CARTILAGE RESPONSE TO *IN VITRO* MODELS OF INJURY IN COMBINATION WITH GROWTH FACTOR AND ANTIOXIDANT TREATMENTS

Cameron A Wheeler
S.B. Mechanical Engineering, MIT, 2003
S.M. Biological Engineering, MIT, 2007

Submitted to the Department of Biological Engineering
in Partial Fulfillment of the Requirements for the Degree of

Doctor of Philosophy in Biological Engineering
at the

Massachusetts Institute of Technology

December 2007
[February 2008]

Signature of Author_____
Cameron A Wheeler
Department of Biological Engineering

Certified by_____
Alan J. Grodzinsky, Thesis Advisor
Professor of Mechanical, Electrical, and Biological Engineering

Accepted by_____
Ram Sasisekharan, Graduate Program Co-Chairman
Professor of Biological Engineering

Thesis Committee:

Alan J. Grodzinsky.....Professor of Biological, Electrical, and Mechanical Engineering
Massachusetts Institute of Technology

Roger D. Kamm.....Professor of Biological and Mechanical Engineering
Massachusetts Institute of Technology

Christopher Evans.....Professor of Orthopedic Surgery
Brigham and Women's Hospital, Harvard Medical School

Abstract

Approximately one in five Americans is affected by arthritis, making it one of the most prevalent diseases and the leading cause of disability in the United States. Post-traumatic arthritis occurs after joint injury (e.g., ACL rupture or intraarticular fracture) and makes up a substantial proportion of the population with arthritis. In previous clinical studies, patients suffering from a traumatic joint injury have shown an increased risk in osteoarthritis (OA), independent of surgical intervention to stabilize the joint. Thus, the early events post-injury have an important effect on tissue within the joint in the long term. To understand the processes involved in the onset of OA and factors leading to OA post-traumatic injury, *in vitro* models have been developed to isolate components of the complex processes occurring *in vivo*. While *in vitro* models do not mimic true physiologic conditions *in vivo*, by isolating the effects of mechanical compression, cytokine treatment, and cartilage co-cultured with adjacent tissue, *in vitro* models can give insight into key biological and mechanical pathways occurring *in vivo*.

This study focuses on changes in cartilage gene and protein expression and associated cartilage matrix degradation in response to static or injurious compression of the tissue in the presence or absence of cytokines including TNF-α and IL-6. In addition, normal or injuriously compressed cartilage explants were co-cultured with injured (excised) joint capsule tissue, another in vitro model of post-traumatic cellular behavior. Both young bovine cartilage and human cartilage from a wide range of ages were used. The growth factors insulin-like growth factor-1 (IGF-1) and Osteogenic protein-1 (OP-1), as well as the antioxidant, superoxide dismutase mimetic (SODm), were tested to examine if they had the capability to abrogate the negative effects of these injury models. Taking a systems approach, the effects of these stimuli on expression of over 48 genes (in cartilage as well as joint capsule) were quantified, along with measures of chondrocyte viability, biosynthesis, protein expression, and GAG loss.

Chondrocyte gene expression was differentially regulated by 50% static compression or IGF-1 treatment or the combination of compression and IGF-1. Results showed that IGF-1 stimulated aggrecan biosynthesis in a transcriptionally regulated manner, whereas compression inhibited aggrecan synthesis in a manner not regulated by transcriptional activity. The injury plus co-culture model was examined in detail, and OP-1 and IGF-1 were unable to rescue changes in transcriptional expressions due to injury. However, these growth factors were able to rescue cells from apoptosis, and slightly increase biosynthesis rates. Human tissue was used to further validate the model of mechanical injury (INJ) combined with co-culture (Co). Immunohistochemical analysis of human cartilage explants after INJ+Co treatment revealed changes in versican and aggrecan protein expression, as well as changes in surface tissue morphology, that mimicked certain changes observed in human osteochondral plugs taken from patients at the time of notchplasty surgery (post ACL reconstruction) at 1, 3, or 57 months post-ACL rupture.

The oxidative stress involved in a cytokine plus injury model showed that SODm had no ability to selectively diminish protease transcriptional activity. Cartilage treated with this antioxidant showed significant increases in GAG loss to the medium, but diminished levels of chondrocyte apoptosis. Taken together, this work supports further investigation of the mechanisms of action of OP-1, IGF-1, and SODm in order to elucidate their possible therapeutic value, and demonstrates the usefulness of these complementary *in vitro* models of cartilage injury.

Acknowledgements

I want to thank my advisor, Alan Grodzinsky for all the help he has given me in editing and guiding my research. His open personality and approach to research has given me an opportunity to explore my ideas and concentrate on my scientific interests. My thesis committee, Roger and Chris, have given me useful suggestions as well as important question that have shaped my work. I am extremely grateful for the open environment which exists in Al's group and the interactions I've been able to have with amazing members of the lab. In particular, Jon Fitzgerald, Mike DiMicco, and Jenny Lee guided my thinking and training, and were always available for all my questions. They gave me directly or indirectly a framework for thinking about research which enabled me to develop my own ideas and understand the tools and techniques to explore those ideas. Jon particularly was always patient in the teaching process which was invaluable. I also would like to thank the current members of the group, Sangwon, Bobae, Rachel, Diana, Shuodan, Paul, Detlef, Eric, Yi, and Sui-Yi for their contribution to wonderful working environment. A special thank you is also in order for the constants in the lab equation, Han-Hwa, Linda, and Elliot. All I have relied on to accomplish things I could not do myself, and am grateful for their approachability. Lastly, I want to thank my family, who have always supported me these past four years, and who are my biggest fans. I cherish those relationships and am grateful that they will always be with me. The past four years have been an amazing time for my own development both personally and scientifically, and I am humbled and grateful for those opportunities.

Table of Contents

List of Figures

List of Tables

Chapter 1

Mechanobiology: Introduction, Background, and Significance

* This chapter has appeared as a review paper in Current Opinions in Orthopaedics (*Wheeler, Cameron A; Fitzgerald, Jonathan B; Grodzinsky, Alan* **Cartilage mechanobiology: the response of chondrocytes to mechanical force.** Current Opinion in Orthopedics. 16(5):346-353, October 2005.)

1.1 Purpose of the Chapter

A comprehensive understanding of chondrocyte mechanobiology is critically important for a clear understanding of the etiopathology and treatment of osteoarthritis (OA) as well as for the long-term survival of tissue engineered implants for cartilage repair.

Recent Findings

A large body of evidence has emerged documenting the effects of various mechanical loading modalities on chondrocyte biosynthesis and gene expression. Many physical forces and flows occur in cartilage during loading *in vivo*. For example, dynamic compression of cartilage results in deformation of cells and the extracellular matrix, hydrostatic pressurization of the tissue fluid, pressure gradients and the accompanying flow of fluid within the tissue, and streaming potentials and currents induced by fluid convection of counter-ions through the negatively charged extracellular matrix (ECM). In addition, local changes in tissue volume caused by compression also lead to alterations in matrix water content, ECM fixed charge density, mobile ion concentrations, and osmotic pressure. Any of these mechanical and physicochemical phenomena in the micro-environment of chondrocytes may affect cellular metabolism. While specific components of certain mechanotransduction pathways have been identified, the exact mechanisms by which mechanical forces influence the biological activity of chondrocytes are not yet fully understood. New genomic and proteomic technologies and methodologies including systems biological analyses are being applied to better understand cellular mechanotransduction.

Summary

Investigators have focused on mechano-regulation of upstream signaling and responses at the level of gene transcription, protein translation and post-translational modifications. Intracellular pathways including those involving integrin signaling, mitogen activated protein kinases (MAPKs), and release of intracellular calcium have been confirmed in several laboratories.

1.2 Introduction

Articular cartilage is an avascular, aneural, alymphatic tissue that provides a low friction weight bearing surface for joint locomotion. During joint loading *in vivo*, cartilage is subjected to mechanical stresses and strains that span a wide range of amplitudes and frequencies [1, 2]. Peak stresses can reach 10–20 MPa (100–200 atm) during activities such as stair climbing [3]. While compressive strains of 15% – 40% may occur in response to long-term or "static" loads within the physiological range [1], compressions of only a few percent occur during normal ambulation (e.g., the "dynamic" strains that occur at walking frequencies of ~1 Hz). Chondrocytes occupy 3% to 5% of tissue volume in adult human cartilage [1]. These cells maintain a mechanically functional extra-cellular matrix (ECM) by mediating the synthesis, assembly, and degradation of proteoglycans (PGs), collagens, glycoproteins, and other matrix molecules. It is well known that chondrocytes can sense and respond to their mechanical environment; however, the mechanotransduction pathways by which mechanical forces influence the biological activity of chondrocytes are not fully understood.

1.3 Systems for Studying Chondrocyte Mechanotransduction

Since mechanotransduction mechanisms are difficult to quantify *in vivo*, model systems such as cartilage explant organ culture and three dimensional chondrocyte/gel culture have been used. Cartilage explants preserve native tissue structure and cell-matrix interactions and thereby enable quantitative correlations between mechanical loading parameters and biological responses such as gene expression and biosynthesis. Muir [4] emphasized the important but complex role of the native ECM and chondrocyte-ECM interactions in chondrocyte response to load; thus, investigators [4] have cautioned that the use of isolated, plated chondrocytes that are depleted of ECM must be approached with care regarding the potential for chondrocyte dedifferentiation and the interpretation of the results in relation to the behavior of cartilage. In native tissue, however,

the coupling between mechanical, chemical, and electrical forces and flows within the ECM can complicate the identification of specific physical stimuli, necessitating specialized experimental and theoretical modeling approaches. Therefore, three-dimensional agarose [5], alginate [6], and other scaffold culture systems have also been used to study chondrocyte response to mechanical compression[7-9], hydrostatic pressure [10], stretch [11], physicochemical stimuli (pH and osmolarity [12], and electrical currents [13]). Finally, a variety of specialized, incubator-housed instruments have been developed to mimic mechanical stimuli found *in vivo* and apply components of compression, shear, stretching, hydrostatic or osmotic pressure to explants, isolated cells, or cell-encapsulated gel constructs *in vitro* [14-17], shown schematically in Fig. 1.1.

1.4 Chondrocyte biosynthesis and gene expression

Static compression (Fig. 1.1a) of animal and human cartilage explants [18, 19] as well as high *hydrostatic pressure* applied to chondrocyte monolayers [20] can cause a dose-dependent decrease in the biosynthesis of proteoglycans, collagens, and other ECM proteins as quickly as one hour after application of compression. Complete recovery of biosynthesis can occur after release of compression, but at different rates for different ECM macromolecules [21], strongly suggesting that specific transduction pathways are involved. In contrast, *dynamic compression and shear* (Fig 1.1b,c) [18, 22, 23] and cyclic hydrostatic compression [20, 24] can markedly upregulate ECM biosynthesis in a manner dependent on compression amplitude and frequency [20, 22], as well as the developmental stage and the depth from the articular surface of the cartilage sample [14, 25, 26]. Tissue-level and cell-level quantitative autoradiography have been used to visualize the spatial distribution of newly-synthesized ECM molecules in response to compression and shear [23, 27, 28], and to compare with the theoretically predicted profiles of

physical stimuli, highlighting the roles of ECM and cell deformation as well as intratissue fluid flow (shown schematically in Fig. 1.1).

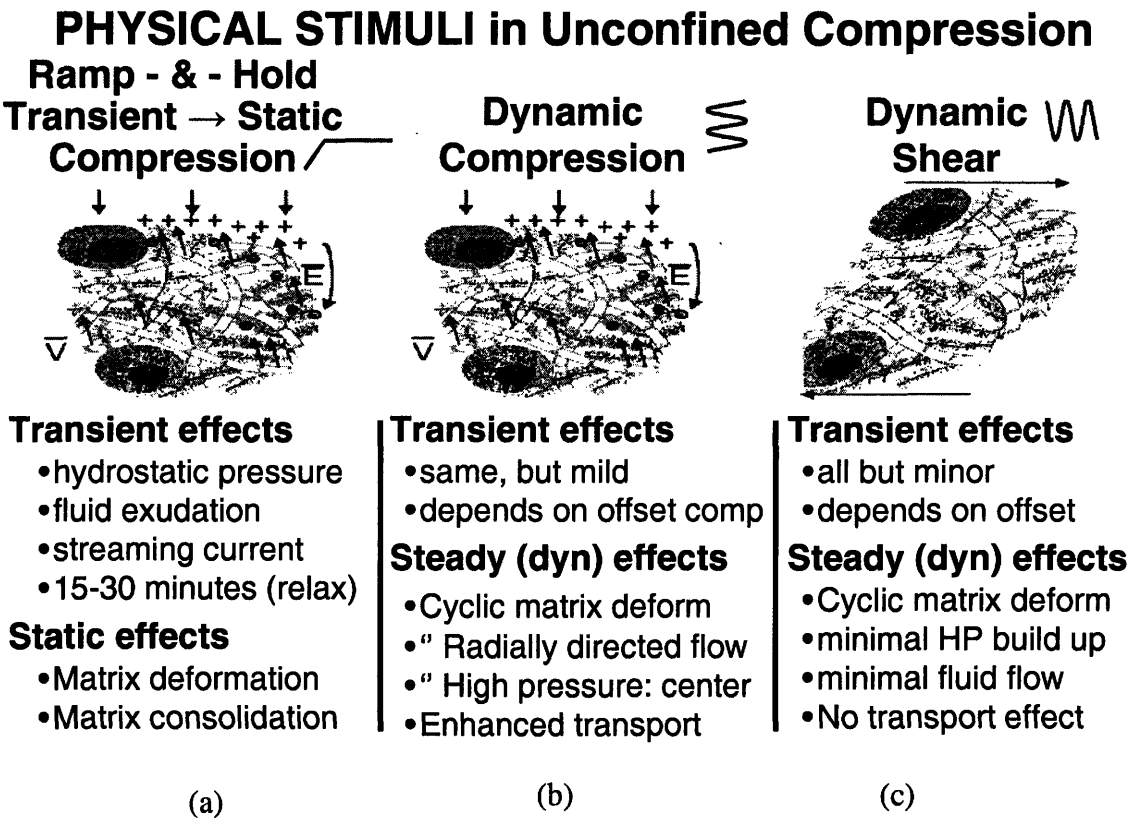

Figure 1.1: Schematic of physical forces and flows occurring during mechanical loading of cartilage in vivo, that can be stimulated in vitro by means of (a) static compression, (b) dynamic compression, and (c) dynamic tissue shear.

Mechanical forces can also influence aggrecan gene expression [29-33] and the transcription of many matrix proteins and proteases in chondrocytes and other connective tissue cells [33-36]. Investigators have also found that *fluid shear flow* [37-40] can alter aggrecan synthesis and the expression of aggrecan, TIMP-1, IL-6 and MMP-9. The induction of MMP-9 gene expression appeared to be mediated via the JNK signaling pathway [38], and the aggrecan promoter via the ERK pathway [39]. While the fluid velocities in these experiments were much

higher than physiological for cartilage, the resulting shear stresses may be relevant. When isolated bovine and human chondrocytes were *cyclically stretched on flexible membranes*, aggrecan and type II collagen mRNA expression were increased [40], consistent with a role for cell deformation and membrane perturbation. Cyclic (1 Hz square wave) uniaxial stretch (5% elongation) of embryonic chick sternal chondrocytes seeded into a 3D collagen sponge induced expression of Indian hedgehog (Ihh) and also upregulated bone morphogenic proteins 2 and 4 downstream of Ihh which, in combination, stimulated cell proliferation [11]. Interestingly, mechanical induction of Ihh mRNA was abolished by blocking stretch activated channels [11].

1.5 Upstream Signaling

Investigators have been trying to map the sequential intracellular signaling pathways through which mechanical forces can modify the gene expression of specific molecules. Major roles have been identified for certain classical signaling pathways including those involving integrins, mitogen activated protein kinases (MAPKs), and release of intracellular calcium.

Integrin signaling pathways

Evidence suggests that integrins can convert extracellular mechanical stimuli into intracellular signals in a variety of cell types [41]. In chondrocytes, the alpha $\alpha5\beta1$ fibronectin-binding integrins have been implicated as part of a mechanotransduction complex that involves tyrosine protein kinases, cytoskeletal proteins, ion channels, and second-messenger signaling cascades [42, 43]. Researchers have also shown that the $\alpha5\beta1$ integrin complex is present in OA chondrocytes, but results in different downstream effects when activated or blocked compared to normal chondrocytes [44]. Application of hydrostatic pressure to chondrocyte monolayers in a manner that induced strain on the culture dish and plated cells caused interleukin-4 (IL-4) secretion via $\alpha5\beta1$ integrin and subsequent intracellular calcium release followed by cell hyperpolarization [42, 45]. One possible connecting link is the N-methyl-D-aspartate (NMDA)

receptor, since integrin signaling has been shown to influence the activity of this receptor in other cells [46]. NMDA is phosphorylated by protein kinases including protein kinase C (PKC) and phosphotidylinositol 3-kinase (PI3K) [47]. Salter el al. observed that the NMDA receptor induced depolarization in OA chondrocytes and hyperpolarization in normal chondrocytes, suggesting a possible alteration in chondrocytic mechanotransduction as a consequence of the function of the NMDA receptor during OA [48].

Mitogen activated protein kinase pathways

Investigators have been trying to map the sequential intracellular signaling pathways through which mechanical forces may modify chondrocyte gene expression of specific molecules. Several recent studies have demonstrated a role for mitogen activated protein kinases (MAPKs) [49, 50] which can alter matrix gene expression and changes in matrix production by chondrocytes within compressed cartilage and in chondrocyte monolayers [51]. This family of ubiquitous signaling molecules includes extracellular-signal regulated protein kinases (ERK1/2), c-Jun N-terminal kinase (JNK) and p38. Activated MAP kinases are thought to translocate to the nucleus, where they may induce phosphorylation of transcriptional factors and eventual upregulation of various genes.

Fanning et al. [52] examined the effects of slow ramp-and-hold compression of cartilage explants to final static strains up to 50% that were held for a range of compression durations; these compression conditions were found previously to inhibit chondrocyte biosynthesis but not to affect cell viability. Mechanical compression caused (1) a rapid induction of ERK1/2 phosphorylation at 10 min followed by a rapid decay, as well as a sustained level of ERK2 phosphorylation that persisted for at least 24 hrs; (2) phosphorylation of p38 in strictly a transient fashion, with maximal phosphorylation occurring at 10 min; and (3) stimulation of SEK1 phosphorylation with a maximum at the relatively delayed time point of 1hr and with a higher amplitude than ERK1/2 and p38 phosphorylation. (SEK1is an immediate upstream specific

activator of JNKs 1,2 and 3 [53], and the JNK and p38 kinases together constitute the SAPK sub-family of MAPKs [54]). Fanning et al. [50] proposed that the rapid activation of ERK1/2 and p38 may be due to the cell deformation, fluid flow and pressurization, while the SEK1 pathway was activated only under static compression without fluid flow or pressurization [50]. Thus, it was suggested that the initial transient ERK1/2 response was due to the dynamic components of static compression, consistent with the results of Li et al. [49], who found a significant upregulation of ERK1/2 activation in response to dynamic compression.

ATP and Ca2+

Ion channels have been identified as another important factor in mechanotransduction, including effects of cell stretching on chondrocyte hyperpolarization and depolarization [55]. ATP has been shown to be involved in signaling in many cell types. Under compressive conditions, bovine chondrocytes can release ATP [56, 57] which, in the extracellular space, can then bind to membrane receptors and initiate a signaling cascade including stimulation of proteoglycan synthesis [58]. While ATP can induce anabolic signaling in normal chondrocytes, OA chondrocytes do not show upregulation of matrix production. Mechanical stimulation can also increase the concentration of intracellular calcium ions, derived either from intracellular stores or from the extracellular space and transported into the cell via stretch activated ion channels. While hyperosmotic stress can initiate intracellular Ca^{2+} signaling in chondrocytes [59], Erickson et al. demonstrated that the stretch activated ion channels were not necessarily responsible for Ca^{2+} transients under these conditions. Cell volume was also shown to decrease under hyperosmotic stress and, hence, the stretch effect was explained by an inhomogeneity in the cell surface [59]. The role of intracellular calcium in native cartilage explants was studied by Vahlmu and Raia [60]; using blockers of intracellular Ca^{2+} and protein kinase C, they demonstrated that regulation of aggrecan mRNA levels under creep compression involved Ca^{2+}/calmodulin and myo-inositol 1,4,5-triphosphate signaling processes. Fitzgerald et al. also

found that compression of cartilage explants induces multiple time-dependent gene expression patterns that involve intracellular calcium and cyclic AMP [61].

1.6 Pro-inflammatory pathways in normal and injurious compression

Acute traumatic joint injury increases the risk for subsequent development of OA [62]. In order to quantify the events following cartilage and joint injury, investigators have turned to a variety of *in vitro* and animal models. Studies have shown that threshold levels of compressive strain, strain rate, and peak stress can cause cartilage matrix disruption, tissue swelling, cell necrosis and apoptosis, and increased loss of matrix macromolecules [63-70]. As a baseline control for changes in gene expression in bovine calf cartilage explants, mRNA levels measured in non-injured free swelling tissue was found to vary over five orders of magnitude, with matrix molecules being the most highly expressed of the genes tested and cytokines, matrix metalloproteinases (MMPs), aggrecanases (ADAMTSs), and transcription factors showing lower levels of expression [71]. While the matrix molecules showed little change in expression after injurious compression, MMP-3 increased ~250-fold, ADAMTS-5 increased ~40-fold, and TIMP-1 increased ~12-fold over free swelling levels [66]. In addition, injurious compression results in a decrease in biosynthetic rates in the remaining viable cells, and these viable cells no longer respond to the stimulatory effects of moderate dynamic compression seen in normal cartilage [70]. Taken together, these studies suggest that mechanical overload can cause long-term cell mediated changes in matrix quality and turnover.

Deschner et al. recently summarized the interaction between loading and inflammatory pathways [72], which may be activated by excessive loads and inhibited by moderate cyclical loading [42, 45, 73]. Thus, these interactions appear to depend on the magnitude and loading rate (frequency).

Mechanical forces can influence production of NO [16, 74, 75], PGE2 [37], and IL-6 [76]. Interestingly, cross-talk between NO and PGE2 pro-inflammatory pathways, and between NOS2 and COX2 (upstream of NO and PGE2), can be regulated by mechanical stimuli [77]. These pathways have been traditionally associated with inflammatory cytokines such as IL-1, an initiator of cartilage degradation [42, 45, 73, 78-80]. Dynamic compression (15% strain amplitude, 1Hz, 48 hr) could inhibit NO synthesis by equine chondrocytes in agarose gel constructs [81] ,and could inhibit NO and PGE2 release by superficial zone equine chondrocytes stimulated by IL-1β [82].

Cell microenvironment and organelle morphology

Loading of cartilage (Fig. 1.2a) produces cellular deformation [83, 84] in proportion to the local deformation of the ECM, and in a manner consistent with the depth-dependent compressive properties of the bulk tissue [85]. Deformations within the pericellular matrix (Fig. 1.2b) also affect the physicochemical microenvironment of the chondrocyte [28, 86] and may, in turn, signal the cell to modulate its biosynthetic response. Deformation-induced fluid flow in the pericellular region enhances transport of soluble factors to cell receptors, and alters the local concentration of mobile ions leading to electrochemical changes such as shifts in pH[87]. Cell-surface connections to the ECM enable pericellular deformations to be transmitted through the cell membrane to intracellular organelles via cytoskeletal elements such as actin microfilaments, microtubules, and intermediate filaments[20, 83, 88]. Compression can also dramatically affect the morphology of intracellular organelles that regulate cell biosynthesis and metabolism by altering gene transcription, intracellular transport and trafficking, and protein translation and post-translational processing. Using chemical fixation, high-pressure freezing, and electron microscopy, Szafranski et al. [89] observed that compression of bovine cartilage explants caused a concomitant reduction in the volume of the extracellular matrix, chondrocyte, nucleus, rough endoplasmic reticulum, and mitochondria. Interestingly, however, the Golgi apparatus was able

to resist loss of intraorganelle water and retain a portion of its volume relative to the remainder of the cell. These combined results suggested the hypothesis that organelle volume changes were driven mainly by osmotic interactions while shape changes were mediated by structural factors, such as cytoskeletal interactions that may be linked to extracellular matrix deformations. The observed volume and shape changes of the chondrocyte organelles and the differential behavior between organelles during tissue compression provides evidence for an important mechanotransduction pathway linking translational and post-translational events. For example, since the Golgi is the site of post-translational modifications of aggrecan (e.g., glycosylation and sulfation) [89, 90], changes in Golgi morphology and function with compression may play a critical role in the known changes in GAG chain length and sulfation caused by compression [21]. Such changes in GAG and aggrecan structure, which also occur naturally with age (Fig. 1.2c) may profoundly influence aggrecan function. Such functional mechanical changes can now be measured directly using atomic force microscopy methodologies [91, 92] (Fig. 1.2d).

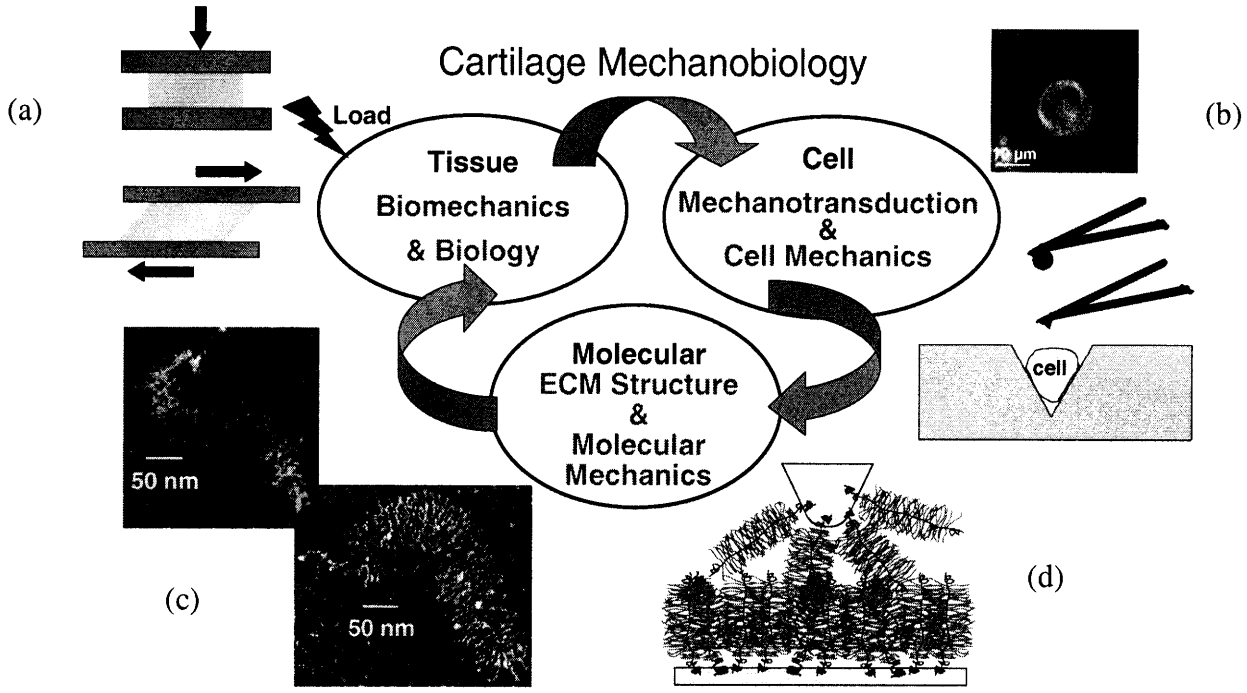

Figure 1.2

Figure 1.2 : Loading of cartilage explants (a), or direct mechanical stimulation of cells (b) can produce mechanical stimuli that may be sensed by the cell and its pericellular microenvironment (b). These mechanical stimuli may alter the rate of synthesis as well as the molecular structure of ECM molecules such as aggrecan (c) which, in turn, could ultimately affect tissue-level biomechanical properties in a feedback fashion (a). New cell-level and molecular-level measurement techniques, such as those based on atomic force microscopy, are being used to quantify the molecular mechanical properties of ECM macromolecules (d) as well as cellular mechanical properties (b).

1.7 Systems biology approaches

Real time PCR and gene clustering analyses have been used to study intermediate-size gene sets (20-48 genes) thought to be involved with cartilage mechanotransduction. Fitzgerald et al. [33] examined the kinetics of mechano-regulation of gene transcription in response to static compression of bovine calf cartilage explants for periods between 1-24 hours in the presence or absence of an intracellular calcium chelator or an inhibitor of cyclic AMP activated protein kinase A. Cluster analysis of the data revealed four main expression patterns: two groups that contained either transiently upregulated or duration-enhanced expression profiles could each be

subdivided into genes that did or did not require intracellular calcium release and cyclic AMP activated protein kinase A for their mechano-regulation. Transcription levels for aggrecan, type II collagen, and link protein were upregulated approximately 2 to 3-fold during the first 8 hrs of 50% compression and subsequently down-regulated to levels below that of free-swelling controls by 24hrs. Transcription levels of matrix metalloproteinases-3,9,13, aggrecanase-1 and the matrix protease regulator cyclooxygenase-2 increased with the duration of 50% compression 2 to 16-fold up to by 24 hrs. Thus, transcription of proteins involved in matrix remodeling and catabolism dominated over anabolic matrix proteins as the duration of static compression increased. These approaches are also being used to study responses to dynamic compression and tissue shear of cartilage explants.

Researchers have begun to integrate genomic and proteomic approaches with the computational tools of systems biology for applications in musculoskeletal research, including medical diagnostics, and drug discovery [93]. DNA microarray technology is being used to explore the complex feedback loops in transcription factors and layered signaling pathways underlying the mechanotransduction as well as the pathobiology of osteoarthritis. Aigner et al. [94-96] examined transcript levels of matrix components and matrix degrading proteinases using DNA arrays. By comparing normal chondrocytes with early and late stage OA chondrocytes, they examined expression trends involving up and down regulation of MMPs, TIMPS, proteoglycans, and collagens [96]. Such approaches can be directly applied to the study of mechanotransduction. While DNA arrays can sample large numbers of genes, they are limited in their sensitivity and they do not measure posttranscriptional regulation or modifications [94]. While recognizing these limitations, the potential of such profiling approaches is clear [95, 97], since the results can be used to formulate hypotheses about specific molecules and mechanisms in ways that are complementary to the traditional one-gene or one-protein hypothesis-testing approach.

1.8 Conclusion

Chondrocytes can sense and respond to mechanical forces in an extraordinarily sensitive and robust manner. These cells can distinguish between compression, tension and shear deformation of the surrounding ECM, and respond in a manner that varies with the rate (frequency) of loading. Recent studies have identified several intracellular signaling pathways that are involved in chondrocyte mechanotransduction and the regulation of cartilage and exhibit levels of overlap or crosstalk in their signaling. These complex signals are responsible for activation of ECM molecules proteinases, inflammatory factors, and regulatory proteins which govern tissue homeostasis. Significant technical advances have enabled the study of transduction mechanisms by chondrocytes within their native, dense ECM. Advanced genomic and proteomic technologies should lead to a further rapid increase understanding the fundamental link between chondrocyte mechanobiology, physiology, and tissue homeostatis in health and disease, with direct application to cartilage repair and tissue engineering.

Acknowledgements

This work supported by NIH Grants AR33236 and AR45779.

1.9 References and recommended reading

1. Herberhold, C., S. Faber, T. Stammberger, et al., *In situ measurement of articular cartilage deformation in intact femoropatellar joints under static loading.* J. Biomech., 1999. **32**(12): p. 1287-1295.
2. Ateshian, G.A., S.D. Kwak, L.J. Soslowsky, and V.C. Mow, *A Stereophotogrammetric Method for Determining in-Situ Contact Areas in Diarthroidal Joints, and a Comparison with Other Methods.* Journal of Biomechanics, 1994. **27**(1): p. 111-124.
3. Hodge, W.A., R.S. Fijan, K.L. Carlson, et al., *Contact Pressures in the Human Hip-Joint Measured Invivo.* Proc. Natl. Acad. Sci. U.S.A., 1986. **83**(9): p. 2879-2883.
4. Muir, H., *The chondrocyte, architect of cartilage.* BioEssays, 1995(17): p. 1039-1048.
5. Benya, P.D. and J.D. Shaffer, *Dedifferentiated chondrocytes reexpress the differentiated collagen phenotype when cultured in agarose gels.* Cell, 1982. **30**(1): p. 215-24.

** A classic in the field and important for all applications in cartilage tissue engineering.

6. Hauselmann, H.J., R.J. Fernandes, S.S. Mok, et al., *Phenotypic stability of bovine articular chondrocytes after long-term culture in alginate beads.* J Cell Sci, 1994. **107** (**Pt 1**): p. 17-27.
7. Buschmann, M.D., Y.A. Gluzband, A.J. Grodzinsky, and E.B. Hunziker, *Mechanical Compression Modulates Matrix Biosynthesis in Chondrocyte Agarose Culture.* Journal of Cell Science, 1995. **108**: p. 1497-1508.
8. Ragan, P.M., V.I. Chin, H.H. Hung, et al., *Chondrocyte extracellular matrix synthesis and turnover are influenced by static compression in a new alginate disk culture system.* Arch. Biochem. Biophys., 2000. **383**(2): p. 256-64.
9. Hung, C.T., R.L. Mauck, C.C. Wang, et al., *A paradigm for functional tissue engineering of articular cartilage via applied physiologic deformational loading.* Ann Biomed Eng, 2004. **32**(1): p. 35-49.

* A very good review of applications of chondrocyte mechanobiology to tissue cartilage engineering

10. Domm, C., J. Fay, M. Schunke, and B. Kurz, *[Redifferentiation of dedifferentiated joint cartilage cells in alginate culture. Effect of intermittent hydrostatic pressure and low oxygen partial pressure].* Orthopaedic, 2000. **29**(2): p. 91-9.
11. Wu, Q., Y. Zhang, and Q. Chen, *Indian hedgehog is an essential component of mechanotransduction complex to stimulate chondrocyte proliferation.* J Biol Chem, 2001. **276**(38): p. 35290-6.

** An important example of cell signaling in response to mechanical stretching of chondrocytes

12. Hung, C.T., M.A. LeRoux, G.D. Palmer, et al., *Disparate aggrecan gene expression in chondrocytes subjected to hypotonic and hypertonic loading in 2D and 3D culture.* Biorheology, 2003. **40**(1-3): p. 61-72.
13. Szasz, N.H., H. Sen, S. Grodzinsky, A, *Electric field regulation of chondrocyte biosynthesis in agarose gel constructs.* Trans Orthop Res Soc, 2003(28): p. 672.
14. Torzilli, P.A., R. Grigiene, C. Huang, et al., *Characterization of cartilage metabolic response to static and dynamic stress using a mechanical explant test system.* J Biomech, 1997. **30**(1): p. 1-9.

15. Frank, E.H., M. Jin, A.M. Loening, et al., *A versatile shear and compression apparatus for mechanical stimulation of tissue culture explants.* Journal of Biomechanics, 2000. **33**(11): p. 1523-1527.
16. Fermor, B., J.B. Weinberg, D.S. Pisetsky, et al., *The effects of static and intermittent compression on nitric oxide production in articular cartilage explants.* J Orthop Res, 2001. **19**(4): p. 729-37.
17. Vanderploeg, E.J., S.M. Imler, K.R. Brodkin, et al., *Oscillatory tension differentially modulates matrix metabolism and cytoskeletal organization in chondrocytes and fibrochondrocytes.* J Biomech, 2004. **37**(12): p. 1941-52.
18. Sah, R.L.Y., Y.J. Kim, J.Y.H. Doong, et al., *Biosynthesis Response to Cartilage Explants to Dynamic Compression.* J. Orthop. Res., 1989. **7**: p. 619-636.
19. Guilak, F., B.C. Meyer, A. Ratcliffe, and V.C. Mow, *The effects of matrix compression on proteoglycan metabolism in articular cartilage explants.* Osteoarthr. Cartilage, 1994. **2**: p. 91-101.
20. Jortikka, M.O., J.J. Parkkinen, R.I. Inkinen, et al., *The role of microtubules in the regulation of proteoglycan synthesis in chondrocytes under hydrostatic pressure.* Archives of Biochemistry and Biophysics, 2000. **374**(2): p. 172-180.
21. Kim, Y.J., A.J. Grodzinsky, and A.H. Plaas, *Compression of cartilage results in differential effects on biosynthetic pathways for aggrecan, link protein, and hyaluronan.* Arch. Biochem. Biophys., 1996. **328**(2): p. 331-40.
22. Kim, Y.J., R.L. Sah, A.J. Grodzinsky, et al., *Mechanical regulation of cartilage biosynthetic behavior: physical stimuli.* Arch. Biochem. Biophys., 1994. **311**(1): p. 1-12.
23. Jin, M., E.H. Frank, T.M. Quinn, et al., *Tissue shear deformation stimulates proteoglycan and protein biosynthesis in bovine cartilage explants.* Arch Biochem Biophys, 2001. **395**(1): p. 41-8.
24. Parkkinen, J.J., M.J. Lammi, A. Pelttari, et al., *Altered Golgi-Apparatus in Hydrostatically Loaded Articular-Cartilage Chondrocytes.* Annals of the Rheumatic Diseases, 1993. **52**(3): p. 192-198.
25. Wong, M., M. Siegrist, and X. Cao, *Cyclic compression of articular cartilage explants is associated with progressive consolidation and altered expression pattern of extracellular matrix proteins.* Matrix Biol, 1999. **18**(4): p. 391-9.
26. Li, K.W., A.K. Williamson, A.S. Wang, and R.L. Sah, *Growth responses of cartilage to static and dynamic compression.* Clin Orthop Relat Res, 2001(391 Suppl): p. S34-48.

** A good review the effects of tissue age on the response of cartilage to mechanical loading.

27. Buschmann, M.D., Y.J. Kim, M. Wong, et al., *Stimulation of aggrecan synthesis in cartilage explants by cyclic loading is localized to regions of high interstitial fluid flow.* Archives of Biochemistry and Biophysics, 1999. **366**(1): p. 1-7.
28. Quinn, T.M., A.J. Grodzinsky, M.D. Buschmann, et al., *Mechanical compression alters proteoglycan deposition and matrix deformation around individual cells in cartilage explants.* Journal of Cell Science, 1998. **111**: p. 573-583.
29. Valhmu, W.B., E.J. Stazzone, N.M. Bachrach, et al., *Load-Controlled Compression of Articular Cartilage induces a transient stimulation of Aggrecan gene expression.* Arch. Biochem. Biophys., 1998. **353**(1): p. 29-36.
30. Smith, R.L., S.F. Rusk, B.E. Ellison, et al., *In vitro stimulation of articular chondrocyte mRNA and extracellular matrix synthesis by hydrostatic pressure.* J Orthop Res, 1996. **14**(1): p. 53-60.

31. Takahashi, K., T. Kubo, K. Kobayashi, et al., *Hydrostatic pressure influences mRNA expression of transforming growth factor-beta 1 and heat shock protein 70 in chondrocyte-like cell line.* J Orthop Res, 1997. **15**(1): p. 150-8.
32. Suh, J.K., G.H. Baek, A. Aroen, et al., *Intermittent sub-ambient interstitial hydrostatic pressure as a potential mechanical stimulator for chondrocyte metabolism.* Osteoarthritis Cartilage, 1999. **7**(1): p. 71-80.
33. Fitzgerald, J.B., M. Jin, D. Dean, et al., *Mechanical compression of cartilage explants induces multiple time-dependent gene expression patterns and involves intracellular calcium and cyclic AMP.* Journal of Biological Chemistry, 2004. **279**(19): p. 19502-19511.

** A good example of a study of mechanical regulation of gene expression including the use of clustering algorithms for statistical analysis of multiple gene responses

34. Fehrenbacher, A., E. Steck, M. Rickert, et al., *Rapid regulation of collagen but not metalloproteinase 1, 3, 13, 14 and tissue inhibitor of metalloproteinase 1, 2, 3 expression in response to mechanical loading of cartilage explants in vitro.* Arch. Biochem. Biophys., 2003. **410**(1): p. 39-47.
35. Upton, M.L., J. Chen, F. Guilak, and L.A. Setton, *Differential effects of static and dynamic compression on meniscal cell gene expression.* J Orthop Res, 2003. **21**(6): p. 963-9.
36. Chen, J., W. Yan, and L.A. Setton, *Static compression induces zonal-specific changes in gene expression for extracellular matrix and cytoskeletal proteins in intervertebral disc cells in vitro.* Matrix Biol, 2004. **22**(7): p. 573-83.
37. Smith, R.L., B.S. Donlon, M.K. Gupta, et al., *Effects of fluid-induced shear on articular chondrocyte morphology and metabolism in vitro.* J Orthop Res, 1995. **13**(6): p. 824-31.
38. Jin, G., R.L. Sah, Y.S. Li, et al., *Biomechanical regulation of matrix metalloproteinase-9 in cultured chondrocytes.* Journal of Orthopaedic Research, 2000. **18**(6): p. 899-908.
39. Hung, C.T., D.R. Henshaw, C.C.B. Wang, et al., *Mitogen-activated protein kinase signaling in bovine articular chondrocytes in response to fluid flow does not require calcium mobilization.* Journal of Biomechanics, 2000. **33**(1): p. 73-80.
40. Holmvall, K., L. Camper, S. Johansson, et al., *Chondrocyte and chondrosarcoma cell integrins with affinity for collagen type II and their response to mechanical stress.* Exp Cell Res, 1995. **221**(2): p. 496-503.
41. Wang, N., J.P. Butler, and D.E. Ingber, *Mechanotransduction across the cell surface and through the cytoskeleton.* Science, 1993. **260**(5111): p. 1124-7.
42. Salter, D.M., S.J. Millward-Sadler, G. Nuki, and M.O. Wright, *Integrin-interleukin-4 mechanotransduction pathways in human chondrocytes.* Clinical Orthopaedics and Related Research, 2001(391): p. S49-S60.
43. Chowdhury, T.T., D.M. Salter, D.L. Bader, and D.A. Lee, *Integrin-mediated mechanotransduction processes in TGFbeta-stimulated monolayer-expanded chondrocytes.* Biochem Biophys Res Commun, 2004. **318**(4): p. 873-81.

* A good example of integrin interactions and mechanotransduction

44. Millward-Sadler, S.J., M.O. Wright, H. Lee, et al., *Altered electrophysiological responses to mechanical stimulation and abnormal signaling through alpha5beta1 integrin in chondrocytes from osteoarthritic cartilage.* Osteoarthritis Cartilage, 2000. **8**(4): p. 272-8.

45. Millward-Sadler, S.J., M.O. Wright, H. Lee, et al., *Integrin-regulated secretion of interleukin 4: A novel pathway of mechanotransduction in human articular chondrocytes.* J. Cell. Biol., 1999. **145**(1): p. 183-9.
46. Chavis, P. and G. Westbrook, *Integrins mediate functional pre- and postsynaptic maturation at a hippocampal synapse.* Nature, 2001. **411**(6835): p. 317-21.
47. Hisatsune, C., H. Umemori, M. Mishina, and T. Yamamoto, *Phosphorylation-dependent interaction of the N-methyl-D-aspartate receptor epsilon 2 subunit with phosphatidylinositol 3-kinase.* Genes Cells, 1999. **4**(11): p. 657-66.
48. Salter, D.M., M.O. Wright, and S.J. Millward-Sadler, *NMDA receptor expression and roles in human articular chondrocyte mechanotransduction.* Biorheology, 2004. **41**(3-4): p. 273-81.

* A good review of specialized receptors and their role in signaling in mechanotransduction

49. Li, K.W., A.S. Wang, and R.L. Sah, *Microenvironment regulation of extracellular signal-regulated kinase activity in chondrocytes - Effects of culture configuration, interleukin-1, and compressive stress.* Arthritis Rheum., 2003. **48**(3): p. 689-699.
50. Fanning, P.J., G. Emkey, R.J. Smith, et al., *Mechanical regulation of mitogen-activated protein kinase signaling in articular cartilage.* J. Biol. Chem., 2003. **278**(51): p. 50940-50948.

* A thorough study of the kinetics of MAPK pathways in reaction to transient ramp-and-hold compression of cartilage.

51. Kim, S.J., S.G. Hwang, I.C. Kim, and J.S. Chun, *Actin cytoskeletal architecture regulates nitric oxide-induced apoptosis, dedifferentiation, and cyclooxygenase-2 expression in articular chondrocytes via mitogen-activated protein kinase and protein kinase C pathways.* J Biol Chem, 2003. **278**(43): p. 42448-56.

* A very good example of the role of the actin cytoskeleton in a variety of different signaling pathways.

52. Fanning, P., G. Emkey, A.J. Grodzinsky, and S. Trippel, *Response of Cartilage to Mechanical Loading is correlated with sustained ERK1/2 Activation.* ORS 47th Annual Meeting, 2001.
53. Dhanasekaran, N., S.T. Tsim, J.M. Dermott, and D. Onesime, *Regulation of cell proliferation by G proteins.* Oncogene, 1998. **17**(11 Reviews): p. 1383-94.
54. Tibbles, L.A. and J.R. Woodgett, *The stress-activated protein kinase pathways.* Cell Mol Life Sci, 1999. **55**(10): p. 1230-54.
55. Millward-Sadler, S.J., M.O. Wright, P.W. Flatman, and D.M. Salter, *ATP in the mechanotransduction pathway of normal human chondrocytes.* Biorheology, 2004. **41**(3-4): p. 567-75.
56. Elfervig, M.K., R.D. Graff, G.M. Lee, et al., *ATP induces Ca(2+) signaling in human chondrons cultured in three-dimensional agarose films.* Osteoarthritis Cartilage, 2001. **9**(6): p. 518-26.
57. Graff, R.D., E.R. Lazarowski, A.J. Banes, and G.M. Lee, *ATP release by mechanically loaded porcine chondrons in pellet culture.* Arthritis Rheum, 2000. **43**(7): p. 1571-9.
58. Croucher, L.J., A. Crawford, P.V. Hatton, et al., *Extracellular ATP and UTP stimulate cartilage proteoglycan and collagen accumulation in bovine articular chondrocyte pellet cultures.* Biochim Biophys Acta, 2000. **1502**(2): p. 297-306.

59. Erickson, G.R., L.G. Alexopoulos, and F. Guilak, *Hyper-osmotic stress induces volume change and calcium transients in chondrocytes by transmembrane, phospholipid, and G-protein pathways.* J Biomech, 2001. **34**(12): p. 1527-35.
60. Valhmu, W.B. and F.J. Raia, *myo-Inositol 1,4,5-trisphosphate and Ca2+/calmodulin-dependent factors mediate transduction of compression-induced signals in bovine articular chondrocytes.* Biochem. J., 2002. **361**: p. 689-696.

** An excellent study of the role of intracellular calcium on aggrecan gene expression

61. Hodge, W.A., R.S. Fijan, K.L. Carlson, et al., *Contact pressures in the human hip joint measured in vivo.* Proc Natl Acad Sci U S A, 1986. **83**(9): p. 2879-83.
62. Gelber, A.C., M.C. Hochberg, L.A. Mead, et al., *Joint injury in young adults and risk for subsequent knee and hip osteoarthritis.* Ann Intern Med, 2000. **133**(5): p. 321-8.
63. Farquhar, T., Y. Xia, K. Mann, et al., *Swelling and fibronectin accumulation in articular cartilage explants after cyclical impact.* J Orthop Res, 1996. **14**(3): p. 417-23.
64. Quinn, T.M., A.J. Grodzinsky, E.B. Hunziker, and J.D. Sandy, *Effects of injurious compression on matrix turnover around individual cells in calf articular cartilage explants.* J Orthop Res, 1998. **16**(4): p. 490-9.
65. Loening, A.M., I.E. James, M.E. Levenston, et al., *Injurious mechanical compression of bovine articular cartilage induces chondrocyte apoptosis.* Arch Biochem Biophys, 2000. **381**(2): p. 205-12.
66. Patwari, P., J. Fay, M.N. Cook, et al., *In vitro models for investigation of the effects of acute mechanical injury on cartilage.* Clin Orthop Relat Res, 2001(391 Suppl): p. S61-71.
67. Jeffry, J., L. Thomson, and R. Aspden, *Matrix damage and chondrocyte viability following a single impact load on articular cartilage.* Arch Biochem Biophys, 1995. **322**: p. 87-96.
68. Quinn, T., R. Allen, B. Schalet, et al., *Matrix and cell injury due to sub-impact loading of adult bovine articular cartilage explants: effects of strain rate and peak stress.* J Orthop Res, 2001. **19**: p. 242-249.
69. Chen, C.T., N. Burton-Wurster, C. Borden, et al., *Chondrocyte necrosis and apoptosis in impact damaged articular cartilage.* J Orthop Res, 2001. **19**(4): p. 703-11.
70. Kurz, B., M. Jin, P. Patwari, et al., *Biosynthetic response and mechanical properties of articular cartilage after injurious compression.* J Orthop Res, 2001. **19**(6): p. 1140-6.
71. Lee, J.H., J.B. Fitzgerald, M.A. DiMicco, and A.J. Grodzinsky, *Mechanical Injury of Cartilage Explants Causes Specific Time Dependent Changes in Chondrocyte Gene Expression.* Arthritis & Rheumatism, 2005. **(in press)**.

* A very comprehensive study of gene expression of a variety in proteins, proteases and signaling molecules following mechanical injury of cartilage

72. Deschner, J., C.R. Hofman, N.P. Piesco, and S. Agarwal, *Signal transduction by mechanical strain in chondrocytes.* Curr Opin Clin Nutr Metab Care, 2003. **6**(3): p. 289-93.
73. Frenkel, S.R. and P.E. Di Cesare, *Degradation and repair of articular cartilage.* Front Biosci, 1999. **4**: p. D671-85.
74. Fermor, B., B. Haribabu, J.B. Weinberg, et al., *Mechanical stress and nitric oxide influence leukotriene production in cartilage.* Biochem Biophys Res Commun, 2001. **285**(3): p. 806-10.

75. Fermor, B., J.B. Weinberg, D.S. Pisetsky, et al., *Induction of cyclooxygenase-2 by mechanical stress through a nitric oxide-regulated pathway.* Osteoarthr. Cartilage, 2002. **10**(10): p. 792-8.
76. Mohtai, M., M.K. Gupta, B. Donlon, et al., *Expression of interleukin-6 in osteoarthritic chondrocytes and effects of fluid-induced shear on this expression in normal human chondrocytes in vitro.* J Orthop Res, 1996. **14**(1): p. 67-73.
77. Guilak, F., B. Fermor, F.J. Keefe, et al., *The role of biomechanics and inflammation in cartilage injury and repair.* Clin Orthop, 2004(423): p. 17-26.

** An excellent review of the role of inflammatory factors and mechanical loading.

78. Williams, J.M., M. Moran, E.J. Thonar, and R.B. Salter, *Continuous passive motion stimulates repair of rabbit knee articular cartilage after matrix proteoglycan loss.* Clin Orthop, 1994(304): p. 252-62.
79. Salter, R.B., *History of rest and motion and the scientific basis for early continuous passive motion.* Hand Clin, 1996. **12**(1): p. 1-11.
80. Salter, R.B., *The physiologic basis of continuous passive motion for articular cartilage healing and regeneration.* Hand Clin, 1994. **10**(2): p. 211-9.
81. Wiseman, M., F. Henson, D.A. Lee, and D.L. Bader, *Dynamic compressive strain inhibits nitric oxide synthesis by equine chondrocytes isolated from different areas of the cartilage surface.* Equine Vet J, 2003. **35**(5): p. 451-6.
82. Chowdhury, T.T., D.L. Bader, and D.A. Lee, *Dynamic compression counteracts IL-1 beta-induced release of nitric oxide and PGE2 by superficial zone chondrocytes cultured in agarose constructs.* Osteoarthritis Cartilage, 2003. **11**(9): p. 688-96.
83. Guilak, F., A. Ratcliffe, and V.C. Mow, *Chondrocyte deformation and local tissue strain in articular cartilage: a confocal microscopy study.* J Orthop Res, 1995. **13**(3): p. 410-21.
84. Buschmann, M.D., A.M. Maurer, E. Berger, and E.B. Hunziker, *A method of quantitative autoradiography for the spatial localization of proteoglycan synthesis rates in cartilage.* J Histochem Cytochem, 1996. **44**(5): p. 423-31.
85. Schinagl, R.M., D. Gurskis, A.C. Chen, and R.L. Sah, *Depth-dependent confined compression modulus of full-thickness bovine articular cartilage.* J Orthop Res, 1997. **15**(4): p. 499-506.
86. Guilak, F. and V.C. Mow, *The mechanical environment of the chondrocyte: a biphasic finite element model of cell-matrix interactions in articular cartilage.* J Biomech, 2000. **33**(12): p. 1663-73.
87. Maroudas, A., *Physico-chemical properties of articular cartilage*, in *Adult Articular Cartilage*, M.A.R. Freeman, Editor. 1979, Pitman: England. p. 215-290.
88. Lee, D.A., M.M. Knight, J.F. Bolton, et al., *Chondrocyte deformation within compressed agarose constructs at the cellular and sub-cellular levels.* J Biomech, 2000. **33**(1): p. 81-95.
89. Szafranski, J.D., A.J. Grodzinsky, E. Burger, et al., *Chondrocyte mechanotransduction: effects of compression on deformation of intracellular organelles and relevance to cellular biosynthesis.* Osteoarthritis Cartilage, 2004. **12**(12): p. 937-46.

** A very good example of the effects of mechanical deformation on intracellular organelle morphology and implications for post translational processing.

90. Lohmander, L.S. and J.H. Kimura, *Biosynthesis of Cartilage Proteoglycan.* Articular Cartilage Biochemistry, ed. K. Kuettner, R. Schleyerbach, and V.C. Hascall. 1986, New York. 93-111.

91. Seog, J., D. Dean, B. Rolauffs, et al., *Nanomechanics of opposing glycosaminoglycan macromolecules.* Journal of Biomechanics, 2005. **(in press)**.
92. Dean, D., L. Han, C. Ortiz, and A.J. Grodzinsky, *Nanoscale conformation and compressibility of cartilage aggrecan using microcontact printing and atomic force microscopy.* Macromolecules, *38*, 4047-4049, 2005.
* A direct measurement of aggrecan compressibility via atomic force microscopy: identifies methods for quantifying the effects of mechano-induced changes in post-translational processing of aggrecan.
93. Young, R.A., *Biomedical discovery with DNA arrays.* Cell, 2000. **102**(1): p. 9-15.
** An excellent review of microarray technology.
94. Aigner, T. and J. Dudhia, *Genomics of osteoarthritis.* Curr Opin Rheumatol, 2003. **15**(5): p. 634-40.
95. Aigner, T., A. Zien, D. Hanisch, and R. Zimmer, *Gene expression in chondrocytes assessed with use of microarrays.* J Bone Joint Surg Am, 2003. **85-A**(Suppl 2): p. 117-23.
** An excellent overview of high throughput data via microarray and its application to cartilage research.
96. Aigner, T., A. Zien, A. Gehrsitz, et al., *Anabolic and Catabolic Gene Expression Pattern Analysis in Normal versus Osteaoarthritic Cartilage using Complementary DNA-Array Technology.* Arthritis & Rheumatism, 2001. **44**(12): p. 2777-2789.
97. Attur, M.G., M.N. Dave, and A.R. Amin, *Functional genomics approaches in arthritis.* Am J Pharmacogenomics, 2004. **4**(1): p. 29-43.
** An excellent in-depth review of functional genomics and it's application to arthritis.

Chapter 2

Current *in vitro* Injury Models

2.1 Introduction

Approximately one in five Americans is affected by arthritis, making it one of the most prevalent diseases and the leading cause of disability in the United States [1]. Post-traumatic arthritis occurs after a traumatic joint injury (ACL rupture [2, 3] or intraarticular fracture [4, 5]) and makes up a significant proportion of the population with arthritis [6]. In previous clinical studies, patients suffering from a traumatic joint injury have shown an increased risk in osteoarthritis (OA), independent of surgical intervention to stabilize the joint [7-11]. Thus, the early events post-injury have an important effect on tissue within the joint in the long term. Studies have shown a dramatic increase in concentration of inflammatory cytokines IL-1β and TNF-α in the synovial fluid within twenty-four hours post injury [12] and have shown them to remain at high levels in the synovial fluid for longer periods of times (months to years) [4, 13, 14]. The interplay between mechanical forces and cellular response to these forces are thought to play a crucial role in understanding the onset of OA [15, 16]. Aggrecan molecules and collagen matrix play an essential role in cartilage homeostasis, and the degradation of this matrix and loss of aggrecan from cartilage is a crucial event in osteoarthritis [17, 18].

To understand the processes involved in the onset of OA and factors leading to OA post-traumatic injury, *in vitro* models have been developed to isolate components of the complex processes occurring *in vivo*. While *in vitro* models do not mimic true physiologic conditions *in vivo*, by isolating the effects of mechanical compression, cytokine treatment, and cartilage co-cultured with adjacent tissue (to name a few models), *in vitro* models can give insight into key biological and mechanical processes occurring *in vivo*.

The aim of this chapter is to review and analyze the current *in vitro* models of injury. While many *in vivo* animal models exist mimicking the injury process [19-21], this chapter will focus on experiment models which isolate the components of such *in vivo* models.

2.2 Models of Mechanical Injury

In vitro mechanical injury has been shown to increase hydraulic permeability [22] and water content [23-25], decrease stiffness [24, 26], increase collagen lost to the medium[22], and increase glycosaminoglycan (GAG) lost to the medium [24, 27-29]. Cells subject to this mechanical injury have been shown to decrease biosynthesis rates [24], undergo apoptosis and necrosis[23, 24, 30, 31], and have elevated levels of protease transcript activity within the first 3 hours post-injury [32] and within the first 24 hours post-injury [33].

There exist significant differences between loading of articular cartilage *in vivo* and mechanically loading explants. *In vivo*, articular cartilage is prone to experience different stress concentrations throughout the tissue due to the rigid topography of the osteochondral cartilage interface. Stress concentration *in vivo* probably corresponds to irregularities in subchondral bone, or to a local variation in cartilage composition [34]. While explant loading may have different stress profiles than *in vivo* loading, the advantage of *in vitro* mechanical loading is the specific and accurate measure of the load applied to the explant and the resulting peak stress, strain, and strain rate. Under these controlled conditions, the strain, strain rate, and peak stress can be measured with precision, and since the three are interdependent, one or two of these

factors can be controlled for as the dependent variables, while the remaining variables are considered the independent variables.

The application of these loads are applied in various different manners, including impact loading (drop tower-type devices [35], material testing machines[36], and free flight masses [37]) and injurious compression [38]. Researchers have suggested that there may be a threshold level of peak stress that separates injurious compression from non-injurious compression [23, 39, 40]. Injurious compression techniques tend to explore the stress-strain response of articular cartilage and how it and other tissues attenuate impact load. Studies have shown that when applied compression reaches 50% strain, chondrocyte viability decreases [24, 26, 40-42] and cartilage surfaces become physically disrupted, with generation of fissures [42]. A recent study investigated the effect of indentation probing used as a diagnostic tool during or after surgical procedures and its effect on chondrocyte viability [43]. This study reported that 30% strain performed in arthroscopy decreased cell viability. The effect of strain rates has been investigated by varying speed of impact and has been shown to be an important parameter in defining mechanical injury [24, 44]. Articular cartilage generally behaves as a visco- or poro-elastic fibre-composite material, and as such, its material properties depend on the rate of loading [45]. For example, at high rates, cartilage acts as a quasi-elastic material provided the stress is not too high. Studies have found that fissuring and cell death occurred in the superficial zone with a higher release of glycosaminoglycan (GAGs) when the strain rate was increased [42] and apoptosis was increased as peak stress increased [26]. Alternatively, loads can be applied in a load-rate dependent manner. A high load-rate of 600 MPa/sec caused concentrated cell death in the superficial zone of articular cartilage, and a lower load-rate (30 MPa/sec) showed a more

diffuse pattern of cell death [23, 42, 46]. In a separate experiment, load-rates of 900 MPa/sec and 40 MPa/sec were applied to cartilage explants. Matrix damage increased at the high load-rate and caused substantial cell death around fissures and fractures while cell death was diffuse throughout the explants at the low rates, as seen before [47]. Recently, peak stress has been shown to not be an important cause of GAG loss from human cartilage in a model of 65% total strain at a relatively high strain rate of 400%/sec [48].

Mechanical injury has also been shown to stimulate chondrocytes to produce harmful reactive oxygen species (ROS) which depolymerize hyaluronic acid and kill chondrocytes [30, 49, 50]. After mechanical injury, cell death was abrogated by blocking NO synthesis, and since NO synthesis is unlikely in itself to cause cell death, it is likely that the high levels of NO in combination with ROS react to form toxic compounds like peroxynitrite [50-52].

2.3 Cytokine treatment Models of Injury

Interleukin-1 (IL-1), a pro-inflammatory cytokine considered to play a pivotal role in OA, is used often as a catabolic stimulant in *in vitro* studies [53, 54]. Studies have shown that IL-1 increases expression of matrix metalloproteinases (MMPs) and aggrecanases involved in cartilage matrix catabolism [32, 55] and mediates matrix degradation [56]. Treatment with IL-1α at concentrations of 10 ng/ml and TNF-α at 100 ng/ml had a significant increase in GAG loss compared to free swell conditions for immature bovine cartilage [27]. In both adult human knee and ankle, IL-1α had no affect on GAG loss after three days in culture. TNF-α also showed no

significant difference in GAG loss of human knee cartilage three days or seven days post TNF-α treatment [27].

Interleukin-6 (IL-6) is a cytokine involved in the regulation of inflammatory and immunological responses and has been shown to be produced by human chondrocytes [57]. The known inflammatory and destructive cytokines, IL-1 and TNF-α, have been shown to stimulate IL-6 production, which acts in an autocrine fashion to increase production of interleukin-6 receptor (IL-6R) [58]. Initially IL-6 and IL-6R were proposed as critical mediators in controlling the catabolic effects of pro-inflammatory cytokines like IL-1 and TNF-α [59]. Recently IL-6 and IL-6R have been shown to synergistically increase cartilage breakdown and collagenase production in combination with IL-1α [60], and have been shown to be upregulated in the synovial fluid in patients who have undergone anterior cruciate ligament injuries (32 weeks post-surgery) [61].

2.4 Synovium-Joint Capsule co-culture models of Injury

Co-culturing un-injured cartilage with damaged joint capsule (JC) *in vitro* has resulted in a decrease in cartilage biosynthesis rates [62, 63], as well as a loss of proteoglycan and collagen, as seen through histology staining [64]. GAG release from cartilage co-cultured with synovial or capsular tissue was not decreased with the inhibition of IL-1β, TNF-α, and ACITIC [65]. Under the same conditions of cartilage co-cultured with joint capsule, GAG loss was blocked by treatment with EDTA [65]. Interestingly, studies have shown that the presence of dead joint capsule as well as joint capsule with viable cells produce similar degradation effects. This

suggests that the factors contributed from the joint capsule need not be actively produced by cells within the joint capsule and may reside in the extracellular space or ECM of the tissue [66]. While the effects of JC co-culture appear to accelerate degradation, studies have also shown that synoviocytes from joint capsule tissue provide chondrocytes with protection against reactive oxygen species, which are known to induce membrane damage and lipid peroxidation [67].

Synovial cells from normal bovine or osteoarthritic human tissue have been shown to produce aggrecanase-2 (ADAMTS-5). Yet interestingly, aggrecanase activity or expression were not induced by IL-1α or retinoic acid [65, 68], two mediators that are known to induce aggrecanase expression in cartilage [69, 70]. The specific factor or factors from joint capsule and/or synovial cells responsible for increased cartilage degradation still remain to be determined.

2.5 Combination Models of Injury

An *in vitro* model of injury has been established in our lab incorporating the effects of a mechanical injury and injured joint capsule (JC) tissue [62, 66]. Mechanical injury of cartilage explants followed by co-culture with excised joint capsule results in further reduction of biosynthesis found after injury or co-culture alone [62]. Initial studies have also been performed on gene expression up to 24 hours post-injury [66]. These studies found there were significant changes in gene expression of key enzymes measured in response to joint capsule co-cultured with un-injured cartilage and mechanically-injured cartilage and co-culture with joint capsule.

Chapters 4 and 5 explore this model of injury in greater depth. Chapter 4 introduces a combination of growth factors and measures their effect on the combination of injury and co-culture. Chapter 5 applies this model to human tissue.

Recent studies showed treatment with cytokines (e.g., IL-1, TNF-α, IL-6 [27, 71]) following injurious compression *in vitro* increased GAG loss and decreased biosynthesis greater than either mechanical injury or cytokine treatment alone. Both bovine and human tissue exhibited a synergistic increase in proteoglycan loss in response to TNF-α or IL-1α treatment combined mechanical injury [27, 72]. Also, new findings have shown that with the addition of an anti-IL-6 Fab fragment, an inhibitor of IL-6, GAG loss was decreased when both mechanical injury and TNF-α were present [71]. This result supports the idea that IL-6 is either endogenously present in cartilage tissue and/or is produced by the chondrocytes in reaction to injury and/or TNF-α treatment. Recent data has shown that IL-6 is produced in response to TNF-α treatment in cartilage, supporting previously reported results [58, 72]. The combinatorial injury model of TNF-α, IL-6, IL-6R, and mechanical compression is further explored on a transcriptional level in Chapter 6.

Whether the combination of these factors and mechanical injury is simply a result of increased ability for factors to diffuse through the cartilage due to the micro-damage within the tissue associated with injurious load or is a result of the synergistic effect of a biological stimulus combined with a mechanical stimulus acting on the chondrocyte itself remains to be seen.

2.6 Conclusion

In vitro cartilage injury models have provided important insights into the basic understanding of the acute effects of injury and the development of posttraumatic OA *in vivo*. These models are the principle avenue for investigating specific components of *in vivo* joint trauma and allow the complex model of joint injury to be understood through compartmentalized studies. While many joint injury models exist, the four models discussed here are mechanical injury of cartilage, cytokine treatment, co-culture models that incubate adjacent tissue and cell types with cartilage, and combination models composed of the combination of mechanical injury, cytokine treatment, and co-culture. An understanding of how cartilage responds to complex models of injury (such as co-culture of mechanically injured cartilage with excised joint capsule) along with the characterization of cell and tissue mechanics and mechanisms of cartilage degradation will, aid clinicians and researchers in treating posttraumatic osteoarthritis.

2.7 References

1. *Arthritis: The Nation's Leading Cause of Disability.* 2007, http://www.cdc.gov.
2. Brandt, K.D., E.M. Braunstein, D.M. Visco, B. O'Connor, D. Heck, and M. Albrecht, *Anterior (cranial) cruciate ligament transection in the dog: a bona fide model of osteoarthritis, not merely of cartilage injury and repair.* J Rheumatol, 1991. **18**(3): p. 436-46.
3. Johnson, D.L., W.P. Urban, Jr., D.N. Caborn, W.J. Vanarthos, and C.S. Carlson, *Articular cartilage changes seen with magnetic resonance imaging-detected bone bruises associated with acute anterior cruciate ligament rupture.* Am J Sports Med, 1998. **26**(3): p. 409-14.
4. Lohmander, L.S., L.A. Hoerrner, L. Dahlberg, H. Roos, S. Bjornsson, and M.W. Lark, *Stromelysin, Tissue Inhibitor of Metalloproteinases and Proteoglycan Fragments in Human Knee-Joint Fluid after Injury.* J. Rheumatol., 1993. **20**(8): p. 1362-1368.
5. Lohmander, L.S., M. Ionescu, H. Jugessur, and A.R. Poole, *Changes in joint cartilage aggrecan after knee injury and in osteoarthritis.* Arthritis Rheum, 1999. **42**(3): p. 534-44.
6. Borrelli, J., Jr. and W.M. Ricci, *Acute effects of cartilage impact.* Clin Orthop Relat Res, 2004(423): p. 33-9.
7. Gelber, A.C., M.C. Hochberg, L.A. Mead, N.Y. Wang, F.M. Wigley, and M.J. Klag, *Joint injury in young adults and risk for subsequent knee and hip osteoarthritis.* Ann Intern Med, 2000. **133**(5): p. 321-8.
8. Roos, H., T. Adalberth, L. Dahlberg, and L.S. Lohmander, *Osteoarthritis of the knee after injury to the anterior cruciate ligament or meniscus: the influence of time and age.* Osteoarthritis Cartilage, 1995. **3**(4): p. 261-7.
9. Roos, H., M. Lauren, T. Adalberth, E.M. Roos, K. Jonsson, and L.S. Lohmander, *Knee osteoarthritis after meniscectomy: prevalence of radiographic changes after twenty-one years, compared with matched controls.* Arthritis Rheum, 1998. **41**(4): p. 687-93.
10. Davis, M.A., W.H. Ettinger, J.M. Neuhaus, S.A. Cho, and W.W. Hauck, *The association of knee injury and obesity with unilateral and bilateral osteoarthritis of the knee.* Am J Epidemiol, 1989. **130**(2): p. 278-88.
11. von Porat, A., E.M. Roos, and H. Roos, *High prevalence of osteoarthritis 14 years after an anterior cruciate ligament tear in male soccer players: a study of radiographic and patient relevant outcomes.* Ann Rheum Dis, 2004. **63**(3): p. 269-73.
12. Irie, K., E. Uchiyama, and H. Iwaso, *Intraarticular inflammatory cytokines in acute anterior cruciate ligament injured knee.* Knee, 2003. **10**(1): p. 93-6.
13. Cameron, M., A. Buchgraber, H. Passler, M. Vogt, E. Thonar, F. Fu, and C.H. Evans, *The natural history of the anterior cruciate ligament-deficient knee. Changes in synovial fluid cytokine and keratan sulfate concentrations.* Am J Sports Med, 1997. **25**(6): p. 751-4.
14. Marks, P.H. and M.L. Donaldson, *Inflammatory cytokine profiles associated with chondral damage in the anterior cruciate ligament-deficient knee.* Arthroscopy, 2005. **21**(11): p. 1342-7.
15. Aigner, T., B. Kurz, N. Fukui, and L. Sandell, *Roles of chondrocytes in the pathogenesis of osteoarthritis.* Curr Opin Rheumatol, 2002. **14**(5): p. 578-84.

16. Felson, D.T., R.C. Lawrence, P.A. Dieppe, R. Hirsch, C.G. Helmick, J.M. Jordan, R.S. Kington, N.E. Lane, M.C. Nevitt, Y. Zhang, M. Sowers, T. McAlindon, T.D. Spector, A.R. Poole, S.Z. Yanovski, G. Ateshian, L. Sharma, J.A. Buckwalter, K.D. Brandt, and J.F. Fries, *Osteoarthritis: new insights. Part 1: the disease and its risk factors.* Ann Intern Med, 2000. **133**(8): p. 635-46.
17. Glasson, S.S., R. Askew, B. Sheppard, B. Carito, T. Blanchet, H.L. Ma, C.R. Flannery, D. Peluso, K. Kanki, Z. Yang, M.K. Majumdar, and E.A. Morris, *Deletion of active ADAMTS5 prevents cartilage degradation in a murine model of osteoarthritis.* Nature, 2005. **434**(7033): p. 644-8.
18. Stanton, H., F.M. Rogerson, C.J. East, S.B. Golub, K.E. Lawlor, C.T. Meeker, C.B. Little, K. Last, P.J. Farmer, I.K. Campbell, A.M. Fourie, and A.J. Fosang, *ADAMTS5 is the major aggrecanase in mouse cartilage in vivo and in vitro.* Nature, 2005. **434**(7033): p. 648-52.
19. Borrelli, J., Jr., M.E. Burns, W.M. Ricci, and M.J. Silva, *A method for delivering variable impact stresses to the articular cartilage of rabbit knees.* J Orthop Trauma, 2002. **16**(3): p. 182-8.
20. Borrelli, J., Jr., K. Tinsley, W.M. Ricci, M. Burns, I.E. Karl, and R. Hotchkiss, *Induction of chondrocyte apoptosis following impact load.* J Orthop Trauma, 2003. **17**(9): p. 635-41.
21. Ewers, B.J., B.T. Weaver, E.T. Sevensma, and R.C. Haut, *Chronic changes in rabbit retro-patellar cartilage and subchondral bone after blunt impact loading of the patellofemoral joint.* J Orthop Res, 2002. **20**(3): p. 545-50.
22. Thibault, M., A.R. Poole, and M.D. Buschmann, *Cyclic compression of cartilage/bone explants in vitro leads to physical weakening, mechanical breakdown of collagen and release of matrix fragments.* J. Orthop. Res., 2002. **20**(6): p. 1265-1273.
23. Torzilli, P.A., R. Grigiene, J. Borrelli, Jr., and D.L. Helfet, *Effect of impact load on articular cartilage: cell metabolism and viability, and matrix water content.* J Biomech Eng, 1999. **121**(5): p. 433-41.
24. Kurz, B., M. Jin, P. Patwari, D.M. Cheng, M.W. Lark, and A.J. Grodzinsky, *Biosynthetic response and mechanical properties of articular cartilage after injurious compression.* J Orthop Res, 2001. **19**(6): p. 1140-6.
25. Chen, C.T., N. Burton-Wurster, G. Lust, R.A. Bank, and J.M. Tekoppele, *Compositional and metabolic changes in damaged cartilage are peak-stress, stress-rate, and loading-duration dependent.* J Orthop Res, 1999. **17**(6): p. 870-9.
26. Loening, A.M., I.E. James, M.E. Levenston, A.M. Badger, E.H. Frank, B. Kurz, M.E. Nuttall, H.H. Hung, S.M. Blake, A.J. Grodzinsky, and M.W. Lark, *Injurious mechanical compression of bovine articular cartilage induces chondrocyte apoptosis.* Arch Biochem Biophys, 2000. **381**(2): p. 205-12.
27. Patwari, P., M.N. Cook, M.A. DiMicco, S.M. Blake, I.E. James, S. Kumar, A.A. Cole, M.W. Lark, and A.J. Grodzinsky, *Proteoglycan degradation after injurious compression of bovine and human articular cartilage in vitro: Interaction with exogenous cytokines.* Arthritis Rheum., 2003. **48**(5): p. 1292-301.
28. DiMicco, M.A., P. Patwari, P.N. Siparsky, S. Kumar, M.A. Pratta, M.W. Lark, Y.J. Kim, and A.J. Grodzinsky, *Mechanisms and kinetics of glycosaminoglycan release following in vitro cartilage injury.* Arthritis and Rheumatism, 2004. **50**(3): p. 840-848.

29. D'Lima, D.D., S. Hashimoto, P.C. Chen, C.W. Colwell, Jr., and M.K. Lotz, *Human chondrocyte apoptosis in response to mechanical injury.* Osteoarthritis Cartilage, 2001. **9**(8): p. 712-9.
30. Kurz, B., A. Lemke, M. Kehn, C. Domm, P. Patwari, E.H. Frank, A.J. Grodzinsky, and M. Schunke, *Influence of tissue maturation and antioxidants on the apoptotic response of articular cartilage after injurious compression.* Arthritis Rheum, 2004. **50**(1): p. 123-30.
31. Chen, C.T., N. Burton-Wurster, C. Borden, K. Hueffer, S.E. Bloom, and G. Lust, *Chondrocyte necrosis and apoptosis in impact damaged articular cartilage.* J Orthop Res, 2001. **19**(4): p. 703-11.
32. Chan, P.S., A.E. Schlueter, P.M. Coussens, G.J. Rosa, R.C. Haut, and M.W. Orth, *Gene expression profile of mechanically impacted bovine articular cartilage explants.* J Orthop Res, 2005. **23**(5): p. 1146-51.
33. Lee, J.H., J.B. Fitzgerald, M.A. Dimicco, and A.J. Grodzinsky, *Mechanical injury of cartilage explants causes specific time-dependent changes in chondrocyte gene expression.* Arthritis Rheum, 2005. **52**(8): p. 2386-95.
34. Adams, M.A., *The mechanical environment of chondrocytes in articular cartilage.* Biorheology, 2006. **43**(3-4): p. 537-45.
35. Jeffry, J., L. Thomson, and R. Aspden, *Matrix damage and chondrocyte viability following a single impact load on articular cartilage.* Arch Biochem Biophys, 1995. **322**: p. 87-96.
36. Bowker, R.M., P.J. Atkinson, T.S. Atkinson, and R.C. Haut, *Effect of contact stress in bones of the distal interphalangeal joint on microscopic changes in articular cartilage and ligaments.* Am J Vet Res, 2001. **62**(3): p. 414-24.
37. Atkinson, P.J., B.J. Ewers, and R.C. Haut, *Blunt injuries to the patellofemoral joint resulting from transarticular loading are influenced by impactor energy and mass.* J Biomech Eng, 2001. **123**(3): p. 293-5.
38. Aspden, R.M., J.E. Jeffrey, and L.V. Burgin, *Impact loading of articular cartilage.* Osteoarthritis Cartilage, 2002. **10**(7): p. 588-9; author reply 590.
39. Newberry, W.N., J.J. Garcia, C.D. Mackenzie, C.E. Decamp, and R.C. Haut, *Analysis of acute mechanical insult in an animal model of post-traumatic osteoarthrosis.* J Biomech Eng, 1998. **120**(6): p. 704-9.
40. Clements, K.M., Z.C. Bee, G.V. Crossingham, M.A. Adams, and M. Sharif, *How severe must repetitive loading be to kill chondrocytes in articular cartilage?* Osteoarthritis Cartilage, 2001. **9**(5): p. 499-507.
41. D'Lima, D.D., S. Hashimoto, P.C. Chen, M.K. Lotz, and C.W. Colwell, Jr., *Cartilage injury induces chondrocyte apoptosis.* J Bone Joint Surg Am, 2001. **83-A Suppl 2**(Pt 1): p. 19-21.
42. Quinn, T., R. Allen, B. Schalet, P. Perumbuli, and E. Hunziker, *Matrix and cell injury due to sub-impact loading of adult bovine articular cartilage explants: effects of strain rate and peak stress.* J Orthop Res, 2001. **19**: p. 242-249.
43. Bae, W.C., B.L. Schumacher, and R.L. Sah, *Indentation probing of human articular cartilage: Effect on chondrocyte viability.* Osteoarthritis Cartilage, 2007. **15**(1): p. 9-18.
44. Morel, V., C. Berutto, and T.M. Quinn, *Effects of damage in the articular surface on the cartilage response to injurious compression in vitro.* J Biomech, 2006. **39**(5): p. 924-30.
45. Burgin, L.V. and R.M. Aspden, *Impact testing to determine the mechanical properties of articular cartilage in isolation and on bone.* J Mater Sci Mater Med, 2007.

46. Krueger, J.A., P. Thisse, B.J. Ewers, D. Dvoracek-Driksna, M.W. Orth, and R.C. Haut, *The extent and distribution of cell death and matrix damage in impacted chondral explants varies with the presence of underlying bone.* J Biomech Eng, 2003. **125**(1): p. 114-9.
47. Ewers, B.J., D. Dvoracek-Driksna, M.W. Orth, and R.C. Haut, *The extent of matrix damage and chondrocyte death in mechanically traumatized articular cartilage explants depends on rate of loading.* J Orthop Res, 2001. **19**(5): p. 779-84.
48. Patwari, P., D.M. Cheng, A.A. Cole, K.E. Kuettner, and A.J. Grodzinsky, *Analysis of the relationship between peak stress and proteoglycan loss following injurious compression of human post-mortem knee and ankle cartilage.* Biomech Model Mechanobiol, 2007. **6**(1-2): p. 83-9.
49. Yamazaki, K., K. Fukuda, M. Matsukawa, F. Hara, T. Matsushita, N. Yamamoto, K. Yoshida, H. Munakata, and C. Hamanishi, *Cyclic tensile stretch loaded on bovine chondrocytes causes depolymerization of hyaluronan: involvement of reactive oxygen species.* Arthritis Rheum, 2003. **48**(11): p. 3151-8.
50. Green, D.M., P.C. Noble, J.S. Ahuero, and H.H. Birdsall, *Cellular events leading to chondrocyte death after cartilage impact injury.* Arthritis Rheum, 2006. **54**(5): p. 1509-17.
51. Del Carlo, M., Jr. and R.F. Loeser, *Nitric oxide-mediated chondrocyte cell death requires the generation of additional reactive oxygen species.* Arthritis Rheum, 2002. **46**(2): p. 394-403.
52. Loeser, R.F., *Molecular mechanisms of cartilage destruction: mechanics, inflammatory mediators, and aging collide.* Arthritis Rheum, 2006. **54**(5): p. 1357-60.
53. Dingle, J.T., D.P. Page Thomas, and B. Hazleman, *The role of cytokines in arthritic diseases: in vitro and in vivo measurements of cartilage degradation.* Int J Tissue React, 1987. **9**(4): p. 349-54.
54. Smith, R.J., N.A. Rohloff, L.M. Sam, J.M. Justen, M.R. Deibel, and J.C. Cornette, *Recombinant human interleukin-1 alpha and recombinant human interleukin-1 beta stimulate cartilage matrix degradation and inhibit glycosaminoglycan synthesis.* Inflammation, 1989. **13**(4): p. 367-82.
55. Koshy, P.J., C.J. Lundy, A.D. Rowan, S. Porter, D.R. Edwards, A. Hogan, I.M. Clark, and T.E. Cawston, *The modulation of matrix metalloproteinase and ADAM gene expression in human chondrocytes by interleukin-1 and oncostatin M: a time-course study using real-time quantitative reverse transcription-polymerase chain reaction.* Arthritis Rheum, 2002. **46**(4): p. 961-7.
56. L'Hermette, M.F., C. Tourny-Chollet, G. Polle, and F.H. Dujardin, *Articular cartilage, degenerative process, and repair: current progress.* Int J Sports Med, 2006. **27**(9): p. 738-44.
57. Guerne, P.A., D.A. Carson, and M. Lotz, *IL-6 production by human articular chondrocytes. Modulation of its synthesis by cytokines, growth factors, and hormones in vitro.* J Immunol, 1990. **144**(2): p. 499-505.
58. Aida, Y., M. Maeno, N. Suzuki, A. Namba, M. Motohashi, M. Matsumoto, M. Makimura, and H. Matsumura, *The effect of IL-1beta on the expression of inflammatory cytokines and their receptors in human chondrocytes.* Life Sci, 2006. **79**(8): p. 764-71.
59. Silacci, P., J.M. Dayer, A. Desgeorges, R. Peter, C. Manueddu, and P.A. Guerne, *Interleukin (IL)-6 and its soluble receptor induce TIMP-1 expression in synoviocytes and*

chondrocytes, and block IL-1-induced collagenolytic activity. J Biol Chem, 1998. **273**(22): p. 13625-9.

60. Rowan, A.D., P.J. Koshy, W.D. Shingleton, B.A. Degnan, J.K. Heath, A.B. Vernallis, J.R. Spaull, P.F. Life, K. Hudson, and T.E. Cawston, *Synergistic effects of glycoprotein 130 binding cytokines in combination with interleukin-1 on cartilage collagen breakdown.* Arthritis Rheum, 2001. **44**(7): p. 1620-32.
61. Higuchi, H., K. Shirakura, M. Kimura, M. Terauchi, T. Shinozaki, H. Watanabe, and K. Takagishi, *Changes in biochemical parameters after anterior cruciate ligament injury.* Int Orthop, 2006. **30**(1): p. 43-7.
62. Patwari, P., J. Fay, M.N. Cook, A.M. Badger, A.J. Kerin, M.W. Lark, and A.J. Grodzinsky, *In vitro models for investigation of the effects of acute mechanical injury on cartilage.* Clin Orthop Relat Res, 2001(391 Suppl): p. S61-71.
63. Jubb, R.W. and H.B. Fell, *The effect of synovial tissue on the synthesis of proteoglycan by the articular cartilage of young pigs.* Arthritis Rheum, 1980. **23**(5): p. 545-55.
64. Fell, H.B. and R.W. Jubb, *The effect of synovial tissue on the breakdown of articular cartilage in organ culture.* Arthritis Rheum, 1977. **20**(7): p. 1359-71.
65. Vankemmelbeke, M.N., M.Z. Ilic, C.J. Handley, C.G. Knight, and D.J. Buttle, *Coincubation of bovine synovial or capsular tissue with cartilage generates a soluble "Aggrecanase" activity.* Biochem Biophys Res Commun, 1999. **255**(3): p. 686-91.
66. Lee, J.H., *Chondrocyte response to in vitro mechanical injury and co-culture with joint capsule tissue*, in *Biological Engineering Division.* 2005, Massachusetts Institute of Technology: Cambridge, MA. p. 162.
67. Kurz, B., J. Steinhagen, and M. Schunke, *Articular chondrocytes and synoviocytes in a co-culture system: influence on reactive oxygen species-induced cytotoxicity and lipid peroxidation.* Cell Tissue Res, 1999. **296**(3): p. 555-63.
68. Vankemmelbeke, M.N., I. Holen, A.G. Wilson, M.Z. Ilic, C.J. Handley, G.S. Kelner, M. Clark, C. Liu, R.A. Maki, D. Burnett, and D.J. Buttle, *Expression and activity of ADAMTS-5 in synovium.* Eur J Biochem, 2001. **268**(5): p. 1259-68.
69. Arner, E.C., C.E. Hughes, C.P. Decicco, B. Caterson, and M.D. Tortorella, *Cytokine-induced cartilage proteoglycan degradation is mediated by aggrecanase.* Osteoarthritis Cartilage, 1998. **6**(3): p. 214-28.
70. Flannery, C.R., C.B. Little, C.E. Hughes, and B. Caterson, *Expression of ADAMTS homologues in articular cartilage.* Biochem Biophys Res Commun, 1999. **260**(2): p. 318-22.
71. Sui, Y., X.-Y. Song, J. Lee, M. DiMicco, S. Blake, H.-H. Hung, I. James, M. Lark, and A. Grodzinsky. *Mechanical Injury Potentiates the Combined Effects of TNF-α and IL-6/SIL-6R on Proteoglycan Catabolism in Bovine Cartilage.* in *ORS.* 2007. San Diego, CA.
72. Sui, Y., J. Lee, C. Wheeler, H. Hung, A. Plaas, S. Blake, and A. Grodzinsky. *Proteoglycan Catabolism in Response to TNF-A, IL-6/SIL-6R, and Mechanical Injury in Bovine and Human Articular Cartilage.* in *ORS.* 2008. San Francisco, CA.

Chapter 3

Transcriptional Effects of Combined Mechanical Compression and IGF-1 Stimulation on Bovine Cartilage Explants

* This chapter is in preparation for submission to the Journal of Orthopaedics Research (Wheeler, Cameron A and Grodzinsky, Alan J.)

3.1 Abstract

***Introduction*:** Insulin-like growth factor-1 (IGF-1) is a potent anabolic factor capable of endocrine and paracrine/autocrine signaling. Numerous studies have shown that chondrocytes produce this important growth factor, and that IGF-1 can stimulate ECM biosynthesis by chondrocytes in native cartilage and tissue engineered constructs. Previous studies have demonstrated that mechanical compression can regulate the action of IGF-1 on chondrocyte biosynthesis in intact tissue; when applied simultaneously, these stimuli act by distinct cell activation pathways. Our objectives were to elucidate the extent and kinetics of the chondrocyte transcriptional response to combined IGF-1 and static compression in cartilage explants.

Methods: Cartilage explants were harvested as performed previously in our lab. Cartilage plugs were placed in 50% compression and 0% compression with or without 300 ng/ml of IGF-1. RNA was obtained and measured by real-time PCR for 2, 8, 24, 32, 48 hours after treatment and compression.

Results and Discussion: Transcript levels in response to compression alone agreed with previously published data. Key matrix molecules, aggrecan and collagen II, responded positively to the addition of IGF-1 without compression, but this effect was abrogated when compression was applied in combination with IGF-1 treatment. Clustering analysis revealed five distinct groups. TIMP-3 and ADAMTS-5, MMP-1 and IGF-2, and IGF-1 and Collagen II, were all robustly co-expressed under all conditions tested. These co-expressed molecules suggest inherent regulation and positive feedback in chondrocyte gene expression. In comparing gene expression levels to previously measured aggrecan biosynthesis levels, aggrecan synthesis is shown to be transcriptionally regulated by IGF-1, whereas inhibition of aggrecan synthesis by compression is not transcriptionally regulated.

Conclusion: Many genes measured are responsive the effects of IGF-1 under 0% compression and 50% compression. Clustering analysis revealed strong co-expressed gene pairings. IGF-1 stimulates aggrecan biosynthesis in a transcriptionally regulated manner, whereas compression inhibits aggrecan synthesis in a manner not regulated by transcriptional activity.

3.2 Introduction

Insulin-like growth factor-1 (IGF-1) is a 7.6 kDa, 8.5 PI, potent anabolic factor capable of endocrine and paracrine/autocrine signaling. While IGF-1 is primarily produced in the liver and transported throughout the body via the blood stream, numerous studies have shown that chondrocytes produce this important growth factor, and that IGF-1 can stimulate ECM biosynthesis by chondrocytes in native cartilage and tissue engineered constructs. The use of growth factors as therapeutics to reverse or inhibit cartilage degradation has been an underlying focus in cartilage research. The avascular, alymphatic, and aneural nature of cartilage suggests that the growth factor be administered though means of local delivery. Local delivery is complicated due to joint motion and cartilage structure which affects special and temporal diffusion rates.

To investigate the effects of exogenous IGF-1, many studies have examined how chondrocytes respond at the protein level as well as the gene transcript level. General protein levels have been measured using conventional radiolabel incorporation (35S, 3H), and show that chondrocytes respond in a dose dependent manner to IGF-1 [1-6]. The environment the chondrocytes are cultured in varies (explants, gels, monolayer), but generally chondrocyte biosynthesis levels are increased from 150% [4] to 2-6 fold control levels [3, 6-8]. Researchers have also examined particular proteins using western blot analysis. For example, MMP-13 was found to be suppressed in response to IGF-1 treatment [9]. When examining the transcript or gene levels in response to IGF-1, researchers have focused on specific molecules using real-time PCR and reverse transcription PCR. Type II collagen was shown in multiple studies to be significantly upregulated by IGF-1 [3, 10-12]. Aggrecan transcripts have shown no significant

increase [3, 4] or slight upregulation [12] with the addition of IGF-1 in the first 48 hours of IGF-1 treatment, yet were significant upregulation (130%) when treated for 1-3 weeks [10]. IGF-1 transcript levels were shown to peak at 24 hours after IGF-1 treatment, suggesting that IGF-1 has an autocrine response [1]. Sox-9, a transcription factor was also shown to have no significant response to IGF-1 [11].

Chondrocytes have been shown to be responsive to mechanical compression on both the protein and gene transcript levels. Static compression in vitro has been shown to decrease protein biosynthesis levels of type II collagen and proteoglycans in a dose dependent manner [5, 13]. In alginate and type I collagen gels seeded with chondrocytes, 50% static compression was shown to decrease radiolabel incorporation by nearly half in comparison to non-compressed controls [14, 15]. Similar findings have been shown in cartilage explants with proteoglycan and type II collagen synthesis decreasing within 1-2 hours of loading and remaining suppressed for the loading period (24 hrs) [16, 17]. When transcript levels were examined in response to static loading, type II collagen and aggrecan were shown to initially peak anywhere from 1 to 4 hours after compression, followed by a decrease to unaffected level of gene expression [13, 15, 18, 19]. Fitzgerald et al. have investigated 28 different ECM related molecules including matrix proteinases, tissue inhibitors of matrix metalloproteinases (TIMPs), growth factors, cytokines, and structural ECM molecules, under static compression for a 24 hour period and reported 4 distinct patterns associate with gene expression [19].

Bonassar et al. have examined the combination of IGF-1 treatment with static compression at a protein level and found when cartilage explants were treated with IGF-1 under 0% compression

(cut thickness) a 2-3 fold increase was found over 48 hour [5]. Under static compression biosynthesis was decrease by 50% compared to non-compressed conditions. When compressed explants were treated with IGF-1, biosynthesis rates significantly increased, returning to levels comparable to non-compressed, non-treated explants. Thus compression diminished the effects of IGF-1, but did not altogether eliminate them. IGF-1 was still able to upregulate or rescues the synthesis rate of statically compressed cartilage explants.

Chondrocyte gene expression under a combination of IGF-1 treatment and static compression have not been examined thoroughly. Our objectives were to elucidate the extent and kinetics of the chondrocyte transcriptional response to combined IGF-1 and static compression in cartilage explants.

3.3 Methods

Cartilage Harvest, Mechanical Loading, and Growth Factor Treatment: Cartilage-bone plugs were harvested from the patello-femoral groove of 1-2 week old calves. Cartilage disks (1mm thick X 3mm diameter) were cored and punch from the middle zone as described previously [20] and equilibrated for two days under free-swell conditions in the presence of serum-free feeding medium consisting of high glucose Dulbecco's modified essential medium supplemented with 10 nM Hepes Buffer, 0.1 mM nonessential amino acids, 20 μg/ml ascorbate, 100 units/ml penicillin, 100 μg/ml streptomycin, and 0.25 μg/ml amphoericin B. Five anatomically matched disks were separated for each time point (Figure 3.1), and placed in polysulfone loading chambers. Each time point consisted of four separate experiments. With cartilage disks matched for time, 8 disks were allocated to 0% compression (i.e., compressed to 1-mm cut thickness from free swelling), 50% compression, 0% compression + 300 ng/ml IGF-1, and 50% compression + 300 ng/ml IGF-1, the IGF-1 concentration found previously to maximally stimulate similar free-swelling calf cartilage explants [5]. At time zero, all chambers were slowly compressed to specified strains over a 3 minute period to avoid injurious effects of high strain rates. These strains were maintained for each of the four conditions for 2, 8, 24, 32, and 48 hours (Figure 3.1). Upon completion of loading time, disks were promptly removed, flash frozen in liquid nitrogen, and stored at -80° C.

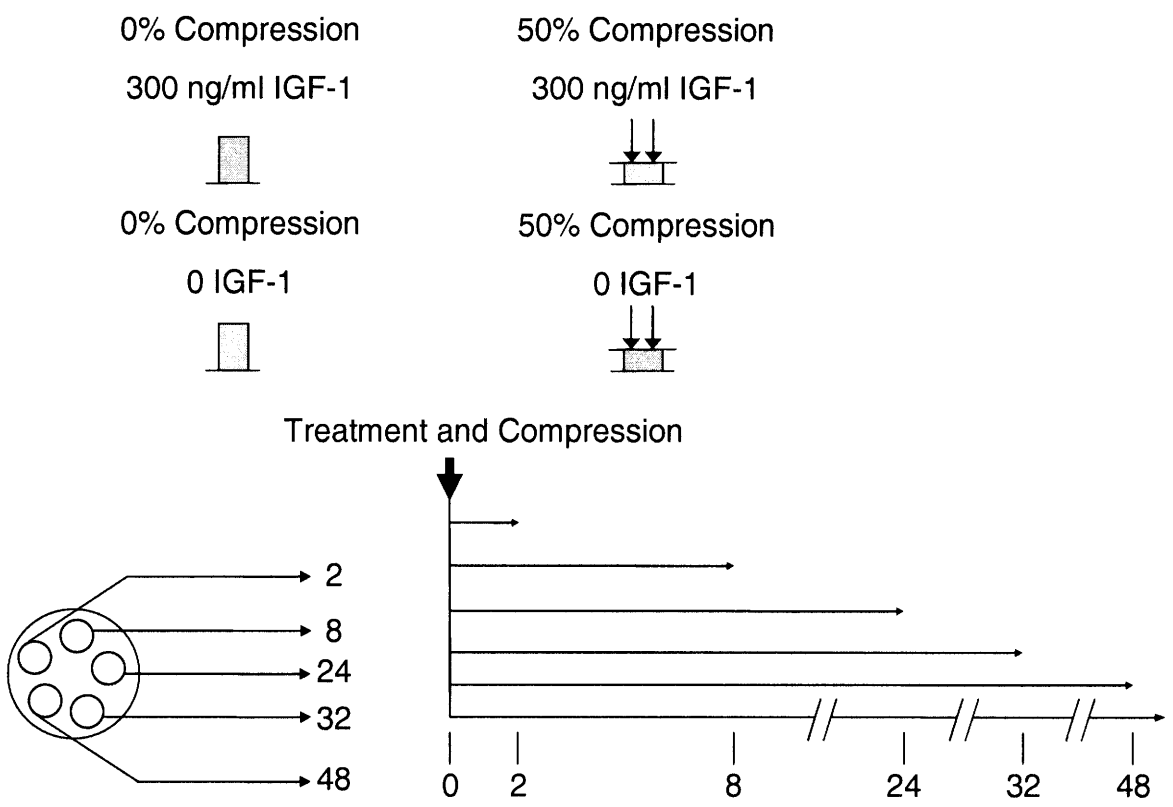

Figure 3.1. A schematic of the four conditions measured. 5 plugs were punched for each time point and matched for time. IGF-1 treatment and static compression were applied at time 0, and plugs were flash frozen at 2, 8, 24, 32, and 48 hours.

RNA Extraction and Quantization, Primer Design, and Real-Time PCR: 8 disks for each time point and condition were taken from -80° C freezer and pulverized. In order to prevent RNA degradation, the pulverizing apparatus was constantly cooled using liquid nitrogen. Once samples had been pulverized, Trizol (sigma, St. Louis) was added and homogenized to thoroughly break down the tissue. After chloroform was added, the mixture was transferred to pre-spun phase gel tubes, and spun at 13,000 rpm for 10 minutes at 4° C. Supernatant was removed, and RNA was extracted using Qiagen RNAeasy mini kit protocol with recommended DNase digest (Qiagen). RNA was stored in 50 μl of RNase free water under -80° C conditions.

RNA quality and amount was quantified by using NanoDrop ND-1000 spectrophotometer. According to RNA measurements, 1μg of RNA was reverse transcribed using Applied Biosystems reagents as previously described [21]. Forward and reverse primers for 24 relent genes (Table 3.1) were designed based on bovine genomic sequences and standard curves were calculated as previously described [19]. Once cDNA was obtained, Real-Time PCR was performed using MJResearch Opticon2 instrument and SYBR Green Master Mix (SGMM, Applied Biosystems). SGMM was combined with RNase free water and cDNA and aliquated into MJResearch 96-well plate. Using a multi-pipette, a premixed solution of forward and reverse primer for 24 different genes was added to each well. Measured threshold values (Ct) were converted to RNA copy number according to previously calculated standard curves.

Matrix Molecules	Proteases	Protease inhibitors	Cytokines	Growth Factors	Transcription Factors	Stress Activated Genes	Housekeeping Gene
Type II Collagen	MMP1	Timp-1	TNF-a	IGF-1	c-Jun	HSP90	18s
Aggrecan	MMP3	Timp-2	IL-1	IGF-2	c-Fos	Txnip	
Link Protein	MMP13	Timp-3	IL-4	TGF-B	Sox-9		
Fibronectin	ADAMTS-5		IL-6				

Table 3.1. 24 Cartilage Relevant Genes. Primers were designed Primer3 software (www.genome.wi.mit.edu/cgi-bin/primer/primer3www.cgi). Standard dilutions were used to calculate relative mRNA copy number.

Data Normalization and Statistical Analysis: Under each loading condition and time point, each gene RNA copy number was normalized to the 18s housekeeping gene from that same condition and time point [22]. To examine the time course of gene expression, 0% compression + IGF-1, 50% compression, and 50% compression + IGF-1 were normalized to 0% compression levels. Thus, if a gene expression value was below or above 1, it represented a decrease or increase of gene expression respectively compared to 0% compression. Expression levels due to experimental error were removed. To assign statistical significance to expression

levels, a non-parametric test was used to ensure unbiased results by avoiding the assumption of a parameter based distribution. The Wilcoxon sign ranked test was used to judge significance which incorporates the amount of data in the significance statistic. Significance was assigned if the Wilcoxon sign ranked test statistic produced a p-value less than 0.07. The minimum p-value using the Wilcoxon sign ranked test is 0.068 due to the fact that there are only four replicates. Thus, significance of 0.07 was chosen because with this non-parametric test and amount of data, 0.05 cannot be obtained.

Clustering Analysis: In order to understand general transcriptional patterns in the data, clustering analysis was performed on all normalized conditions (0% compression + IGF-1, 50% compression, and 50% compression + IGF-1) and time points (2, 8, 24, 32, 48 hours) over 23 genes. This resulted in a 15 x 23 matrix which was standardized by expression amplitude as described previously [19], in order to accentuate gene expression patterns as appose to expression magnitudes. The 15 gene expression array vectors were clustered using k-means clustering. Principle component analysis (PCA) was used to determine the components that contain the greatest variance in the expression data[23, 24]. Once the 15 principle components had been calculated, the k-means clustering algorithm was applied to the 15 principle components and clustered into k groups. The average and variance of each projected coordinate group was calculated to compose a group centroid. Centroid vectors were formed by combining the three main principal components weighted by their projected centroid coordinate. The uniqueness of each Group's expression patterns were evaluated by the Wilcoxon sign ranked test.

3.4 Results

Effects of static compression: Cartilage disks were subject to 2, 8, 24, 32, and 48 hours of compression applied in a ramp and hold fashion. The disks experience a peak stress when the compression is applied, followed by a slow stress relaxation due to the poroelastic properties of cartilage. The five time points were chosen to capture the kinetics of gene expression in repose to the changes in stress. Twenty-four different genes were measured at each one of the five time points and were normalized to 18s, a housekeeping gene, and 0% compression with no added IGF-1 was used as a control. 8 of the 23 genes measured were up-regulated for 3 or more of the time points examined. These included ADAM-TS5, MMP-13, MMP-3, TGF-β, c-Fos, c-Jun, and Sox-9 (Figure 3.2, Appendix 3.8.1). Matrix metalloproteinase- 3 (MMP-3) was significantly up-regulated at 8, 24, 32, and 48 hours with a peak expression level of 30-fold compared to control at 32 hours (Figure 3.2A). ADAM-TS5 and MMP-13 displayed a transient increase in expression levels peaking at 48 hours with >6-fold and >17-fold up-regulation respectively (Figure 3.2B, Appendix 3.8.1). TGF-β was consistently up-regulated 2.5-fold from 8 hours to 32 hours (Figure 3.2D). Supporting previously reported data[19], c-Fos and c-Jun were significantly up-regulated in response to 50% static compression at all time points measured (Appendix 3.8.1). Interestingly, c-Fos, c-Jun and Sox-9 were all maximized at 8 hours (23-fold, 30-fold, and 6.8-fold respectively) (Appendix 3.8.1). Displaying a transient decrease, IGF-1 was the only gene measured that showed a significant down-regulation in the presence of 50% strain for at least 3 of the measured time points. IGF-1 was significantly down-regulated by 50% at 24 hours and up to 70% at 48 hours (Appendix 3.8.1).

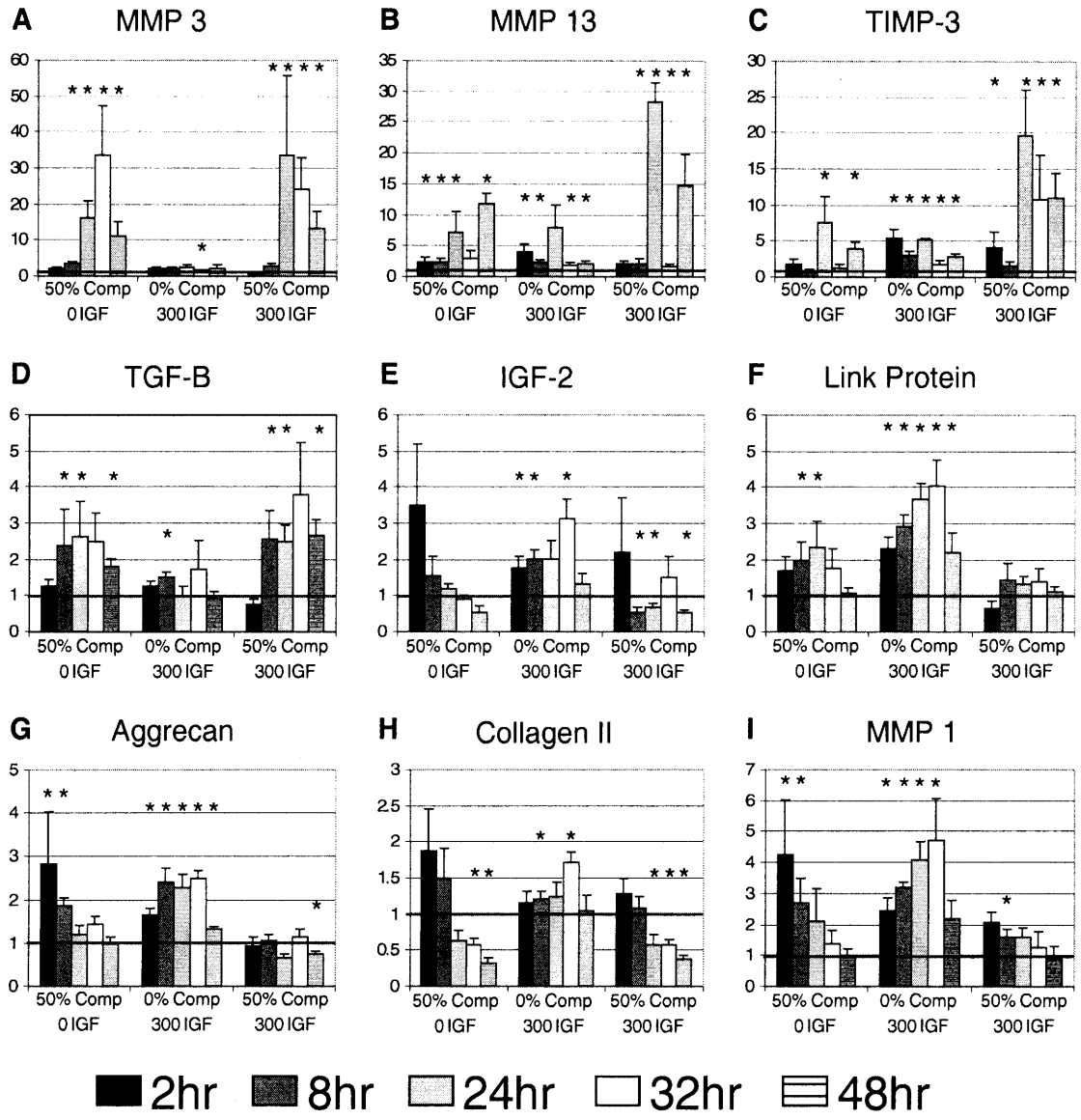

Figure 3.2. Gene expression of proteinases, growth factors, and ECM molecules. 8 cartilage disks were pooled for each time point for each experiment. All genes were normalized to 18s and plotted relative to 0% compression 0 IGF-1. Significance was measured by the Wilcoxon sign ranked test compared to 0% compression 0 IGF-1 (* p-value <0.07). Mean ± SE (n=4)

Effects of IGF-1: To examine the effect of IGF-1 on cartilage explants, disks were incubated for 2, 8, 24, 32, and 48 hours with 300 ng/mL IGF-1 under 0% compression. 10 of the 23 genes were upregulated with the treatment of IGF-1. IGF-1 up-regulated for three or more

time points, MMP-13, MMP-1, TNF-α, and IL-1β, which traditionally are thought to play catabolic roles in cartilage. MMP-13, TNF-α, and IL-1β were significantly up-regulated and peaked at 24 hours to the level of 8-fold, 2.5-fold, and 2.75-fold respectively (Figure 3.2B and Appendix 3.8.1). MMP-1 and IGF2 were transiently up-regulated to a significant level until a 32 hour peak (4.75-fold and 3-fold respectively), after which expression levels returned to control (Figure 3.2I, 3.2E). Link and Aggrecan were also transiently up-regulated with a peak of 32 hours (4-fold and 2.5-fold respectively), but expression levels at 48 hours were still significantly above control (Figure 3.2F, 3.2G). As in 50% static compression, Sox-9 was significantly up-regulated at 8 hours to a comparable level of 6.3-fold (Appendix 3.8.1). TIMP-3 and HSP90 were significantly upregulated at all time points and both displayed an initial peak of expression (5-fold and 3-fold respectively), followed by a transient decrease of expression over time (Figure 3.2C, Appendix 3.8.1). No genes measured were significantly down-regulated by the treatment of IGF-1.

Effects of IGF-1 and static compression: Combining the treatment of 300 ng/mL of IGF-1 and static compression to a level of 50% strain, 11 of the 23 genes were significantly different than the 0% control for 3 or more time points. MMP-13, MMP-3, TGF-β, c-Fos, c-Jun, TIMP-3, and HSP90 were significantly up-regulated in at least 3 of the measured time points. MMP-13 and MMP-3 were significantly upregulated 4 out of the 5 time points and had peak values of 28-fold and 33-fold respectively at 24 hours (Figure 3.2B, 3.2A). TGF-β and HSP90 were transiently upregulated to a peak level of 3.8-fold and 2.25-fold respectively, at 32 hours (Figure 3.2D, Appendix 3.8.1). c-Fos and c-Jun were again significantly up-regulated for all time points with expression peaks at 24 and 8 hours (Appendix 3.8.1). The peak value of c-Fos, 22-fold, was

similar to the expression levels found in 50% static compression alone. Alternatively, the peak value of c-Jun had decreased from 30-fold under 50% static compression to 16-fold under 50% static compression with IGF-1. TIMP-3 showed a slow increase of expression which peaked at 24 hours to a level of 19-fold, followed by an up-regulated level of 10-fold (Figure 3.2C). Col2, IGF-2, TIMP-2, and TXNIP were significantly down-regulated for 3 or more time points measured. IGF-2 and TXNIP showed a transient decrease of expression over time and bottomed out at 48 hours decreasing 45% and 52% expression below control (Figure 3.2E, Appendix 3.8.1). Col2 and TIMP-2 were drastically decreased under 50% static compression with IGF-1. Col2 was transiently down-regulated, decreasing expression levels by 43% at 24 hours, to 62% at 48 hours (Figure 3.2H). TIMP-2 was also transiently down-regulated, decreasing expression levels by 50% at 24 hours and 92% at 48 hours (Appendix 3.8.1).

Comparing effects of IGF-1 under 0% and 50% compression: To elucidate the different effects of IGF-1, the effects of IGF-1 were isolated by normalized gene expression to like loading conditions. 50% static compression with IGF-1 was normalized by 50% static compression, and 0% static compression with IGF-1 was normalized to 0% static compression. When examining the effects of IGF-1 under non-loaded conditions (0% static compression), 9 of the 23 genes were significantly altered for 3 or more time points by the addition of IGF-1. Under loading conditions (50% static compression), 4 of the 23 genes were significantly altered for 3 or more time points by the addition of IGF-1 (Appendix 3.8.2). Of the significantly affected genes, aggrecan, IGF-2, and TIMP-3 were significantly affected by IGF-1 in both loaded and un-loaded conditions (Figure 3.3). Aggrecan, IGF-2, and Link were all up-regulated when treated with IGF-1 under un-loaded conditions, and down-regulated when treated with IGF-1 under loaded

conditions (Figure 3.3A, 3.3B, 3.3C). Aggrecan in particular was significantly up-regulated for all time points by IGF-1 under un-loaded conditions, and significantly down-regulated for all time points by IGF-1 under loaded conditions (Figure 3.3A). In contrast, TIMP-3 was up-regulated significantly under both un-loaded and loaded conditions (Figure 3.3D). MMP-1 was up-regulated significantly with treatment of IGF-1 under un-loaded conditions, but was unaffected by the treatment of IGF-1 when loading conditions were present (Figure 3.3E).

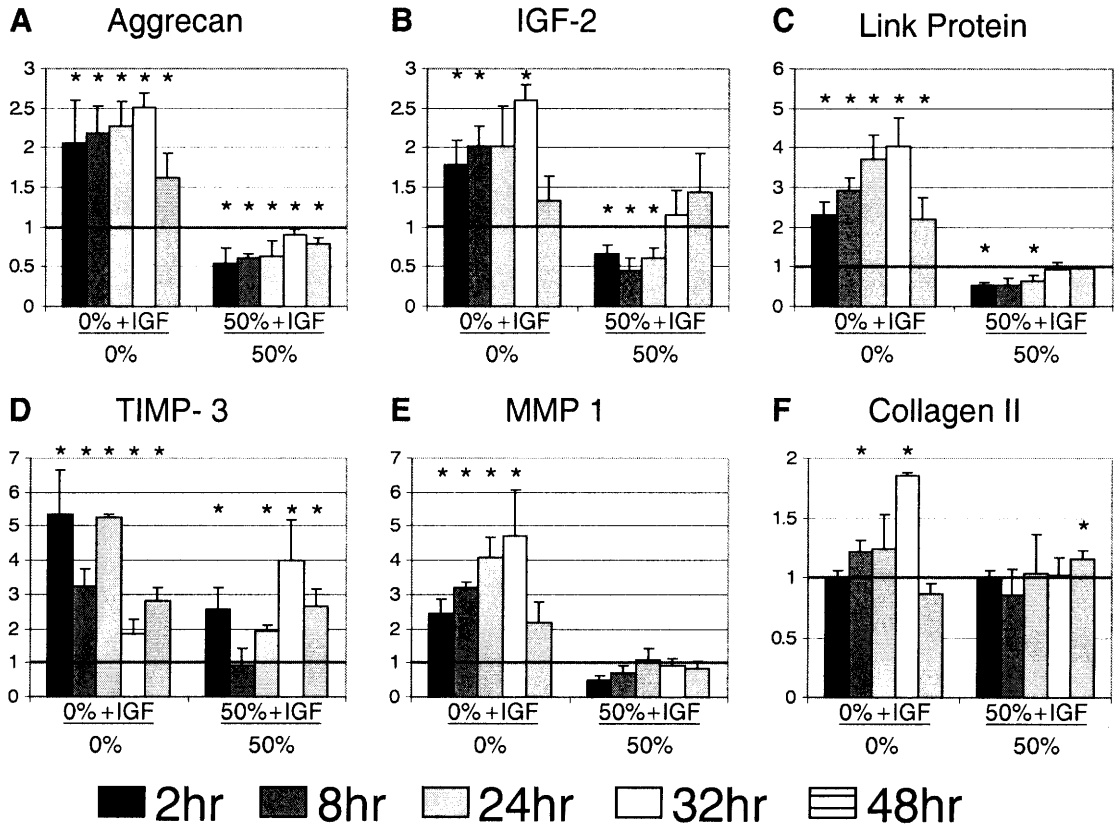

Figure 3.3. Effects of IGF-1. Gene expression was plotted normalized to like loading condition in order to elucidate the effects of IGF-1 under compression or non-compression. Aggrecan (A) and Link (C) respond to IGF-1 in a compression dependent manner, while TIMP-3 (D) and Collagen II (F) respond to IGF-1 in a compression independent manner. Significance was measured by the Wilcoxon sign ranked test compared to like compression 0 IGF-1. (* p-value <0.07). Mean ± SE (n=4)

Expression Trends and Groupings: After normalization of the data, using principle component analysis (PCA), the 15 dimensional space was reduced to a three dimensional space, by calculating three eigenvectors or principle components that represent 80% of the variance in the data. With three principle components, each standardized gene was projected in to the principle component space and can be visualized as shown in figure 3.4. All 15 dimensions of each gene were used in the k-means clustering technique to ensure that smaller gene variations were represented in the grouping. After dividing the genes into 2 to 8 cluster groups and visually comparing the distinctness of the groups, 5 groups appeared to be an adequate number of groupings (Figure 3.4). These 5 groups contained 4 to 7 genes as shown in Table 3.3A. The mean expression level is represented by a centroid (Figure 3.4) and the mean expression profile of the 5 groups is shown in Figure 3.5. The centroids were shown to be significantly separated by taking the euclidean distance between centroids and calculating the gene to centroid variance[22]. (Table 3.2).

P-value of Centroid Separation	Centroid 1	Centroid 2	Centroid 3	Centroid 4
Centroid 2	0.032			
Centroid 3	0.017	0.034		
Centroid 4	0.007	0.073	0.016	
Centroid 5	0.001	0.015	0.006	0.042

Table 3.2. P-value of Centroid Profile Separation. P-values were obtained through student T-test, comparing centroid to centroid Euclidean distance. Degrees of freedom were taken as the number of genes in each group.

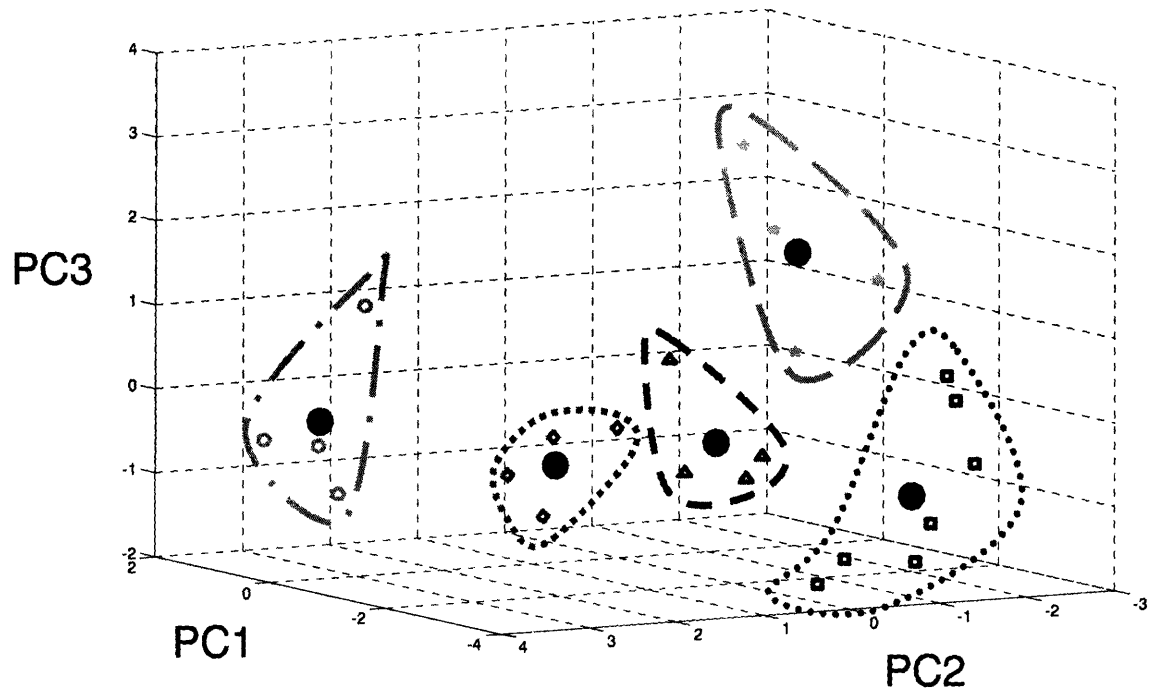

Figure 3.4. Standardized gene expression visualized in principle component space. Principle component 1, 2, and 3 represent 80% of the variance in the data. Genes were allocated to one of five distinct groups by way of k-means clustering. Large solid black circles denote the centroid of the corresponding group.

Group 1 was significantly upregulated for all conditions and all time points (Figure 3.5A). Under treatment of IGF-1, a 2-fold increase was observed at 24 hours and under loading conditions a > 6-fold increase was observed at 24 hours as well. When combining the treatment of IGF-1 and compression, it appears the expression levels of IGF-1 treatment dominate initially (2 hours). At 24 hours there appears to be an additive effect of compression and IGF-1 treatment as the combined compression and IGF-1 levels are about 9-fold. (>6 + 2). At 32 and 48 hours, the effects of compression appear to dominate the effects of IGF-1 treatment. Group 2 under treatment, compression, and compression with treatment, are initially significantly upregulated, but return to control expression levels at 48 hours (Figure 3.5B). In both compression and

treatment conditions, group 2 responds strongly by reaching > 3-fold and 2.5-fold respectively. When IGF-1 treatment and compression are combined, all significantly upregulated time points (2-32 hours) in treatment and compression are reduced with a peak value of 2-fold. Under treatment conditions, with a strong significant up-regulated for the first three time points, (peaked at > 3.5-fold) group 3 appears to be strongly upregulated by IGF-1 (Figure 3.5C). Under compression, group 3 has no significant initial changes, but at 48 hours in upregulated > 2-fold. When combining compression and treatment all time points are reduced to control levels, apart from 24 hours, which is still significantly upregulated, but reduced to 2-fold from > 3.5-fold in treatment alone. Group 4 under IGF-1 treatment conditions is increasing significantly up-regulated until 32 hours (2.5-fold) before it returns to near control levels at 48 hours (Figure 3.5D). Under compression conditions, group 4 exhibits a near opposite effect as in the treatment conditions, by initially being up-regulated (3-fold), and decreasing over time to return to control levels. Previous data has shown that Aggrecan, a member of this group, acts in a similar expression profile with a initial upregulation with compression followed by a return to control levels [19]. Combining compression and treatment, no time points are significantly different than control, but artifacts of the initial peak at 2 hours from compression alone and peak at 32 hours from IGF-1 treatment alone appear. Group 5 showed very little change under IGF-1 treatment with a significant upregulation at 32 hours of 1.5-fold (Figure 3.5E). Under compression conditions, group 5 was upregulated significantly at 2 and 8 hours with a peak of 1.6-fold, but by 24 hours until 48 hours was significantly decreasingly down-regulated to a minimum point at 48 hours, loosing greater than 50% expression compared to control. When combining compression and IGF-1 treatment, all time points were lower than either compression or IGF-1 treatment

alone, and 24-48 hour were decreasingly down-regulated to a significant level, loosing greater than 60% expression compared to control at 48 hours.

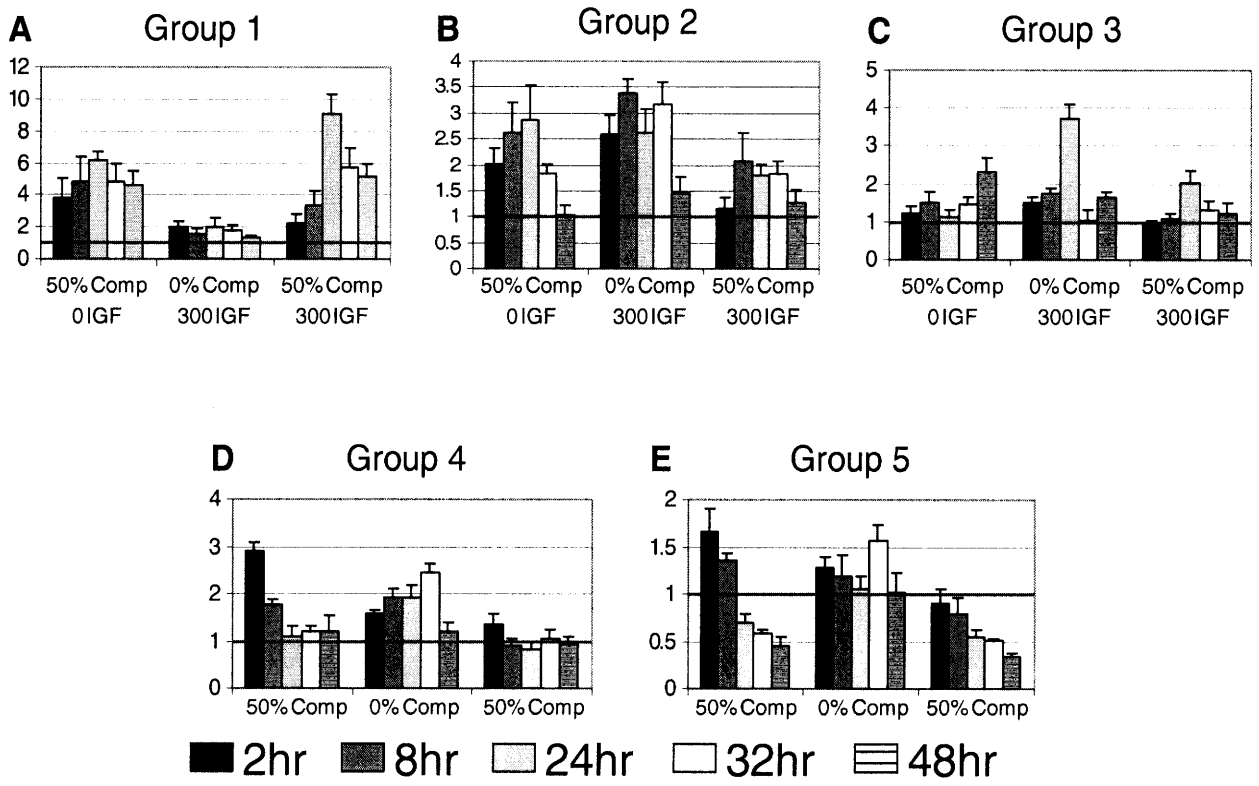

Figure 3.5. Five expression profiles represent the combination of 0% compression 300 ng/ml of IGF-1, 50% compression 0 ng/ml of IGF-1, and 50% compression 300 ng/ml of IGF-1. Centroid profiles were calculated through the average projection coordinates of genes in each group, and transformed from principle component space through use of the calculated principle components. Mean ± SE (n varies based on group component number)

3.5 Discussion

To understand the transcriptional responses under different conditions, the 23 genes observed were clustered according to IGF-1 treatment alone, 50% static compression alone, and

the combination of static compression and IGF-1 treatment. Lastly, to understand a more global view of transcriptional activity, all conditions and time points were clustered together. The groupings assigned by clustering analysis can be seen in Table 3.3A. Looking at the groupings under IGF-1 treatment alone, Link, type II collagen, and aggrecan which were significantly upregulated, were grouped together, while TXNIP, thioredoxin interacting protein, the only molecule that was significantly down regulated by IGF-1 treatment for multiple time points is uniquely grouped (Table 3.3B). Groupings of compression alone isolate IL-6, highly non-responsive to compression over the time course measured, in its own group. Transcription factors, highly initially upregulated genes, were grouped together while transiently upregulated proteinases were allocated to a different grouped, both of which support previous findings for compression (Table 3.3C) [19]. Examining the combination of the treatments, Fibronectin was partitioned to a unique group for its seemingly non-responsive behavior to compression and IGF-1 treatment. The majority of proteinases were also grouped together (Table 3.3D). Looking at all three sets of clusters, of note, MMP-1 and IGF-2 were grouped together under the three different conditions, as well as link protein, and the components of the AP-1 complex, c-Fos and c-Jun. Type II collagen and IGF-1, TIMP-3 and MMP-3, Sox-9 and TIMP-1 were allocated in the same group for all three conditions. Compiling all conditions observed into an expression vector, cluster analysis revealed that all cytokines were grouped together, and were significantly upregulated under IGF-1 treatment alone compared to controls. Under compression alone and IGF-1 and compression experiments this extensive upregulation was not observed, suggesting that IGF-1 has a stimulatory effect on cytokines which is mitigated when compression is present. Also of note, Aggrecan, type II collagen, and link protein were all in separate groupings, suggesting that there may be different mechanisms involved in the activation of these molecules.

Of the strongly upregulated group, transcription factors, growth factors, protease inhibitors, and proteinases were grouped together, namely c-Fos, c-Jun, TGF-β, TIMP-3, MMP-3, MMP-13, and ADAMTS-5.

A

Group	Genes	Centroid Coordinates (PC1, PC2, PC3)
1	TGF-B, c-Fos, c-Jun, Timp-3, ADAMTS-5, MMP13, MMP3	(-2.46, 2.37, -0.33)
2	Sox-9, HSP90, Timp-1, Link	(-3.10, 0.95, -0.07)
3	TNF-a, IL-1, IL-4, IL-6	(-2.78, -1.50, -0.94)
4	IGF-2, MMP1, Fibronectin, Aggrecan	(-2.71, -0.24, 2.03)
5	IGF-1, Txnip, Timp-2, Collagen II	(0.32, 3.21, -0.19)

B

Group	Genes	Centroid Coordinates (PC1, PC2, PC3)
1	TGF-B, Sox-9, Timp-2, Timp-1, Fibronectin	(-1.81, 0.93, 0.43)
2	Txnip	(1.11, 0.91, -1.55)
3	IGF-2, IGF-1, c-Jun, c-Fos, ADAMTS-5, MMP1, Link, Collagen II, Aggrecan	(-2.05, 0.39, -0.25)
4	TNF-a, IL-6, IL-4, MMP13	(-1.48, -1.58, -0.22)
5	IL-1, HSP90, Timp-3, MMP3	(-2.03, -0.57, -0.05)

C

Group	Genes	Centroid Coordinates (PC1, PC2, PC3)
1	IGF-1, Timp-2, Collagen II	(0.44, 2.03, -0.13)
2	IGF-2, Txnip, MMP1, Fibronectin, Aggrecan	(-1.41, 1.42, -0.48)
3	TNF-a, IL-4, IL-1, Timp-3, ADAMTS-5, MMP13, MMP3	(-1.92, 0.16, 0.56)
4	TGF-B, c-Jun, c-Fos, Sox-9, HSP-90, Timp-1, Link	(-1.73, -0.86, -0.37)
5	IL-6	(0.59, -1.18, -1.76)

D

Group	Genes	Centroid Coordinates (PC1, PC2, PC3)
1	IGF-2, MMP1	(-0.52, 0.62, -1.65)
2	IL-6, IL-4, IL-1, Timp-3, ADAMTS-5, MMP13, MMP3	(-1.88, -0.49, 0.14)
3	TGF-B, TNF-a, c-Jun, c-Fos, Sox-9, HSP90, Timp-1, Link	(-1.88, 0.62, 0.05)
4	Fibronectin	(1.34, -1.62, -0.59)
5	IGF-1, Txnip, TIMP-2, Collagen II, Aggrecan	(1.77, 0.70, 0.14)

Table 3.3. Gene clustering groupings. Resulted gene sorting according to extent and kinetics of expression. Specific gene allocation and centroid coordinates when all data are clustered (A), 0% compression 300 ng/ml IGF-1 data clustered (B), 50% compression 0 IGF-1 data clustered (C), and 50% compression 300 ng/ml IGF-1 data clustered (D).

With the 4 different sets of data clustered, (compression, IGF-1, compression + IGF-1, all conditions) three interesting pairings were always present: MMP-1 and IGF-2, TIMP-3 and

ADAMTS-5, type II collagen and IGF-1. MMP-1 or collagenase-1 is shown to cleave key ECM molecules including collagen I, collagen II, aggrecan (at the MMP cleavage site in the interglobular domain), fibronectin, and link protein [25]. MMP-1 has been shown to play a role in the regulation of paracrine signals, through the degradation of cytokines such as IL-1β [26]. Collagenase-1 has also been shown to degrade insulin-like growth factor binding proteins (IGFBP) 3 and 5, which indirectly increases presence of free (unbound) IGF [27, 28]. IGF-1 and IGF-2 are known to bind IGFBP-3, the most abundant IGF binding protein in human serum [29]. IGF-2 is known to stimulate DNA and proteoglycan synthesis in chondrocytes [30] and has been shown to act in an autocrine fashion [31]. IGF-2 has also been shown to stimulate type 1 IGF receptor, a key receptor for IGF-1 and also IGF-2 with lesser affinity [32, 33]. The co-expression of MMP-1 and IGF-2 suggests that the two contain each other through their anabolic and catabolic activities and have the capability of a strong anabolic response, due to the stimulatory secondary effects of MMP-1.

TIMPs act in a stochiometric fashion to reversibly inhibit metallo-proteinases [34]. Of the four known TIMPs (1-4), TIMP-3 has been shown to be a strong inhibitor of Aggrecanase-1 (ADAM-TS4) and Aggrecanase-2 (ADAM-TS5) with K_i values in the subnanomolar range [35, 36]. When added exogenously to bovine nasal and porcine articular cartilage, TIMP-3 retains the ability to inhibit aggrecanase activity induced by catabolic factors [37]. In the current study, TIMP-3 is shown to be significantly upregulated with the addition of IGF-1, and acts in a compression independent manner (Figure 3.3). Although Aggrecan can be degraded by multiple members of the matrix metalloproteinase family, it has recently been shown that ADAMTS-5 is the primary aggrecanase responsible for aggrecan degradation in a murine model of osteoarthritis [38]. The constant grouping based on expression profile of TIMP-3 and ADAMTS-5 suggests a

biological control may present to ensure the turn over of aggrecan and the regulation of anabolic and catabolic factors. Supporting these ideas, past clustering analysis with cartilage under multiple conditions also grouped ADAMTS-5 and TIMP-3 together [19].

Type II Collagen, a key matrix protein, adds structure and strength to articular cartilage. IGF-1 has been shown to elevate levels of type II collagen under a number of different conditions [3, 10]. The co-expression of type II collagen and IGF-1 under compressive and/or IGF-1 treated conditions suggests a positive feedback loop between IGF-1 and type II collagen. Under IGF-1 treatment both are upregulated, while under compression, both are down regulated. This supports previous data suggesting that IGF-1 acts in an autocrine fashion [1, 32]. Further studies using promoter analysis must be performed to confirm if these pairings are co-expressed or if these results are an artifact of the selected genes measured.

In contrast with previously published reports [3, 10, 11], the current results show only a slight upregulation of type II collagen in response to IGF-1 alone, compared to a significant upregulation (Figure 3.2H). A possible explanation for the discrepancy in the magnitude of type II collagen expression induced by IGF-1 was the 0% compression control present in the current study, where free swell conditions were used in previously published studies. Aggrecan was previously shown to have no significant change in the first 48 hours [3], which this study supports (Figure 3.2F). Previously published data show that MMP-1, MMP-3, and MMP-13 were unaffected by the addition of IGF-1 after 48 hours, while the current data suggests a significant increase for 4 out of the 5 time points in MMP-1 and MMP-13 (Figure 3.2I, 3.2B). Again, reasons for this discrepancy may be due to the 0% static compression present during IGF-1 treatment. IGF-1 mRNA levels were maximum at 32 hours (Appendix 3.8.1), where previous

studies reported them to peak at 24 hours [1]. Nixon et al. examined time points at 0, 4, 14, 24, 48, and 72 hours, thus finding a maximum of 32 hours is not in direct contradiction to the previously published finding. Sox-9 expression was shown to be significantly upregulated by IGF-1 at 4 of the 5 measured time points (2, 8, 32, 48), which previously was shown to be unresponsive to IGF-1 at 72 hours (Appendix 3.8.1). Many differences in the two experiments exist possibly explaining the difference in IGF-1 response, i.e., bovine vs. human, young tissue vs. old tissue, explant tissue vs. monolayer, 300 ng/mL IGF-1 vs. 100 ng/mL IGF-1.
In agreement with previously published data [13, 15, 18, 19], under static compression, type II collagen and aggrecan were initially upregulated and then down regulated to nearly control levels (Figure 3.2H, 3.2G).

Examining the transcriptional effects of IGF-1 on aggrecan and link, IGF-1 appears to act via a compression-dependent manner (Figure 3.3A, 3.3C), whereas the transcriptional effects of IGF-1 on collagen II and fibronectin appear to be independent of compression (Figure 3.3F, Appendix 3.8.2). This phenomenon could easily be explained by the compacted ECM present under compression, dramatically restricting transport of IGF-1 to chondrocytes. To test this idea, experiments were performed allowing IGF-1 to be incubated for 24 hours (transport studies performed by Bonassar *et al.* [5]), to allow IGF-1 to diffuse completely into the cartilage explant. Results of this experiment replicate the trends seen in Figure 3.3A, 3.3C, suggesting that aggrecan and link act in a compression-dependent manner when treated with IGF-1. Whether this change is due to decreased receptor-ligand affinity, or to mechanotransduction intracellular signaling interference, remains to be determined.

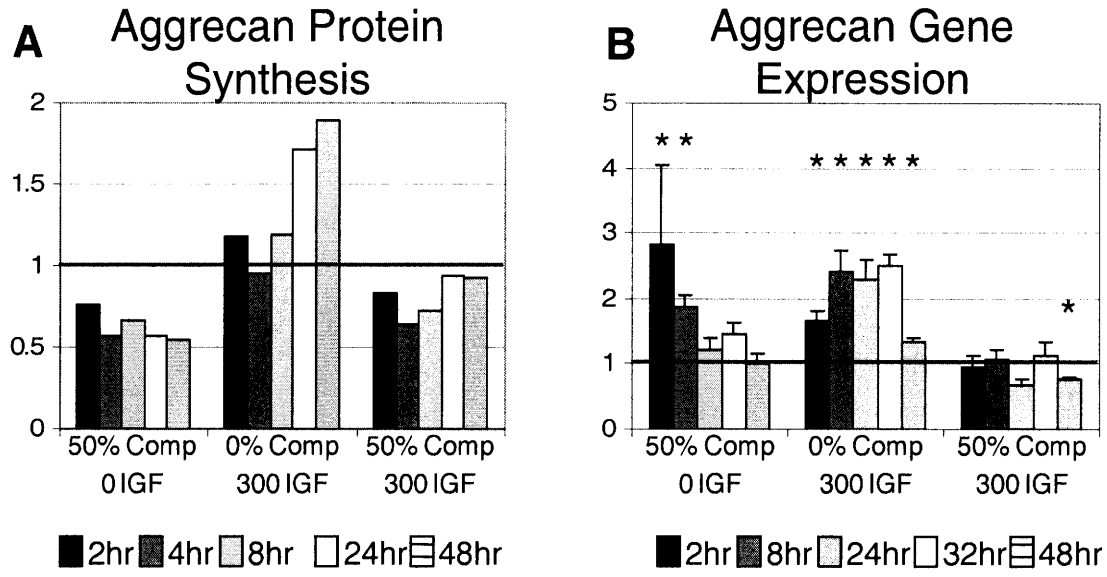

Figure 3.6. Aggrecan Protein Synthesis compared to Aggrecan Gene Expression. (A) Aggrecan protein synthesis as measured by 35S radiolabel incorporation normalized to 0% compression 0 IGF-1 adapted from Bonassar et al [5]. Mean plotted. (B) Aggrecan gene expression normalized to 18s and plotted relative to 0% compression 0 IGF-1. Significance was measured by the Wilcoxon sign ranked test compared to like compression 0 IGF-1. (* p-value <0.07).

At the transcriptional level, the current study points out the anabolic response due to the treatment of IGF-1 under 0% compression loading, and the mixed anabolic and catabolic signals under 50% static compression coupled with IGF-1. To further investigate the transcriptional response to the protein synthesis under IGF-1 treatment and compression, Figure 3.6 shows the levels of aggrecan protein synthesis, normalized to 0% compression 0 IGF-1 compared to gene expression of aggrecan. Aggrecan gene expression under 0% compression, 300 ng/ml IGF-1 is upregulated compared to control for all 5 time points measured (Figure 3.6B). Examining the corresponding aggrecan protein level at 0% compression, 300 ng/ml IGF-1, there is a strong increase in aggrecan synthesis at 8, 24, and 48 hours (Figure 3.6A). These data suggest that aggrecan synthesis is transcriptionally regulated by IGF-1. Examining the gene expression of aggrecan under 50% compression 0 IGF-1, there is an initial bolus of transcript at early time

points, followed by a return to control levels (Figure 3.6B). Examining the protein synthesis levels of aggrecan, at the same early time points, aggrecan synthesis is reduced below control and this reduction is sustained for all time points measured, suggesting that the inhibition of aggrecan synthesis by compression, with no IGF-1, is not transcriptionally regulated (Figure 3.6A). Thus, in attempts to reconcile the responsiveness of aggrecan under 50% static compression at the translational level with the unresponsiveness of aggrecan at the transcriptional level, the authors support the hypothesis [4] that under static compression, proteoglycan synthesis is regulated through post-transcriptional machinery.

3.6 Conclusion

Experiments have been performed to assess expression levels of a range of ECM related genes in response to static loading in the presence and absence of IGF-1. Through k-means clustering analysis, major co-expression trends were elucidated, grouping genes into highly responsive, non-responsive, and differentially active gene profile groups. The gene pairs MMP-1 and IGF-2, TIMP-3 and ADAMTS-5, and type II collagen and IGF-1 were consistently co-expressed in multiple clustering conditions, suggesting the possibility of strong regulation and control relationships between members of each pair. Aggrecan and link protein responded to IGF-1 in a compression-dependent manner, whereas type II collagen and fibronectin appeared to respond to IGF-1 in a manner independent of compression. While aggrecan transcripts were significantly upregulated with the addition of IGF-1 under 0% compression, IGF-1 was unable to upregulate aggrecan when the cartilage explants were statically compressed to 50% strain. In comparing aggrecan gene expression to aggrecan synthesis, these data suggest that aggrecan synthesis is transcriptionally regulated by IGF-1 while the inhibition of aggrecan synthesis by

compression is not transcriptionally regulated. However, more studies are needed to elucidate the specific stimulatory mechanism(s) induced by IGF-1 and the post-transcriptional inhibitory effects of compression.

3.7 References

1. Nixon, A.J., R.A. Saxer, and B.D. Brower-Toland, *Exogenous insulin-like growth factor-I stimulates an autoinductive IGF-I autocrine/paracrine response in chondrocytes.* J Orthop Res, 2001. **19**(1): p. 26-32.
2. Sah, R.L., A.C. Chen, A.J. Grodzinsky, and S.B. Trippel, *Differential effects of bFGF and IGF-I on matrix metabolism in calf and adult bovine cartilage explants.* Arch Biochem Biophys, 1994. **308**(1): p. 137-47.
3. Bau, B., L.A. McKenna, S. Soeder, Z. Fan, A. Pecht, and T. Aigner, *Hepatocyte growth factor/scatter factor is not a potent regulator of anabolic and catabolic gene expression in adult human articular chondrocytes.* Biochem Biophys Res Commun, 2004. **316**(4): p. 984-90.
4. Starkman, B.G., J.D. Cravero, M. Delcarlo, and R.F. Loeser, *IGF-I stimulation of proteoglycan synthesis by chondrocytes requires activation of the PI 3-kinase pathway but not ERK MAPK.* Biochem J, 2005. **389**(Pt 3): p. 723-9.
5. Bonassar, L.J., A.J. Grodzinsky, A. Srinivasan, S.G. Davila, and S.B. Trippel, *Mechanical and physicochemical regulation of the action of insulin-like growth factor-I on articular cartilage.* Arch. Biochem. Biophys., 2000. **379**(1): p. 57-63.
6. Smith, P., F.D. Shuler, H.I. Georgescu, S.C. Ghivizzani, B. Johnstone, C. Niyibizi, P.D. Robbins, and C.H. Evans, *Genetic enhancement of matrix synthesis by articular chondrocytes: comparison of different growth factor genes in the presence and absence of interleukin-1.* Arthritis Rheum, 2000. **43**(5): p. 1156-64.
7. Studer, R.K., R. Bergman, T. Stubbs, and K. Decker, *Chondrocyte response to growth factors is modulated by p38 mitogen-activated protein kinase inhibition.* Arthritis Res Ther, 2004. **6**(1): p. R56-R64.
8. Veilleux, N. and M. Spector, *Effects of FGF-2 and IGF-1 on adult canine articular chondrocytes in type II collagen-glycosaminoglycan scaffolds in vitro.* Osteoarthritis Cartilage, 2005. **13**(4): p. 278-86.
9. Im, H.J., C. Pacione, S. Chubinskaya, A.J. Van Wijnen, Y. Sun, and R.F. Loeser, *Inhibitory effects of insulin-like growth factor-1 and osteogenic protein-1 on fibronectin fragment- and interleukin-1beta-stimulated matrix metalloproteinase-13 expression in human chondrocytes.* J Biol Chem, 2003. **278**(28): p. 25386-94.
10. Darling, E.M. and K.A. Athanasiou, *Growth factor impact on articular cartilage subpopulations.* Cell Tissue Res, 2005. **322**(3): p. 463-73.
11. Aigner, T., P.M. Gebhard, E. Schmid, B. Bau, V. Harley, and E. Poschl, *SOX9 expression does not correlate with type II collagen expression in adult articular chondrocytes.* Matrix Biol, 2003. **22**(4): p. 363-72.
12. Messai, H., Y. Duchossoy, A.M. Khatib, A. Panasyuk, and D.R. Mitrovic, *Articular chondrocytes from aging rats respond poorly to insulin-like growth factor-1: an altered signaling pathway.* Mech Ageing Dev, 2000. **115**(1-2): p. 21-37.
13. Ragan, P.M., A.M. Badger, M. Cook, V.I. Chin, M. Gowen, A.J. Grodzinsky, and M.W. Lark, *Down-regulation of chondrocyte aggrecan and type-II collagen gene expression correlates with increases in static compression magnitude and duration.* J. Orthop. Res., 1999. **17**(6): p. 836-42.

14. Ragan, P.M., V.I. Chin, H.H. Hung, K. Masuda, E.J. Thonar, E.C. Arner, A.J. Grodzinsky, and J.D. Sandy, *Chondrocyte extracellular matrix synthesis and turnover are influenced by static compression in a new alginate disk culture system.* Arch. Biochem. Biophys., 2000. **383**(2): p. 256-64.
15. Hunter, C.J., S.M. Imler, P. Malaviya, R.M. Nerem, and M.E. Levenston, *Mechanical compression alters gene expression and extracellular matrix synthesis by chondrocytes cultured in collagen I gels.* Biomaterials, 2002. **23**(4): p. 1249-59.
16. Guilak, F., B.C. Meyer, A. Ratcliffe, and V.C. Mow, *The effects of matrix compression on proteoglycan metabolism in articular cartilage explants.* Osteoarthr. Cartilage, 1994. **2**: p. 91-101.
17. Kim, Y.J., A.J. Grodzinsky, and A.H. Plaas, *Compression of cartilage results in differential effects on biosynthetic pathways for aggrecan, link protein, and hyaluronan.* Arch. Biochem. Biophys., 1996. **328**(2): p. 331-40.
18. Valhmu, W.B., E.J. Stazzone, N.M. Bachrach, F. Saed-Nejad, S.G. Fischer, V.C. Mow, and A. Ratcliffe, *Load-Controlled Compression of Articular Cartilage induces a transient stimulation of Aggrecan gene expression.* Arch. Biochem. Biophys., 1998. **353**(1): p. 29-36.
19. Fitzgerald, J.B., M. Jin, D. Dean, D.J. Wood, M.H. Zheng, and A.J. Grodzinsky, *Mechanical compression of cartilage explants induces multiple time-dependent gene expression patterns and involves intracellular calcium and cyclic AMP.* Journal of Biological Chemistry, 2004. **279**(19): p. 19502-19511.
20. Sah, R.L.Y., Y.J. Kim, J.Y.H. Doong, A.J. Grodzinsky, A.H.K. Plaas, and J.D. Sandy, *Biosynthesis Response to Cartilage Explants to Dynamic Compression.* J. Orthop. Res., 1989. **7**: p. 619-636.
21. Lee, J.H., J.B. Fitzgerald, M.A. Dimicco, and A.J. Grodzinsky, *Mechanical injury of cartilage explants causes specific time-dependent changes in chondrocyte gene expression.* Arthritis Rheum, 2005. **52**(8): p. 2386-95.
22. Lee, C.R., S. Grad, J.J. Maclean, J.C. Iatridis, and M. Alini, *Effect of mechanical loading on mRNA levels of common endogenous controls in articular chondrocytes and intervertebral disk.* Anal Biochem, 2005. **341**(2): p. 372-5.
23. Alter, O., P.O. Brown, and D. Botstein, *Singular value decomposition for genome-wide expression data processing and modeling.* Proc Natl Acad Sci U S A, 2000. **97**(18): p. 10101-6.
24. Holter, N.S., M. Mitra, A. Maritan, M. Cieplak, J.R. Banavar, and N.V. Fedoroff, *Fundamental patterns underlying gene expression profiles: simplicity from complexity.* Proc Natl Acad Sci U S A, 2000. **97**(15): p. 8409-14.
25. Sternlicht, M.D. and Z. Werb, *How matrix metalloproteinases regulate cell behavior.* Annu Rev Cell Dev Biol, 2001. **17**: p. 463-516.
26. Ushiki, T., J. Hitomi, S. Ogura, T. Umemoto, and M. Shigeno, *Atomic force microscopy in histology and cytology.* Arch. Histol. Cytol., 1996. **59**: p. 421-31.
27. Fowlkes, J.L., D.M. Serra, H. Nagase, and K.M. Thrailkill, *MMPs are IGFBP-degrading proteinases: implications for cell proliferation and tissue growth.* Ann N Y Acad Sci, 1999. **878**: p. 696-9.
28. Kiepe, D., S. Ciarmatori, A. Hoeflich, E. Wolf, and B. Tonshoff, *Insulin-like growth factor (IGF)-I stimulates cell proliferation and induces IGF binding protein (IGFBP)-3*

and IGFBP-5 gene expression in cultured growth plate chondrocytes via distinct signaling pathways. Endocrinology, 2005. **146**(7): p. 3096-104.
29. Ali, O., P. Cohen, and K.W. Lee, *Epidemiology and biology of insulin-like growth factor binding protein-3 (IGFBP-3) as an anti-cancer molecule.* Horm Metab Res, 2003. **35**(11-12): p. 726-33.
30. Davenport-Goodall, C.L., R.C. Boston, and D.W. Richardson, *Effects of insulin-like growth factor-II on the mitogenic and metabolic activities of equine articular cartilage with and without interleukin 1-beta.* Am J Vet Res, 2004. **65**(2): p. 238-44.
31. Takahashi, K., T. Kubo, K. Kobayashi, J. Imanishi, M. Takigawa, Y. Arai, and Y. Hirasawa, *Hydrostatic pressure influences mRNA expression of transforming growth factor-beta 1 and heat shock protein 70 in chondrocyte-like cell line.* J Orthop Res, 1997. **15**(1): p. 150-8.
32. Loeser, R.F. and G. Shanker, *Autocrine stimulation by insulin-like growth factor 1 and insulin-like growth factor 2 mediates chondrocyte survival in vitro.* Arthritis Rheum, 2000. **43**(7): p. 1552-9.
33. Armstrong, D.G., C.G. Gutierrez, G. Baxter, A.L. Glazyrin, G.E. Mann, K.J. Woad, C.O. Hogg, and R. Webb, *Expression of mRNA encoding IGF-I, IGF-II and type 1 IGF receptor in bovine ovarian follicles.* J Endocrinol, 2000. **165**(1): p. 101-13.
34. Edwards, D., N.J. Clendeninn, and K. Appelt, *The Tissue Inhibitors of Metalloproteinases (TIMPs): Biology and Regulation. Matrix metalloproteinase inhibitors in cancer therapy.* Cancer drug discovery and development. 2001, Totowa, N.J.: Humana Press. 67-84.
35. Kashiwagi, M., M. Tortorella, H. Nagase, and K. Brew, *TIMP-3 is a potent inhibitor of aggrecanase 1 (ADAM-TS4) and aggrecanase 2 (ADAM-TS5).* J Biol Chem, 2001. **276**(16): p. 12501-4.
36. Hashimoto, G., T. Aoki, H. Nakamura, K. Tanzawa, and Y. Okada, *Inhibition of ADAMTS4 (aggrecanase-1) by tissue inhibitors of metalloproteinases (TIMP-1, 2, 3 and 4).* FEBS Lett, 2001. **494**(3): p. 192-5.
37. Gendron, C., M. Kashiwagi, C. Hughes, B. Caterson, and H. Nagase, *TIMP-3 inhibits aggrecanase-mediated glycosaminoglycan release from cartilage explants stimulated by catabolic factors.* FEBS Lett, 2003. **555**(3): p. 431-6.
38. Glasson, S.S., R. Askew, B. Sheppard, B. Carito, T. Blanchet, H.L. Ma, C.R. Flannery, D. Peluso, K. Kanki, Z. Yang, M.K. Majumdar, and E.A. Morris, *Deletion of active ADAMTS5 prevents cartilage degradation in a murine model of osteoarthritis.* Nature, 2005. **434**(7033): p. 644-8.

3.8 Appendix

Appendix 3.8.1- Gene Expression relative to Control

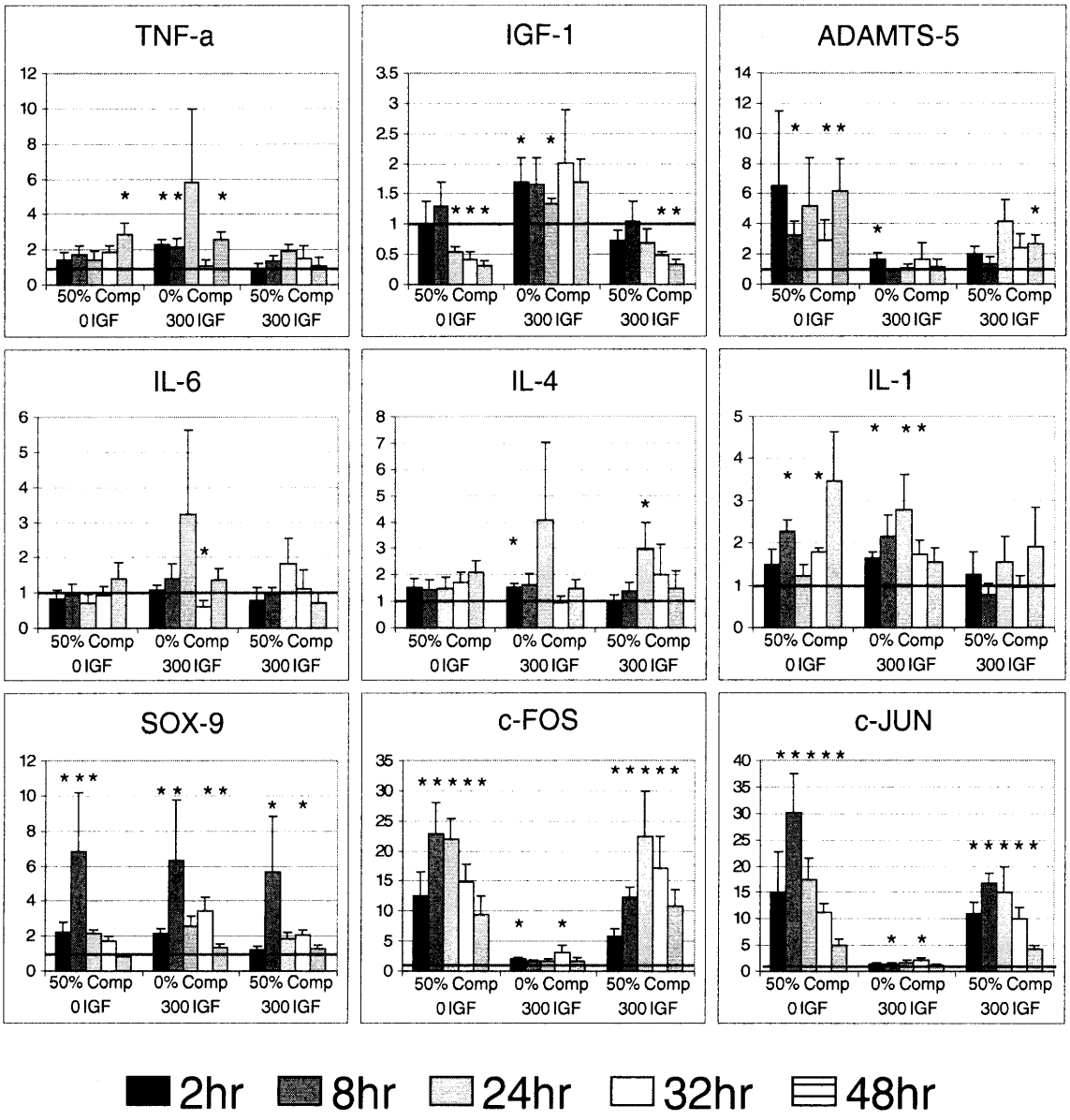

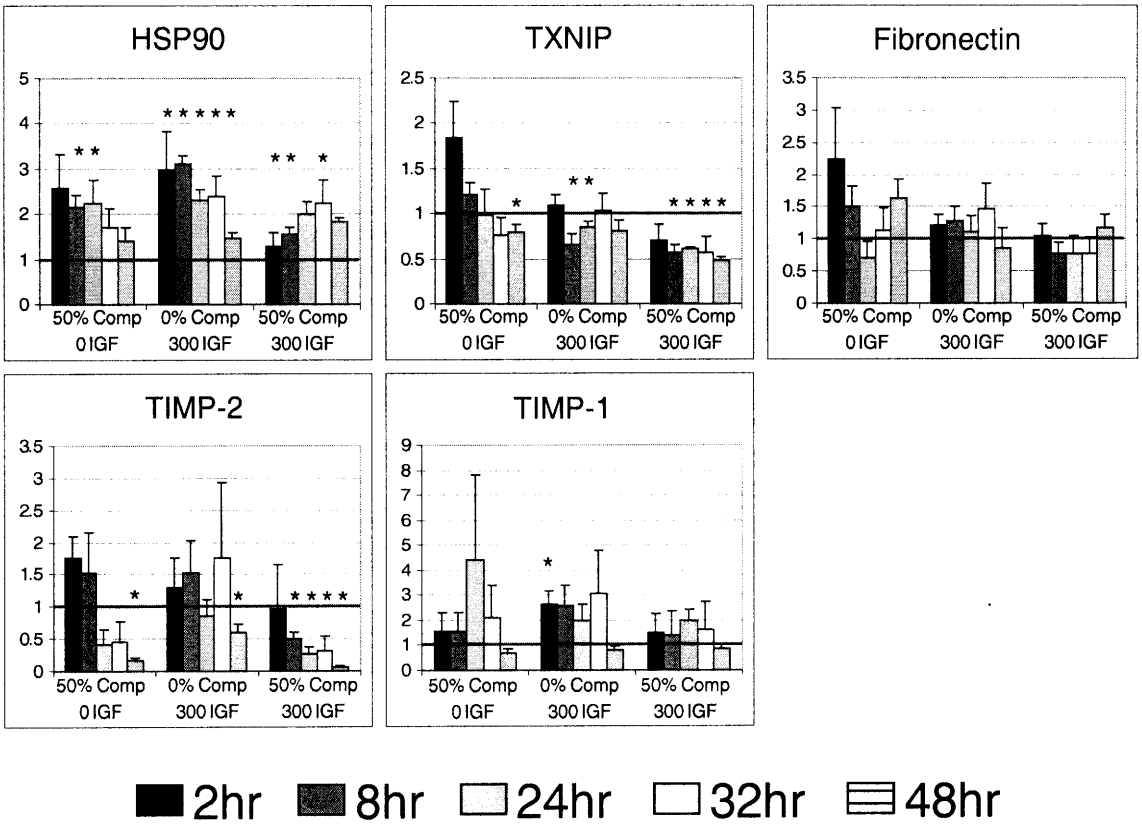
HSP90
TXNIP
Fibronectin
TIMP-2
TIMP-1
50% Comp 0 IGF
0% Comp 300 IGF
50% Comp 300 IGF
2hr
8hr
24hr
32hr
48hr

Appendix 3.8.2- The Effects of IGF-1 on Gene Expression

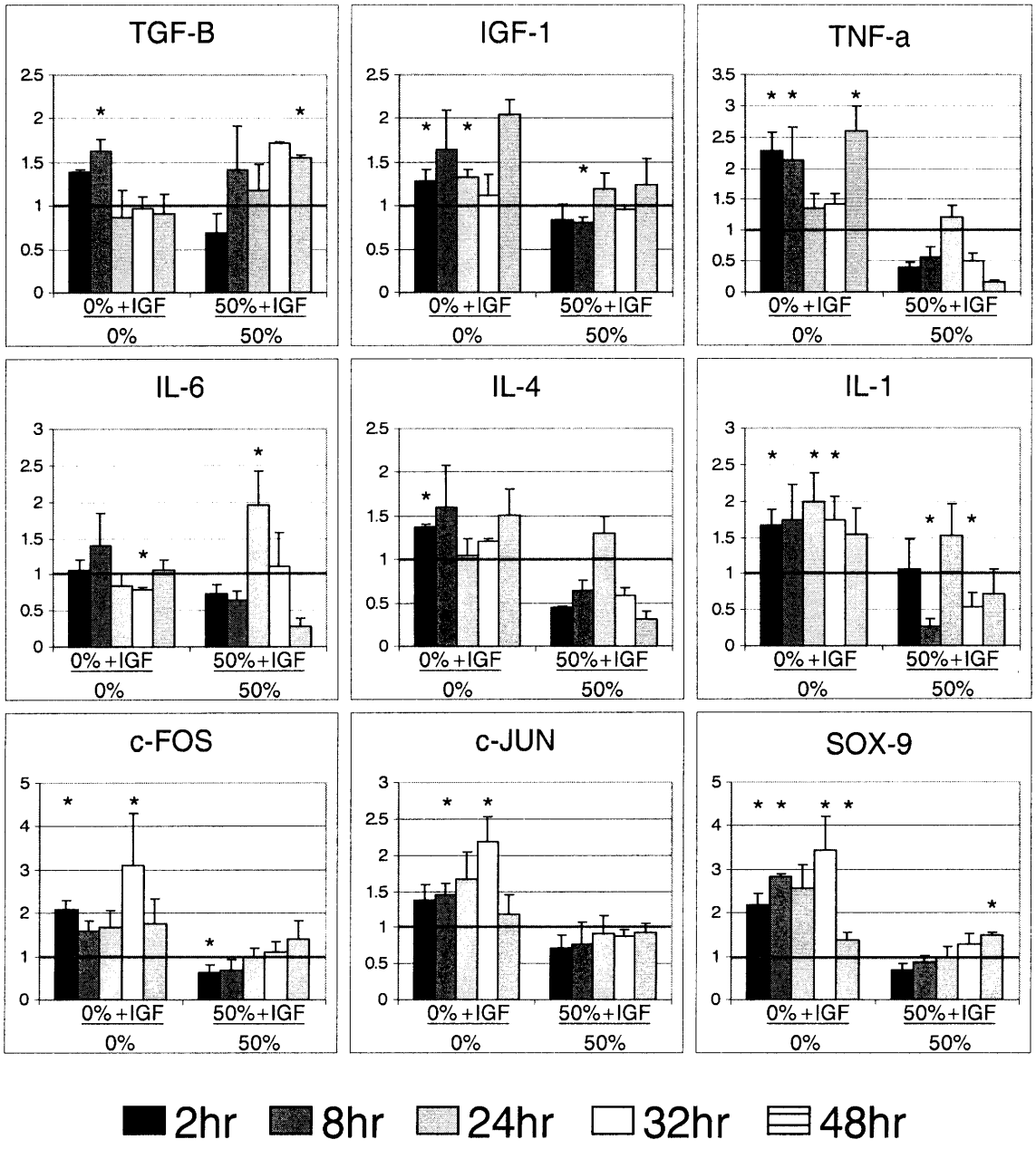

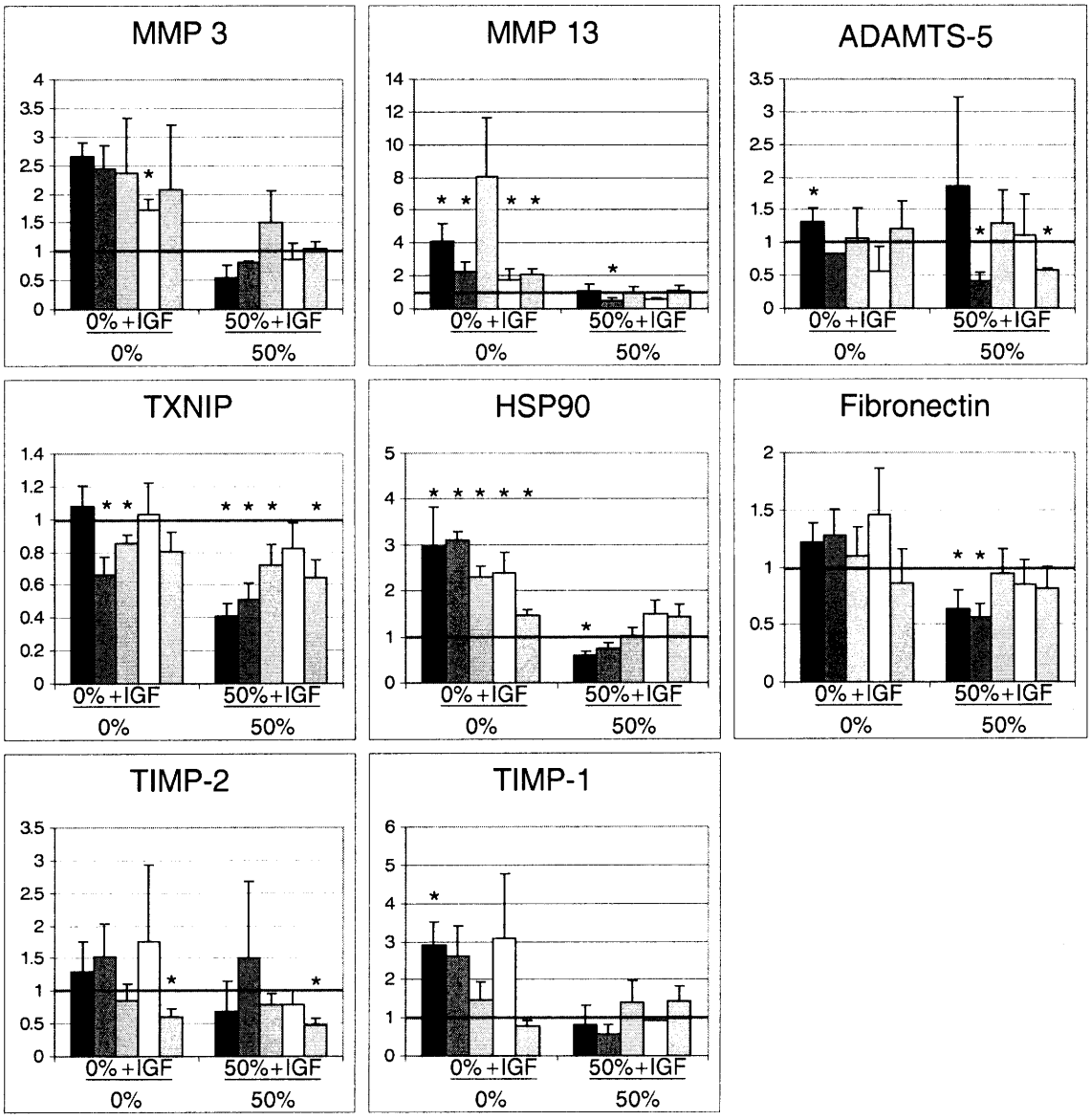
MMP 3
MMP 13
ADAMTS-5
TXNIP
HSP90
Fibronectin
TIMP-2
TIMP-1
0% +IGF
50%+IGF
0%
50%
2hr
8hr
24hr
32hr
48hr

Chapter 4

Influence of OP-1 and IGF-1 on Cartilage Subjected to Combined Mechanical Injury and Co-culture with Joint Capsule

* This chapter is a manuscript in preparation for submission
(Wheeler, Cameron A., Wilkinson, Samuel, Perez, Anthony R., Kurz, Bodo, and Grodzinsky, Alan J.)

4.1 Introduction

Osteogenic Protein-1 (OP-1), or Bone Morphogenetic Protein-7 (BMP-7), is a potent growth factor and belongs to the TGF-β super family [1]. Bone morphogenetic proteins have a variety of effects on biologic activity, including: cell proliferation, apoptosis, differentiation, migration, embryogenesis, development, and supporting tissue homeostasis [1-3]. For the past 30 years, studies have been compiled and therapeutics have been developed documenting and exploiting the effects of OP-1 and BMPs on bone formation [4]; for the past ten years, studies have shown the possible use of this growth factor in cartilage [5]. OP-1 is found in many tissues, and was recently found to be expressed in articular cartilage [6-8]. The apparent advantage of OP-1 over other members of the TGF-β family for the treatment of cartilage pathologies is the ability of OP-1 to upregulate chondrocyte metabolic activities and proteoglycan synthesis while avoiding uncontrolled cell proliferation and differentiation [5, 8-10]. Studies have shown that OP-1 stimulates key extracellular cartilage proteins such as collagen type II, VI, aggrecan, decorin, fibronectin, hyaluronan, and superficial zone protein (lubricin) [5, 11-14] while others have shown that OP-1 has little stimulatory effect on gene expression [15]. OP-1 also stimulates proteoglycan synthesis in osteoarthritic and non-osteoarthritic chondrocytes [16]. In addition to stimulating key extracellular matrix (ECM) molecules, OP-1 has been shown to modulate various growth factors, i.e., IGF-1, TGF-β, BMPs, and cytokine mediators (IL-6 family of cytokines) [17]. OP-1 has also been able to regulate synthesis of chondrocyte cytoskeleton proteins such as talin, paxillin, and focal adhesion kinase (FAK) while enhancing expression of tissue inhibitor of metalloproteinases (TIMP) in human normal and OA chondrocytes [8]. OP-1 has been linked to cell survival [10-12] and appears to act in a distinct regulatory pathway

independent of other growth factors, including IGF-1, while augmenting IGF-1 anabolic effects. OP-1 has been reported to increase levels of IGF-1, IGF-1 receptor, and IGF-1 binding proteins, and authors speculate that this augmentation acts to restore in part the responsiveness of adult human chondrocytes to IGF-1 lost through aging [9, 10, 17, 18]. IGF-1 has also been well documented in its anabolic effects on cartilage tissue [19-21], and OP-1 combined with IGF-1 has shown a synergistic effect on cell survival and matrix synthesis, hinting at the use of both OP-1 and IGF-1 in combination therapy [11]. Interestingly, recent studies have shown that the effects of the combination of these two potent growth factors can be reversed with the addition of basic fibroblast growth factor (bFGF or FGF-2); proteoglycan synthesis induced by OP-1 and IGF-1 either independently or together were strongly inhibited by bFGF [12]. Acting in an anti-catabolic fashion, OP-1 has been shown to effectively counteract the effects of IL-1β treatment [22], as well as harmful fibronectin fragments [23] and HA hexasaccharides [24]. Studies have also shown that OP-1 blocks gene expression of MMP-1 and MMP-13 in response to cytokine treatment [17].

Endogenous OP-1 is also very important to cartilage homeostasis. Normal adult human cartilage tissue contains approximately 50 ng of OP-1 per gram of dry tissue, which is within the concentration range of recombinant OP-1 (50-200 ng/ml) used in various studies [9]. OP-1 has also been detected in synovium, ligament, tendon, menisci [18], and synovial fluid from normal, OA, and RA joints [25]. Recent studies have shown that through a gene silencing technique (antisense) in which OP-1 was inhibited, there was a significant decrease of aggrecan mRNA expression and a ~50% decrease in proteoglycan synthesis. Recovery experiments with the addition of recombinant OP-1 were able to partially restore proteoglycan production [25].

Showing an anabolic response to injury, active OP-1 was highly elevated in response to a capsular incision in a rabbit model [26].

OP-1 has been suggested to aid long-term healing of cartilage defects [27] and has been recently used in a reparative fashion in horses, sheep, goats, and rabbits. OP-1 was put on an adenoviral vector and delivered to a focal chondral defect via transfected allogenic chondrocytes in a horse model [28]. The defects seeded with chondrocytes enhanced with the OP-1 vector showed significantly better healing at four weeks post injection and more hyaline-like morphology. Recent data from rabbits subjected to an ACL transection showed that OP-1 had a protective effect on cartilage degradation [29], and in goats OP-1 has been shown to promote cartilage formation in subchondral defects [30]. OP-1 also prevented post-traumatic osteoarthritis in a sheep model when intra-articular injections were administered at time of mechanical injury and one week post injury [31].

An *in vitro* model of injury has been established in our laboratory incorporating the effects of a mechanical injury and injured joint capsule (JC) tissue [32, 33]. *In vitro* mechanical injury to cartilage alone has been shown to increase hydraulic permeability [34] and water content [35-37], decrease stiffness [36, 38], and increase glycosaminoglycan (GAG) lost to the medium [36, 39-41]. Cells with cartilage subject to this mechanical injury have been shown to decrease biosynthesis rates [36], undergo apoptosis and necrosis[35, 36, 42, 43], and have elevated levels of protease transcript activity within the first 24 hours [44]. Co-culturing un-injured cartilage with damaged joint capsule *in vitro* has resulted in a decrease in cartilage biosynthesis rates [32, 45], as well as a loss of proteoglycan and collagen as seen though histology staining [46]. GAG release from cartilage co-cultured with synovial or capsular tissue was not decreased with the inhibition of IL-1β, TNF-α, and ACITIC [47]. Under the same

conditions of cartilage co-cultured with joint capsule, GAG loss was blocked by treatment with EDTA [47]. While the effects of JC co-culture appear to accelerate degradation, studies have also shown that synoviocytes from joint capsule tissue provide chondrocytes with protection against reactive oxygen species, which are known to induce membrane damage and lipid peroxidation [48].

The objectives of this study was to (1) more fully explore the degradative effects of mechanical injury co-cultured with excise joint capsule through changes in transcript levels, protein biosynthesis rates, and apoptosis, and (2) to test whether combined treatment with IGF-1 and OP-1 could mitigate those degradative effects on a short time scale (3 days) and a longer time scale (16 days).

4.2 Materials and Methods

Tissue Harvest

Cartilage-bone plugs (9mm in diameter) were harvested from the patello-femoral groove of 1-2 week old calves. Cartilage disks (1mm thick x 3mm diameter) were sliced and punched from the middle zone as described previously[49] and equilibrated for two days under free-swell conditions (37°C, 5% CO_2) in the presence of serum-free, 1% ITS supplemented feeding medium consisting of high glucose Dulbecco's modified essential medium supplemented with 10 nM Hepes Buffer, 0.1 mM nonessential amino acids, 20 μg/ml ascorbate, 100 units/ml penicillin, 100 μg/ml streptomycin, and 0.25 μg/ml amphoericin B. Joint capsule was excised adjacent to the medial and lateral femoral condyles, cut into approximately 5mm x 5mm squares, and

equilibrated for two days (37°C, 5% CO_2). Each section of JC included a section of synovial tissue and was approximately 0.5mm thick.

Injury

After two days of equilibration, disks were allocated into 1 of 8 conditions: (1) free swell, (2) normal cartilage co-cultured with JC (Co), (3) cartilage mechanically injured, and (4) injured cartilage co-cultured with joint capsule (INJ+Co), (5-8) conditions (1)-(4) repeated with addition of growth factors (100ng/ml OP-1 + 300ng/ml IGF-1) throughout culture duration. Growth factor concentration was determined through dose-dependent measure of OP-1 and IGF-1 independently, as previously presented [50]. A custom designed incubator-housed loading apparatus [51] was used to compress cartilage disks. Each cartilage disk designated for mechanical injury was loaded individually in a polysulfone chamber allowing for radially-unconfined compression [36, 39, 40]. Cartilage disks were measured for height, compressed to a final strain of 50% at a velocity of 1mm/sec, and promptly removed and placed in fresh culture media as described previously [44]. Application of this strain and strain rate produced a peak stress on the order of 20MPa. Three to five pieces (to ensure equal amounts of JC tissue) of cut joint capsule were added to Co and INJ+Co conditions.

Short and Longer Term Gene Expression Time Courses

Short Term: Due to the limited amount of cartilage available in young bovine knee joints, experiments were divided into three distinct groups, each containing a control (FS) and control plus treatment (FS+GF). The three experiments consisted of 4 conditions each; all contained FS and FS+GF, the first consisted of Co and Co+GF, the second of INJ and INJ+GF, and the third of INJ+Co and INJ+Co+GF. At time = 0 plugs were injured or treated as prescribed, incubated at 37°C, 5% CO_2, and flash frozen in liquid N_2 at 2, 8, 24, 48, and 72 hours, and placed in -80°C

(medium changed every 48 hours). Each of the time point-conditions in the three experiments contained 6 cartilage disks which were pooled and purposely matched across depth, location, and time to prevent any bias in the results. Joint capsule was also flash frozen in liquid nitrogen at 2, 8, 24, 48, and 72 hours for the Co and Co+GF experiment. *Longer Term*: To examine gene expression for longer periods of time, in a separate experiment, cartilage disks were subjected to the same 8 conditions and were cultured for 1, 4, 8, and 16 days, whereupon the plugs were flash frozen in liquid N_2 and stored in -80°C (medium changed every 2 days) . The shorter term gene expression experiment was repeated six times, using six different animals for each of the three experiments for an n=6. The longer term gene expression experiments were repeated five times, for an n=5.

RNA Extraction and Quantization, Primer Design, and Real-Time PCR

6 disks for each time point and condition were taken from the -80° C freezer and pulverized. In order to prevent RNA degradation, the pulverizing apparatus was constantly cooled using liquid nitrogen. Trizol (Sigma, MO) was added and the tissue was thoroughly homogenized. After chloroform was added, the mixture was transferred to pre-spun phase gel tubes, and spun at 13,000 rpm for 10 minutes at 4° C. The supernatant was removed, and RNA was extracted using Qiagen RNAeasy mini kit protocol with recommended DNase digest (Qiagen). RNA was stored in 50 µl of RNase free water under -80° C conditions. RNA abundance and purity was measured using NanoDrop ND-1000 (NanoDrop Technologies, DE) with abundance ~80ug/ml and purity ~2 (260nm/280nm). 1µg of RNA was reverse transcribed using Applied Biosystems reagents as previously described [44]. Forward and reverse primers for 48 relevant genes (Table 4.1) were designed using Primer3 Software (http://fokker.wi.mit.edu/primer3/input.htm) and Primer Express (Applied Biosystems, CA)

based on bovine genomic sequences, and standard curves were calculated as previously described [52].

Table 4.1. List of Cartilage relevant genes measured by qPCR

ECM	ECM	Proteases	Protease Inhibitors	Transcription Factors	Growth Factors
Aggrecan	Link	MMP-1	TIMP-1	SOX-9	IGF-1
Collagen II	CD-44	MMP-3	TIMP-2	c-Fos	IGF-2
Collagen IX	HAS2	MMP-9	TIMP-3	c-Jun	OP-1
Collagen XI	COMP	MMP-13			bFGF
Fibromodulin	β-actin	ADAMTS-1			TGF-β
Fibronectin		ADAMTS-4			VEGF
Decorin		ADAMTS-5			
Assorted Genes	**Cytokines**	**Oxidation Genes**	**Stress Induced Genes**	**Housekeeping Gene**	
Cox-2	LIF	ALPL	TXNIP	18s	
iNOS	IL-1β	SOD1	HSP90		
Osteocalcin	IL-4	SOD2			
Caspase-3	IL-6	GPX-3			
	TNF-α				
	IL-6R				

Table 4.1 List of 48 cartilage relevant genes measured by qPCR. Primer3 and Primer Express were used to design primers. Standard dilutions were used to calculate relative mRNA copy number.

Once cDNA was obtained, Real-Time PCR was performed using Applied Biosystems ABI 7900ht instrument and SYBR Green Master Mix (SGMM, Applied Biosystems, CA). SGMM was combined with cDNA, and RNase free water was combined with forward and reverse primers. Using a multi-pipette, 8 different samples of cDNA and SGMM were aliquoted into a 384 well plate, followed by 48 different primer and water mixes. Plates were run and inspected for proper amplification and melting curves using SDS 2.3 (Applied Biosystems, CA). Measured threshold values (Ct) were obtained through SDS 2.3 and converted to RNA copy number according to previously calculated primer efficiencies using standard curves.

Protein Biosynthesis

Radiolabel incorporation was measured at days 1, 4, 8, 12, and 16 post-injury. Bovine explants were cultured in fresh media 24 hours prior to 1, 4, 8, 12, and 16 days in 5 μCi/ml $^{35}SO_4$ and 10 μCi/ml ^{3}H-proline. After culture, cartilage explants were washed four times over 60 minutes in 1ml phosphate-buffered saline (PBS) supplemented with 0.8 mM sodium sulfate and

0.5 mM proline to remove free radiolabel, and digested in 1 ml protease K solution (100 pg/ml in SO mM Tris-HCI and 1 mM CaClz at pH 8) at 60°C for 12-18 h. Digested explants were homogenized in Optiphase Supermix scintillation fluid and measured using a Microbeta plate reader.

Apoptosis

At 1, 4, 8, and 16 days post-injury, disks were fixed in 4% paraformaldahyde supplemented with 0.1% 1M NaOH as previously described [42]. In brief, disks were embedded in Paraplast, cut into serial sections (7μm), and sectioned sagitally throughout the entire thickness of the disk. Sections were immobilized on glass slides and stained with Mayer's hematoxylin to quantify the percentage of cells showing nuclear blebbing. Each explant was evaluated in 3–5 sections, as previously described [42]. Since cutting of the explants induces apoptosis at the edges of the tissue, the margins of the sections (~150μm thickness) were excluded. Using a Zeiss Axiophot microscope (Zeiss, Wetzlar, Germany) with a 40x objective, positive and negative cells were counted in 3 optical fields in each section (60–100 cells/field). One optical field was located in the center of the explant sections and 2 were located more peripherally, near the corners of the sections (but not including the margins). The mean value from each field was recorded. In a secondary analysis, cell apoptosis rates in the central and peripheral fields were compared. Encoded labels were used on all samples to ensure blind scoring.

Gene Expression Data Analysis

All data are shown as mean ± SEM. Under each condition and time point, each gene RNA copy number was normalized to the 18s housekeeping gene from that same condition and time point [44, 52]. 18s was chosen in light of recent studies showing the variation in expression

of alternative housekeeping genes (i.e., GAPDH, β-actin) in response to certain conditions of loading of cartilage explants [53]. To examine the time course of gene expression, all conditions were normalized to their corresponding free swell condition. Thus, gene expression values below or above 1 represent a decrease or increase in expression, respectively, compared to FS. Expression levels due to experimental error, as defined by 6σ from mean, were removed. The Wilcoxon sign-ranked test (a non-parametric test which incorporates the amount of data in the significance statistic and avoids the assumption of a parameter-based distribution) was used to judge significance at a p-value less than 0.05. *Clustering and Principle Component Analyses*: In addition to measuring changes in the expression magnitude of each gene, we further explored patterns of co-expression using principle component analysis (PCA) and clustering analysis, performed on all normalized conditions (fold change compared to FS) and time points (2, 8, 24, 48, 72 hours, short term and 1, 4, 8, 16 days, long term) over 47 genes. This resulted in a 35 x 47 (short term) and a 28 x 47 (long term) matrix which were each standardized by expression amplitude as described previously [52]. After normalization of the data using PCA, the maximal dimensional space was reordered according to greatest dimensional variance, where the first three detentions or principle components represent ~70% of the variance in the data [54, 55]. Once the principle components had been calculated, a k-means clustering algorithm was applied to cluster the components into k groups. The average and variance of each projected coordinate group was calculated to give the group centroid. Centroid vectors were formed by combining the three main principal components weighted by their projected centroid coordinate. The uniqueness of each group's expression patterns was evaluated by the Wilcoxon sign-ranked test, and special separation between the centroids was measured and deemed significant through euclidean distance and student's t-test.

Biosynthesis and Apoptosis Data Analysis

All data are represented as mean ± SEM. A three-way analysis of variance was used to test significant differences in biosynthesis data. P-values less than 0.05 were considered significant.

4.3 Results

Short Term Cartilage Gene Expression

Matrix Molecules: Key ECM molecules were downregulated over the three-day period under the *in vitro* injury model. Uninjured cartilage co-cultured with excised joint capsule significantly downregulated Aggrecan (Figure 4.1A), Collagen IX (Figure 4.1B), Collagen XI, Fibromodulin, and HAS2 in a transient manner (Appendix 4.7.1).

Figure 4.1 Aggrecan and Collagen IX gene expression

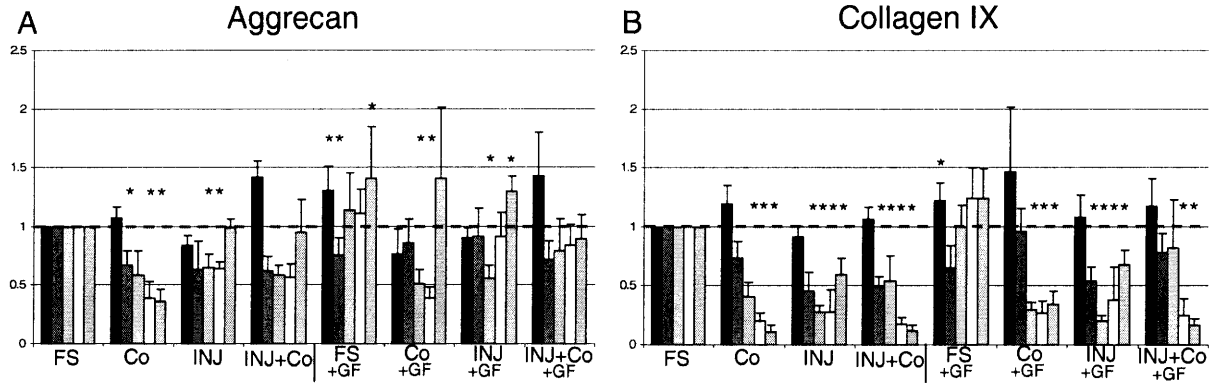

Figure 4.1 Aggrecan and Collagen type IX short-term gene expression. Data was plotted relative to FS conditions, and stars indicate significance (p-values < 0.05) between condition and corresponding FS value. Mean ± SEM. Time points: ■ 2 Hrs, ■ 8 Hrs, □ 24 Hrs, □ 48 Hrs, ▤ 72 Hrs.

At 72 hours, gene expression reached below 0.5 FS values (Aggrecan 0.36, Collagen IX 0.11, Collagen XI 0.19, Fibromodulin 0.18, and HAS2 0.30). While Aggrecan, Collagen XI,

Fibromodulin, and HAS2 showed slight downregulation with INJ and INJ+Co, Collagen IX was significantly downregulated when mechanical injury was present, with or without Co. Fibronectin, Decorin, and CD-44 were significantly upregulated under the injury models, and were most responsive to INJ+Co; reaching maximal values of 4.8-, 4.8-, and 16.6-fold FS values respectively (24hrs) (Appendix 4.7.1). Collagen II was significantly downregulated with INJ alone and INJ+Co but was unaffected with co-culture alone (Appendix 4.7.1). Link Protein, Osteocalcin, and COMP were slightly upregulated with INJ alone, downregulated with co-culture alone, and no different than FS with INJ+Co (Appendix 4.7.1). β-actin was generally unresponsive to the injury models and GF treatment (Appendix 4.7.1). Aggrecan was significantly upregulated when GF was added under FS conditions (Appendix 4.7.2). Fibromodulin was significantly upregulated at 2hrs, followed by a significant downregulation at 8, 48, and 72 hrs. Collagen II, Collagen IX, Collagen XI, Fibronectin, Decorin, Link, CD-44, HAS2, Osteocalcin, and COMP were not dramatically altered by GF treatment under FS (Appendix 4.7.2). Treatment of the GF combination had no effect on Aggrecan, Collagen II, Collagen IX, Collagen XI, Fibromodulin, Fibronectin, Decorin, Link, CD-44, and Osteocalcin under INJ, Co, or INJ+Co, and appeared to marginally upregulate HAS2 and COMP under the same three injury conditions (Appendix 4.7.2).

Proteinases: MMP-3 (stromelysin) was significantly upregulated for 2, 8, 24, and 48 hrs under Co alone, INJ alone, and INJ+Co and returned to FS levels at 72 hrs (Appendix 4.7.1). INJ+Co facilitated the greatest fold upregulation (47x 8hrs) compared to co-culture alone (23x 24hrs) and injury alone (16x 8hrs). In a like manner, MMP-9 and MMP-13 were maximally expressed with INJ+Co (Figure 4.2A, Appendix 4.7.1). MMP-9 and MMP-13 were transiently upregulated and both peaked at the last time-point measured (72hrs). MMP-9 was significantly

upregulated at 8, 24, 48, and 72 hrs and peaked at 47x FS, while MMP-13 was significantly upregulated at 24, 48, and 72 hrs and peaked at 46x FS.

Figure 4.2 MMP-9 and TIMP-1 gene expression

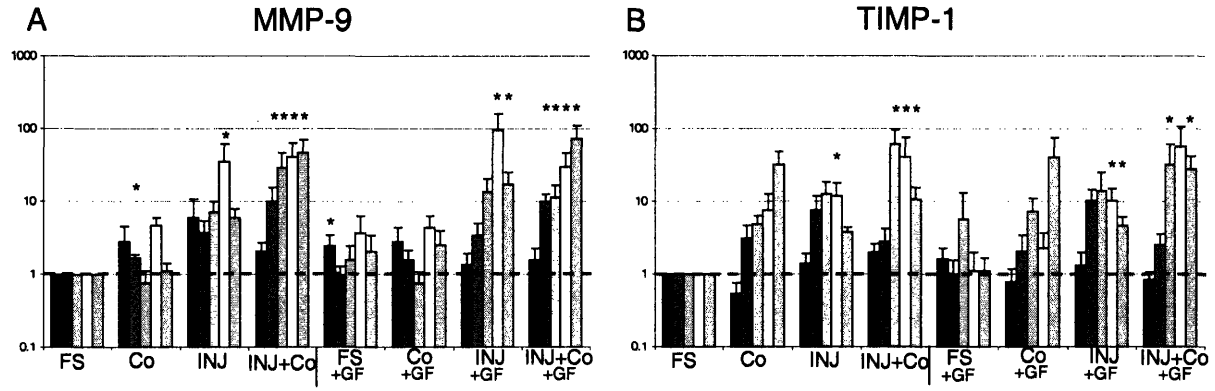

Figure 4.2 MMP-9 and TIMP-1 short-term gene expression. Data was plotted relative to FS conditions, and stars indicate significance (p-values < 0.05) between condition and corresponding FS value. Mean ± SEM. Time points: ■ 2 Hrs, ■ 8 Hrs, ▨ 24 Hrs, □ 48 Hrs, ▤ 72 Hrs.

MMP-1 was slightly upregulated with INJ+Co, but was unaffected by Co and INJ alone (Appendix 4.7.1). Growth factors appeared to stimulate MMP-9 expression by nearly doubling expression under INJ, (35x to 95x) and INJ+Co (47x to 74x) (Appendix 4.7.2). MMP-3 and MMP-13 showed a slight decrease in expression levels when GF was added to INJ+Co, but were unaffected by GF under all other culture conditions (Appendix 4.7.2). MMP-1 was not clearly regulated by GF treatment for all conditions (Appendix 4.7.2). All matrix metalloproteinases showed little to no response to GF treatment under FS conditions. ADAMTS-1 was highly responsive to INJ (40x 8hrs) and INJ+Co (58x 24hrs) but showed little significant difference with Co alone (Figure 4.3A).

Figure 4.3 ADAMTS-1 and iNOS gene expression

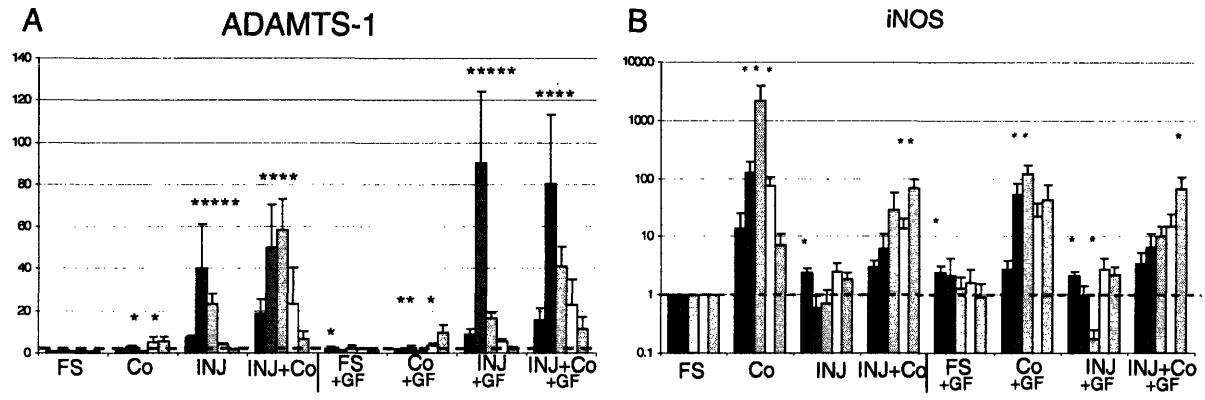

Figure 4.3 ADAMTS-1 and iNOS short-term gene expression. Data was plotted relative to FS conditions, and stars indicate significance (p-values < 0.05) between condition and corresponding FS value. Mean ± SEM. Time points: ■ 2 Hrs, ■ 8 Hrs, □ 24 Hrs, □ 48 Hrs, ▤ 72 Hrs.

ADAMTS-4 was upregulated under Co, INJ, and INJ+Co, but again, the combination of INJ+Co served as the most stimulant (Appendix 4.7.1). ADAMTS-5 appeared to be unresponsive to INJ or Co alone, but the combination of the two lead to a synergistic transient increase of expression, peaking at 14x FS (Appendix 4.7.1). Growth Factor treatment increased expression of ADAMTS-1 and ADAMTS-5 (Appendix 4.7.2). ADAMTS-1 expression was increased at 8hrs for both INJ (40x to 90x) and INJ+Co (49x to 81x) (Figure 4.3A and Appendix 4.7.2). ADAMTS-5 retained the transient upregulation, as seen in the absence of GF, and reached values of 18x FS. ADAMTS-4 showed a slight increase with GF treatment in magnitude of expression for Co, INJ, and INJ+Co (Appendix 4.7.2).

TIMPS: TIMP-1, a general inhibitor of protease activity, was upregulated for INJ and Co alone, but was significantly upregulated when the two were combined (INJ+Co) (Figure 4.2B). Under this condition, TIMP-1 reached a maximum of 61x FS values at 24hrs. To a lesser effect, TIMP-2 was stimulated by INJ, Co, and INJ+Co, and like TIMP-1 was maximally stimulated under INJ+Co (5.7x FS) at 24hrs (Appendix 4.7.1). TIMP-3, an inhibitor which binds at high

affinity to ADAMTS-4, was also maximally stimulated at 24hrs, and in the combination of INJ+Co, reached values 15x greater than FS condition (Appendix 4.7.1). GF treatment had little effect on the TIMPS measured under FS conditions. While the changes in GF treatment were on the same order of magnitude as without GF treatment, it appeared that the addition of GF slightly stimulated all three TIMPS under the conditions of Co, INJ, and INJ+Co (Appendix 4.7.2).

Transcription Factors: c-Jun and c-Fos, both members of the AP-1 complex, were both initially highly responsive to INJ and INJ+Co, but decreased over the time course (Appendix 4.7.1). After 2hr, c-Jun in INJ (23x) and INJ+Co (25x) returned to FS values and was not responsive to Co alone. Alternatively, c-Fos was significantly upregulated for all time points under INJ (transiently decreasing, 13x to 2x) and significantly upregulated for the first 48 hrs (transiently decreasing, 19x to 8x) for INJ+Co. Sox-9 showed little response to Co, INJ, or INJ+Co (Appendix 4.7.1). GF had little effect on expression of transcription factors measured (Appendix 4.7.2).

Enzyme Mediators: Inducible Nitric Oxide Synthase (iNOS) was highly regulated when Co was present (Figure 4.3B). In Co alone, iNOS expression peaked at 24hrs at a magnitude of over 2000 times greater than FS values. iNOS was transiently upregulated under INJ+Co peaking at 69x at 72hrs. INJ alone showed little effect on the production of iNOS. GF treatment was effective in significantly lowering the transcript levels of iNOS under Co alone (2140x to 120x at 24hrs) but did not effect expression under INJ+Co (Figure 4.3B, Appendix 4.7.2). Cox-2 was significantly induced by Co and INJ+Co at early time points, reaching levels of 42x (Co) and 50x (INJ+Co), followed by a return to free swell levels at 72hrs (Appendix 4.7.1). GF showed little difference in Cox-2 expression, with the exception of a slight decrease in expression under INJ+Co (Appendix 4.7.2).

Growth Factors: IGF-2 showed sustained significant downregulation for INJ alone, while IGF-1 was predominantly unaffected by Co, INJ, and INJ+Co (Appendix 4.7.1). OP-1 and VEGF were significantly upregulated at 24 hrs in response to Co alone at magnitudes of 24x and 9x respectively (Appendix 4.7.1). Both were marginally upregulated by INJ alone, and upregulated slightly with INJ+Co. bFGF and TGF-β were upregulated for all conditions and both were maximally expressed at 24hrs under INJ+Co (17x and 11x respectively) (Appendix 4.7.1). GF treatment had little to no effect on IGF-1, IGF-2, bFGF, and TGF-β (Appendix 4.7.2). OP-1 and VEGF showed a slight increase in expression with the GF under Co and INJ+Co conditions (Appendix 4.7.2).

Cytokines: Leukemia Inhibitory Factor (LIF) was maximally expressed under the combination of INJ+Co (76x 2hr), displaying a synergistic effect (Figure 4.4A). IL-4 and IL-1β were both significantly upregulated at 48 hrs under Co (4.7x and 4.0x) and showed an increase of expression under INJ+Co (Appendix 4.7.1). IL-6 and its receptor, IL-6R, were upregulated under Co (5.4x and 4.2x) and INJ+Co (5.4x and 4.6x) (Appendix 4.7.1). TNF-α was significantly upregulated under INJ+Co (Appendix 4.7.1). GF treatment affected the measured cytokines in a minimal amount, with the exception of IL-1β expression returning to FS levels from statistically upregulated levels for INJ+Co (Appendix 4.7.2).

Stress Induced: TXNIP was primarily downregulated by Co alone and HSP90 was significantly upregulated at 2 and 24hrs under INJ+Co (Appendix 4.7.1). GF showed little to no effect on both TXNIP and HSP90 (Appendix 4.7.2).

Figure 4.4 LIF and Caspase-3 gene expression

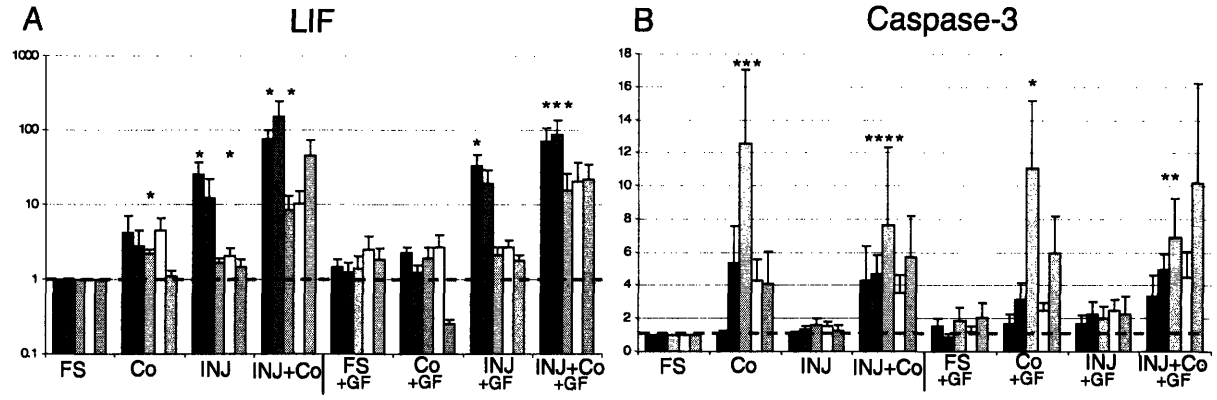

Figure 4.4 LIF and Caspase-3 short-term gene expression. Data was plotted relative to FS conditions, and stars indicate significance (p-values < 0.05) between condition and corresponding FS value. Mean ± SEM. Time points: ■ 2 Hrs, ■ 8 Hrs, □ 24 Hrs, □ 48 Hrs, ▤ 72 Hrs.

Apoptosis and Oxidation Factors: Caspase-3 was significantly upregulated under Co conditions, reaching a > 12x FS level at 24hrs (Figure 4.4B). Caspase-3 was also significantly upregulated under INJ+Co for 2, 8, 24, and 48hrs after injury. Interestingly, caspase-3 under INJ did not show significant difference from the corresponding FS values. When GF was added, caspase-3 levels for Co alone and INJ+Co slightly decreased (Appendix 4.7.2). ALPL and GPX-3 were synergistically upregulated under INJ+Co (Appendix 4.7.1). ALPL showed a peak at 24 hrs (8.4x FS) where GPX-3 was transiently upregulated achieving at value of 9.5x FS at 72hrs. Superoxide Dismutase-1 (SOD1) and Superoxide Dismutase-2 (SOD2) were both slightly upregulated with INJ+Co, reaching levels less than 4 fold FS at 24hrs (Appendix 4.7.1). GF treatment showed little to no effect on ALPL, GPX-3, SOD1, and SOD2 (Appendix 4.7.2).

Clustering: The 47 normalized genes were clustered using PCA and k-means clustering algorithms. After multiple iterations of groups, it was determined through analytical (Pareto plot and euclidean distance separation) measures that there existed 5 distinct groups of genes. The

groups were plotted in the first three principle components, as seen in Figure 4.5, where the first three principle components represent 80% of the variation in the data.

Figure 4.5 Genes Clustered in PC Space

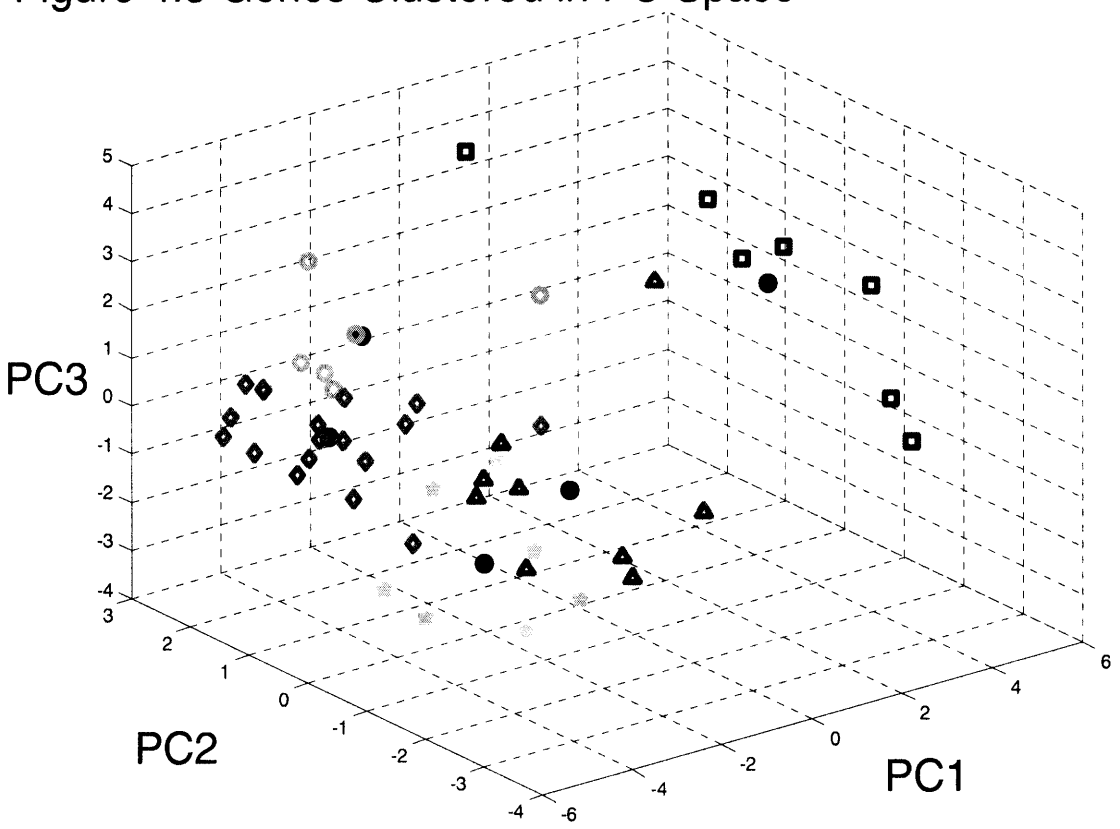

Genes Grouped According to K-means Clustering

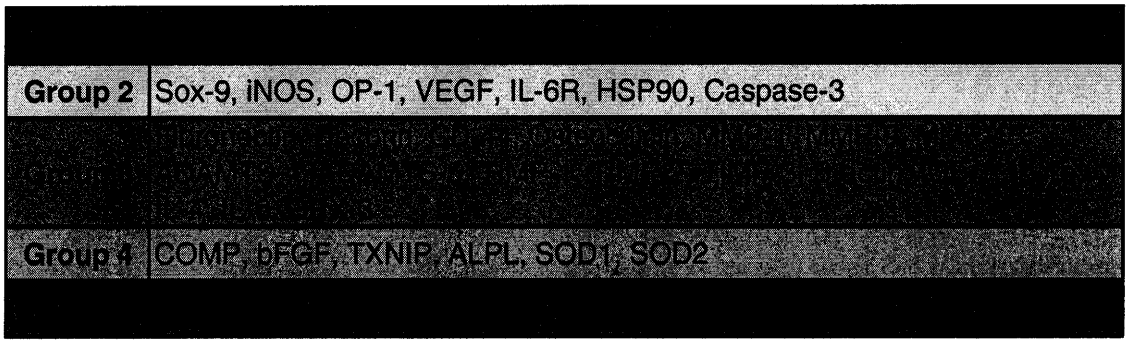

Figure 4.5 Standardized gene expression visualized in principle component space. Principle components 1, 2, and 3 represent 80% of the variance in the data. Genes were allocated to one of five distinct groups by way of k-means clustering. Large solid black circles denote the centroid of the corresponding group.

The corresponding genes in each grouping are shown in Table 4.2. The centroid profile for each of the 5 groupings were converted from principle component space and plotted relative to FS values, as seen in Figure 4.6. The first group, Figure 4.6A, was composed of aggrecan, collagen II, collagen IX, collagen XI, Fibromodulin, Link, and IGF-2. This profile was characterized by the strong downregulation of expression due to Co, INJ, and INJ+Co. The growth factor treatment slightly stimulated the expression of this centroid, but did not dramatically overcome the effects of Co or INJ or the combination of INJ+Co. Group 2 is composed of Sox-9, iNOS, OP-1, VEGF, IL-6R, HSP90, and Caspse-3 (Figure 4.6B). This centroid was characterized by a very strong upregulation to Co (6.5x FS at 24hrs) and to a lesser extent, INJ+Co (3x at 24hrs). GF treatment appeared to change the dynamics of the Co response showing a peak at 72 hrs, but in other conditions GF treatment showed no magnitudinous changes in expression. The third group was composed of fibronectin, decorin, CD-44, Osteocalcin, MMP-1, MMP-9, MMP-13, ADAMTS-4, ADAMTS-5, TIMP-1, TIMP-2, TIMP-3, β-actin, IGF-1, IL-1β, IL-4, IL-6, and GPX-3 (Figure 4.6C). This centroid was characterized by the strong upregulation of expression due to INJ+Co. This centroid profile peaked at 24 hrs at 4x FS. GF treatment showed little significant effect, but appeared to change the temporal dynamics of expression with INJ+Co by altering the peak 24 hr expression to a clear transient upregulation ending at 72hrs (~4x FS). Group 4 was characterized by a slight upregulation due to GF treatment and was composed of COMP, bFGF, TXNIP, ALPL, SOD1 and SOD2 (Figure 4.6D). While INJ+Co stimulated this centroid at levels on the order of 3x (24 hrs), when GF was added to INJ+Co, the centroid reached values of 8x (24 hrs). The Group 5 centroid profile was similar to the Group 3 centroid profile in that it was strongly induced by the combination of INJ+Co. Differing from Group 3, Group 5 showed an increase in expression magnitude, on the order of 2x Group 3. Group 5 was

composed of HAS2, MMP-3, ADAMTS-1, c-FOS, c-JUN, TGF-β, LIF, TNF-α, and Cox-2 (Figure 4.6E). This group was upregulated by Co and INJ alone, but the combination of INJ+Co increased levels of gene expression >6x FS conditions at 8hrs. GF treatment did not appear to show a significant effect on centroid profile for any of the measured conditions for Group 5.

Figure 4.6 Centroid Profiles of Gene Clustering

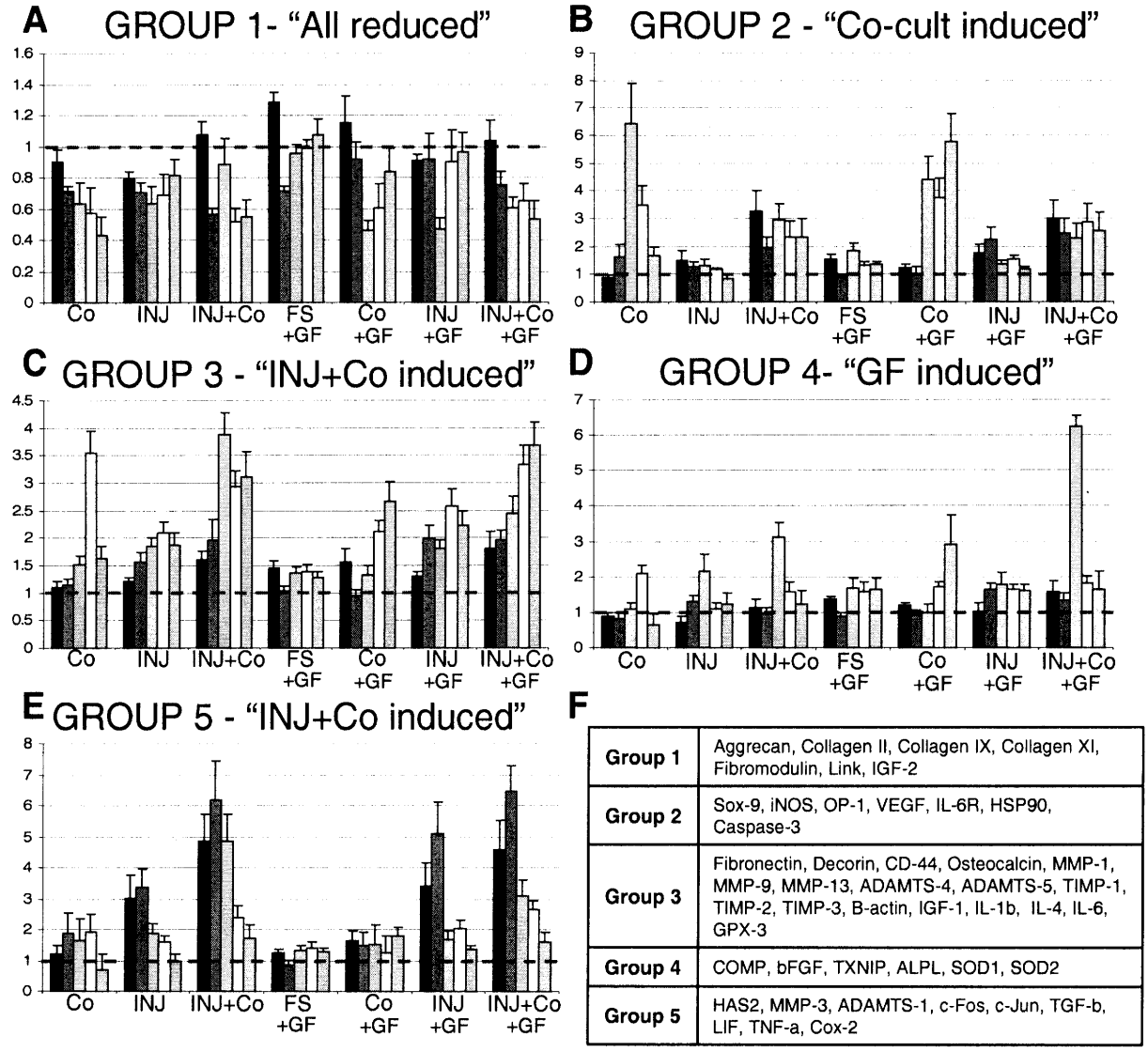

F

Group 1	Aggrecan, Collagen II, Collagen IX, Collagen XI, Fibromodulin, Link, IGF-2
Group 2	Sox-9, iNOS, OP-1, VEGF, IL-6R, HSP90, Caspase-3
Group 3	Fibronectin, Decorin, CD-44, Osteocalcin, MMP-1, MMP-9, MMP-13, ADAMTS-4, ADAMTS-5, TIMP-1, TIMP-2, TIMP-3, B-actin, IGF-1, IL-1b, IL-4, IL-6, GPX-3
Group 4	COMP, bFGF, TXNIP, ALPL, SOD1, SOD2
Group 5	HAS2, MMP-3, ADAMTS-1, c-Fos, c-Jun, TGF-b, LIF, TNF-a, Cox-2

Figure 4.6 Five expression profiles represent the combination of conditions and treatments. Centroid profiles were calculated through the average projection coordinates of genes in each group and transformed from principle component space through use of the calculated principle components. Mean ± SEM (n varies based on group component number). Time points: ■ 2 Hrs, ▩ 8 Hrs, □ 24 Hrs, □ 48 Hrs, ▤ 72 Hrs.

Short-Term Joint Capsule Gene Expression

Understanding that there are multiple cell types and tissues in the joint capsule that may contribute to cartilage homeostasis or degradation, the object of this section was to determine the levels of expression of cartilage-relevant genes and to assess if GF had a stimulatory effect on the JC. Gene expression of joint capsule was taken from the Co experiment, where uninjured cartilage was co-cultured with excised joint capsule, with the addition or absence of GF. The same 48 genes were measured in the JC and, interestingly, all 48 transcript levels were detected. Examining the JC basal level of expression, many proteinases were abundantly expressed. The basal level of gene expression in JC was compared to cartilage in Figure 4.7, where gene transcript abundance was normalized to the least abundant gene (GPX-3 for JC and cartilage).

FIGURE 4.7. BASAL GENE EXPRESSION: JC vs. CARTILAGE

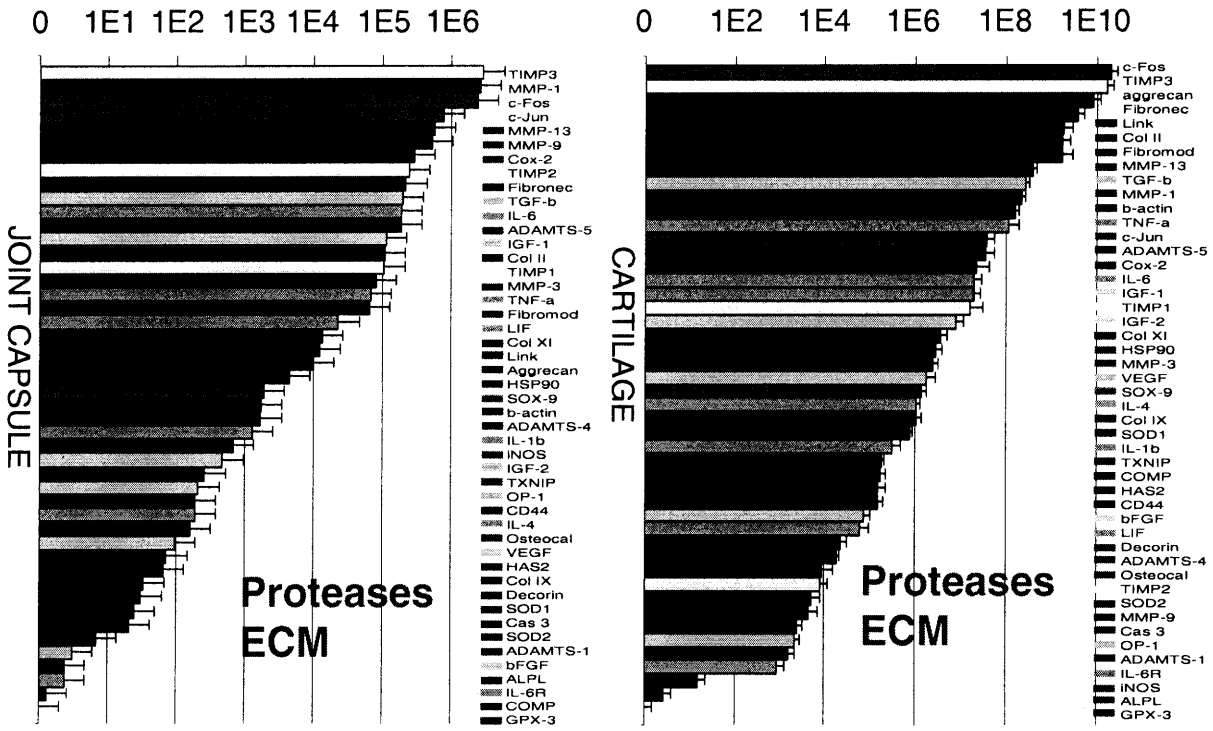

Figure 4.7 Basal levels of gene expression for joint capsule and cartilage relative to the least abundant gene. Proteinases are colored in red; ECM molecules are colored in blue.

All measured proteases were expressed proportionally higher in JC compared to cartilage. Cartilage had a much higher level of abundance compared to JC, but with this difference, MMP-9 and TIMP-2 were more abundantly expressed in JC vs. cartilage (MMP-9 100x higher in JC, TIMP-2 15x higher in JC). The effect of the growth factor on the JC gene expression was primarily and predominantly stimulatory (Appendix 4.7.3). Almost all genes, with the exception of ADAMTS-5, were strongly upregulated, and most genes showed a peak of expression at the 8hr time point. ADAMTS-5 was downregulated for the first 24 hours, returning eventually to non-GF treated JC levels.

Longer-Term Cartilage Gene Expression

Matrix Molecules: Aggrecan, Collagen IX, and Collagen XI continued to be significantly downregulated through day 4 under Co alone. At days 8 and 16, expression levels for Co alone returned to FS levels (Figure 4.8A, Appendix 4.7.4). INJ alone showed no significant difference from FS up to day 16, with the exception of a slight upregulation of Collagen IX at day 8 (1.3x FS). INJ+Co showed no significant difference at later time points compared to FS values.

Figure 4.8 Aggrecan and Fibronectin gene expression

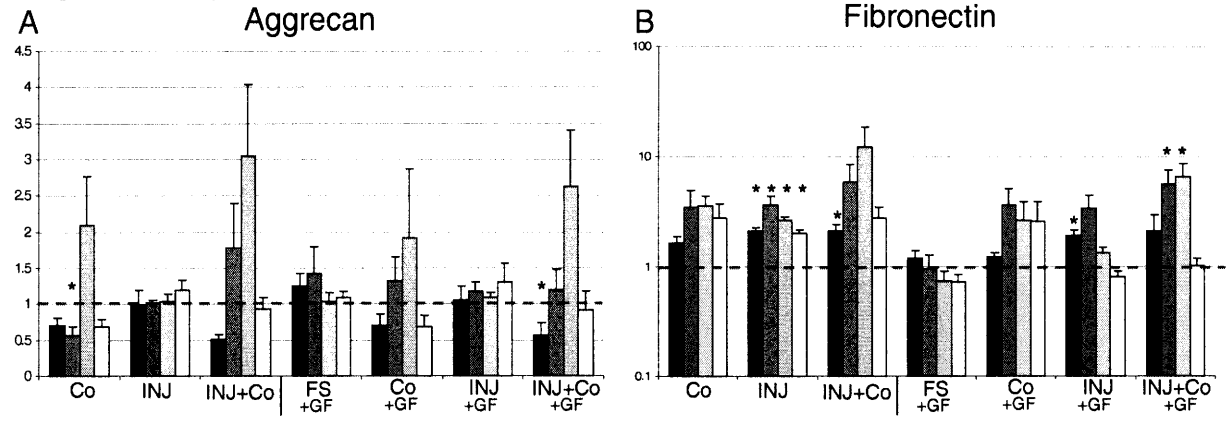

Figure 4.8 Aggrecan and Fibronectin longer-term gene expression. Data was plotted relative to FS conditions, and stars indicate significance (p-values < 0.05) between condition and corresponding FS value. Mean ± SEM. Time points: ■ Day 2, ■ Day 4, □ Day 8, □ Day 16

When growth factors were added for the time course, a significant upregulation was seen in Collagen IX under FS and INJ conditions compared to FS (Appendix 4.7.5). Growth factor treatment showed little significant increase in transcript levels in aggrecan (3x under Co at day 4), collagen IX (2x under Co at day 8, 1.5x under FS at day 16), and collagen XI (1.9x under Co at day 4) (Appendix 4.7.5). Collagen II and osteocalcin showed no significant differences for the time course in Co, INJ, or INJ+Co. When growth factor was present, collagen II was significantly downregulated under INJ at day 1 and day 4 compared to FS, where osteocalcin was unaffected. There was no significant change in expression when comparing the effects of the growth factor treatment to like conditions (Appendix 4.7.5).

Fibromodulin, HAS2, and COMP were significantly downregulated at day 1 under Co, and COMP was significantly downregulated through day 4 under Co (Appendix 4.7.4). Day 8 and day 16 were consistent with FS levels for the three genes under INJ and INJ+Co. When growth factor was added, Co alone resulted in no significant differences at days 4, 8, and 16 compared with FS (Appendix 4.7.5). Under injury, fibromodulin showed a slight increase in

expression at day 4 (1.2x FS) followed by a decrease in expression at days 8 and 16. HAS2 was slightly upregulated at day 8 under INJ+GF (1.4x FS), where COMP was significantly upregulated in a transient fashion, peaking at day 16 with a magnitude of 2.5x FS (Appendix 4.7.4). Fibromodulin, HAS2, and COMP showed no significant differences under INJ+Co compared to FS for days 4, 8, and 16. Further examining the effects of GF treatment under like loading conditions, HAS2 appeared unaffected by GF treatment while fibromodulin appeared to be downregulated, particularly under INJ, and COMP was upregulated for FS, Co, INJ, and INJ+Co (Appendix 4.7.5).

Fibronectin and decorin expression was consistent with FS values under Co, but both were significantly upregulated under INJ (Figure 4.8B, Appendix 4.7.4). Fibronectin was upregulated for all time points measured, with a peak value of 3.6x FS at day 4, and decorin was upregulated at days 4 and 16 with a peak value of 4x FS at day 4. Under INJ+Co, fibronectin was not significantly different than FS for days 4, 8, and 16, while decorin was upregulated at days 4 (2.6x FS) and 8 (6.5x FS). With the addition of GF treatment, there appeared to be no dramatic effect compared to FS (Appendix 4.7.5). When examining the effects of the growth factor under similar injurious conditions, fibronectin and decorin were both dramatically downregulated, with fibronectin significantly downregulated at days 8 and 16 of INJ, and decorin downregulated at day 8 under Co and INJ (Appendix 4.7.5).

Link and CD-44 were not significantly different than FS values for days 4, 8, and 16 under Co and INJ+Co (Appendix 4.7.4). Under INJ alone, link was significantly upregulated at days 4 and 8, while CD-44 was significantly upregulated at day 4. GF treatment appeared to have little effect on Link when comparing the FS values, and a slight increase in expression was found in CD-44 under Co and INJ+Co conditions. Looking at the effects of GF treatment under

like conditions, GF had no effect on CD-44 expression under all conditions and had a slight effect on link under INJ and INJ+Co (Appendix 4.7.5). β-actin showed a slight but significant upregulation under INJ for days 4, 8, and 16 (Appendix 4.7.4). When GF was added, there was no dramatic change in expression compared to FS or like injury condition (Appendix 4.7.5).

Proteinases: MMP-9 showed sustained and dramatic upregulation for Co (peak 144x FS at day 16), INJ (peak 13.3x FS at day 8) and INJ+Co (peak 46x FS at day 16) at days 4, 8, and 16 (Figure 4.9B).

Figure 4.9 MMP-3 and MMP-9 gene expression

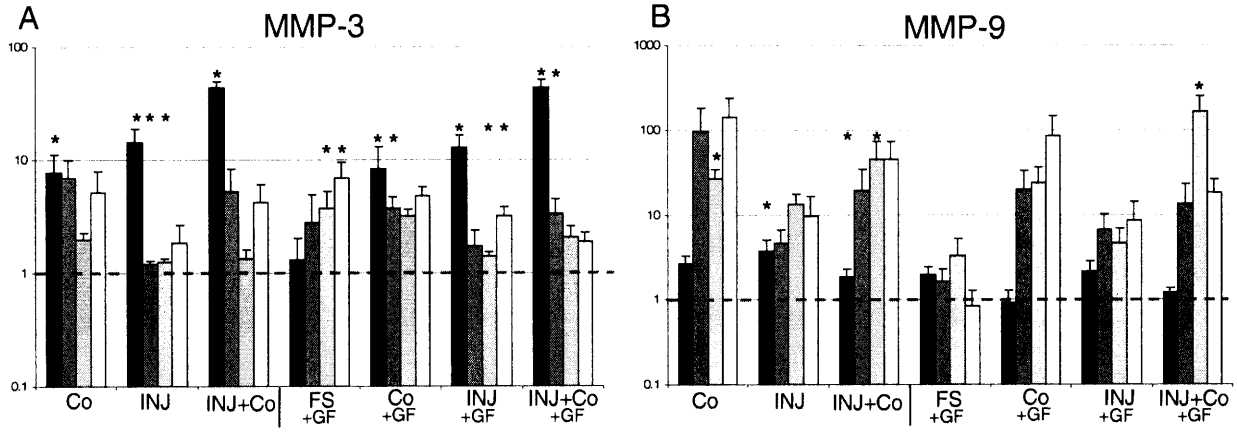

Figure 4.9 MMP-3 and MMP-9 longer-term gene expression. Data was plotted relative to FS conditions, and stars indicate significance (p-values < 0.05) between condition and corresponding FS value. Mean ± SEM. Time points: ■ Day 2, ■ Day 4, □ Day 8, □ Day 16 GF treatment appeared to slightly decrease the levels of MMP-9 in Co and INJ compared to FS. Normalizing the effects of GF by like injury condition, the data revealed there was no significant difference with the GF treatment (Appendix 4.7.5). MMP-1 transcript levels were consistent with FS for Co and INJ for days 4, 8, and 16 (Appendix 4.7.4). Under INJ+Co, there appeared to be a trend of upregulation, with day 8 values significantly different than FS (4x FS). Growth factor treatment had no significant effect on MMP-1 expression compared to FS, but when examining treatment under like conditions, MMP-1 was slightly downregulated at day 4 under INJ alone (Appendix 4.7.5). MMP-3 and ADAMTS-1 were initially upregulated under INJ and

INJ+Co followed by a decrease to FS conditions at day 16 (Figure 4.9A, Appendix 4.7.4). MMP-3 was significantly upregulated at days 4 and 8 of culture under INJ, and ADAMTS-1 was significantly upregulated at day 4 under INJ+Co. When GF treatment was added, MMP-3 and ADAMTS-1 were significantly upregulated at later time points. MMP-3 was transiently upregulated under FS conditions, peaking at a significant 6.9x FS at day 16. MMP-3 was also significantly upregulated at day 16 under INJ (3.2x FS) and day 4 under INJ+Co (3.4x FS).

ADAMTS-1 was significantly upregulated for all time points under INJ+GF with a sustained 2.7x FS at day 16. GF treatment appeared to have no effect on ADAMTS-1 under Co and FS conditions. Looking at GF treatment under like loading conditions, MMP-3 was strongly stimulated by GF under FS conditions and was stimulated to a lesser extent by Co and INJ (Appendix 4.7.5). GF transiently stimulated ADAMTS-1 expression under Co conditions, while uniformly upregulating expression under INJ (Appendix 4.7.5). MMP-13 and ADAMTS-5 were both not statistically different than FS under Co, INJ, and INJ+Co at days 4, 8, and 16, with or without the treatment of GF (Appendix 4.7.4). MMP-13 and ADAMTS-5 were slightly downregulated under INJ and INJ+Co when GF treatment was normalized by like injury conditions (Appendix 4.7.5). ADAMTS-4 was initially upregulated followed by a transient return to slightly above FS levels under INJ and INJ+Co (Appendix 4.7.4). Under Co, ADAMTS-4 showed a trend of upregulation over 16 days, but was not statistically different than FS levels. GF treatment had little to no effect on each of the conditions when compared to FS or when comparing like injury conditions (Appendix 4.7.5).

TIMPS: TIMP-1 and TIMP-3 showed a significant initial increase of expression followed by a transient decrease in expression, returning to FS levels over the 16 days under Co, INJ, and INJ+Co (Figure 4.10A, Appendix 4.7.4). GF treatment did not alter the magnitude of kinetics of

transcript expression of TIMP-1 or TIMP-3 for any of the conditions measured (Appendix 4.7.5). TIMP-2 showed a trend of sustained upregulation under INJ and an initial upregulation followed by a transient return to FS values under Co (Appendix 4.7.4). GF treatment did not induce significant changes in the conditions when compared to FS, but when examining the effect of GF treatment normalized to like injury condition, GF significantly decreased levels of TIMP-2 under INJ conditions (.14x INJ alone at day 16) (Appendix 4.7.5).

Figure 4.10 TIMP-1 and c-Fos gene expression

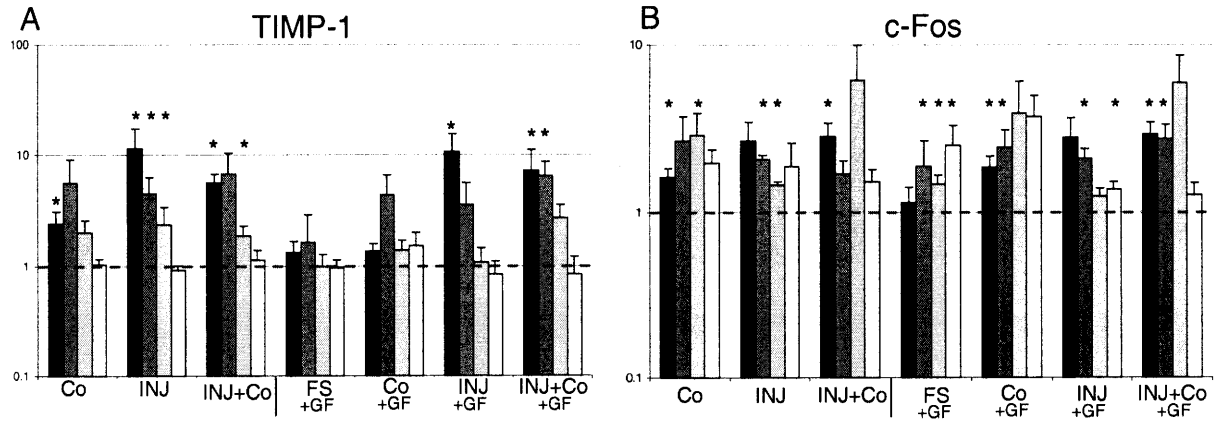

Figure 4.10 TIMP-1 and c-Fos longer-term gene expression. Data was plotted relative to FS conditions, and stars indicate significance (p-values < 0.05) between condition and corresponding FS value. Mean ± SEM. Time points: ■ Day 2, ■ Day 4, □ Day 8, □ Day 16

Transcription Factors: Sox-9 showed no significant difference from FS at days 4, 8, and 16 for Co, INJ, and INJ+Co (Appendix 4.7.4). When GF was present and values were normalized to like injury condition, there were no significant alterations of expression with the exception of Co+GF, where day 4 was significantly upregulated compared to Co. c-Fos showed significant slight upregulation under Co (day 8) and INJ (day 4, 8) (Figure 4.10B). When GF was added, there was an increase in time points that were significantly upregulated (compared to FS), but none were upregulated above 3x FS values. Isolating the effects of GF by normalizing by like injury condition, GF significantly increased c-Fos at days 8 and 16 but had no effect on

Co, INJ, or INJ+Co (Appendix 4.7.5). c-Jun followed a similar trend as c-Fos, where in the absence of GF, there were few values significantly different than free swell, and under GF, many time points were significantly different than FS (FS+GF day 8, 16; INJ+GF day 4, 16) (Appendix 4.7.4). Isolating the effects of the GF treatment, only FS+GF showed any significant change (Appendix 4.7.5).

Enzyme Mediators: iNOS was initially upregulated under Co conditions, and returned to FS levels over the 16-day period (Appendix 4.7.4). GF treatment strongly stimulated iNOS expression under Co (24x at day 4) and INJ+Co (7.3x at day 8). Normalizing to like loading conditions, iNOS was slightly stimulated or not affected by GF (Appendix 4.7.5). Though not significantly different compared to FS, Cox-2 expression tended to increase over the 16-day time course for Co, INJ, and INJ+Co (3x, 2.3x, 4x, respectively at day 16) (Appendix 4.7.4). GF treatment appeared to decrease levels of Cox-2 but no significant differences were seen when isolating the effects of GF (Appendix 4.7.5).

Growth Factors: After slightly above or below FS levels of expression, IGF-1 and IGF-2 appeared to be upregulated at days 8 and 16 under Co, INJ, and INJ+Co (Appendix 4.7.4). Under the treatment of GF, IGF-2 showed a strong upregulation due to GF under FS and Co conditions (Appendix 4.7.5). IGF-1 showed little to no effect when treated with GF (Appendix 4.7.5). OP-1 and VEGF showed significant upregulation at day 8 under Co conditions (2x FS, 6.4x FS respectively). They both also showed little long-term response under INJ alone but an upregulation under INJ+Co at day 8. With GF present, the magnitude of expression of both OP-1 and VEGF declined under Co at day 8 (Appendix 4.7.4). GF treatment on other conditions and time points had little effect. bFGF and TGF-β were both upregulated for later time points (days 8 and 16) under Co and INJ+Co. Under INJ, bFGF and TGF-β were initially upregulated at days

1 and 4 and returned to FS levels at days 8 and 16 (Appendix 4.7.4). The treatment of GF induced a significant increase of expression at day 8 of FS+GF for TGF-β and appeared to have a negative or downregulatory effect on bFGF expression for Co, INJ, and INJ+Co (Appendix 4.7.5).

Cytokines: IL-1β and TNF-α were generally consistent with FS values for days 1, 4, and 8, but tended to increase expression at day 16 for all conditions (Appendix 4.7.4). GF treatment had little effect on IL-1β or TNF-α (Appendix 3.7.5). IL-6 and its receptor, IL-6R, were both upregulated under Co and INJ+Co and unaffected by INJ alone (Appendix 4.7.4). When GF treatment was added, IL-6 showed a slight decrease in expression for Co, INJ, and INJ+Co for days 4, 8, and 16, while IL-6R appeared to be decreased to a lesser degree for INJ and INJ+Co at days 4, 8, and 16 (Appendix 4.7.5). IL-4 and LIF both exhibited trends of transiently increasing expression under Co, INJ, and INJ+Co (Appendix 4.7.4). The effects of GF on IL-4 and LIF expression appeared to slightly downregulate expression at days 4, 8, and 16 under INJ (Appendix 4.7.5).

Stress Induced Factors: TXNIP and HSP90 were both upregulated in response to Co alone. HSP90 was also strongly upregulated under INJ+Co, whereas TXNIP did not appear to respond to INJ and INJ+Co at later time points (Appendix 4.7.4). GF treatment seemed to decrease TXNIP and HSP90 expression compared to FS. TXNIP was significantly downregulated by GF when data was normalized to like injury conditions at day 4 for INJ and INJ+Co (Appendix 4.7.5). HSP90 showed a general increase of expression with the addition of GF, with the exception of INJ+Co, where GF appeared to downregulate HSP90 expression (Appendix 4.7.5).

Apoptotic and Oxidation Factors: Caspase-3 was constantly upregulated for the 4 time points measured for Co and INJ+Co, and to a lesser extent, INJ alone. For each injury condition, Caspase-3 was upregulated at day 1, which was followed by a decrease in expression (Appendix 4.7.4). With the addition of GF, Caspase-3 appeared to be upregulated under INJ and slightly downregulated under Co and INJ+Co. Isolating the effects of GF, GF treatment had very little effect on transcript levels under Co and INJ+Co, and significantly upregulated caspase-3 at day 8 under INJ+GF (1.7x INJ) (Appendix 4.7.5). ALPL and SOD2 showed little to no significant differences compared to FS under Co, INJ, and INJ+Co (Appendix 4.7.4). With the addition of GF, SOD2 showed a slight increase in expression under INJ+Co, and ALPL showed a strong stimulation of expression under INJ and INJ+Co compared to FS at 16 days (Appendix 4.7.5). SOD1 and GPX-3 showed slight upregulation due to Co, INJ, and INJ+Co (Appendix 4.7.4). The treatment of GF decreased expression levels of GPX-3 and SOD1, as seen in INJ+Co. Examining the effects of GF, normalized by like injury condition, GF downregulated GPX-3 at days 4 (INJ, INJ+Co), 8 (Co, INJ+Co), and 16 (INJ, INJ+Co) (Appendix 4.7.5).

Clustering: Clustering analysis revealed three distinct trends for the 47 genes measured (Figure 4.11, Table 4.3).

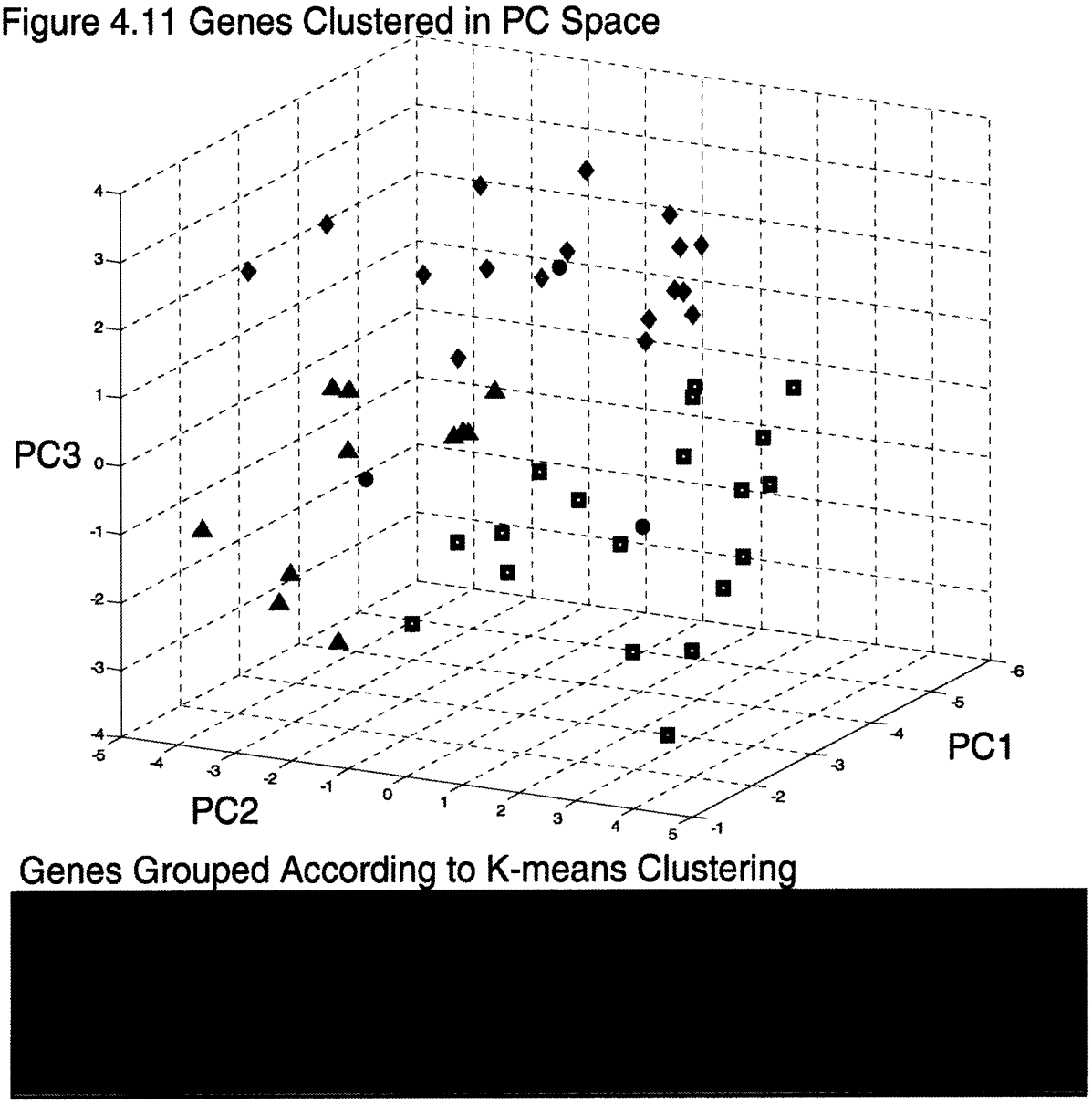

Figure 4.11 Standardized gene expression visualized in principle component space. Principle components 1, 2, and 3 represent 70% of the variance in the data. Genes were allocated to one of five distinct groups by way of k-means clustering. Large solid black circles denote the centroid of the corresponding group.

The first group (11 genes) was composed of Collagen II, Osteocalcin, MMP-13, IGF-1, LIF, IL-1β, IL-4, TNF-α, IL-6R, TXNIP, and GPX-3. This group showed a late response to Co, INJ, and INJ+Co, where all three conditions peaked at 8 or 16 days at a magnitude of 2x FS. The

magnitude of the transcripts was diminished with the addition of GF treatment, while the kinetics of the response was unaffected (Figure 4.12A). Group 2 (17 genes) was composed of Aggrecan, Collagen IX, Collagen XI, Fibromodulin, Fibronectin, Decorin, Link, HAS2, COMP, MMP-1, TIMP-2, SOX-9, c-Jun, β-actin, IGF-2, HSP90, and SOD1.

Figure 4.12 Centroid Profiles of Gene Clustering

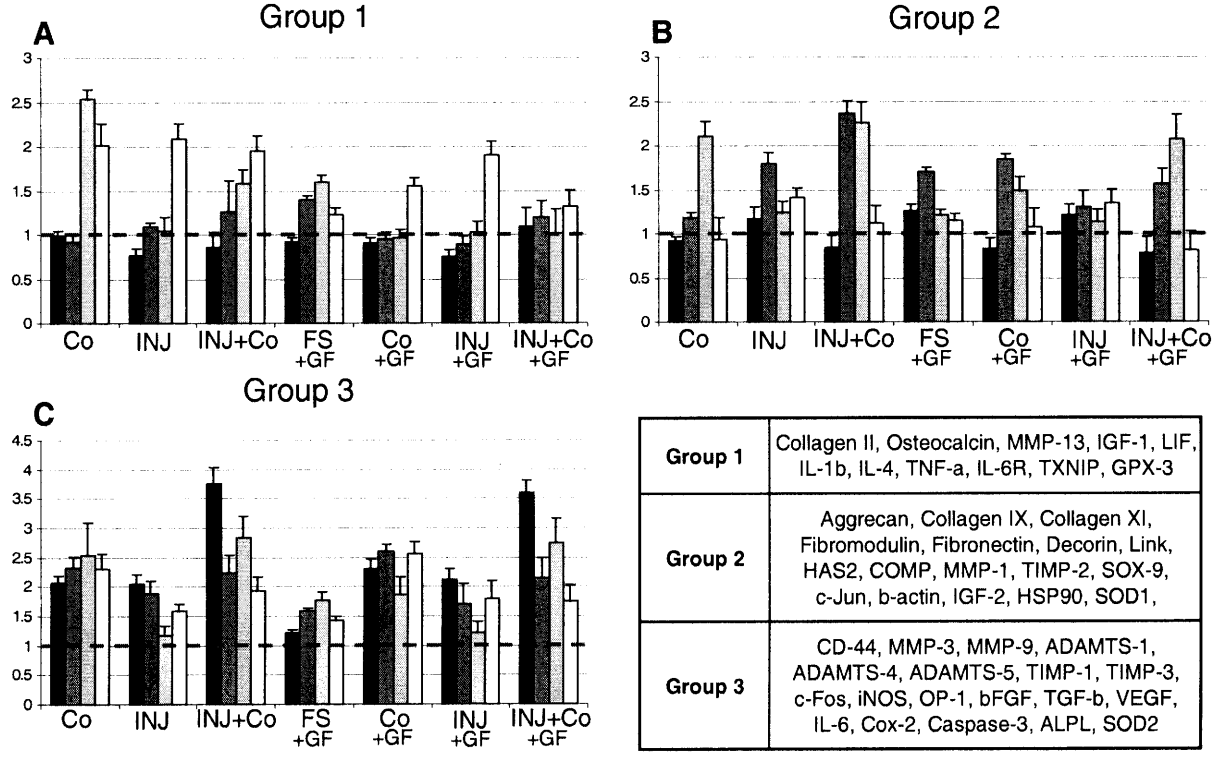

Group 1	Collagen II, Osteocalcin, MMP-13, IGF-1, LIF, IL-1b, IL-4, TNF-a, IL-6R, TXNIP, GPX-3
Group 2	Aggrecan, Collagen IX, Collagen XI, Fibromodulin, Fibronectin, Decorin, Link, HAS2, COMP, MMP-1, TIMP-2, SOX-9, c-Jun, b-actin, IGF-2, HSP90, SOD1,
Group 3	CD-44, MMP-3, MMP-9, ADAMTS-1, ADAMTS-4, ADAMTS-5, TIMP-1, TIMP-3, c-Fos, iNOS, OP-1, bFGF, TGF-b, VEGF, IL-6, Cox-2, Caspase-3, ALPL, SOD2

Figure 4.12 Five expression profiles represent the combination of conditions and treatments. Centroid profiles were calculated through the average projection coordinates of genes in each group and transformed from principle component space through use of the calculated principle components. Mean ± SEM (n varies based on group component number). Time points: ■ Day 2, ▩ Day 4, ▨ Day 8, □ Day 16

With many of the key ECM molecules in this group, the centroid expression was characterized by initial low levels of expression at day 1 compared to FS, followed by increased expression of up to 2x for Co, INJ, and INJ+Co (Figure 4.12B). INJ+Co appeared to be the most effected condition with days 4 and 8 reaching levels above 2x FS. GF slightly increased basal level of expression under the injury models, while FS combined with GF showed an increase in

expression. Group 3 (19 genes) contained CD-44, MMP-3, MMP-9, ADAMTS-1, ADAMTS-4, ADAMTS-5, TIMP-1, TIMP-3, c-Fos, iNOS, OP-1, bFGF, TGF-β, VEGF, IL-6, Cox-2, Caspase-3, ALPL, and SOD2. This group showed sustained upregulation for 16 days with Co alone, decreased expression with INJ, and maximum decreased expression with INJ+Co (Figure 4.12C). GF appeared to have little effect on group 3.

Longer-Term Cartilage Biosynthesis

Radiolabel incorporation was calculated as described previously [32]. Each plug was digested and measured for radiolabeled [^{35}S]-sulfate and [^{3}H]-proline, which was normalized to total DNA. Sulfate incorporation can be seen in Figure 4.13A. Incorporation in all conditions was normalized to incorporation of free swell plugs. Over the 16-day period, INJ+Co showed the most dramatic decrease in incorporation rates and had significantly lower rates at days 1, 8, and 16 compared to FS. INJ alone and Co alone showed no significant change from FS over 16 days. When growth factor was added to the medium, over 16 days there was increased synthesis. INJ alone resulted in a significant improvement in synthesis for days 12 and 16, and INJ+Co significantly improved synthesis for day 8. These growth factor effects on sulfate incorporation can be seen in Figure 4.13B.

Figure 4.13 Sulfate incorporation over 16 days

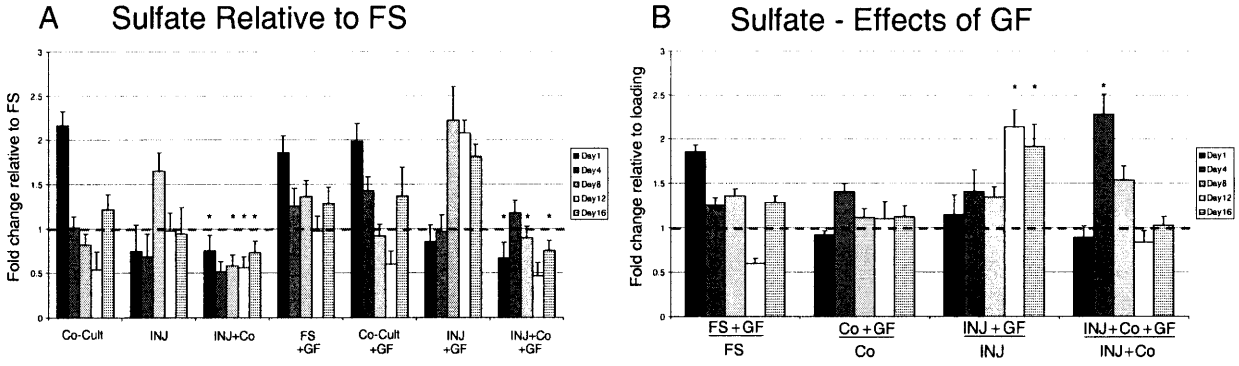

Figure 4.13 Sulfate incorporation measured over 16 days. Data was plotted relative to FS conditions (A) and relative to the corresponding treatment (B). Stars indicate significance (p-values < 0.05) between condition and corresponding FS (A) or treatment (B) value. Mean ± SEM. Time points: ■ Day 2, ▩ Day 4, □ Day 8, □ Day 12, ▤ Day 16.

Examining [^{3}H]-proline incorporation, INJ+Co biosynthesis rates were significantly lower than FS levels, similar to sulfate incorporation results (Figure 4.14A). The addition of growth factor stimulated synthesis in FS, INJ, and INJ+Co conditions relative to FS conditions. There was a significant improvement in biosynthesis for all injury models with the addition of growth factors when comparing to like injury. As seen in Figure 4.14B, when the effects of growth factor treatment are isolated by normalizing to similar injury conditions, there is a significant improvement in biosynthesis rates for all conditions: FS, Co, INJ, and INJ+Co. INJ alone improved greater than 4-fold with the addition of growth factor at days 12 and 16. Slight, but significant, increases were seen at day 4 (FS, INJ+Co), day 8 (FS, INJ+Co), day 12 (FS, Co, INJ+Co), and day 16 (FS, INJ+Co).

Figure 4.14 Proline incorporation over 16 days

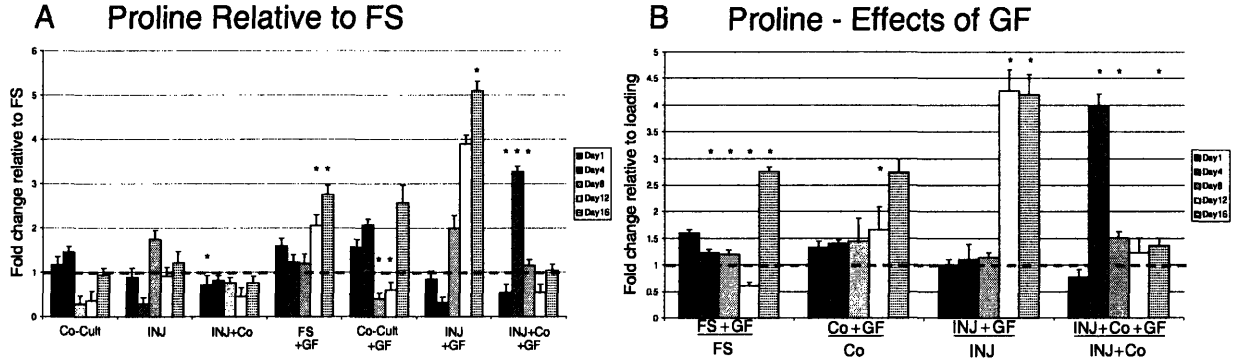

Figure 4.14 Proline incorporation measured over 16 days. Data was plotted relative to FS conditions (A) and relative to the corresponding treatment (B). Stars indicate significance (p-values < 0.05) between condition and corresponding FS (A) or treatment (B) value. Mean ± SEM. Time points: ■ Day 2, ■ Day 4, ▨ Day 8, □ Day 12, ▤ Day 16.

Longer-Term Cartilage Apoptosis

Disks at day 1 showed little to no amounts of apoptosis. Disks at day 4 were sectioned and examined to find the intensity of nuclear blebbing to be insufficient to determine apoptosis accurately. At day 8, INJ and INJ+Co showed significantly larger amounts of apoptosis (Figure 4.15).

Figure 4.15 Levels of Apoptosis at Day 8

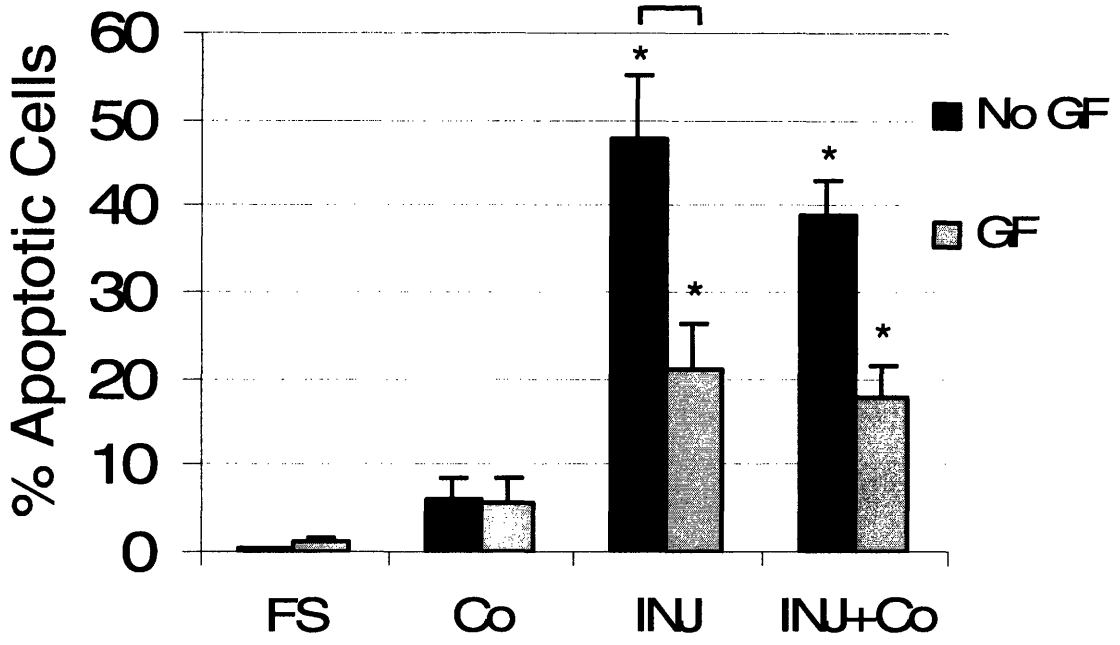

Figure 4.15 Levels of apoptosis 8 days after loading. Percentage apoptotic cells represent the amount of apoptotic cells divided by the total number of cells. Stars indicate significance (p-values < 0.05) between condition and FS. Bar indicates statistical difference (p-values < 0.05) between the two end points. Mean ± SEM.

INJ alone produced 48% apoptotic cells, INJ+Co produced 39% apoptotic cells, and FS produced 0.3%. Co alone produced 6% apoptotic cells and was not statistically different than FS. Examining the effects of GF treatment under INJ alone, GF treatment significantly lowered the amount of apoptosis (p-value = 0.007), from 48% under INJ to 21% under INJ+GF. Day 16 samples were also prepared and can be seen in Figure 4.16. These data show INJ alone has a significant effect on levels of apoptosis after 16 days, where INJ+Co was not significantly different compared to FS conditions. GF treatment reaffirmed the trend seen in the day 8 samples under mechanical injury and mechanical injury co-cultured with joint capsule, though there was no statistically significant difference between GF and non-GF treatment.

Figure 4.16 Levels of Apoptosis at Day 16

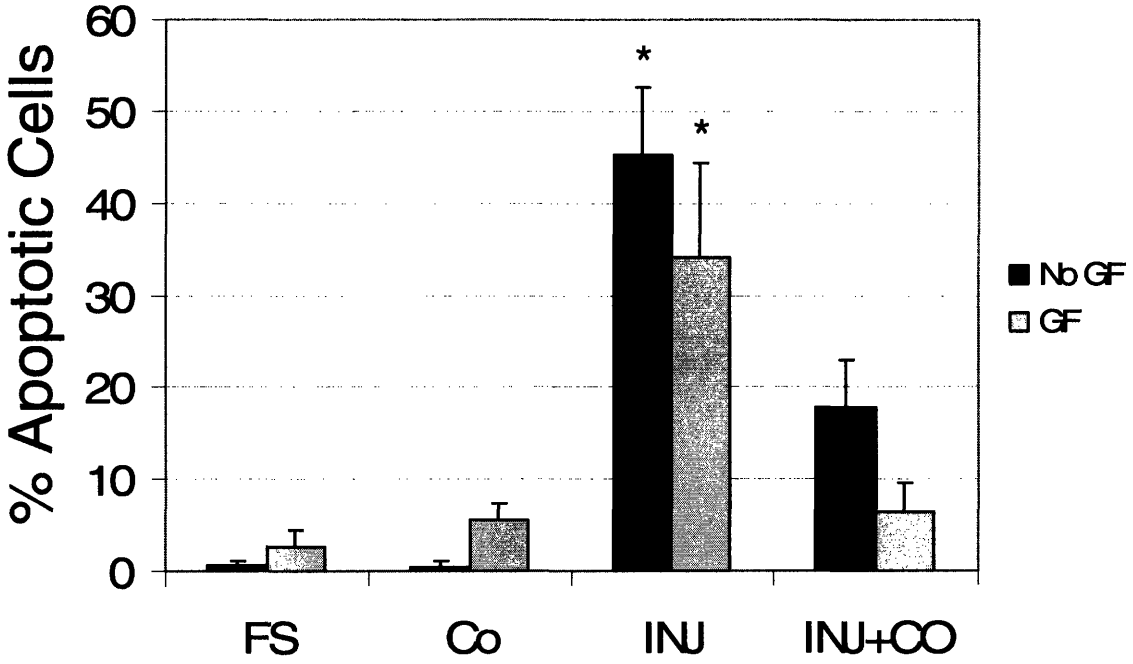

Figure 4.16 Levels of apoptosis 16 days after loading. Percentage apoptotic cells represent the amount of apoptotic cells divided by the total number of cells. Stars indicate significance (p-values < 0.05) between condition and FS. Mean ± SEM.

4.4 Discussion

Short-Term

Mechanical injury co-cultured with excised joint capsule caused modulation of most of the 47 relevant cartilage genes tested by 3 days post-injury. Interestingly, aggrecan, collagen II, collagen IX, collagen XI, fibromodulin, link, and HAS2 were significantly downregulated for Co, INJ, and/or INJ+Co (Figures 4.1). These data agree with previous transcript data reported for aggrecan and collagen type II [33]. The addition of excised joint capsule showed the most significant change in expression for aggrecan, collagen IX, collagen XI, fibromodulin, link, and

HAS2, supporting evidence that there is a key mediator, originating in damaged joint capsule, which has a more suppressive effect on these transcripts' expression than mechanical injury alone.

Having the opposite response as the injury models, fibronectin, decorin, and CD-44 were significantly upregulated when placed in Co, INJ, and/or INJ+Co conditions. The response of CD-44 (a cell-surface glycoprotein known to bind hyaluronic acid and interact with collagens and MMPs) and decorin (proteoglycan that aids structure of collagen network) appears to be an anabolic or reparative response to injury. However, it is unclear whether fibronectin upregulation is an anabolic response, contributing towards its function as a building block of the ECM and cell adhesion, or a catabolic response; when cleaved by proteolytic activity, fibronectin fragments (upregulated in injury models) stimulate protease activity and cartilage degradation [56, 57].

Matrix metalloproteinases 1, 3, 9, and 13 were upregulated and all showed maximal stimulation under the combination of INJ+Co. As previously reported, MMP-1, MMP-3, and MMP-13 were upregulated within the first 24 hours post injury [33, 53, 58], and these data show a continued upregulation of MMP-13 through day 3, reaching 46x FS levels. Not previously reported, MMP-9 was highly upregulated under INJ+Co and mirrored expression of the most highly expressed TIMP, TIMP-1. Both were significantly upregulated under Co, INJ, and INJ+Co (Figure 4.2A, B). This finding supports the notion that TIMP-1, a general inhibitor of protease activity and a known inhibitor of MMP-9 [59, 60], and MMP-9, a collagenase responsible for degrading decorin, collagens, and activating proTNF-α, are co-regulated in chondrocytes in order to maintain a proper balance of proteolytic activity [61-63]. ADAMTS-1, ADAMTS-4, and ADAMTS-5 were maximally expressed under INJ+Co, again showing that the

combination of mechanical injury co-cultured with joint capsule has an additive (ADAMTS-1,2) and synergistic effect (ADAMTS-5) (Figure 4.3A).

iNOS induction has been reported in crushed or injured tendon and synovium [64], and through autocrine signaling coincides with the significant upregulation in cartilage iNOS in response to excised joint capsule shown here (Figure 4.3B). Leukemia inhibitory factor (LIF), an IL-6 class cytokine, was highly upregulated with the addition of Co, INJ, and INJ+Co, reaching values above 100x FS (Figure 4.4A). Previous studies have also shown a strong upregulation of LIF in response to chondrocytes treated with IL-1β [65]. This suggests that IL-1β stimulation and INJ+Co stimulation have common mediators responsible for stimulation of LIF.

Previous studies have shown that OP-1 transcript expression acts in an initial reparative response in reaction of capsular incision [26]; though a different model of injury was used, our data agree with this finding and show that OP-1 transcripts were highly upregulated when excise joint capsule was present (Co and INJ+Co). Following a similar response to OP-1, growth factors bFGF and VEGF were strongly upregulated in the case of Co, INJ, and INJ+Co. Yet unlike OP-1, bFGF at elevated levels has been shown to inhibit and reduce anabolic activity by IGF-1 and OP-1 [12] and has been shown to stimulate matrix metalloproteinases, such as MMP-13 [66]. VEGF, like bFGF, has been shown to promote cartilage degradation pathways [67], and here we report a strong upregulation of VEGF under Co, INJ, and INJ+Co. Together this suggests that VEGF and bFGF result in catabolic responses in our injury models.

Growth factor treatment was generally insufficient to negate the strong catabolic effects of the injury model on the transcript level. The combination of OP-1 and IGF-1 actually appeared to stimulate, not abrogate, protease transcript levels, as seen in MMP-9, ADAMTS-1,

and ADAMTS-5. In addition, known catabolic factors bFGF and VEGF were stimulated to a greater extent with the addition of GF. GF treatment did significantly downregulate the response of inducible nitric oxide synthase, and to a lesser extent, the expression of tumor necrosis factor-α.

Clustering analysis showed genes allocated into 5 significantly separated groups (Table 4.4). Clustering allocated genes into groups that were highly upregulated (Group 2) or downregulated (Group 1) in response to co-culture, the combination of injury and co-culture (Groups 3 and 5), and a slight responsiveness to GF treatment (Group 4) (Figure 4.6). Clustering showed robust grouping of key ECM molecules including aggrecan, collagen II, collagen IX, collagen XI, fibromodulin, and link protein. Interestingly, all proteases and cytokines measured were clustered in groups that were maximally expressed under the combination of mechanical injury co-cultured with joint capsule. This introduces the idea that protease transcripts in chondrocytes are modulated by mechanical forces and factors from surrounding tissues (additive/synergistic manner), whereas iNOS, OP-1, and caspase-3 transcripts are modulated predominantly by factors from the surrounding tissue.

Table 4.2 Centroid Uniqueness- Short Term

P-value of Centroid Separation	Centroid 1	Centroid 2	Centroid 3	Centroid 4
Centroid 2	0.009			
Centroid 3	0.000	0.035		
Centroid 4	0.014	0.049	0.048	
Centroid 5	0.004	0.039	0.023	0.014

Table 4.2. P-value of Centroid Profile Separation. P-values were obtained through student T-test, comparing centroid to centroid Euclidean distance. Degrees of freedom were taken as the number of genes in each group.

Joint capsule is composed of multiple different cell types including synoviocytes, synovial fibroblasts, and lymphocytes [68]. Understanding that multiple cell types may contribute to an analysis of joint capsule gene expression, samples were taken to investigate a global expression level of cartilage relevant genes and the tissue's response to the combination GF treatment. The basal level of joint capsule gene expression reveals a proportionally large number of proteolytic transcripts being produced in the JC (Figure 4.7). MMP-1, MMP-3, MMP-9, and MMP-13 and ADAMTS-1, ADAMTS-4, and ADAMTS-5 were expressed abundantly, as seen in previous experiments [69-72]. In particular, MMP-9 was expressed orders of magnitude greater in joint capsule compared to cartilage. MMP-9 or gelatinase-B has been shown to be increased in osteoarthritis [73]. This tissue also produced small amounts of aggrecan and collagen type II, two transcripts that are characteristic of a chondrocyte phenotype and that have been previously reported within joint capsule cells [74]. GF treatment stimulated all measured genes in the JC with the exception of ADAMTS-5, hinting at a possible positive effect of the treatment in an adjacent tissue (Appendix 4.7.3). This transcriptional data supports the idea that the synovial membrane is a good target for investigation for both the pathogenesis and progression of osteoarthritis [75].

Longer-Term

Examining gene expression over a longer period of time, up to 16 days, showed most ECM molecules return to their respective FS values by day 16. Aggrecan was slightly upregulated with the addition of joint capsule (Co and INJ+Co) at day 8, which was followed by FS levels at day 16 (Figure 4.8A). Fibronectin was dramatically and significantly upregulated by INJ alone for all 4 time points measured (Figure 4.8B). Growth factor treatment tended to

slightly alter dynamics in expression over the 16 days, and collagen IX and COMP were statistically upregulated under FS and INJ conditions for longer time points (days 8 and 16). These data might explain the slight increase in proteoglycan synthesis with growth factor treatment on the same timescale. Also interesting to note, levels of COMP in the synovial fluid has recently been suggested to be a marker for cartilage degradation and possibly play a role in cartilage degradation and inflammation [76-78].

Matrix metallo-proteinases showed significant increases in gene expression over the 16-day period. MMP-9, shown to be extremely active in the first three days post-injury, was upregulated at day 16 under Co and INJ+Co (Figure 4.9B). TIMPs, ADAMs, and transcription factors returned to FS levels by day 16. GF treatment increased transcript levels of MMP-3, c-Fos, and c-Jun at days 8 and 16 (Figure 4.9A, 4.10B). As reported here and previously [44, 50, 52, 79], c-Fos and c-Jun are regulated by injury or mechanical forces on small time scales (i.e. hours). These data show that c-Fos and c-Jun are positively regulated by GF treatment on longer time scales (i.e. days, weeks) as well. The upregulation of components of the activator protein-1 complex (AP-1) due to GF treatment supports the corresponding upregulation of MMP-3 (stromelysin-1) and MMP-9 (gelatinase-B) as previous reports have shown AP-1 to be a promoter of many MMPs, including MMP-3 and MMP-9 [80-83]. Interestingly, TIMP-1 tracked expression of MMP-9 in the first 3 days, but at days 8 and 16, TIMP-1 returned to FS levels while MMP-9 continued high levels of expression (Figure 4.9B, 4.10A). TIMP-2 transcript levels were downregulated at day 16 when joint capsule was present (Co and INJ+Co), and previous studies have shown TIMP-2 to be significantly reduced in canine OA cartilage [84].

Previous studies have shown that in late-stage osteoarthritic chondrocytes GPX-3, SOD2, SOD3, and TXNIP were significantly downregulated in comparison to non-osteoarthritic

chondrocytes [85]. In our longer-term investigation of genes involved in the defense of oxidative damage, TXNIP, SOD1, SOD2, and GPX-3 were not significantly downregulated at day 16, but SOD1, SOD2, and TXNIP showed signs of downregulation under many of the conditions, particularly INJ+Co. This downregulation of oxidation enzymes and TIMP-2, as seen in OA tissue, validates the co-culture model as an *in vitro* model of OA. Interestingly, key cytokines measured, TNF-α, IL-1β, IL-4, and LIF, were highly expressed, though quite variable, after 16 days post-injury. This suggests an additional transcriptional cue that might explain the onset of cartilage degradation on longer-term time scales, similar to MMP-9 expression mentioned previously.

Clustering analysis partitioned the genes in three groups: (1) transcript levels are increased at later time points (days 8. 16), (2) transcript levels peak at days 4 and 8 and return to FS, and (3) transcripts that are generally upregulated under different dynamics with Co, INJ, and INJ+Co (Figure 4.12). These groupings were statistically unique compared to one another (Table 4.5). As seen in expression levels over a shorter-time period, GF treatment generally showed little effect on transcript levels.

Table 4.3 Centroid Uniqueness- Longer Term

P-value of Centroid Separation	Centroid 1	Centroid 2
Centroid 2	0.008	
Centroid 3	0.006	0.009

Table 4.3. P-value of Centroid Profile Separation. P-values were obtained through student T-test, comparing centroid to centroid Euclidean distance. Degrees of freedom were taken as the number of genes in each group.

Proteoglycan incorporation rates showed significantly lower rates under INJ+Co for ^{35}S and ^{3}H. GF treatment showed a significant increase in biosynthesis rates for ^{35}S under INJ for

later time points (days 12 and 16) and INJ+Co (Figure 4.13B). This result is not seen with the aggrecan transcript levels, showing the discrepancy between GF action on transcription compared to translation. When GF treatment was examined for ^{3}H, biosynthesis rates dramatically increased for all conditions (FS, Co, INJ, INJ+Co) (Figure 4.14B). While ^{3}H is not a specific marker of a particular molecule like ^{35}S (aggrecans have abundant sulfated GAG chains), from our clustering data, a majority of the collagens and ECM molecules measured were allocated to group 2, which showed an increase in expression at days 4 and 8. While we cannot definitively state that transcript levels correspond to ^{3}H incorporation, the data suggests a correlation between transcript and translated protein levels.

As seen previously, apoptosis was increased when mechanical injury was present [42]. Although apoptosis has been shown to be initiated as quickly as 24 hours post-injury [38], we found examining later time points distinctly showed the effect of apoptosis on the cartilage explants. Day 8 showed significant levels of apoptosis under injury. While co-culture alone did not show a significant difference compared to FS, there was a trend of Co increasing the amount of apoptosis (Figure 4.15). Caspase-3, cysteine-aspartic acid protease, is a known player in the execution of cell suicide. Caspase-3 transcript was found to be upregulated in the first three days under Co alone (Figure 4.4B), and continued to be upregulated until day 16. Caspase-3 transcript significantly increased with the addition of GF under all conditions, and particularly in injury. Where previous work with human articular chondrocytes and murine bone marrow neutrophils has shown that the inhibition of caspase-3 activity leads to apoptosis mitigation [86, 87], these data show that increase of caspase-3 transcript does not correlate with cell apoptosis.

4.5 Conclusion

This study has examined the transcriptional, translational, and apoptotic effects of various models of cartilage injury in combination with growth factor stimulus. ECM genes were generally downregulated and proteases upregulated in response to Co, INJ, and/or INJ+Co, where genes predominantly responded most dramatically to INJ+Co for both short-term and longer-term expression. GF treatment failed to rescue the downregulation of ECM transcripts and the upregulation of protease transcripts. Clustering analysis of both short-term and longer-term gene expression showed distinct groupings of co-regulated genes. Joint capsule gene expression was also measured and revealed that protease production is much higher in joint capsule when compared to cartilage tissue. Growth factor treatment stimulated all genes measured in the JC, with the exception of ADAMTS-5. Examining the rates of biosynthesis, Co and INJ+Co dramatically affected uptake of ^{35}S and ^{3}H over the 16 day time period measured. After treatment with OP-1 and IGF-1, protein biosynthesis rates (^{3}H-proline incorporation) improved dramatically, while proteoglycan biosynthesis (^{35}S-sulfate incorporation) only slightly increased. Dramatic amounts of apoptosis were measured after mechanical injury. JC appeared to have little effect on apoptosis. Growth factor treatment significantly decreased levels of apoptosis under mechanical injury alone.

In conclusion, the *in vitro* models of injury, Co, INJ, and INJ+Co, mimic certain aspects of joint injury result in changes in cartilage metabolism *in vivo*. Growth factor treatment had a

slightly stimulatory effect on biosynthesis rates, caused a significant decrease apoptosis, and had little effect on recovering gene transcripts after injury. While OP-1 and IGF-1 had a positive effect on apoptosis, these data support the role of OP-1 and IGF-1 as remodeling factors, as opposed to anti-catabolic and pro-anabolic factors as has been previously reported. Further studies are needed to understand the mechanistic action of OP-1 and IGF-1 to clarify their reparative and possible therapeutic capabilities.

4.6 References

1. Wozney, J.M., V. Rosen, A.J. Celeste, L.M. Mitsock, M.J. Whitters, R.W. Kriz, R.M. Hewick, and E.A. Wang, *Novel regulators of bone formation: molecular clones and activities.* Science, 1988. **242**(4885): p. 1528-34.
2. Massague, J. and Y.G. Chen, *Controlling TGF-beta signaling.* Genes Dev, 2000. **14**(6): p. 627-44.
3. Cook, S.D., L.P. Patron, S.L. Salkeld, and D.C. Rueger, *Repair of articular cartilage defects with osteogenic protein-1 (BMP-7) in dogs.* J Bone Joint Surg Am, 2003. **85-A Suppl 3**: p. 116-23.
4. Urist, M.R., A. Mikulski, and A. Lietze, *Solubilized and insolubilized bone morphogenetic protein.* Proc Natl Acad Sci U S A, 1979. **76**(4): p. 1828-32.
5. Flechtenmacher, J., K. Huch, E.J. Thonar, J.A. Mollenhauer, S.R. Davies, T.M. Schmid, W. Puhl, T.K. Sampath, M.B. Aydelotte, and K.E. Kuettner, *Recombinant human osteogenic protein 1 is a potent stimulator of the synthesis of cartilage proteoglycans and collagens by human articular chondrocytes.* Arthritis Rheum, 1996. **39**(11): p. 1896-904.
6. Chubinskaya, S., C. Merrihew, G. Cs-Szabo, J. Mollenhauer, J. McCartney, D.C. Rueger, and K.E. Kuettner, *Human articular chondrocytes express osteogenic protein-1.* J Histochem Cytochem, 2000. **48**(2): p. 239-50.
7. Merrihew, C., B. Kumar, K. Heretis, D.C. Rueger, K.E. Kuettner, and S. Chubinskaya, *Alterations in endogenous osteogenic protein-1 with degeneration of human articular cartilage.* J Orthop Res, 2003. **21**(5): p. 899-907.
8. Fan, Z., S. Chubinskaya, D.C. Rueger, B. Bau, J. Haag, and T. Aigner, *Regulation of anabolic and catabolic gene expression in normal and osteoarthritic adult human articular chondrocytes by osteogenic protein-1.* Clin Exp Rheumatol, 2004. **22**(1): p. 103-6.
9. Chubinskaya, S., B. Kumar, C. Merrihew, K. Heretis, D.C. Rueger, and K.E. Kuettner, *Age-related changes in cartilage endogenous osteogenic protein-1 (OP-1).* Biochim Biophys Acta, 2002. **1588**(2): p. 126-34.
10. Loeser, R.F., C.A. Pacione, and S. Chubinskaya, *The combination of insulin-like growth factor 1 and osteogenic protein 1 promotes increased survival of and matrix synthesis by normal and osteoarthritic human articular chondrocytes.* Arthritis Rheum, 2003. **48**(8): p. 2188-96.
11. Chubinskaya, S., A. Hakimiyan, C. Pacione, A. Yanke, L. Rappoport, T. Aigner, D.C. Rueger, and R.F. Loeser, *Synergistic effect of IGF-1 and OP-1 on matrix formation by normal and OA chondrocytes cultured in alginate beads.* Osteoarthritis Cartilage, 2007. **15**(4): p. 421-30.
12. Loeser, R.F., S. Chubinskaya, C. Pacione, and H.J. Im, *Basic fibroblast growth factor inhibits the anabolic activity of insulin-like growth factor 1 and osteogenic protein 1 in adult human articular chondrocytes.* Arthritis Rheum, 2005. **52**(12): p. 3910-7.
13. Nishida, Y., C.B. Knudson, W. Eger, K.E. Kuettner, and W. Knudson, *Osteogenic protein 1 stimulates cells-associated matrix assembly by normal human articular chondrocytes: up-regulation of hyaluronan synthase, CD44, and aggrecan.* Arthritis Rheum, 2000. **43**(1): p. 206-14.

14. Khalafi, A., T.M. Schmid, C. Neu, and A.H. Reddi, *Increased accumulation of superficial zone protein (SZP) in articular cartilage in response to bone morphogenetic protein-7 and growth factors.* J Orthop Res, 2007. **25**(3): p. 293-303.
15. Saas, J., J. Haag, D. Rueger, S. Chubinskaya, F. Sohler, R. Zimmer, E. Bartnik, and T. Aigner, *IL-1beta, but not BMP-7 leads to a dramatic change in the gene expression pattern of human adult articular chondrocytes--portraying the gene expression pattern in two donors.* Cytokine, 2006. **36**(1-2): p. 90-9.
16. Stove, J., B. Schneider-Wald, H.P. Scharf, and M.L. Schwarz, *Bone morphogenetic protein 7 (bmp-7) stimulates proteoglycan synthesis in human osteoarthritic chondrocytes in vitro.* Biomed Pharmacother, 2006. **60**(10): p. 639-43.
17. Im, H.J., C. Pacione, S. Chubinskaya, A.J. Van Wijnen, Y. Sun, and R.F. Loeser, *Inhibitory effects of insulin-like growth factor-1 and osteogenic protein-1 on fibronectin fragment- and interleukin-1beta-stimulated matrix metalloproteinase-13 expression in human chondrocytes.* J Biol Chem, 2003. **278**(28): p. 25386-94.
18. Chubinskaya, S., M. Hurtig, and D.C. Rueger, *OP-1/BMP-7 in cartilage repair.* Int Orthop, 2007.
19. Bonassar, L.J., A.J. Grodzinsky, A. Srinivasan, S.G. Davila, and S.B. Trippel, *Mechanical and physicochemical regulation of the action of insulin-like growth factor-I on articular cartilage.* Arch. Biochem. Biophys., 2000. **379**(1): p. 57-63.
20. Bonassar, L.J., A.J. Grodzinsky, E.H. Frank, S.G. Davila, N.R. Bhaktav, and S.B. Trippel, *The effect of dynamic compression on the response of articular cartilage to insulin-like growth factor-1.* J. Orthop. Res., 2001. **19**: p. 11-17.
21. Izal, I., C.A. Acosta, P. Ripalda, M. Zaratiegui, J. Ruiz, and F. Forriol, *IGF-1 gene therapy to protect articular cartilage in a rat model of joint damage.* Arch Orthop Trauma Surg, 2007.
22. Huch, K., B. Wilbrink, J. Flechtenmacher, H.E. Koepp, M.B. Aydelotte, T.K. Sampath, K.E. Kuettner, J. Mollenhauer, and E.J. Thonar, *Effects of recombinant human osteogenic protein 1 on the production of proteoglycan, prostaglandin E2, and interleukin-1 receptor antagonist by human articular chondrocytes cultured in the presence of interleukin-1beta.* Arthritis Rheum, 1997. **40**(12): p. 2157-61.
23. Koepp, H.E., K.T. Sampath, K.E. Kuettner, and G.A. Homandberg, *Osteogenic protein-1 (OP-1) blocks cartilage damage caused by fibronectin fragments and promotes repair by enhancing proteoglycan synthesis.* Inflamm Res, 1999. **48**(4): p. 199-204.
24. Nishida, Y., C.B. Knudson, and W. Knudson, *Osteogenic Protein-1 inhibits matrix depletion in a hyaluronan hexasaccharide-induced model of osteoarthritis.* Osteoarthritis Cartilage, 2004. **12**(5): p. 374-82.
25. Chubinskaya, S., B.S. Frank, M. Michalska, B. Kumar, C.A. Merrihew, E.J. Thonar, M.E. Lenz, L. Otten, D.C. Rueger, and J.A. Block, *Osteogenic protein 1 in synovial fluid from patients with rheumatoid arthritis or osteoarthritis: relationship with disease and levels of hyaluronan and antigenic keratan sulfate.* Arthritis Res Ther, 2006. **8**(3): p. R73.
26. Fahlgren, A., S. Chubinskaya, K. Messner, and P. Aspenberg, *A capsular incision leads to a fast osteoarthritic response, but also elevated levels of activated osteogenic protein-1 in rabbit knee joint cartilage.* Scand J Med Sci Sports, 2006. **16**(6): p. 456-62.
27. Trippel, S.B., S.C. Ghivizzani, and A.J. Nixon, *Gene-based approaches for the repair of articular cartilage.* Gene Ther, 2004. **11**(4): p. 351-9.

28. Hidaka, C., L.R. Goodrich, C.T. Chen, R.F. Warren, R.G. Crystal, and A.J. Nixon, *Acceleration of cartilage repair by genetically modified chondrocytes over expressing bone morphogenetic protein-7.* J Orthop Res, 2003. **21**(4): p. 573-83.
29. Badlani N, I.A., Healy R, Coutts R, Ameil D. *The protective effect of OP-1 on articular cartilage in teh development of osteoarthritis.* in *Proceedings ICRS.* 2007.
30. Louwerse, R.T., I.C. Heyligers, J. Klein-Nulend, S. Sugihara, G.P. van Kampen, C.M. Semeins, S.W. Goei, M.H. de Koning, P.I. Wuisman, and E.H. Burger, *Use of recombinant human osteogenic protein-1 for the repair of subchondral defects in articular cartilage in goats.* J Biomed Mater Res, 2000. **49**(4): p. 506-16.
31. Hartig MB, C.S. *The protective effect of OP-1 in early traumatic osteoarthitis-animal studies.* in *5th combined ORS.* 2004.
32. Patwari, P., J. Fay, M.N. Cook, A.M. Badger, A.J. Kerin, M.W. Lark, and A.J. Grodzinsky, *In vitro models for investigation of the effects of acute mechanical injury on cartilage.* Clin Orthop Relat Res, 2001(391 Suppl): p. S61-71.
33. Lee, J.H., *Chondrocyte response to in vitro mechanical injury and co-culture with joint capsule tissue*, in *Biological Engineering Division.* 2005, Massachusetts Institute of Technology: Cambridge, MA. p. 162.
34. Thibault, M., A.R. Poole, and M.D. Buschmann, *Cyclic compression of cartilage/bone explants in vitro leads to physical weakening, mechanical breakdown of collagen and release of matrix fragments.* J. Orthop. Res., 2002. **20**(6): p. 1265-1273.
35. Torzilli, P.A., R. Grigiene, J. Borrelli, Jr., and D.L. Helfet, *Effect of impact load on articular cartilage: cell metabolism and viability, and matrix water content.* J Biomech Eng, 1999. **121**(5): p. 433-41.
36. Kurz, B., M. Jin, P. Patwari, D.M. Cheng, M.W. Lark, and A.J. Grodzinsky, *Biosynthetic response and mechanical properties of articular cartilage after injurious compression.* J Orthop Res, 2001. **19**(6): p. 1140-6.
37. Chen, C.T., N. Burton-Wurster, G. Lust, R.A. Bank, and J.M. Tekoppele, *Compositional and metabolic changes in damaged cartilage are peak-stress, stress-rate, and loading-duration dependent.* J Orthop Res, 1999. **17**(6): p. 870-9.
38. Loening, A.M., I.E. James, M.E. Levenston, A.M. Badger, E.H. Frank, B. Kurz, M.E. Nuttall, H.H. Hung, S.M. Blake, A.J. Grodzinsky, and M.W. Lark, *Injurious mechanical compression of bovine articular cartilage induces chondrocyte apoptosis.* Arch Biochem Biophys, 2000. **381**(2): p. 205-12.
39. Patwari, P., M.N. Cook, M.A. DiMicco, S.M. Blake, I.E. James, S. Kumar, A.A. Cole, M.W. Lark, and A.J. Grodzinsky, *Proteoglycan degradation after injurious compression of bovine and human articular cartilage in vitro: Interaction with exogenous cytokines.* Arthritis Rheum., 2003. **48**(5): p. 1292-301.
40. DiMicco, M.A., P. Patwari, P.N. Siparsky, S. Kumar, M.A. Pratta, M.W. Lark, Y.J. Kim, and A.J. Grodzinsky, *Mechanisms and kinetics of glycosaminoglycan release following in vitro cartilage injury.* Arthritis and Rheumatism, 2004. **50**(3): p. 840-848.
41. D'Lima, D.D., S. Hashimoto, P.C. Chen, C.W. Colwell, Jr., and M.K. Lotz, *Human chondrocyte apoptosis in response to mechanical injury.* Osteoarthritis Cartilage, 2001. **9**(8): p. 712-9.
42. Kurz, B., A. Lemke, M. Kehn, C. Domm, P. Patwari, E.H. Frank, A.J. Grodzinsky, and M. Schunke, *Influence of tissue maturation and antioxidants on the apoptotic response of articular cartilage after injurious compression.* Arthritis Rheum, 2004. **50**(1): p. 123-30.

43. Chen, C.T., N. Burton-Wurster, C. Borden, K. Hueffer, S.E. Bloom, and G. Lust, *Chondrocyte necrosis and apoptosis in impact damaged articular cartilage.* J Orthop Res, 2001. **19**(4): p. 703-11.
44. Lee, J.H., J.B. Fitzgerald, M.A. Dimicco, and A.J. Grodzinsky, *Mechanical injury of cartilage explants causes specific time-dependent changes in chondrocyte gene expression.* Arthritis Rheum, 2005. **52**(8): p. 2386-95.
45. Jubb, R.W. and H.B. Fell, *The effect of synovial tissue on the synthesis of proteoglycan by the articular cartilage of young pigs.* Arthritis Rheum, 1980. **23**(5): p. 545-55.
46. Fell, H.B. and R.W. Jubb, *The effect of synovial tissue on the breakdown of articular cartilage in organ culture.* Arthritis Rheum, 1977. **20**(7): p. 1359-71.
47. Vankemmelbeke, M.N., M.Z. Ilic, C.J. Handley, C.G. Knight, and D.J. Buttle, *Coincubation of bovine synovial or capsular tissue with cartilage generates a soluble "Aggrecanase" activity.* Biochem Biophys Res Commun, 1999. **255**(3): p. 686-91.
48. Kurz, B., J. Steinhagen, and M. Schunke, *Articular chondrocytes and synoviocytes in a co-culture system: influence on reactive oxygen species-induced cytotoxicity and lipid peroxidation.* Cell Tissue Res, 1999. **296**(3): p. 555-63.
49. Sah, R.L.Y., Y.J. Kim, J.Y.H. Doong, A.J. Grodzinsky, A.H.K. Plaas, and J.D. Sandy, *Biosynthesis Response to Cartilage Explants to Dynamic Compression.* J. Orthop. Res., 1989. **7**: p. 619-636.
50. Wheeler CA, C.S., Grodzinsky AJ. *Stimulatory Dose-Dependent Transcriptional Behavior of Mechanically Injured Bovine Cartilage Following OP-1 or IGF-1 Treatment In Vitro.* in *ORS.* 2007. San Diego, CA.
51. Frank, E.H., M. Jin, A.M. Loening, M.E. Levenston, and A.J. Grodzinsky, *A versatile shear and compression apparatus for mechanical stimulation of tissue culture explants.* Journal of Biomechanics, 2000. **33**(11): p. 1523-1527.
52. Fitzgerald, J.B., M. Jin, D. Dean, D.J. Wood, M.H. Zheng, and A.J. Grodzinsky, *Mechanical compression of cartilage explants induces multiple time-dependent gene expression patterns and involves intracellular calcium and cyclic AMP.* Journal of Biological Chemistry, 2004. **279**(19): p. 19502-19511.
53. Lee, C.R., S. Grad, J.J. Maclean, J.C. Iatridis, and M. Alini, *Effect of mechanical loading on mRNA levels of common endogenous controls in articular chondrocytes and intervertebral disk.* Anal Biochem, 2005. **341**(2): p. 372-5.
54. Alter, O., P.O. Brown, and D. Botstein, *Singular value decomposition for genome-wide expression data processing and modeling.* Proc Natl Acad Sci U S A, 2000. **97**(18): p. 10101-6.
55. Holter, N.S., M. Mitra, A. Maritan, M. Cieplak, J.R. Banavar, and N.V. Fedoroff, *Fundamental patterns underlying gene expression profiles: simplicity from complexity.* Proc Natl Acad Sci U S A, 2000. **97**(15): p. 8409-14.
56. Yasuda, T., S.M. Julovi, T. Hiramitsu, M. Yoshida, and T. Nakamura, *Requirement of mitogen-activated protein kinase for collagenase production by the fibronectin fragment in human articular chondrocytes in culture.* Mod Rheumatol, 2004. **14**(1): p. 54-60.
57. Yasuda, T., *Cartilage destruction by matrix degradation products.* Mod Rheumatol, 2006. **16**(4): p. 197-205.
58. Chan, P.S., A.E. Schlueter, P.M. Coussens, G.J. Rosa, R.C. Haut, and M.W. Orth, *Gene expression profile of mechanically impacted bovine articular cartilage explants.* J Orthop Res, 2005. **23**(5): p. 1146-51.

59. Elliott, S. and T. Cawston, *The clinical potential of matrix metalloproteinase inhibitors in the rheumatic disorders.* Drugs Aging, 2001. **18**(2): p. 87-99.
60. Cawston, T., C. Billington, C. Cleaver, S. Elliott, W. Hui, P. Koshy, B. Shingleton, and A. Rowan, *The regulation of MMPs and TIMPs in cartilage turnover.* Ann N Y Acad Sci, 1999. **878**: p. 120-9.
61. Burrage, P.S., K.S. Mix, and C.E. Brinckerhoff, *Matrix metalloproteinases: role in arthritis.* Front Biosci, 2006. **11**: p. 529-43.
62. Kurz, B., A.K. Lemke, J. Fay, T. Pufe, A.J. Grodzinsky, and M. Schunke, *Pathomechanisms of cartilage destruction by mechanical injury.* Ann Anat, 2005. **187**(5-6): p. 473-85.
63. Blain, E.J., *Mechanical regulation of matrix metalloproteinases.* Front Biosci, 2007. **12**: p. 507-27.
64. Darmani, H., J. Crossan, S.D. McLellan, D. Meek, and C. Adam, *Expression of nitric oxide synthase and transforming growth factor-beta in crush-injured tendon and synovium.* Mediators Inflamm, 2004. **13**(5-6): p. 299-305.
65. Gebauer, M., J. Saas, F. Sohler, J. Haag, S. Soder, M. Pieper, E. Bartnik, J. Beninga, R. Zimmer, and T. Aigner, *Comparison of the chondrosarcoma cell line SW1353 with primary human adult articular chondrocytes with regard to their gene expression profile and reactivity to IL-1beta.* Osteoarthritis Cartilage, 2005. **13**(8): p. 697-708.
66. Im, H.J., P. Muddasani, V. Natarajan, T.M. Schmid, J.A. Block, F. Davis, A.J. van Wijnen, and R.F. Loeser, *Basic fibroblast growth factor stimulates matrix metalloproteinase-13 via the molecular cross-talk between the mitogen-activated protein kinases and protein kinase Cdelta pathways in human adult articular chondrocytes.* J Biol Chem, 2007. **282**(15): p. 11110-21.
67. Fay, J., D. Varoga, C.J. Wruck, B. Kurz, M.B. Goldring, and T. Pufe, *Reactive oxygen species induce expression of vascular endothelial growth factor in chondrocytes and human articular cartilage explants.* Arthritis Res Ther, 2006. **8**(6): p. R189.
68. Iwanaga, T., M. Shikichi, H. Kitamura, H. Yanase, and K. Nozawa-Inoue, *Morphology and functional roles of synoviocytes in the joint.* Arch Histol Cytol, 2000. **63**(1): p. 17-31.
69. Distler, J.H., A. Jungel, L.C. Huber, C.A. Seemayer, C.F. Reich, 3rd, R.E. Gay, B.A. Michel, A. Fontana, S. Gay, D.S. Pisetsky, and O. Distler, *The induction of matrix metalloproteinase and cytokine expression in synovial fibroblasts stimulated with immune cell microparticles.* Proc Natl Acad Sci U S A, 2005. **102**(8): p. 2892-7.
70. Bondeson, J., S.D. Wainwright, S. Lauder, N. Amos, and C.E. Hughes, *The role of synovial macrophages and macrophage-produced cytokines in driving aggrecanases, matrix metalloproteinases, and other destructive and inflammatory responses in osteoarthritis.* Arthritis Res Ther, 2006. **8**(6): p. R187.
71. Ilic, M.Z., M.N. Vankemmelbeke, I. Holen, D.J. Buttle, H. Clem Robinson, and C.J. Handley, *Bovine joint capsule and fibroblasts derived from joint capsule express aggrecanase activity.* Matrix Biol, 2000. **19**(3): p. 257-65.
72. Vankemmelbeke, M.N., I. Holen, A.G. Wilson, M.Z. Ilic, C.J. Handley, G.S. Kelner, M. Clark, C. Liu, R.A. Maki, D. Burnett, and D.J. Buttle, *Expression and activity of ADAMTS-5 in synovium.* Eur J Biochem, 2001. **268**(5): p. 1259-68.
73. Soder, S., H.I. Roach, S. Oehler, B. Bau, J. Haag, and T. Aigner, *MMP-9/gelatinase B is a gene product of human adult articular chondrocytes and increased in osteoarthritic cartilage.* Clin Exp Rheumatol, 2006. **24**(3): p. 302-4.

74. Nalin, A.M., T.K. Greenlee, Jr., and L.J. Sandell, *Collagen gene expression during development of avian synovial joints: transient expression of types II and XI collagen genes in the joint capsule.* Dev Dyn, 1995. **203**(3): p. 352-62.
75. Roach, H.I., T. Aigner, S. Soder, J. Haag, and H. Welkerling, *Pathobiology of osteoarthritis: pathomechanisms and potential therapeutic targets.* Curr Drug Targets, 2007. **8**(2): p. 271-82.
76. Halasz, K., A. Kassner, M. Morgelin, and D. Heinegard, *COMP acts as a catalyst in collagen fibrillogenesis.* J Biol Chem, 2007. **282**(43): p. 31166-73.
77. Morozzi, G., M. Fabbroni, F. Bellisai, G. Pucci, and M. Galeazzi, *Cartilage oligomeric matrix protein level in rheumatic diseases: potential use as a marker for measuring articular cartilage damage and/or the therapeutic efficacy of treatments.* Ann N Y Acad Sci, 2007. **1108**: p. 398-407.
78. Gagarina, V., A.L. Carlberg, L. Pereira-Mouries, and D.J. Hall, *Cartilage oligomeric matrix protein (COMP) protects cells against death by elevating members of the IAP family of survival proteins.* J Biol Chem, 2007.
79. Fitzgerald, J.B. and A.J. Grodzinsky, *Involvement of protein synthesis and the MAP kinase pathway in gene transcription induced by static compression of cartilage.* ORS 51st Annual Meeting, 2005.
80. Ray, A., A. Shakya, and B.K. Ray, *Inflammation-responsive transcription factors SAF-1 and c-Jun/c-Fos promote canine MMP-1 gene expression.* Biochim Biophys Acta, 2005. **1732**(1-3): p. 53-61.
81. Lu, T., Y. Achari, J.B. Rattner, and D.A. Hart, *Evidence that estrogen receptor beta enhances MMP-13 promoter activity in HIG-82 cells and that this enhancement can be influenced by ligands and involves specific promoter sites.* Biochem Cell Biol, 2007. **85**(3): p. 326-36.
82. Liacini, A., J. Sylvester, W.Q. Li, and M. Zafarullah, *Inhibition of interleukin-1-stimulated MAP kinases, activating protein- 1 (AP-1) and nuclear factor kappa B (NF-kappa B) transcription factors down-regulates matrix metalloproteinase gene expression in articular chondrocytes.* Matrix Biol., 2002. **21**(3): p. 251-62.
83. Liacini, A., J. Sylvester, W.Q. Li, W. Huang, F. Dehnade, M. Ahmad, and M. Zafarullah, *Induction of matrix metalloproteinase-13 gene expression by TNF-alpha is mediated by MAP kinases, AP-1, and NF-kappaB transcription factors in articular chondrocytes.* Exp. Cell. Res., 2003. **288**: p. 208-217.
84. Clements, D.N., S.D. Carter, J.F. Innes, W.E. Ollier, and P.J. Day, *Analysis of normal and osteoarthritic canine cartilage mRNA expression by quantitative polymerase chain reaction.* Arthritis Res Ther, 2006. **8**(6): p. R158.
85. Aigner, T., K. Fundel, J. Saas, P.M. Gebhard, J. Haag, T. Weiss, A. Zien, F. Obermayr, R. Zimmer, and E. Bartnik, *Large-scale gene expression profiling reveals major pathogenetic pathways of cartilage degeneration in osteoarthritis.* Arthritis Rheum, 2006. **54**(11): p. 3533-44.
86. Nuttall, M.E., D.P. Nadeau, P.W. Fisher, F. Wang, P.M. Keller, W.E. DeWolf, Jr., M.B. Goldring, A.M. Badger, D. Lee, M.A. Levy, M. Gowen, and M.W. Lark, *Inhibition of caspase-3-like activity prevents apoptosis while retaining functionality of human chondrocytes in vitro.* J Orthop Res, 2000. **18**(3): p. 356-63.
87. Lee, D., S.A. Long, J.L. Adams, G. Chan, K.S. Vaidya, T.A. Francis, K. Kikly, J.D. Winkler, C.M. Sung, C. Debouck, S. Richardson, M.A. Levy, W.E. DeWolf, Jr.,

P.M. Keller, T. Tomaszek, M.S. Head, M.D. Ryan, R.C. Haltiwanger, P.H. Liang, C.A. Janson, P.J. McDevitt, K. Johanson, N.O. Concha, W. Chan, S.S. Abdel-Meguid, A.M. Badger, M.W. Lark, D.P. Nadeau, L.J. Suva, M. Gowen, and M.E. Nuttall, *Potent and selective nonpeptide inhibitors of caspases 3 and 7 inhibit apoptosis and maintain cell functionality.* J Biol Chem, 2000. **275**(21): p. 16007-14.

4.7 Appendix of Figures

4.7.1 Short Term Gene Expression

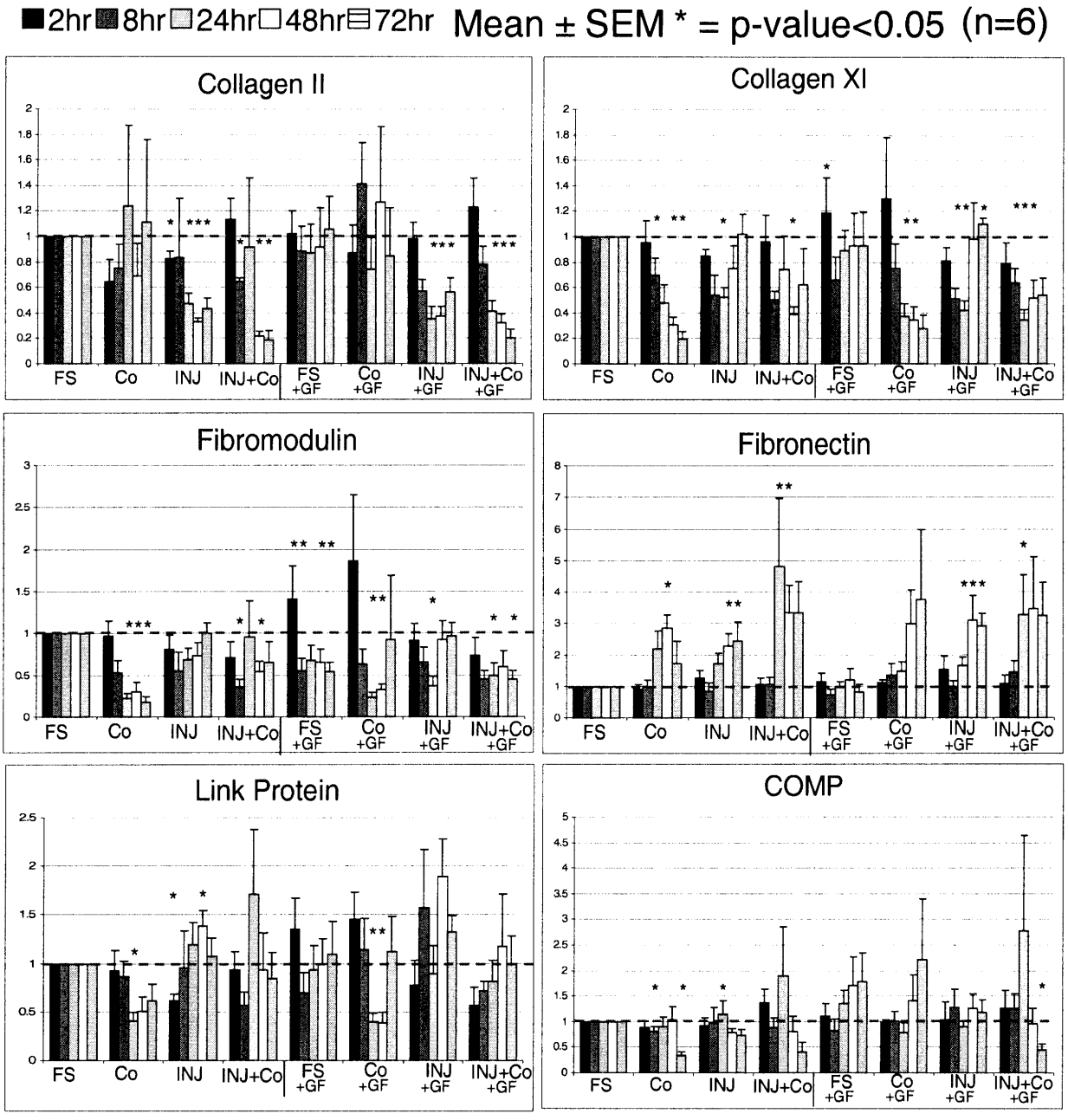

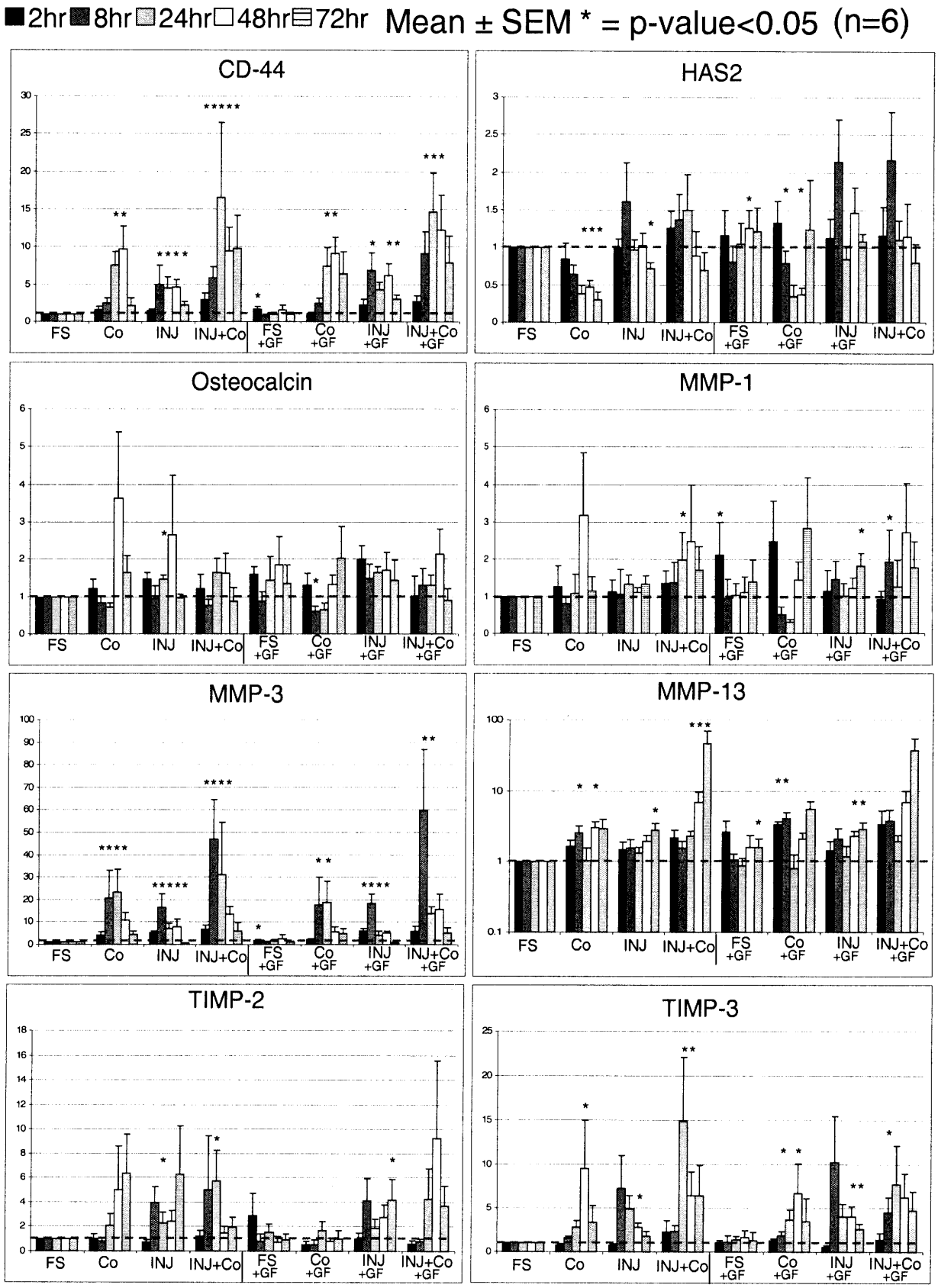
2hr 8hr 24hr 48hr 72hr Mean ± SEM * = p-value<0.05 (n=6)
CD-44
HAS2
Osteocalcin
MMP-1
MMP-3
MMP-13
TIMP-2
TIMP-3
FS
Co
INJ
INJ+Co
FS +GF
Co +GF
INJ +GF
INJ+Co +GF

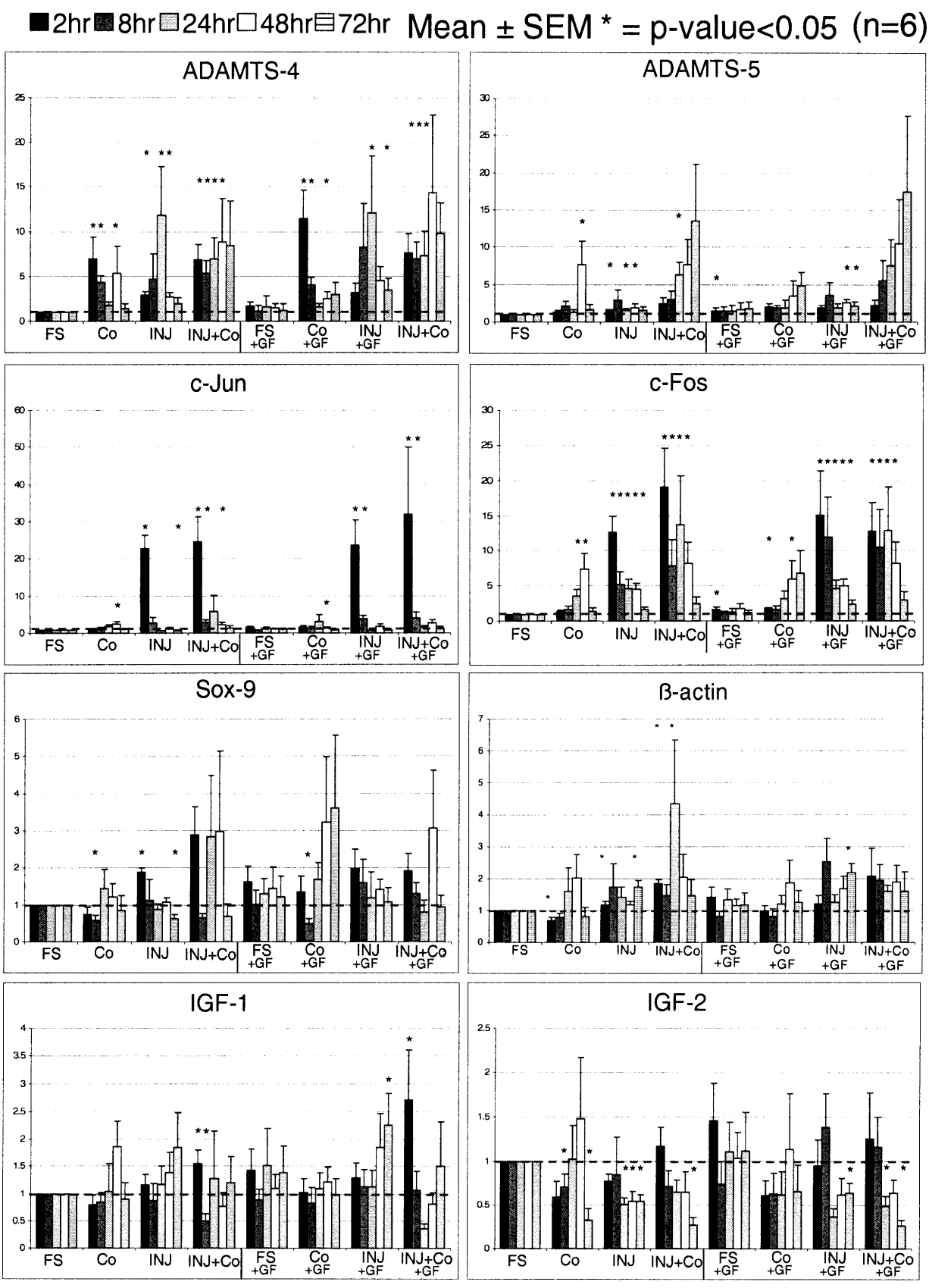
2hr 8hr 24hr 48hr 72hr Mean ± SEM * = p-value<0.05 (n=6)
ADAMTS-4
ADAMTS-5
c-Jun
c-Fos
Sox-9
ß-actin
IGF-1
IGF-2
FS
Co
INJ
INJ+Co
FS +GF
Co +GF
INJ +GF
INJ+Co +GF

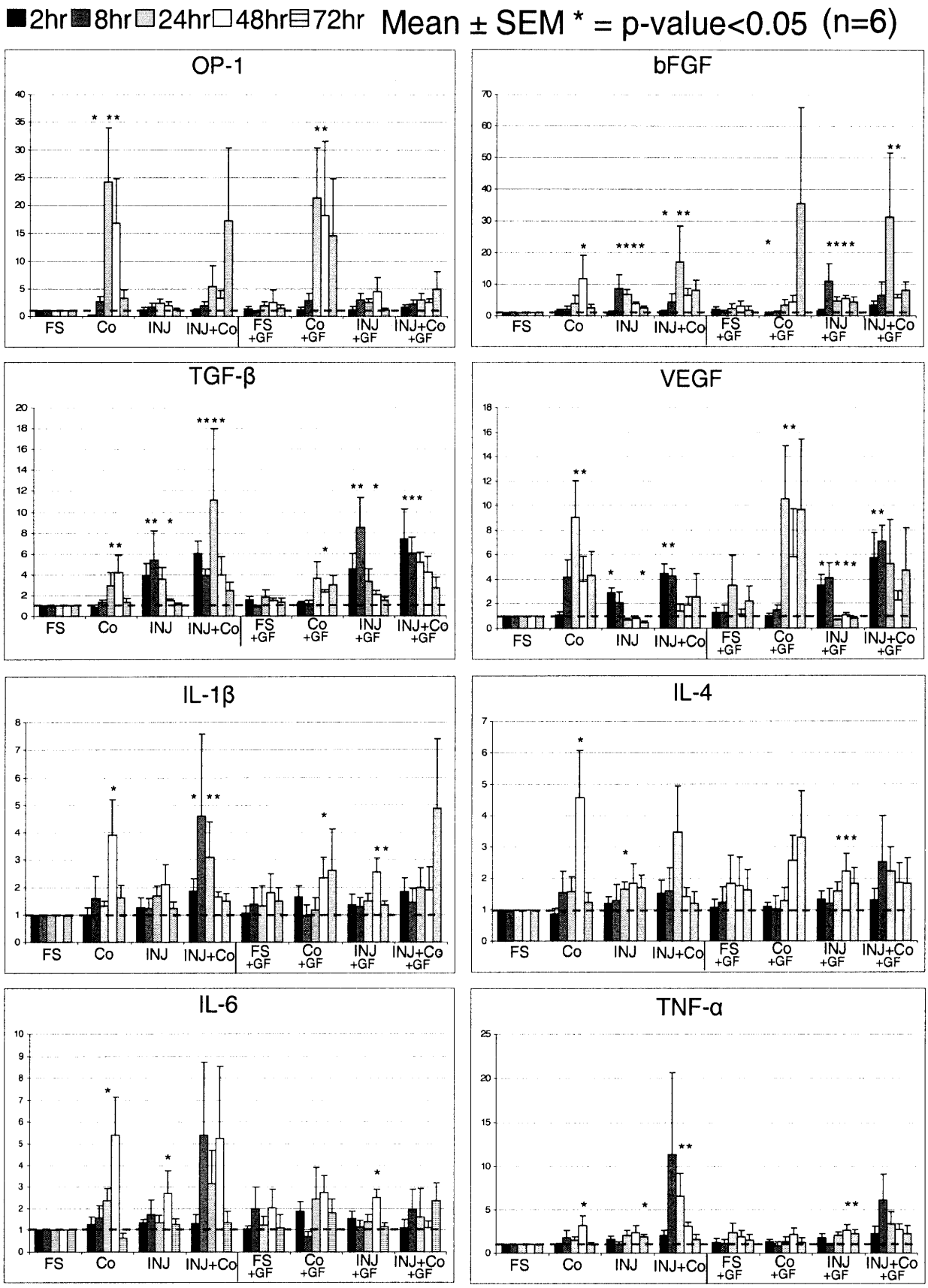
2hr 8hr 24hr 48hr 72hr Mean ± SEM * = p-value<0.05 (n=6)
OP-1
bFGF
TGF-β
VEGF
IL-1β
IL-4
IL-6
TNF-α
FS
Co
INJ
INJ+Co
FS +GF
Co +GF
INJ +GF
INJ+Co +GF

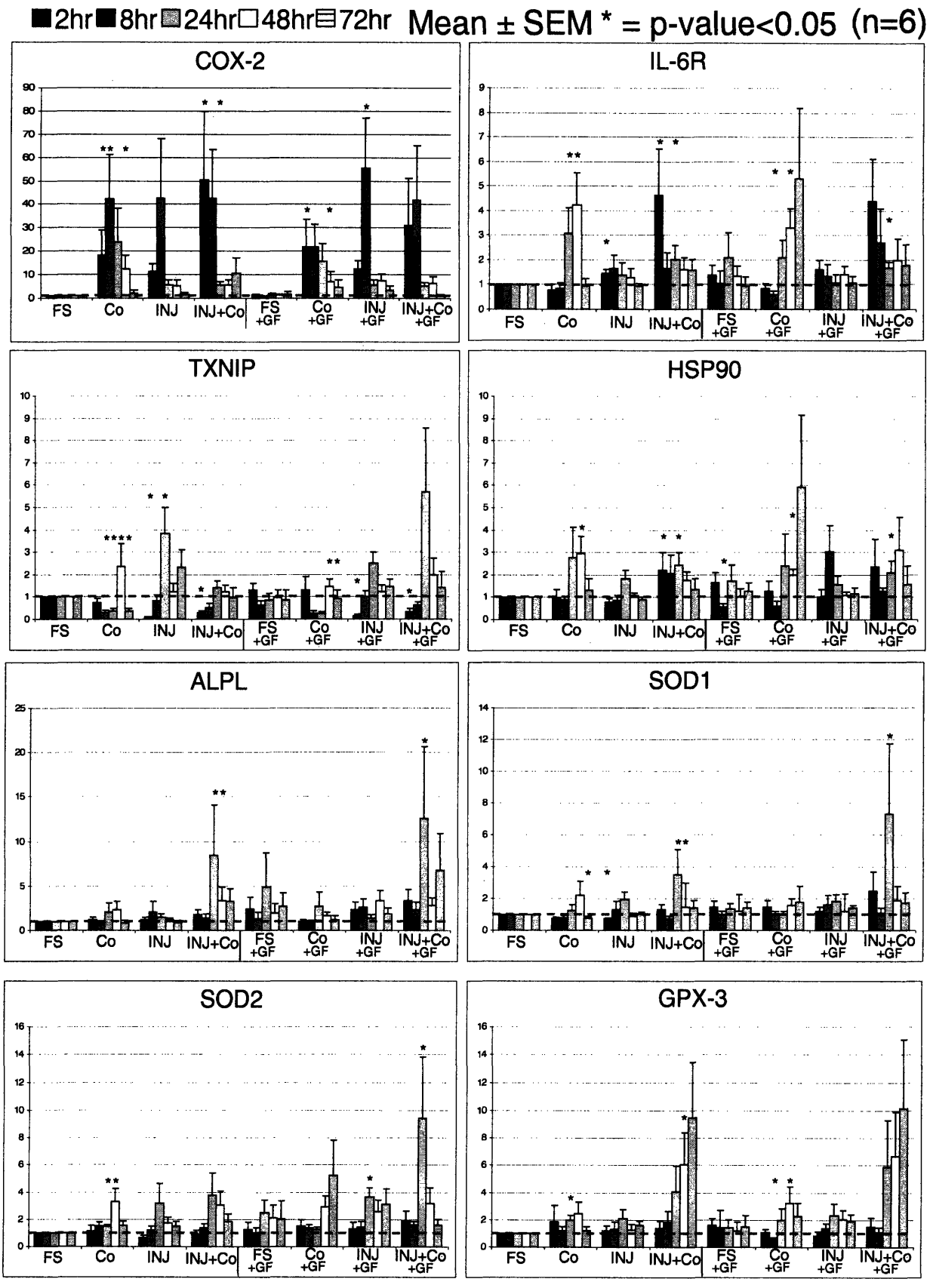
2hr 8hr 24hr 48hr 72hr Mean ± SEM * = p-value<0.05 (n=6)
COX-2
IL-6R
TXNIP
HSP90
ALPL
SOD1
SOD2
GPX-3
FS
Co
INJ
INJ+Co
FS +GF
Co +GF
INJ +GF
INJ+Co +GF

4.7.2 Effects of GF Treatment- Short Term Gene Expression

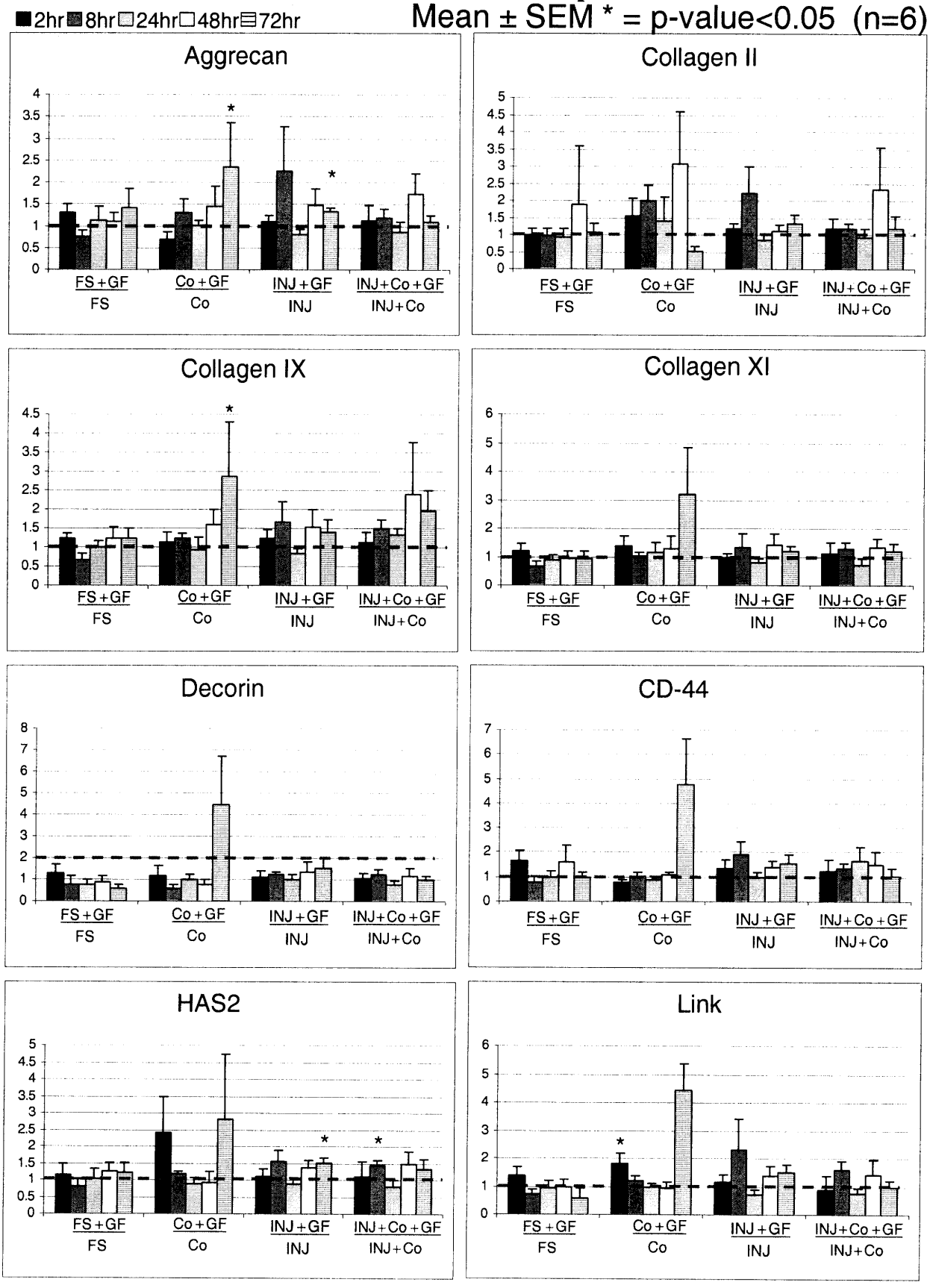

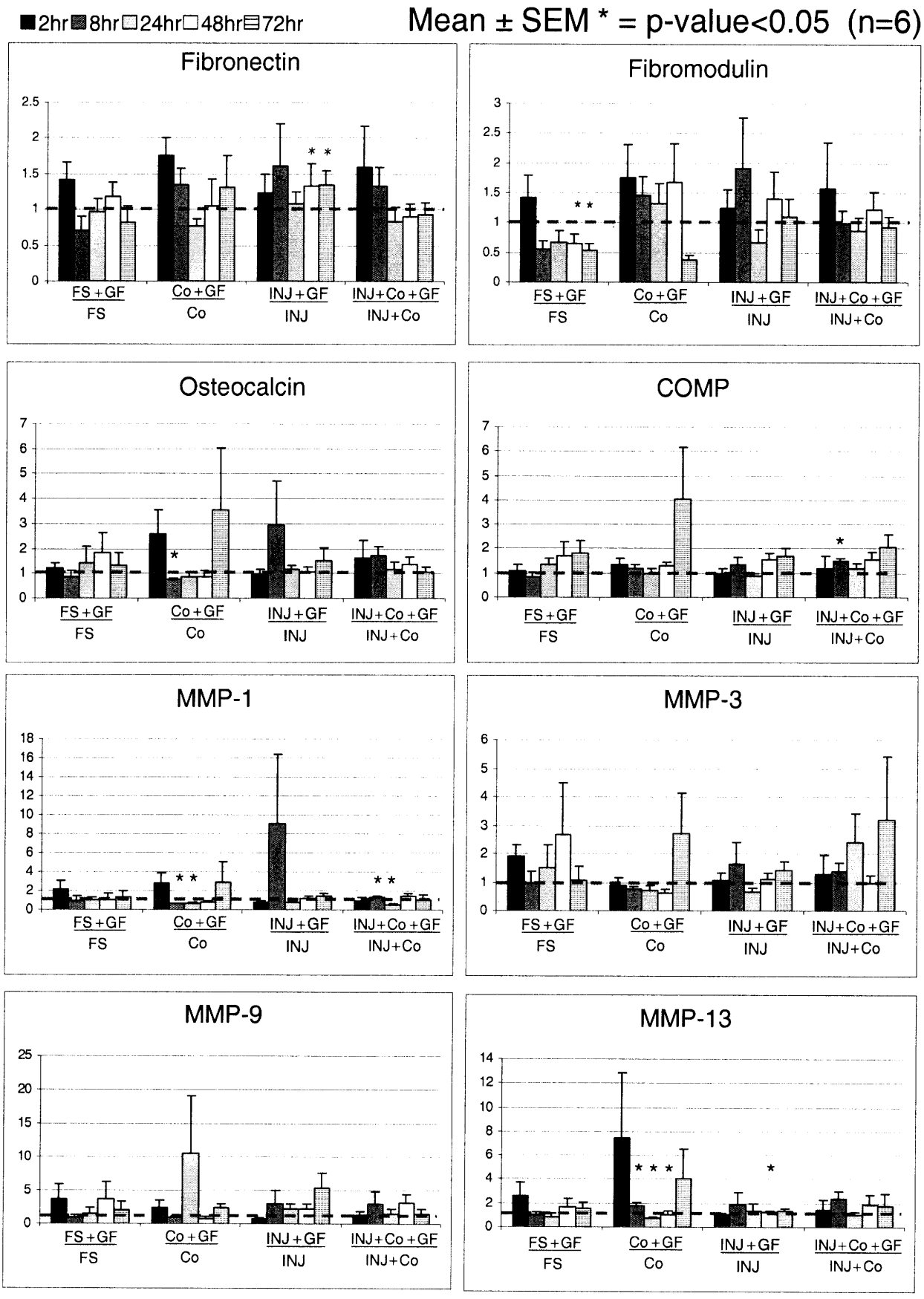
■2hr■8hr□24hr□48hr▤72hr
Mean ± SEM * = p-value<0.05 (n=6)
Fibronectin
Fibromodulin
Osteocalcin
COMP
MMP-1
MMP-3
MMP-9
MMP-13
FS+GF
FS
Co+GF
Co
INJ+GF
INJ
INJ+Co+GF
INJ+Co

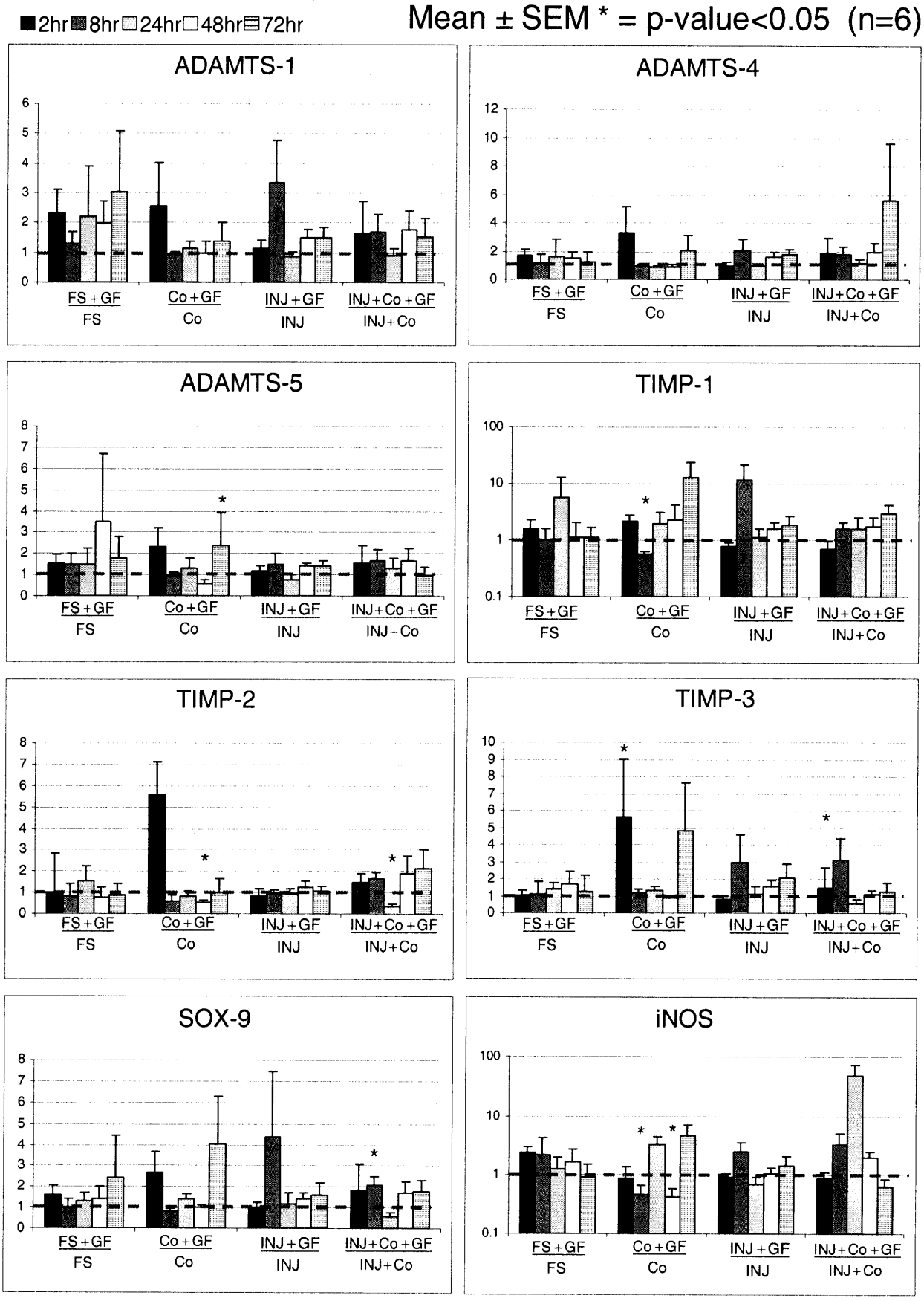
■2hr■8hr□24hr□48hr⊟72hr
Mean ± SEM * = p-value<0.05 (n=6)
ADAMTS-1
ADAMTS-4
ADAMTS-5
TIMP-1
TIMP-2
TIMP-3
SOX-9
iNOS
FS+GF
Co+GF
INJ+GF
INJ+Co+GF
FS
Co
INJ
INJ+Co

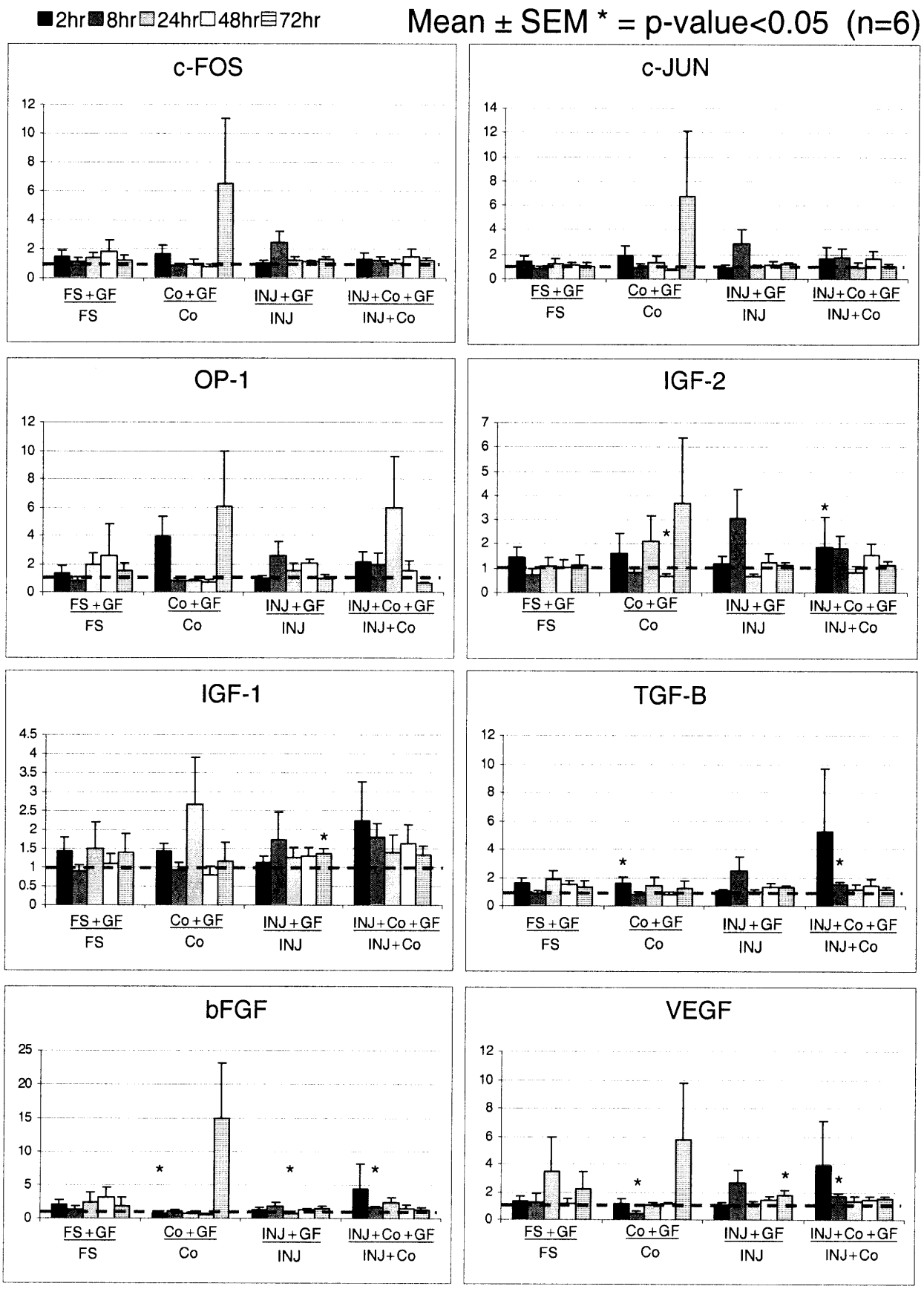
■2hr■8hr□24hr□48hr▤72hr
Mean ± SEM * = p-value<0.05 (n=6)
c-FOS
c-JUN
OP-1
IGF-2
IGF-1
TGF-B
bFGF
VEGF
FS+GF
Co+GF
INJ+GF
INJ+Co+GF
FS
Co
INJ
INJ+Co

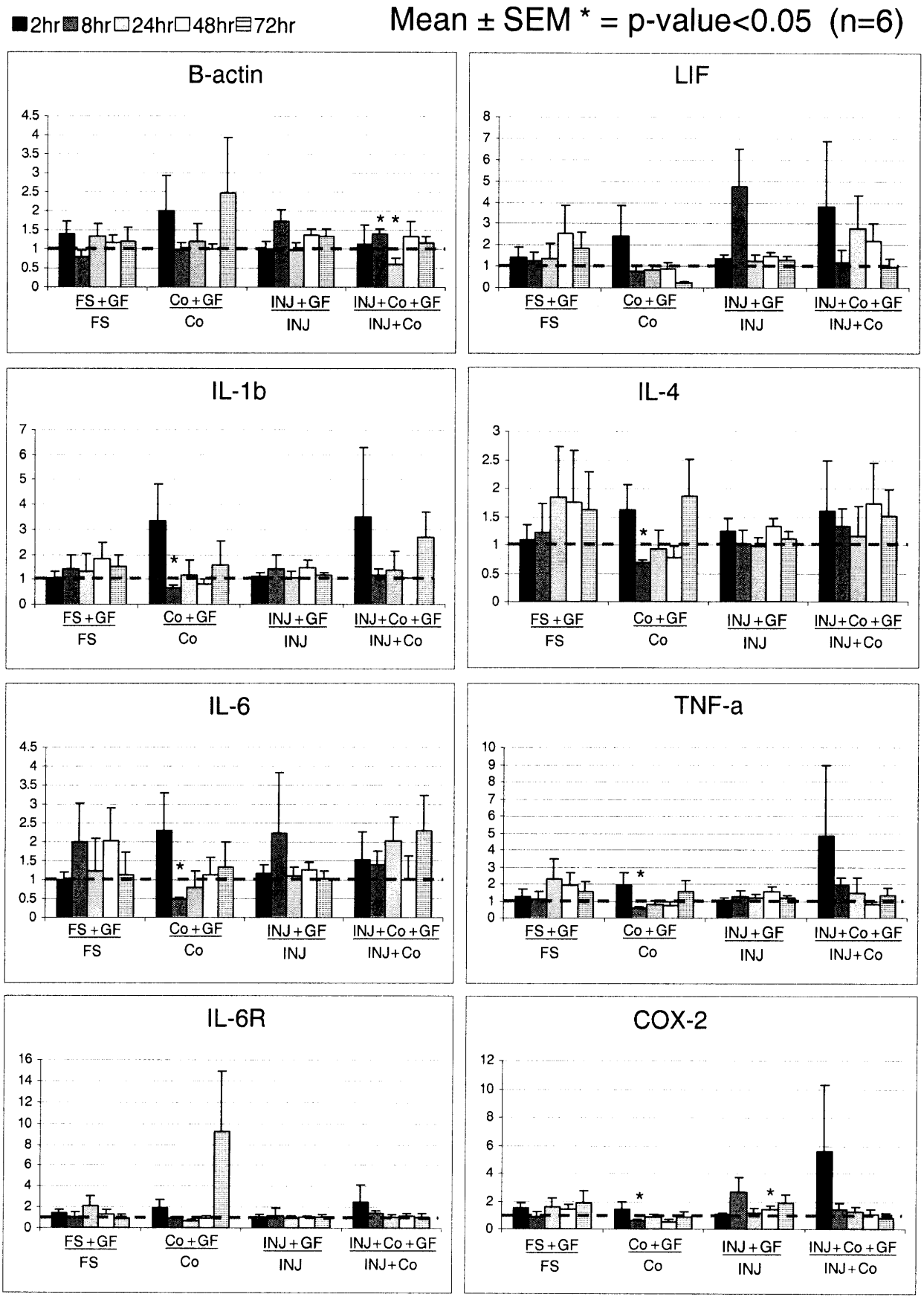
■2hr■8hr□24hr□48hr▤72hr
Mean ± SEM * = p-value<0.05 (n=6)
B-actin
LIF
IL-1b
IL-4
IL-6
TNF-a
IL-6R
COX-2
FS+GF
FS
Co+GF
Co
INJ+GF
INJ
INJ+Co+GF
INJ+Co

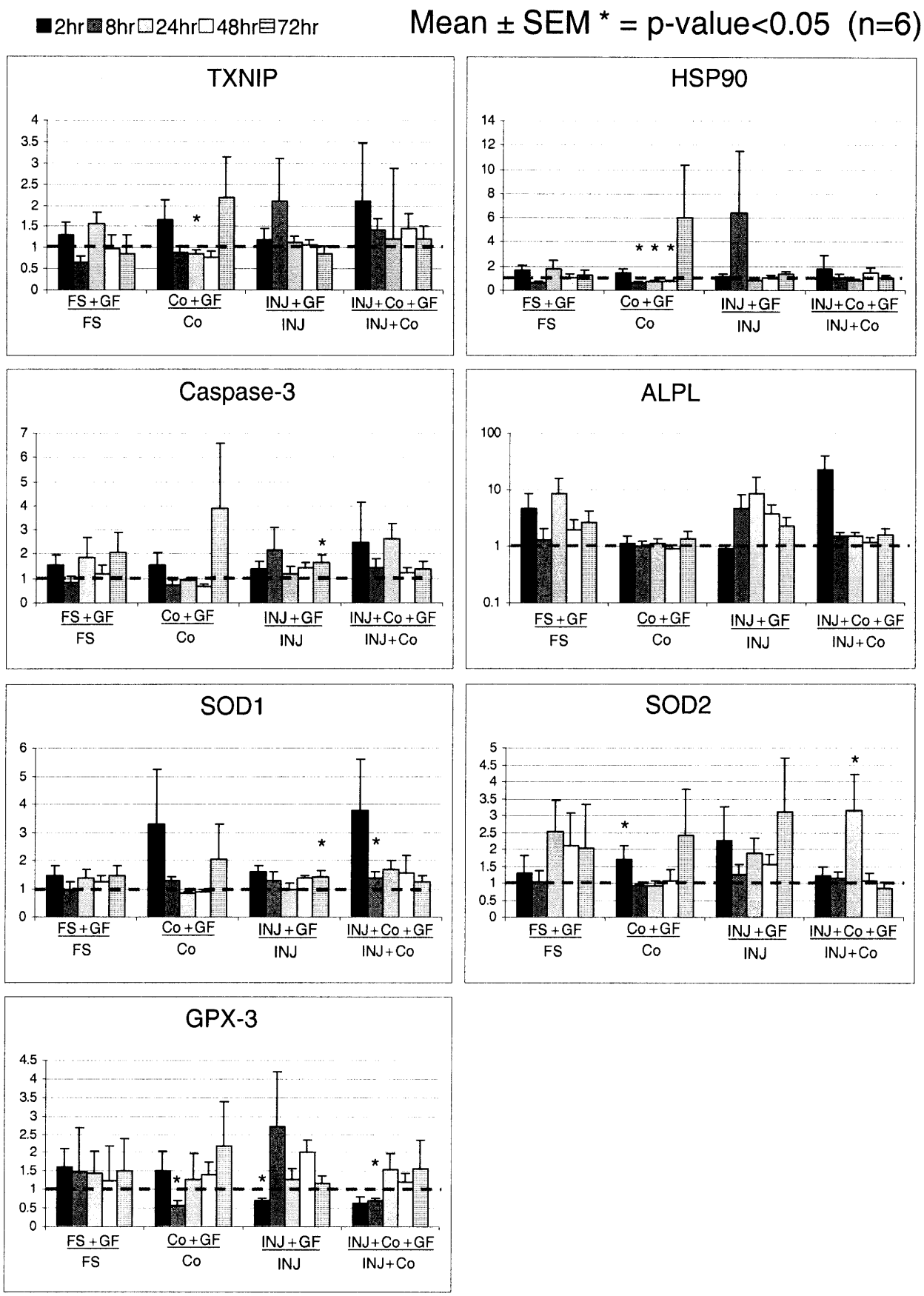
2hr 8hr 24hr 48hr 72hr
Mean ± SEM * = p-value<0.05 (n=6)
TXNIP
HSP90
Caspase-3
ALPL
SOD1
SOD2
GPX-3
FS+GF
FS
Co+GF
Co
INJ+GF
INJ
INJ+Co+GF
INJ+Co

4.7.3 Joint Capsule Gene Expression

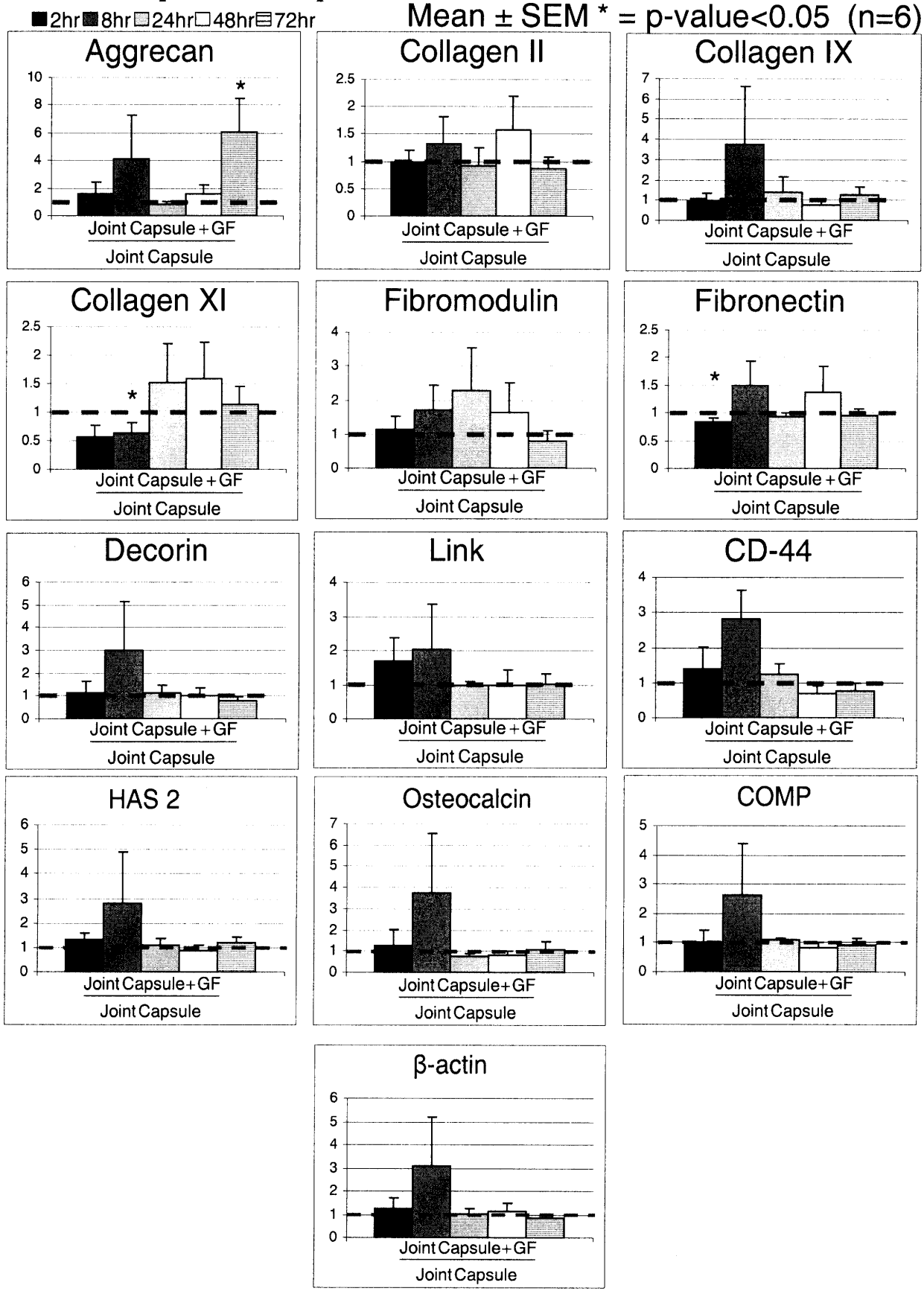

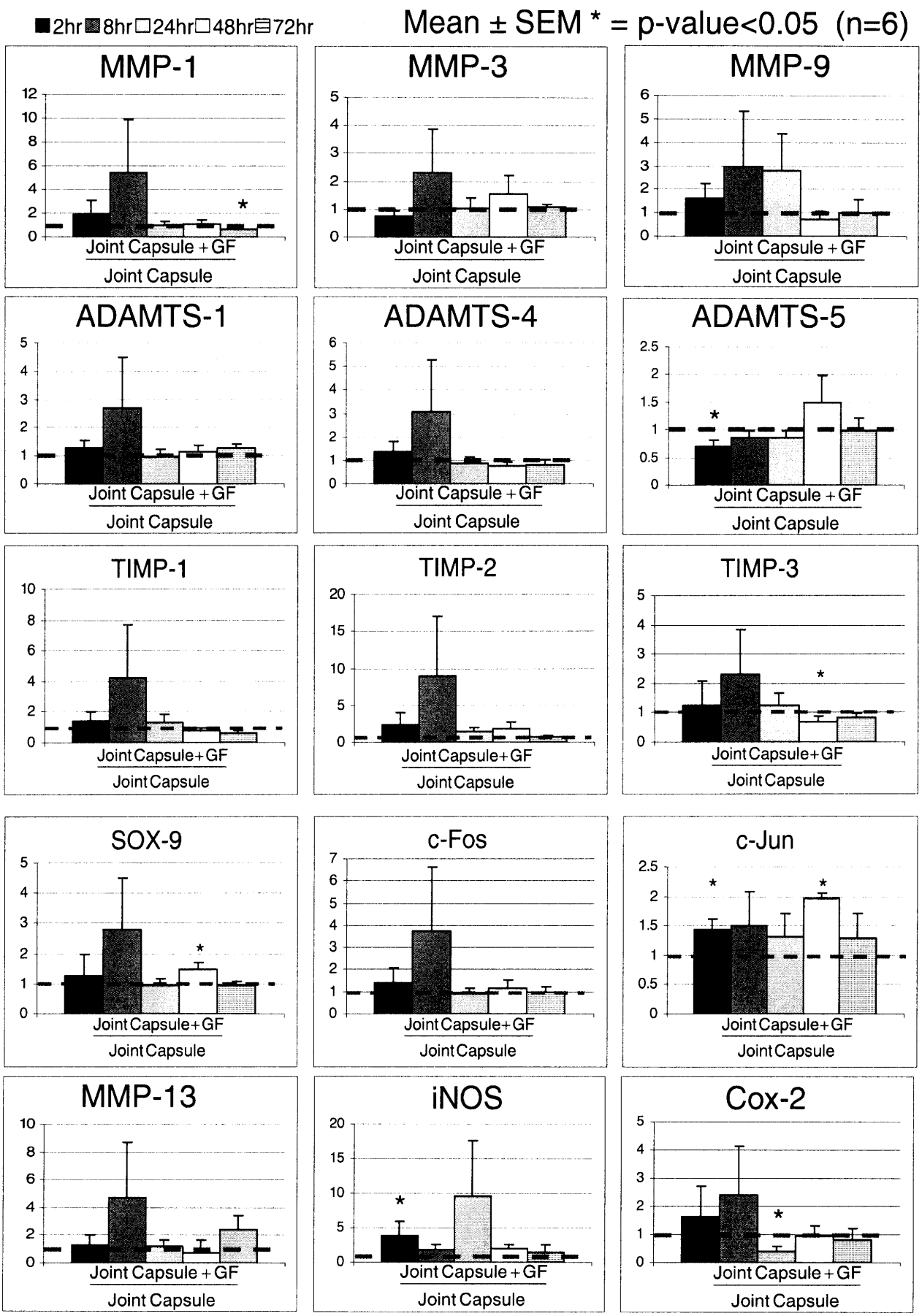
2hr 8hr 24hr 48hr 72hr
Mean ± SEM * = p-value<0.05 (n=6)
MMP-1
MMP-3
MMP-9
ADAMTS-1
ADAMTS-4
ADAMTS-5
TIMP-1
TIMP-2
TIMP-3
SOX-9
c-Fos
c-Jun
MMP-13
iNOS
Cox-2
Joint Capsule + GF
Joint Capsule

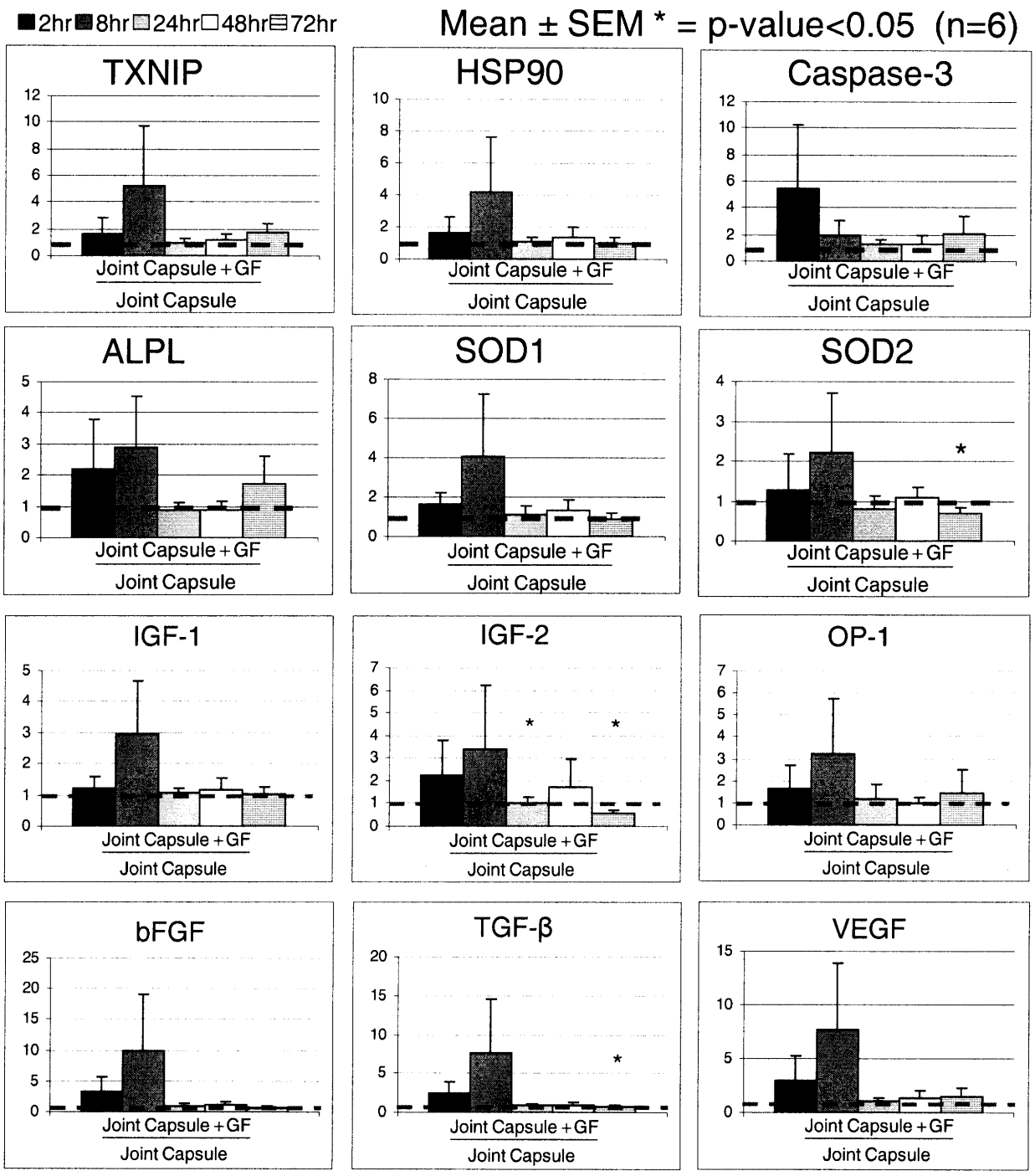
2hr 8hr 24hr 48hr 72hr
Mean ± SEM * = p-value<0.05 (n=6)
TXNIP
HSP90
Caspase-3
ALPL
SOD1
SOD2
IGF-1
IGF-2
OP-1
bFGF
TGF-β
VEGF
Joint Capsule + GF
Joint Capsule

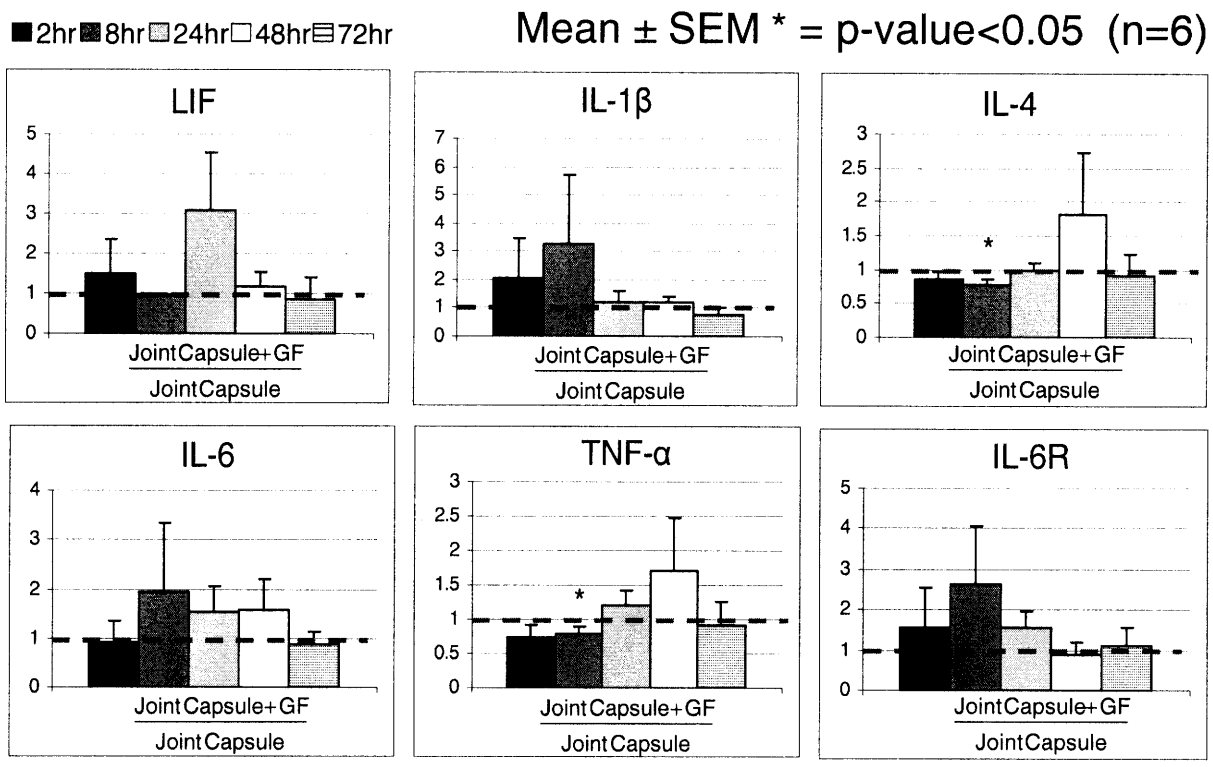
2hr 8hr 24hr 48hr 72hr
Mean ± SEM * = p-value<0.05 (n=6)
LIF
IL-1β
IL-4
IL-6
TNF-α
IL-6R
Joint Capsule+GF
Joint Capsule

4.7.4 Longer Term Gene Expression

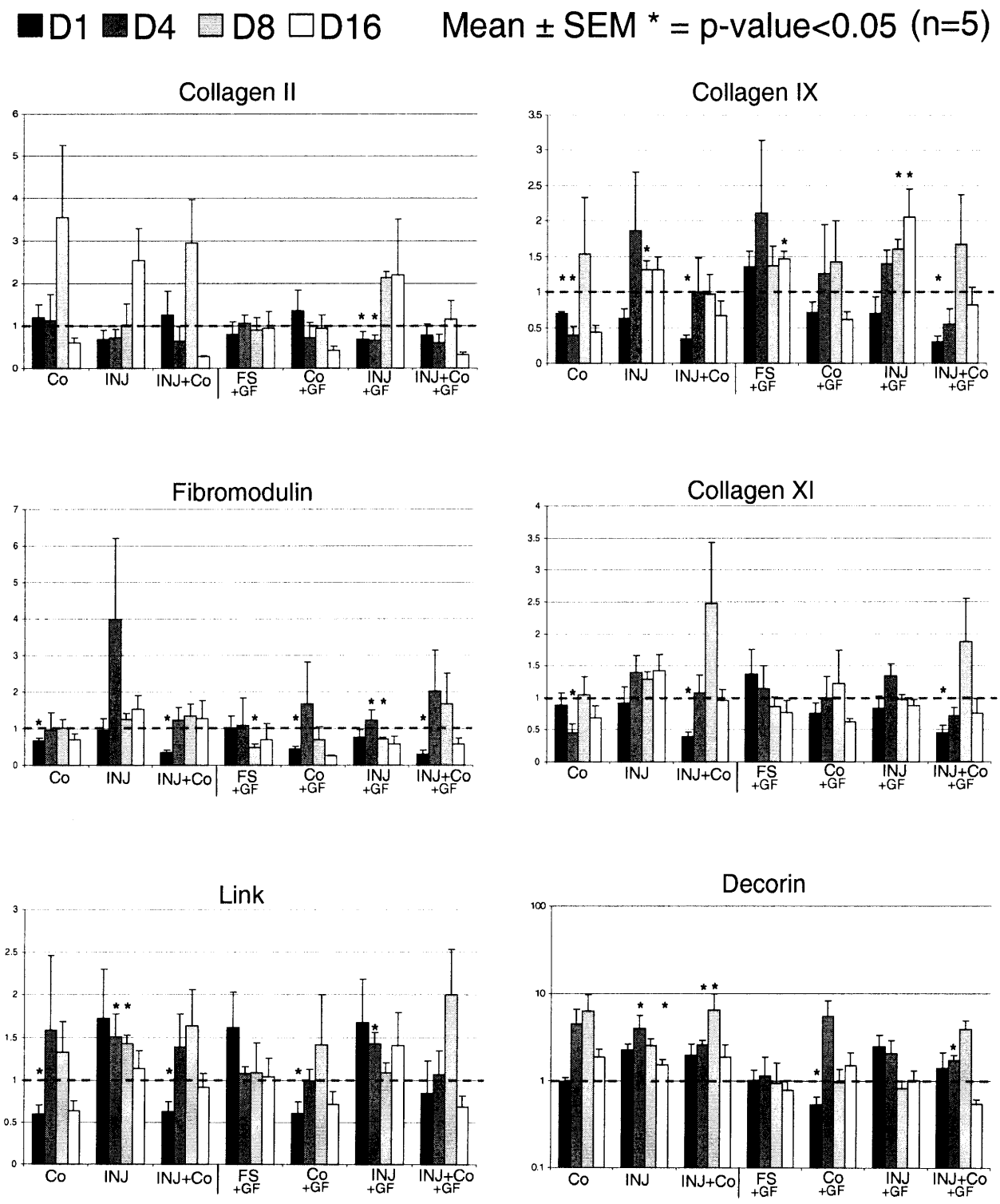

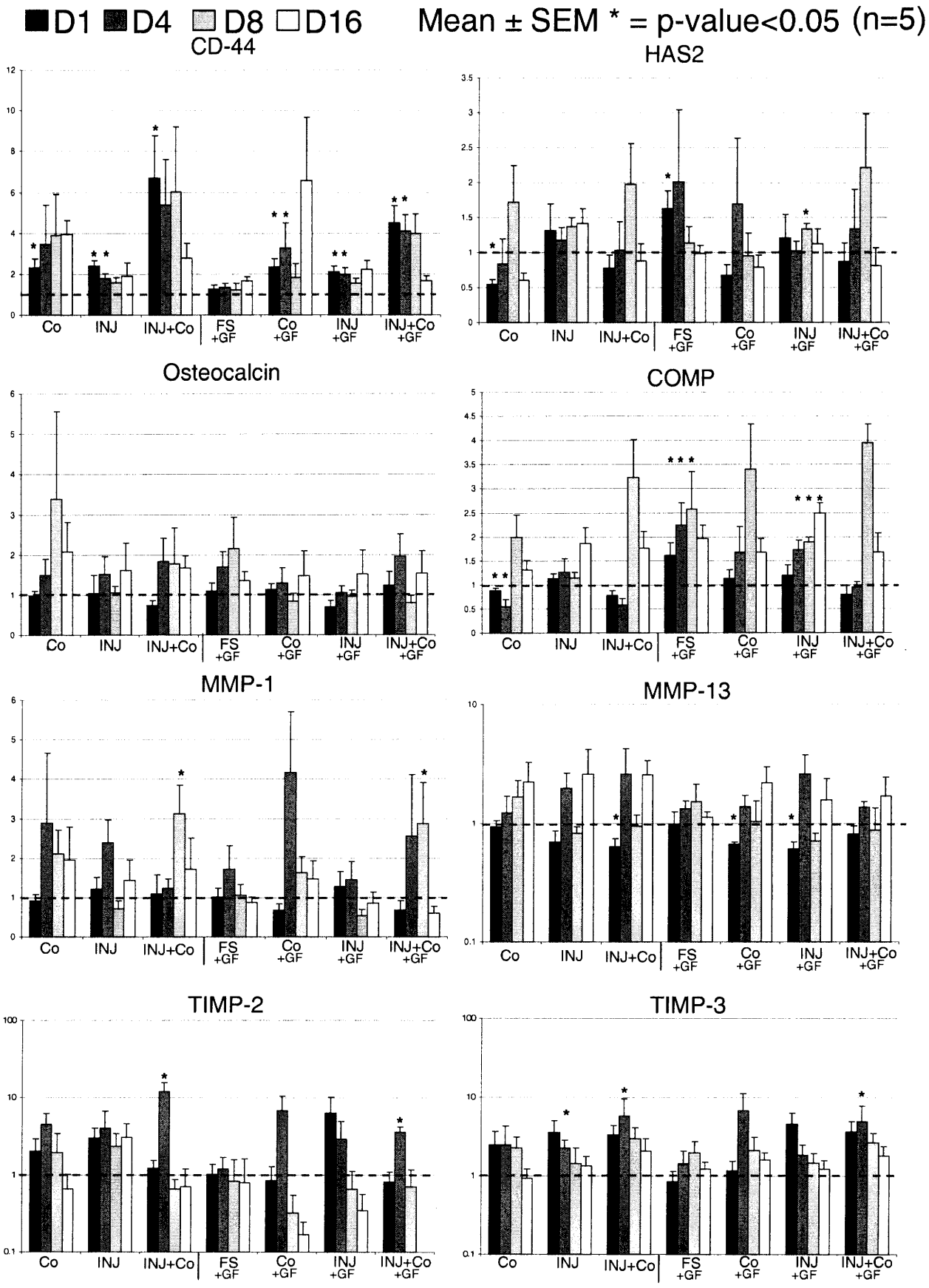
D1 D4 D8 D16
Mean ± SEM * = p-value<0.05 (n=5)
CD-44
HAS2
Osteocalcin
COMP
MMP-1
MMP-13
TIMP-2
TIMP-3
Co
INJ
INJ+Co
FS +GF
Co +GF
INJ +GF
INJ+Co +GF

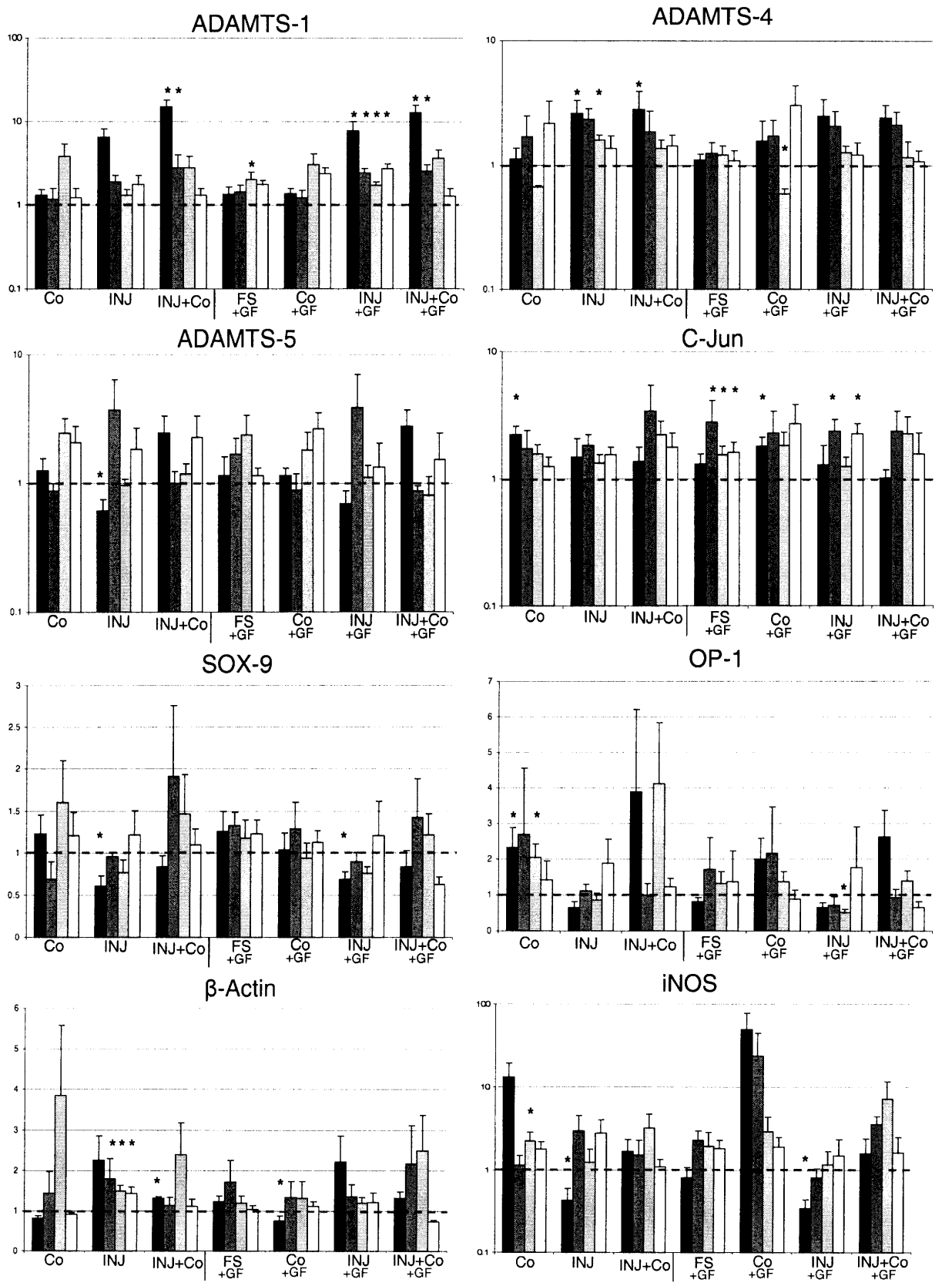
■D1 ■D4 □D8 □D16 Mean ± SEM * = p-value<0.05 (n=5)
ADAMTS-1
ADAMTS-4
ADAMTS-5
C-Jun
SOX-9
OP-1
β-Actin
iNOS
Co
INJ
INJ+Co
FS +GF
Co +GF
INJ +GF
INJ+Co +GF

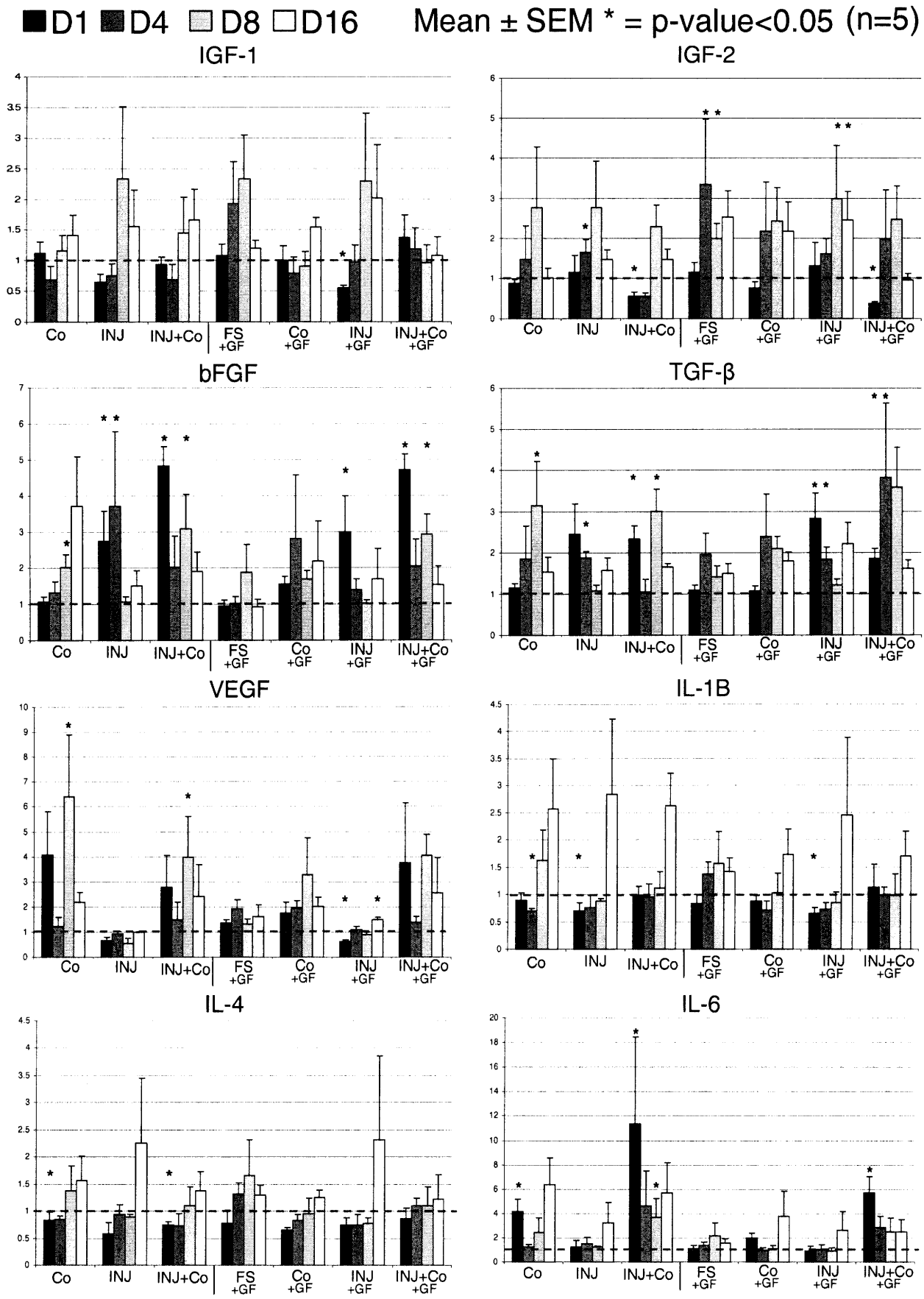
■D1 ■D4 □D8 □D16
Mean ± SEM * = p-value<0.05 (n=5)
IGF-1
IGF-2
bFGF
TGF-β
VEGF
IL-1B
IL-4
IL-6
Co
INJ
INJ+Co
FS +GF
Co +GF
INJ +GF
INJ+Co +GF

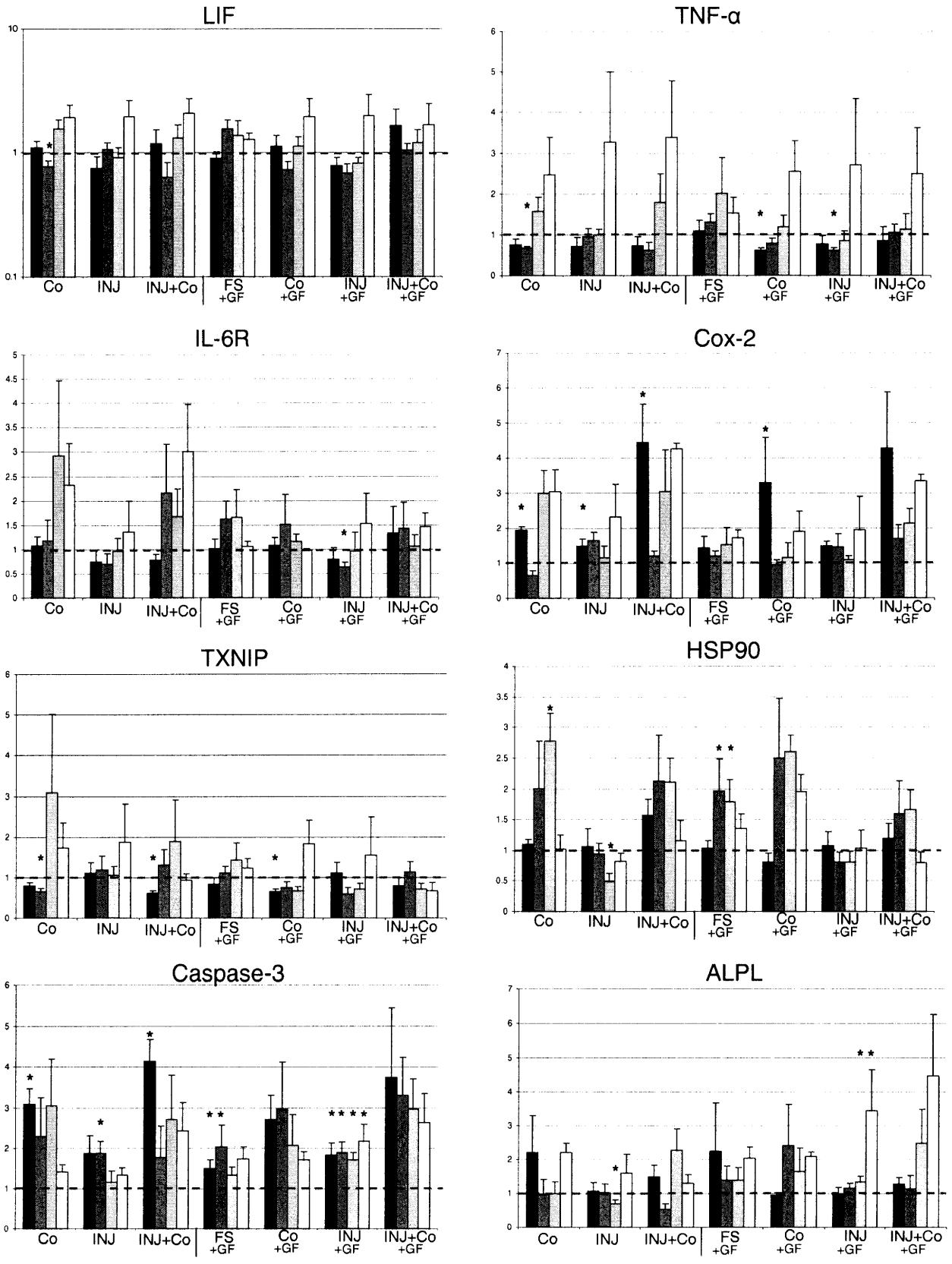
■D1 ■D4 ▨D8 □D16 Mean ± SEM * = p-value<0.05 (n=5)
LIF
TNF-α
IL-6R
Cox-2
TXNIP
HSP90
Caspase-3
ALPL
Co
INJ
INJ+Co
FS +GF
Co +GF
INJ +GF
INJ+Co +GF

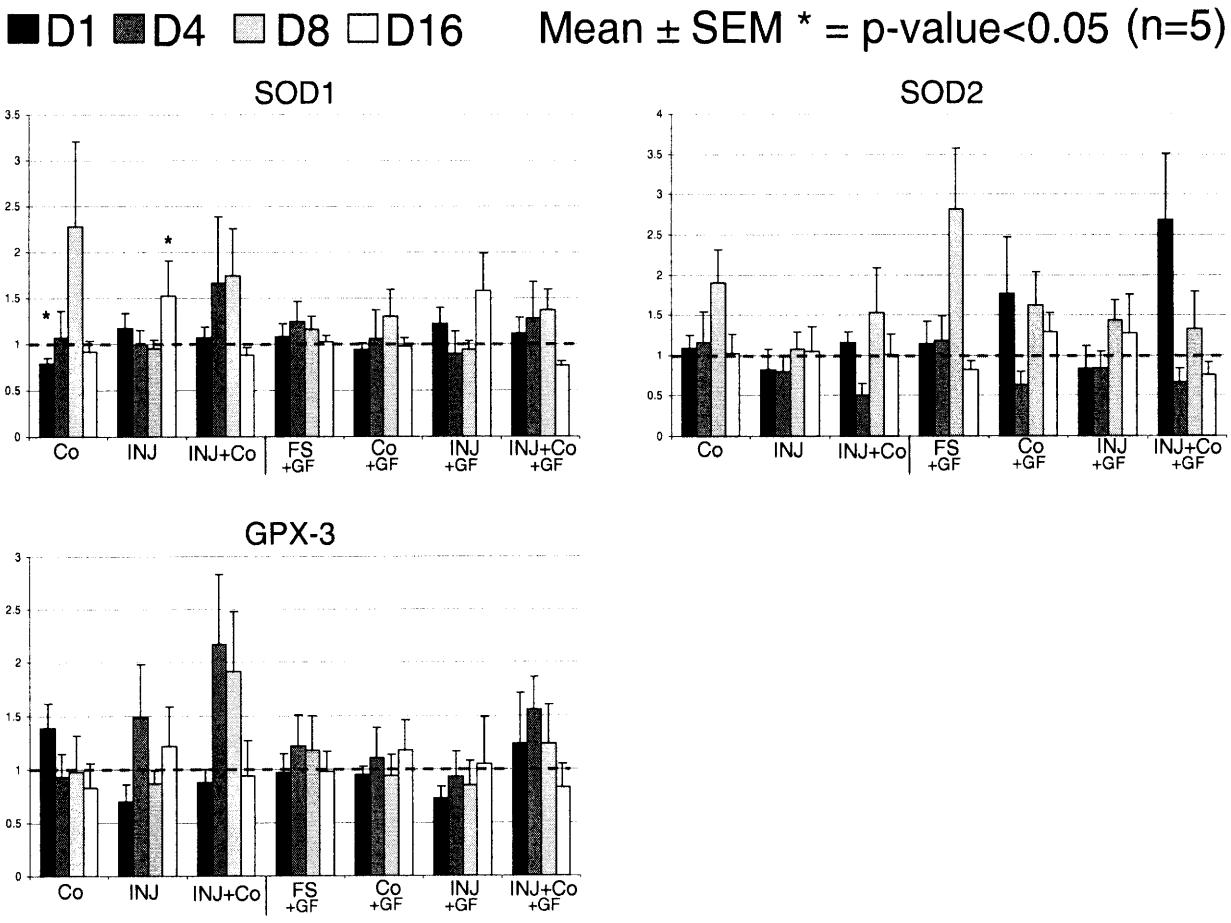
■D1 ■D4 □D8 □D16 Mean ± SEM * = p-value<0.05 (n=5)
SOD1
SOD2
GPX-3
Co
INJ
INJ+Co
FS +GF
Co +GF
INJ +GF
INJ+Co +GF

4.7.5 Effects of GF Treatment- Longer Term Gene Expression

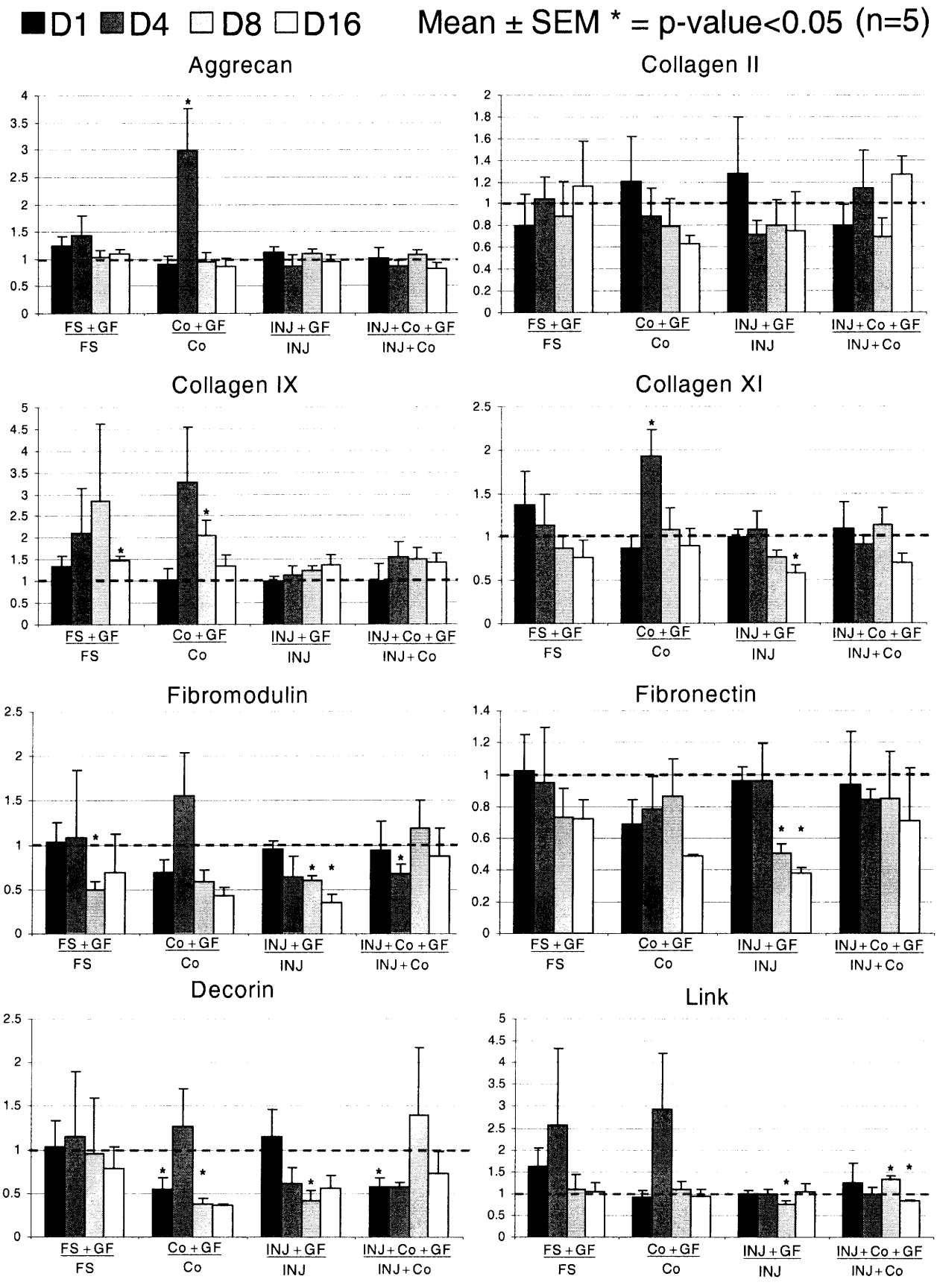

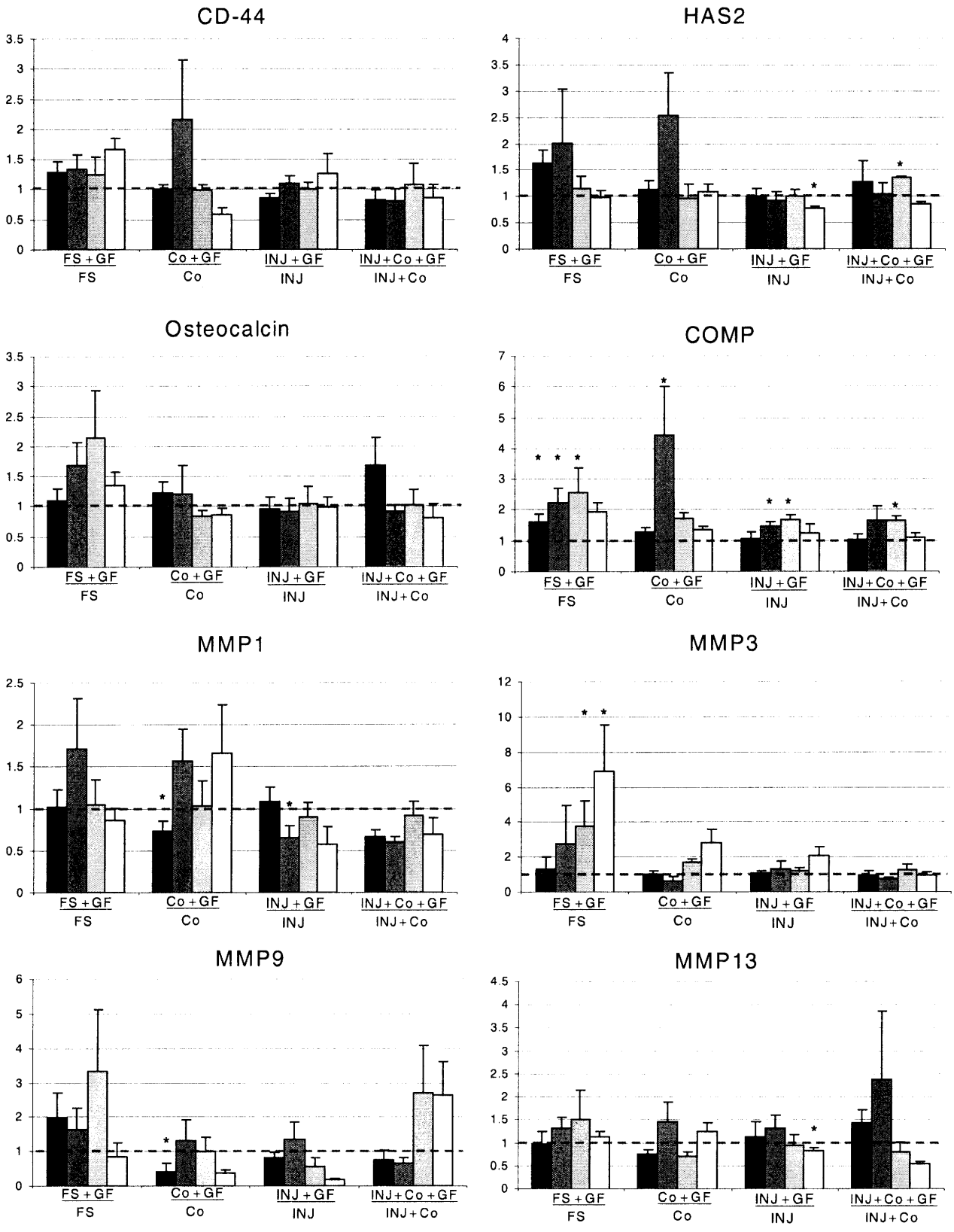
■D1 ■D4 □D8 □D16 Mean ± SEM * = p-value<0.05 (n=5)
CD-44
HAS2
Osteocalcin
COMP
MMP1
MMP3
MMP9
MMP13
FS + GF
Co + GF
INJ + GF
INJ + Co + GF
FS
Co
INJ
INJ + Co

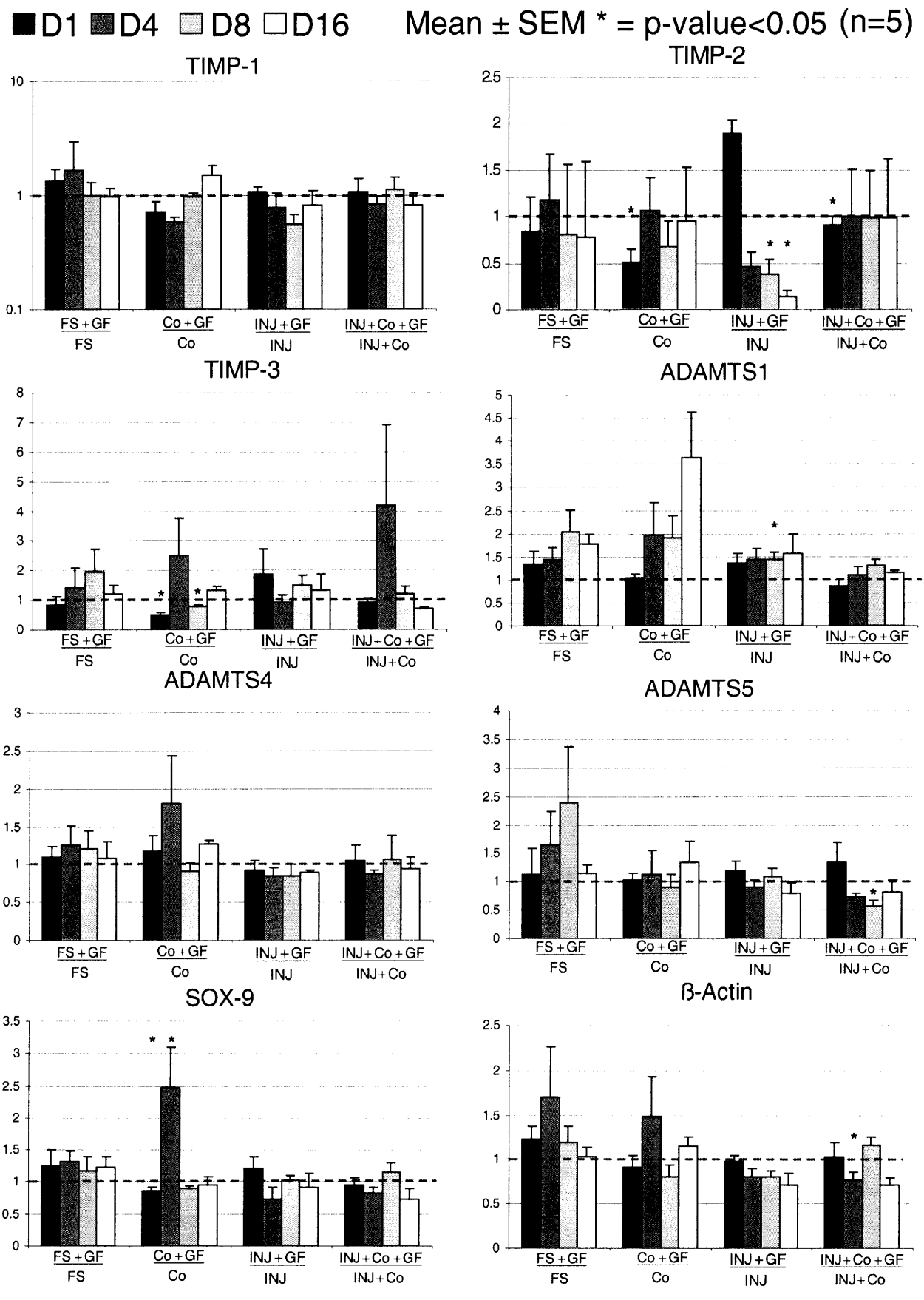
■D1 ■D4 □D8 □D16 Mean ± SEM * = p-value<0.05 (n=5)
TIMP-1
TIMP-2
TIMP-3
ADAMTS1
ADAMTS4
ADAMTS5
SOX-9
ß-Actin
FS + GF
Co + GF
INJ + GF
INJ + Co + GF
FS
Co
INJ
INJ + Co

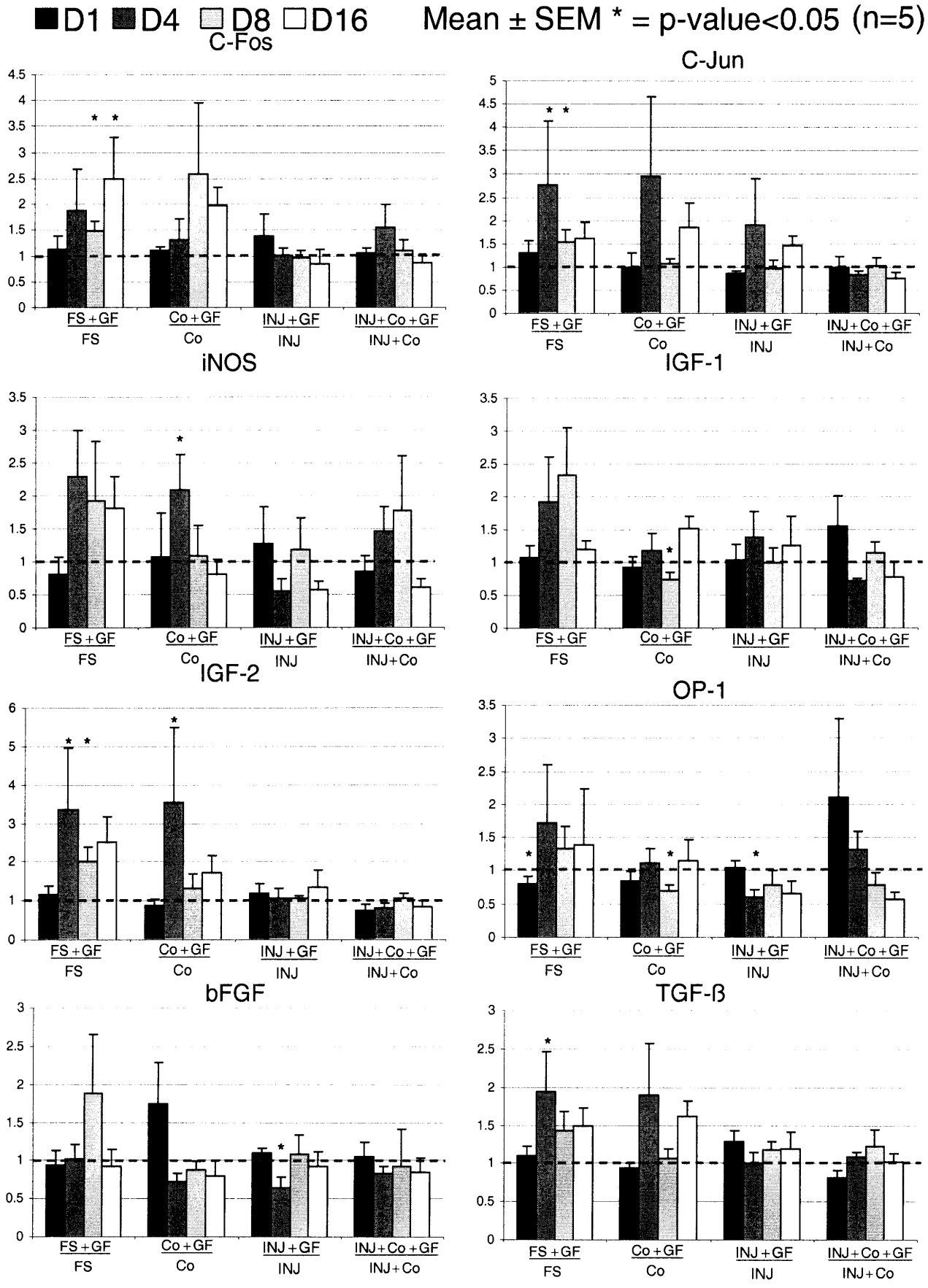
D1 D4 D8 D16
Mean ± SEM * = p-value<0.05 (n=5)
C-Fos
C-Jun
iNOS
IGF-1
IGF-2
OP-1
bFGF
TGF-ß
FS + GF
Co + GF
INJ + GF
INJ + Co + GF
FS
Co
INJ
INJ + Co

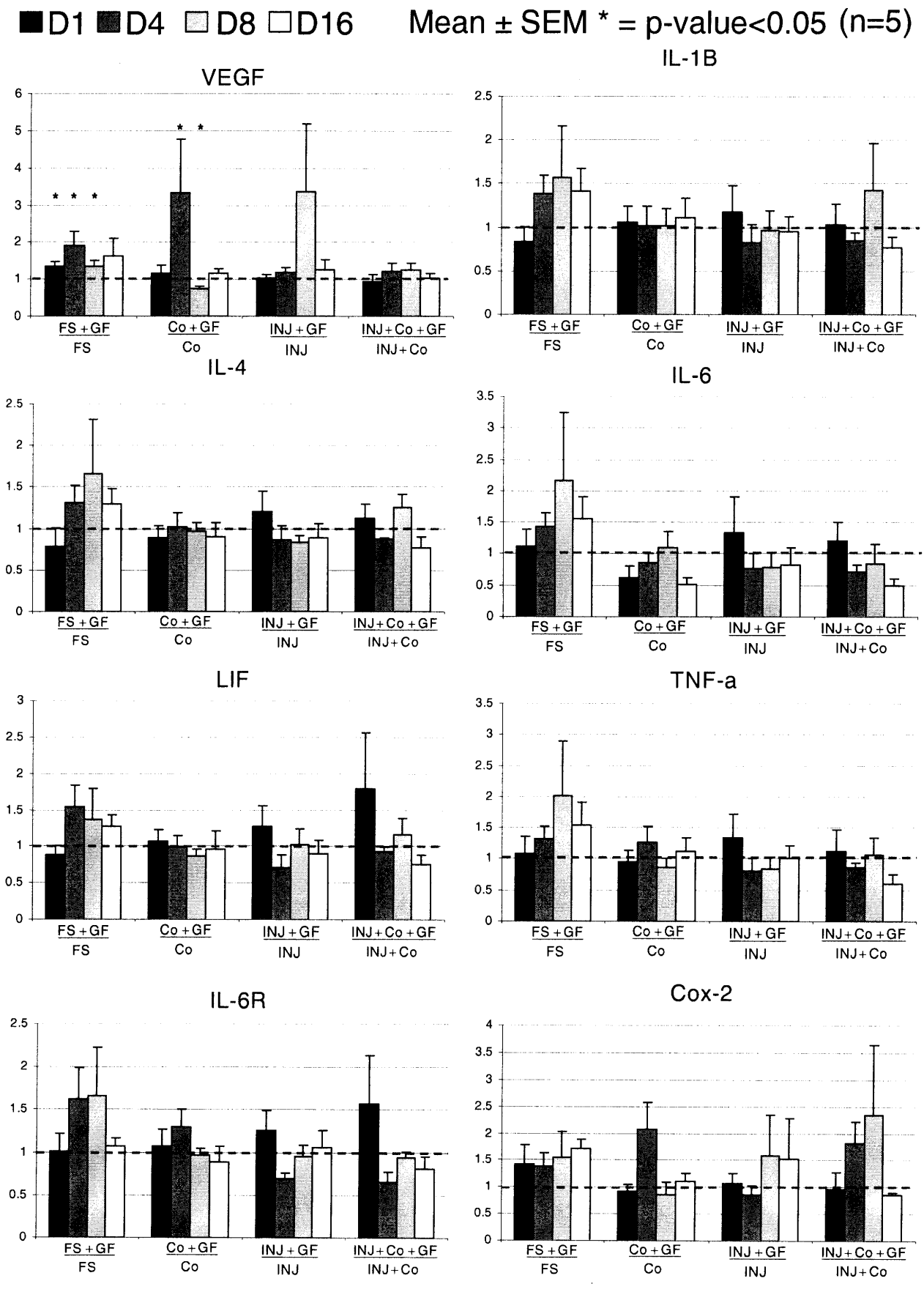
■D1 ■D4 □D8 □D16 Mean ± SEM * = p-value<0.05 (n=5)
VEGF
IL-1B
IL-4
IL-6
LIF
TNF-a
IL-6R
Cox-2
FS + GF
FS
Co + GF
Co
INJ + GF
INJ
INJ + Co + GF
INJ + Co

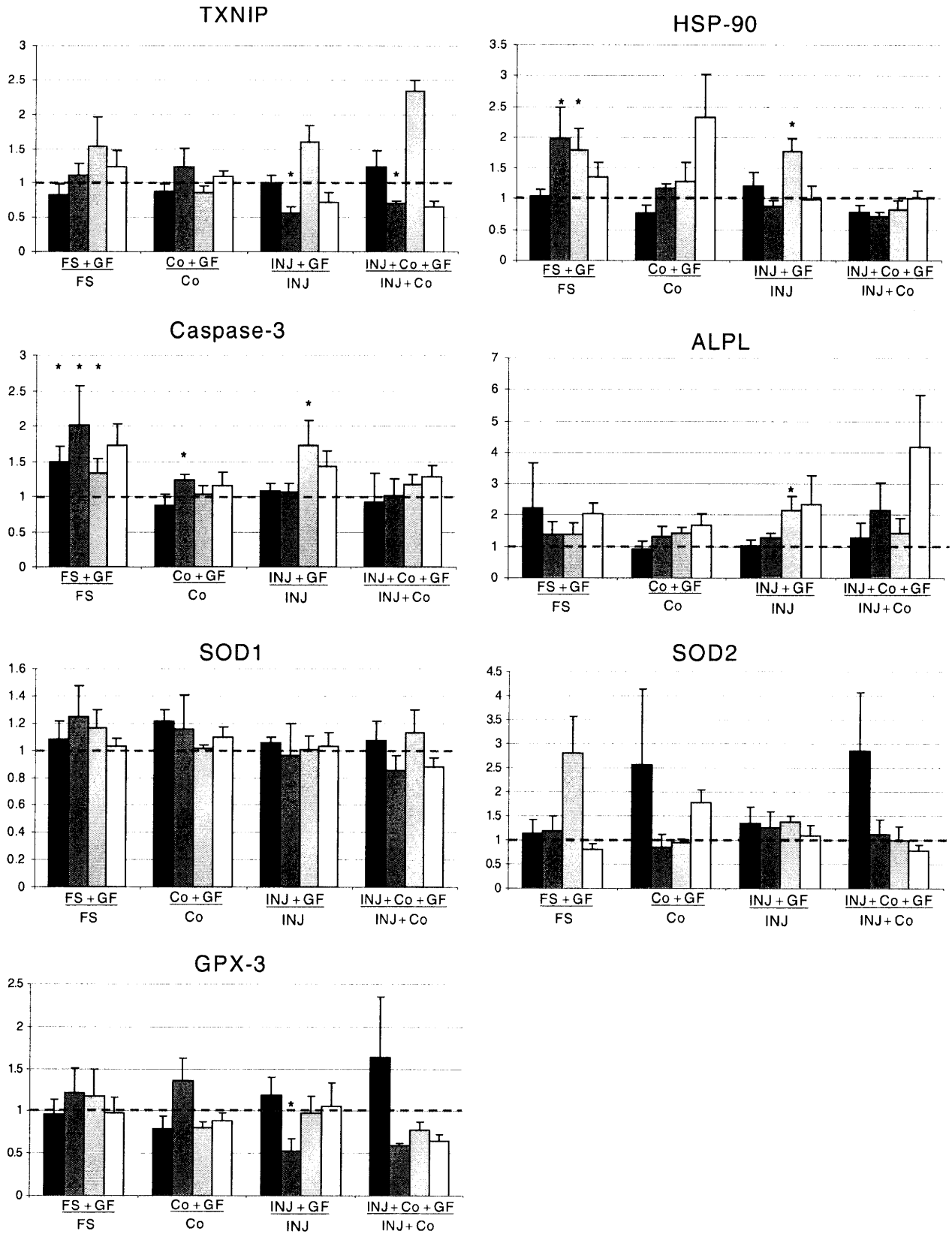
■D1 ■D4 □D8 □D16 Mean ± SEM * = p-value<0.05 (n=5)
TXNIP
HSP-90
Caspase-3
ALPL
SOD1
SOD2
GPX-3
FS + GF
FS
Co + GF
Co
INJ + GF
INJ
INJ + Co + GF
INJ + Co

Chapter 5

Human Tissue Response to Mechanical Injury and Co-culture with excised Joint Capsule

* This study is in collaboration with Professors Anna Plaas and John Sandy, Rush University Medical School, Chicago, IL.

5.1 Introduction

An *in vitro* model of injury has been established in our laboratory incorporating the effects of mechanical injury cartilage co-cultured with injured joint capsule (JC) tissue [1, 2]. *In vitro* mechanical injury of cartilage alone has been shown to increase hydraulic permeability [3] and water content [4-6], decrease stiffness [5, 7], and increase glycosaminoglycan (GAG) lost to the medium [5, 8-10]. Cells in cartilage subjected to this injury have been shown to decrease biosynthesis rates [5], undergo apoptosis and necrosis [4, 5, 11, 12], and have elevated levels of protease transcript activity within the first 24 hours [13]. Co-culturing un-injured cartilage with damaged joint capsule *in vitro* has resulted in a decrease in cartilage biosynthesis rates [1, 14] as well as a loss of proteoglycan and collagen as seen though histology staining [15]. GAG release from cartilage co-cultured with synovial or capsular tissue was not decreased with the inhibition of IL-1β, TNF-α, and ACITIC [16]. Under the same conditions of cartilage co-cultured with joint capsule, GAG loss was blocked by treatment with EDTA [16]. While the effects of JC co-culture appear to accelerate degradation, studies have also shown that synoviocytes from joint capsule tissue provide chondrocytes with protection against reactive oxygen species, which are known to induce membrane damage and lipid peroxidation [17]. This model of injury has not been fully investigated in non-arthritic human cartilage tissue.

The objectives of this study was to more fully explore the degradative effects on human cartilage of mechanical injury combined with co-cultured excise joint capsule as measured by protein biosynthesis rates, the amount of GAG lost to the medium, and the prevalence of select key cartilage proteins, including aggrecan and versican, using western blot analysis and

immunohistochemistry. We hypothesize that the combination of mechanical injury co-cultured with excised joint capsule will have a greater degradation effect compared to either mechanical injury alone or co-cultured joint capsule alone, and that these will be evident in the measures of GAG loss, biosynthesis rates, and protein levels.

5.2 Materials and Methods

Tissue Harvest

Human tissue composed of knees, ankles, and joint capsule were obtained through the Gift of Hope Organ and Tissue Donor Network (Elmhurst, Illinois) and in collaboration with Rush Medical Center (Chicago, Illinois). All research was approved by the Office of Research Affairs at Rush–Presbyterian–St. Luke's Medical Center and by the Committee on the Use of Humans as Experimental Subjects at the Massachusetts Institute of Technology. Five donors with normal body mass index (BMI) levels (less than BMI 24.9) and no history of osteoarthritis or autoimmune disease were obtained. The 5 donors included various ethnic backgrounds, different sexes, and were of the ages 19, 19, 42, 55, and 74. A full description of the donors can be seen in Table 5.1.

Table 5.1 Information on Donor Tissue

Donor	Age	Grade	Tissue	M/F	RACE
Human 1	42	0	Knee	M	Caucasian
Human 2	19	0	Knee and Ankle	M	Caucasian
Human 3	19	0	Knee and Ankle	M	Black
Human 4	74	1	Ankle	M	Asian
Human 5	55	0	Ankle	F	Caucasian

Table 5.1 List of human donor information and tissue provided by Gift of Hope Organ and Tissue Donor Network.

In addition, all joint surfaces were scored as grade 0 or 1 on a modified Collins scale [18], and only cartilage from an area that was smoothly reflective and unfibrillated to visual inspection was harvested for these experiments. Joint capsule was extracted from the knee joint of each donor and taken from the areas adjacent to the medial and lateral condyles (Figure 5.1). Tissue was received and processed within 24 hours of donor death. Upon obtaining the femoral portion of the knee joint and/or talus of the ankle joint, under sterile techniques articular cartilage was removed from the medial and lateral femoral patello groove and medial and lateral condyles (knee) and/or from the trochlear surface, the lateral and medial malleolus, and the anterior and posterior calcaneal surfaces (ankle) and placed in feeding medium. Feeding medium consisted of serum-free, 1% ITS supplemented feeding medium consisting of high glucose Dulbecco's modified essential medium supplemented with 10 nM Hepes Buffer, 0.1 mM nonessential amino acids, 20 μg/ml ascorbate, 100 units/ml penicillin, 100 μg/ml streptomycin, and 0.25 μg/ml amphoericin B. Articular cartilage was punched with a 3mm diameter dermal punch and allowed to equilibrate in medium at 37°C and 5% CO_2 for 1 day. After equilibration, 3mm diameter cylinders were sliced into approximately 800-1000 μm thick disks using a brain cutter instrument (TM-1000, ASI Instruments, Warren, MI). Disks were allocated into 1st mm

(cartilage disks containing superficial zone of articular cartilage) and 2nd mm (cartilage disks absent of superficial zone) pools. These plugs were placed in fresh medium and allowed to equilibrate for 1 day. JC excised adjacent to the lateral and femoral condyles was cut into ~5mm x 5mm sections approximately 0.5mm thick and equilibrated for 2 days in feeding medium.

Figure 5.1 Location of Joint Capsule and Articular Cartilage

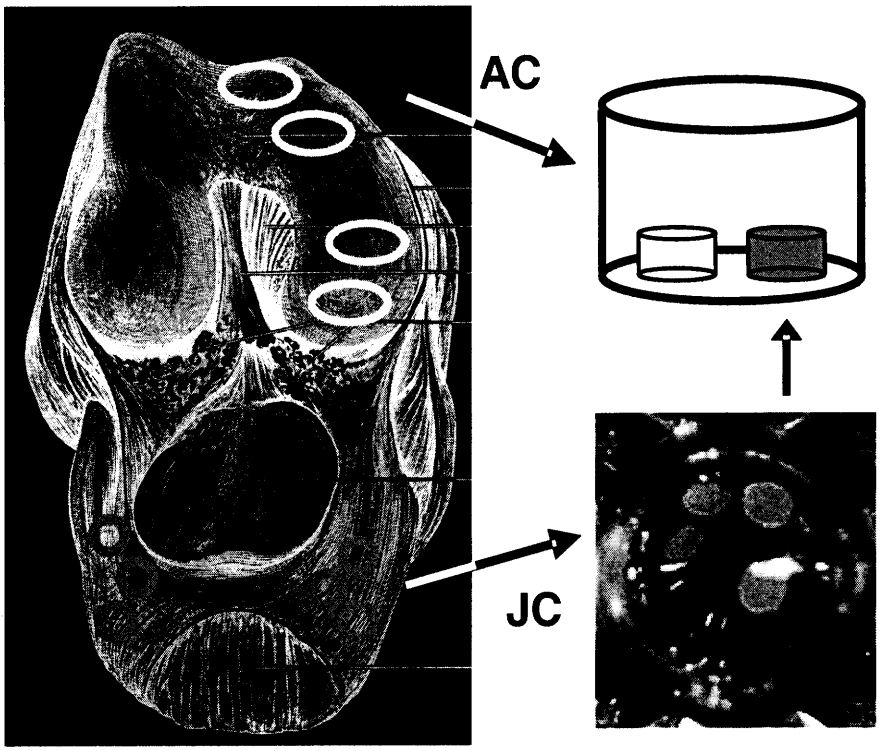

Figure 5.1 Schematic of knee joint where orange circles denote location of joint capsule excision and white ovals denote areas of cartilage harvest. Adapted from Patwari, 2003 [19].

Injury

After two days of equilibration, disks were allocated into one of 4 conditions; (1) free swell, (2) normal cartilage co-cultured with JC (Co), (3) cartilage mechanically injured, and (4) injured cartilage co-cultured with joint capsule (INJ+Co). A custom designed incubator housed loading apparatus[20] was used to compress cartilage disks. Each cartilage disk designated for mechanical injury was loaded individually in a polysulfone chamber allowing for radially-

unconfined compression [5, 8, 9]. Cartilage disks were measured for height, compressed to a final strain of 65% at a velocity of 400% per second, and promptly removed and placed in fresh culture media as described previously [13]. As has been described previously [8], the different size and mechanical properties of human cartilage compared to bovine cartilage necessitates an increase in final strain and strain rate to obtain qualitatively similar mechanical injury. Application of this strain and strain rate produced a peak stress on the order of 20MPa, and after injury, visual inspection revealed most plugs altered their round disk shape to an elliptical shape with samples occasionally showing substantial tissue fracture. Three to five pieces (to ensure equal amounts of JC tissue) of cut joint capsule were added to Co and INJ+Co conditions.

Protein Biosynthesis

Radiolabel incorporation was measured at days 2, 6, and 16 post-injury for knee cartilage, and days 2 and 6 for ankle cartilage. In some cases, due to the lack of cartilage tissue harvested, knee experiments were limited to two time points, days 2 and 6. Human explants were cultured in fresh media 24 hours prior to 2, 6, and 16 days in 10 μCi/ml [^{35}S]-sulfate and 20 μCi/ml [^{3}H]-proline. After culture, cartilage explants were washed four times over 60 minutes in 1ml phosphate-buffer saline (PBS) supplemented with 0.8 mM sodium sulfate and 0.5 mM proline to remove free radiolabel, and digested in 1 ml protease K solution (100 pg/ml in 5O mM Tris-HCI and 1 mM CaClz at pH 8) at 60°C for 12-18 h. Digested explants were homogenized in Optiphase Supermix scintillation fluid and measured using a Microbeta plate reader. Biosynthesis rates were normalized to levels of DNA in the tissue, which was measured by CyQUANT Cell proliferation assay kit (Molecular Probes, Inc. Eugene, OR) and DNAse (Applied Biosystems, Foster City, CA).

Antibodies

Anti-CDAG antibody is used to detect HA binding sequence of aggrecan, versican, and Link protein as well as the NITGE and VDIPEN neoepitopes. CDAG predominantly binds to aggrecan species in cartilage [21]. Anti-DPE antibody binds to the N-terminus of versican, a molecule known for its anabolic response to injury [22, 23].

Western Blotting:

Explants were placed in protease inhibitor and stored at -80°C until extraction. Cartilage was washed in ice-cold phosphate-buffered saline (PBS) (supplemented with proteinase inhibitors), and 6 plugs (~50 μg wet weight) were pooled followed by extraction in 4 M guanidine HCl (supplemented by proteinase inhibitors), 50 mM sodium acetate, pH 7.3, purified by G50 and DE52 chromatography as described [24] and deglycosylated core protein from 75 mg dimethylmethylene blue-glycosaminoglycan (DMMB-GAG) was loaded per lane [25].

Immunohistochemistry

Select plugs were fixed in 10% formalin at appropriate time points, sectioned, treated, and imaged as previously described [25]. IHC probes were individually optimized for sensitivity, specificity and reproducibility. Thin (4 μm) sections were deparaffinized as described [26] and incubated in dilute goat serum (1.5% v/v in PBS) for 20 min, prior to exposure to specific IgGs, diluted to 1, 2, 5 and 10 mg/ml with 1.5% (v/v) goat serum for 30 min at RT. IgG solutions were removed, and sections were washed extensively in PBS before incubation at RT for 30 min with 7.5 mg/ml biotinylated goat anti-rabbit IgG (Vector labs). Sections were rinsed in PBS and then treated with 3% hydrogen peroxide (v/v) in tap water for 10 min, rinsed again in PBS, and incubated with horseradish peroxidase (HRP) labeled avidinebiotin complex (Vector labs) for 30 min at RT, washed with PBS and incubated with 3,30-diaminobenzidine (DAB)

substrate for 30 min. Negative controls (background staining) for each antibody were established by omission of primary antibody and incubation with non-immune rabbit IgG at the same concentration and under the same conditions. Specificity was independently established by Western analysis with human, bovine, and recombinant antigens and antigenic peptide blocking experiments [21, 24, 26-28].

GAG Loss

The amount of sulfated glycosaminoglycan (GAG) content within the condition medium and within each cartilage plug was quantified using dimethylmethylene blue (DMMB) dye-binding assay [29]. Standard curves were generated using known amounts of GAG (Sigma, St. Louis, MO). Cartilage plugs were proteolytically digested through incubating overnight in protease K at 60°C. GAG from plugs was measured though DMMB dye. For ease of comparison, GAG loss data was expressed in percentage of GAG loss to the medium, normalized by the total GAG (GAG in medium + GAG in plug).

GAG Loss and Biosynthesis Analysis

All data are represented as mean ± SEM. A three-way analysis of variance was used to test significant differences in biosynthesis data. P-values less than 0.05 were considered significant.

5.3 Results

Biosynthesis

Generally the rates of biosynthesis measured over the five different subjects decreased over time, having the greatest amount of biosynthesis on day 2, followed by a decrease in biosynthesis on days 6 and 16. *Knee Cartilage*: Knee cartilage not containing the superficial zone (2nd mm) was not significantly responsive to mechanical injury or co-culture treatments, yet cartilage containing the superficial zone (1st mm) was significantly downregulated in the presence of INJ and INJ+Co, for 19-year-old tissue (Sulfate and proline) (Figure 5.2A, B, Appendix 5.7.1), and significantly downregulated 42-year-old tissue by 14% under INJ (Proline) (Appendix 5.7.1).

Figure 5.2 Biosynthesis rates of 1st mm Human 2 (19 years) Mean ± SEM (n=5)

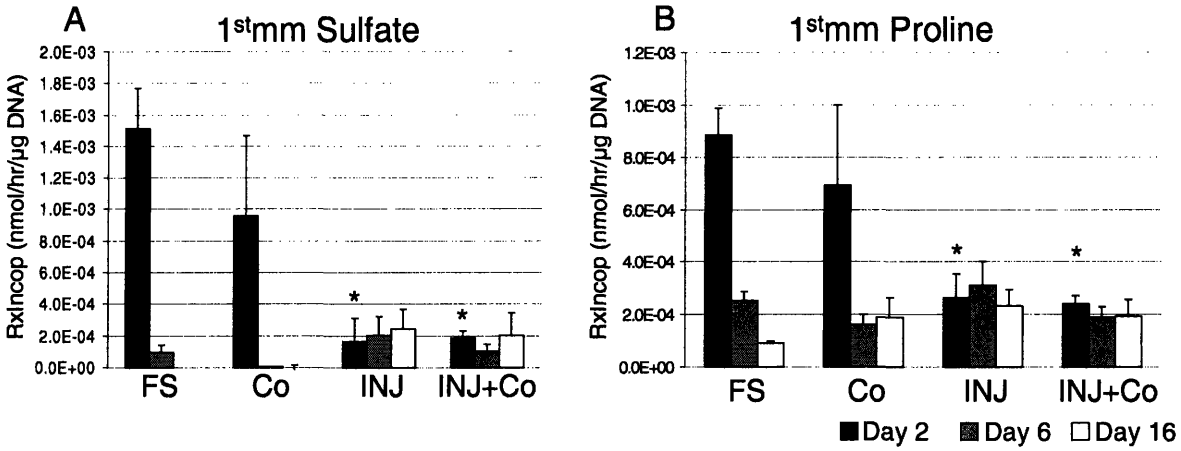

Figure 5.2 Biosynthesis rates of [^{35}S]-Sulfate and [^{3}H]-Proline 1st mm knee tissue in Human 2 (19 years). Stars represent significant difference compared to FS conditions (p-values <0.05).

Ankle Cartilage: Ankle cartilage was not significantly affected by co-culture, mechanical injury, or the combination of co-culture and mechanical injury (Appendix 5.7.1). Interestingly, most of

the conditions for the 4 tissue samples were transiently upregulated from days 2 to 6 (Figure 5.3A, B, Appendix 5.7.1). This trend was apparent in the youngest tissue, 19 years old (Figure 5.3A, B), as well as the oldest tissue tested, 74 years old (Figure 5.4A, B). This was most apparent under all tissue specimens when mechanical injury alone was applied. *Age*: No clear age-dependent trend was apparent when examining biosynthesis data in both knee and ankle cartilage (Appendix 5.7.1).

Figure 5.3 Biosynthesis rates of Ankle Human 3 (19 years) Mean ± SEM (n=5)

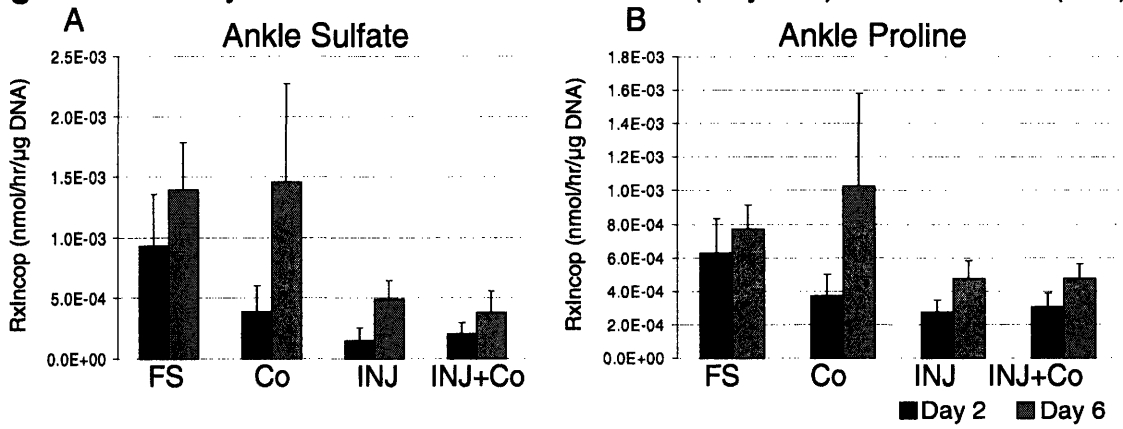

Figure 5.3 Biosynthesis rates of [^{35}S]-Sulfate and [^{3}H]-Proline ankle tissue in Human 3 (19 years).

Figure 5.4 Biosynthesis rates of Ankle Human 5 (74 years) Mean ± SEM (n=5)

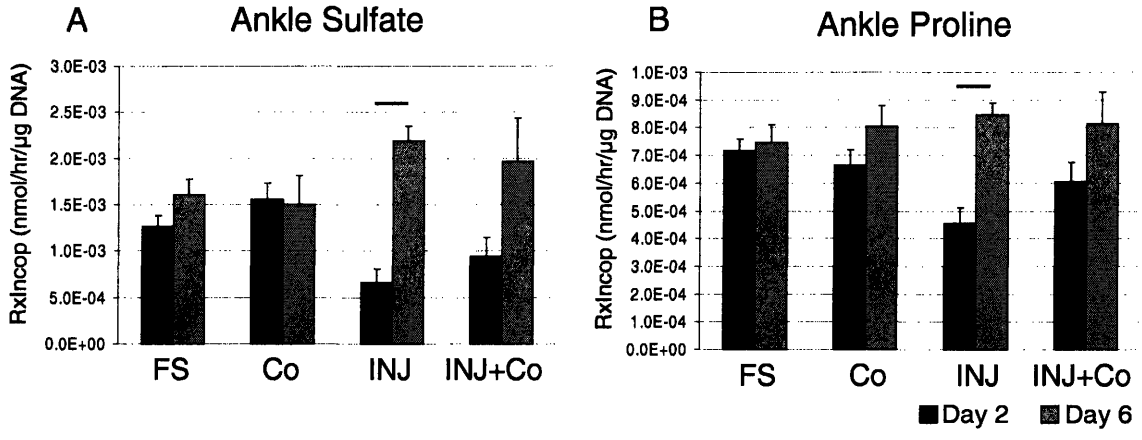

Figure 5.4 Biosynthesis rates of [^{35}S]-Sulfate and [^{3}H]-Proline ankle tissue in Human 5 (74 years). Bars represent statistical significance between ends (p-value < 0.05).

GAG Loss

Total sGAG content varied from donor to donor. *Knee Cartilage*: The combination of mechanical injury and co-cultured JC produced the greatest sGAG loss to the medium in plugs containing the knee superficial zone. The younger 19-year-old 1st mm cartilage appeared more resilient to the combination of joint capsule and mechanical injury (15% sGAG loss day 6) compared to middle-age 1st mm cartilage (age 42) samples (40% sGAG loss, Day 6) (Figure 5.5A, Appendix 5.7.2). This age-dependent degradation was not seen in the 2nd mm (Figure 5.5B, Appendix 5.7.2). The 2nd mm of knee cartilage produced generally greater amounts of GAG loss to the medium, as illustrated in Human 2 (Figure 5.5A, B). Injury had a significant effect on the 19-year-old's GAG loss when comparing the 1st mm of INJ and INJ+Co to FS conditions (Figure 5.5A). This difference was only apparent at the last time point measured, 16 days after the injury.

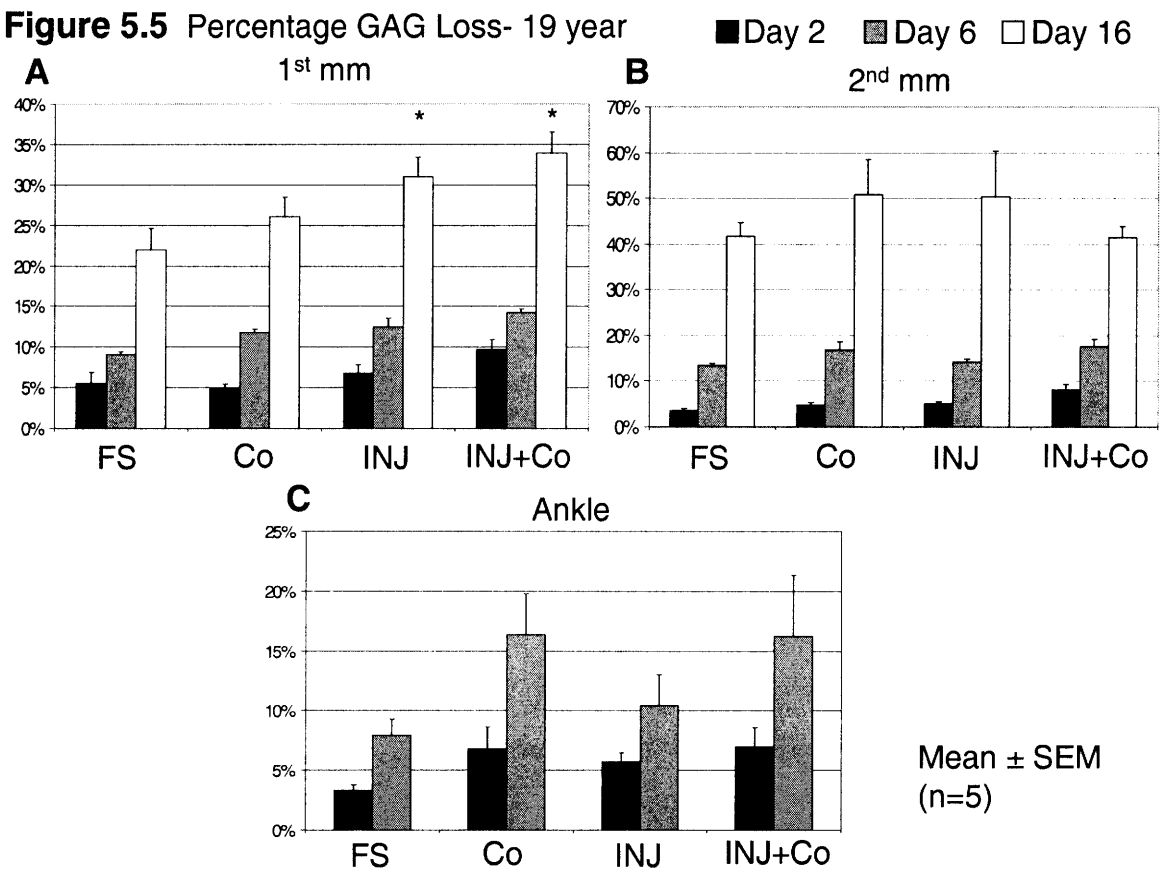

Figure 5.5 GAG loss to the medium in 1st mm Knee, 2nd mm Knee, and Ankle from Human 2 (19 years old). Percentage GAG loss was determined by GAG lost to the medium divided by total GAG measured (GAG lost to medium + GAG in plug). Stars represent statistical significance compared to FS conditions (p-value < 0.05).

Ankle Cartilage: The ankle tissue showed less sGAG loss (generally less than 10% after day 6, depending on tissue) than the knee (generally 15%-20% after day 6) from human 3 (19 year old). The older tissue, from donors 74 and 55, was more affected by INJ+Co compared to the two other younger tissue samples (19 and 19 years) (Appendix 5.7.2).

Western Analysis

Using anti-CDAG antibodies, aggrecan levels were not significantly different under the conditions of mechanical injury, uninjured cartilage co-culture with joint capsule, or

mechanically-injured cartilage co-cultured with joint capsule. G1-NITEGE/VDIPEN levels showed no significant changes in aggrecan species within the tissue over the 4 conditions tested (data not shown).

IHC

Sections were probed using anti-DPE and anti-CDAG antibodies. Versican-DPE showed great abundance in the 1st mm *in vitro* injury model, in both the mechanical injury and mechanical injury co-cultured with joint capsule conditions (Figure 5.6A). Versican, production of which is indicative of an anabolic response to injury, was detected strongly in mechanical injury conditions and, with the addition of joint capsule, was more prevalent in the 2nd mm than in the 1st mm (Figure 5.6A, B).

Figure 5.6 Versican-DPE 19 year

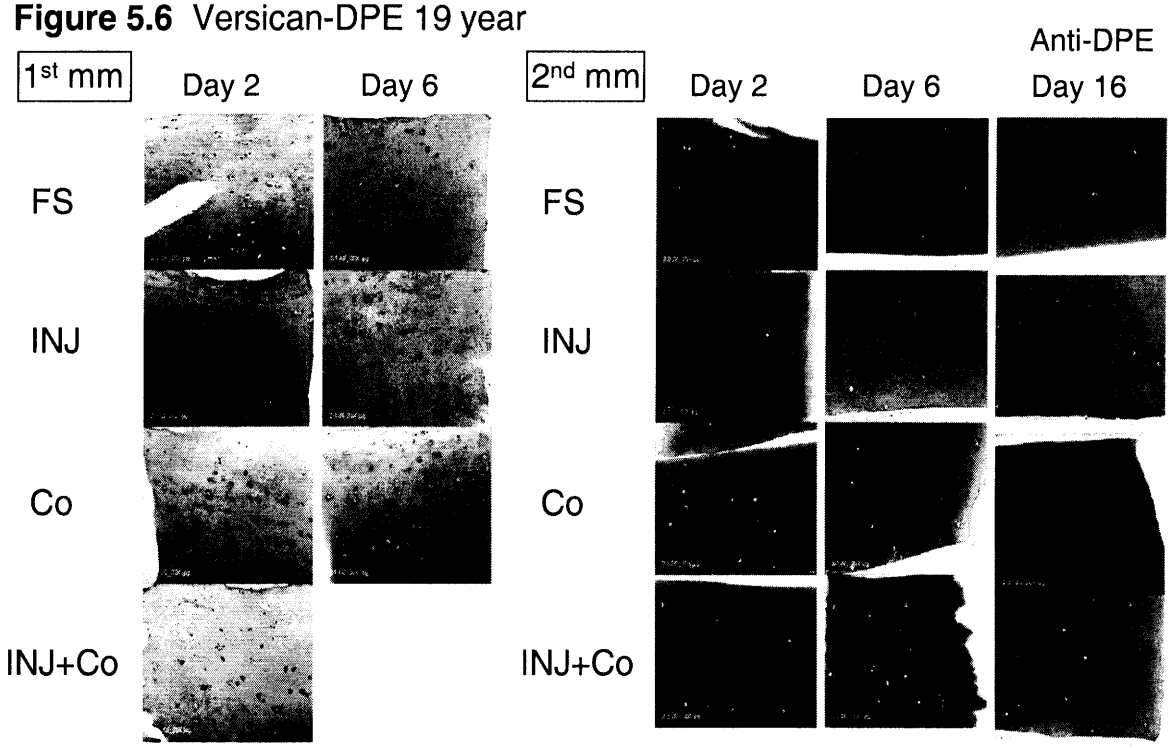

Figure 5.6 IHC samples stained with Anti-DPE targeting Versican expression from 1st mm and 2nd mm knee cartilage from Human 2 (19 years old). Plugs were placed in 10% formalin after 2, 6, and 16 days of treatment post treatment/injury.

Nuclear staining of versican G1 domain is also present in the deeper half of the 1st mm samples (Figure 5.6A). The 2nd mm plugs are more affected by co-culture than the 1st mm plugs, as evidenced by the versican activation (Figure 5.6B). CDAG antibodies pointed out the new population of aggrecan (Figure 5.7A, B). This staining shows cells in a hyper-anabolic state, and cells were activated in groupings. These groupings of aggrecan stimulated cells were randomly activated with no clear trend of spatial or depth dependence.

Figure 5.7 CDAG 19 years

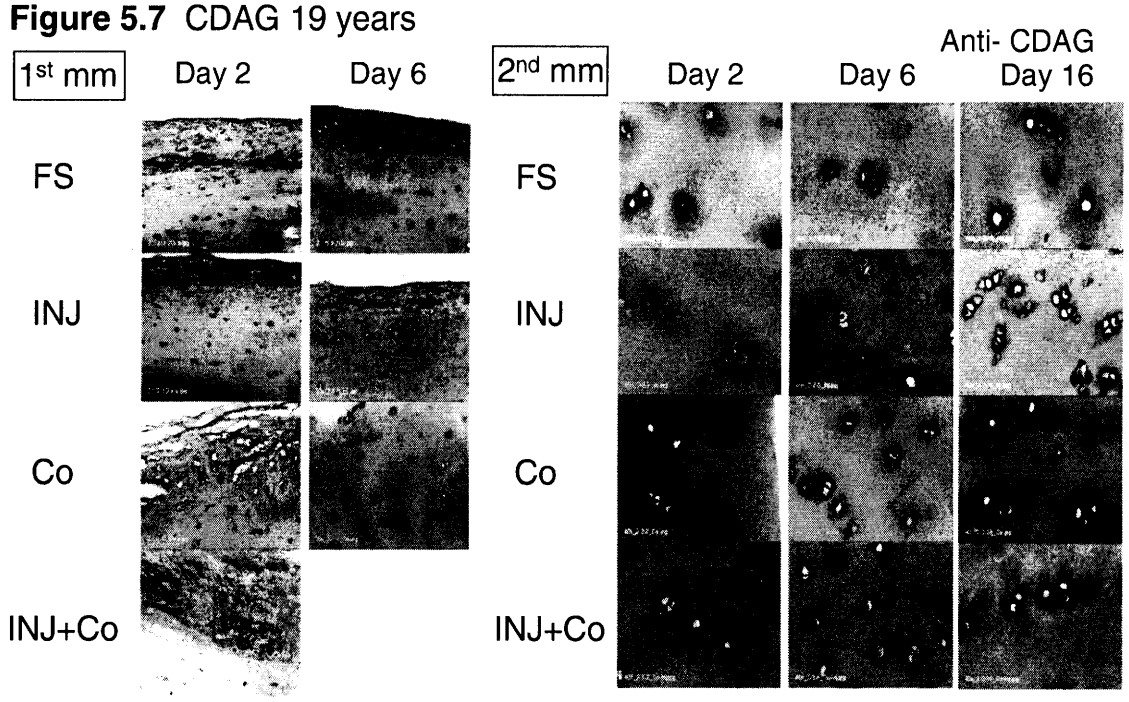

Figure 5.7 IHC samples stained with Anti-CDAG targeting aggrecan expression from 1st mm and 2nd mm knee cartilage from Human 2 (19 years old). Plugs were placed in 10% formalin after 2, 6, and 16 days of treatment post treatment/injury.

5.4 Discussion

The *in vitro* injury model demonstrated little effect on the aggrecan species profile within cartilage, as seen via Western blotting. This result agrees with previous studies [5] from injured and late stage human OA tissue where no major differences in aggrecan were observed. The IHC presented for mechanically-injured cartilage with the addition of joint capsule (INJ+Co) (Figure 5.6, 5.7) have striking similarity to previous IHC where tissue underwent notchplasty post-ACL reconstructive surgery (Figure 5.8, 5.9) [30].

Figure 5.8 Notchplasty injured cartilage- Versican-DPE

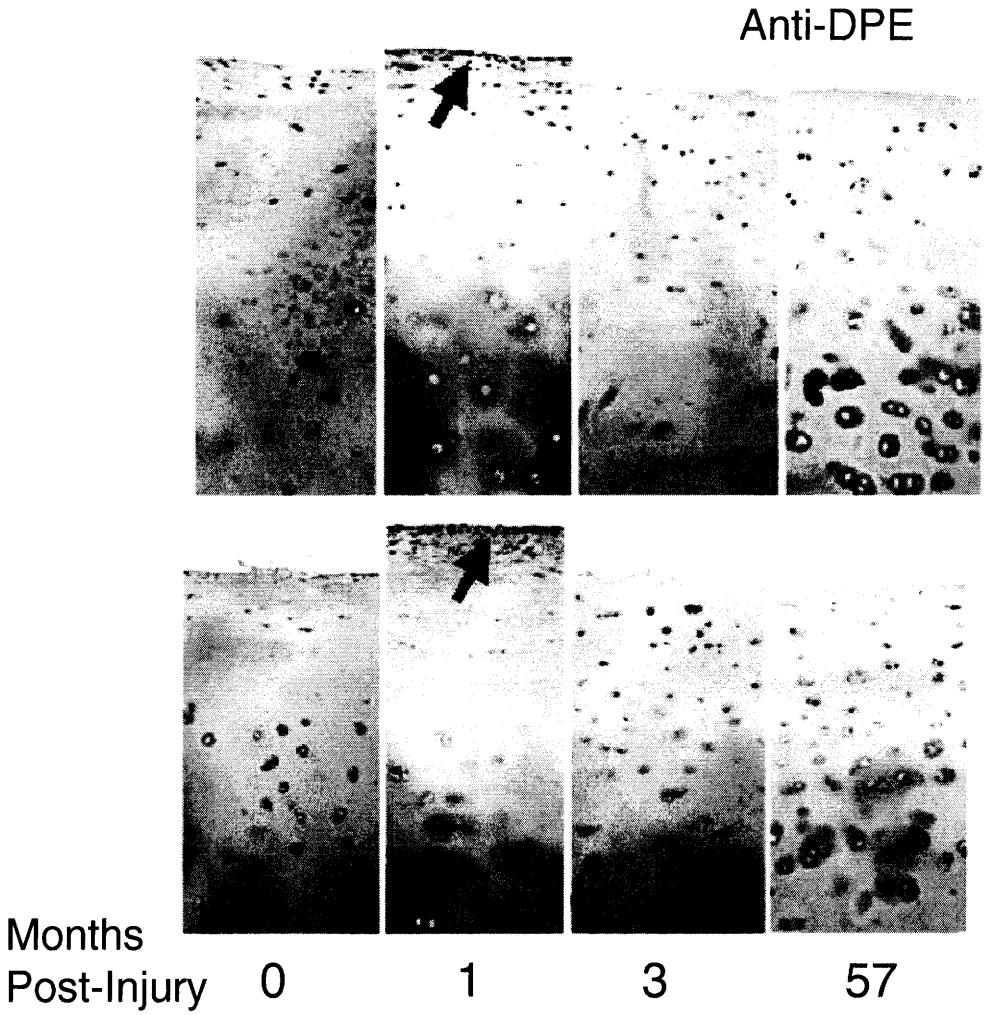

Figure 5.8 IHC samples stained with Anti-DPE targeting versican expression from human cartilage tissue taken from notchplasty experiment post-ACL reconstructive surgery. Tissue was examined 0, 1, 3, and 57 months post-surgery [30].

Human cartilage biopsies were obtained from the lateral femoral condylar notch expansion as part of ACL repair surgery. Similarities exist in the versican-DPE signaling abundance (Figure 5.6, 5.8) as well as the cell-associated localization (Figure 5.6, 5.8). From the IHC, it appears the JC is less effective in the superficial zones of cartilage (1^{st} mm), and more effective in the middle to deep zones (2^{nd} mm) of the cartilage (Figure 5.6, 5.7).

Figure 5.9 Notchplasty injured cartilage- CDAG

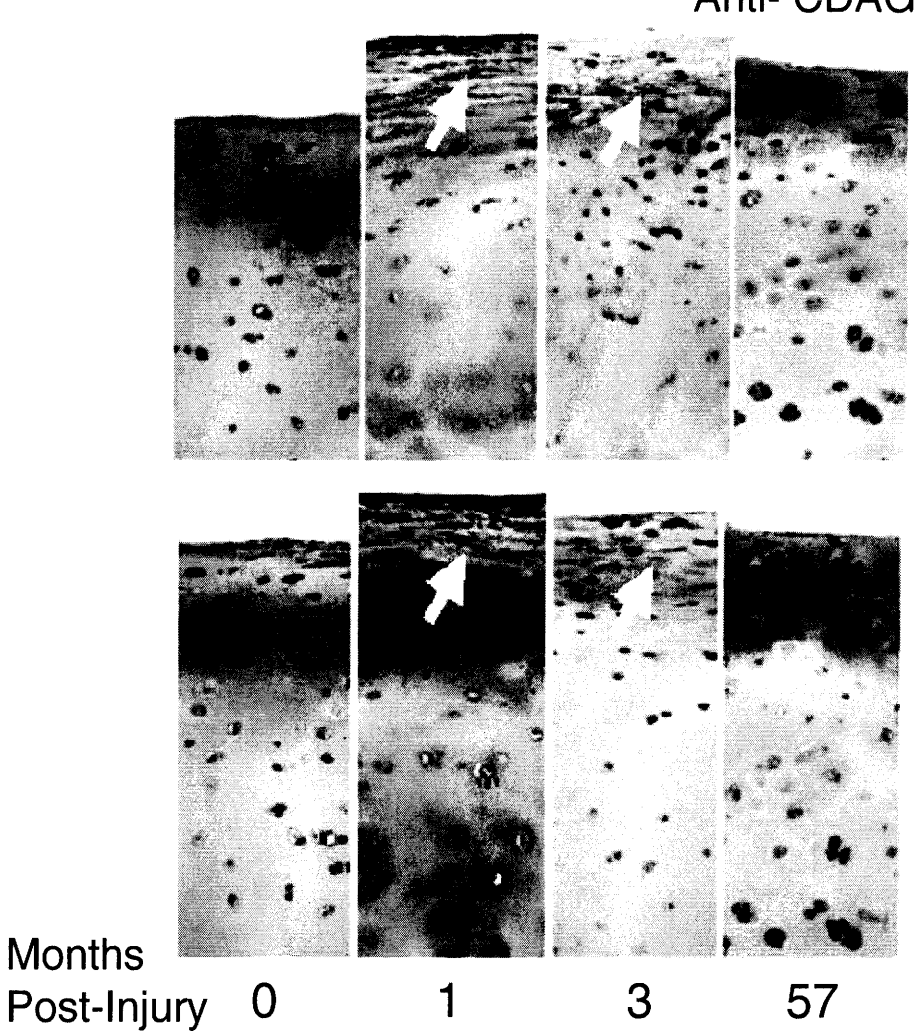

Figure 5.9 IHC samples stained with Anti-CDAG targeting aggrecan expression from human cartilage tissue taken from notchplasty experiment post-ACL reconstructive surgery. Tissue was examined 0, 1, 3, and 57 months post-surgery [30].

Biosynthesis rates of both sulfate and proline were significantly downregulated only at day 2, under mechanical injury and mechanical injury co-cultured with JC for a 10-year-old tissue under the 1st mm. Knee cartilage showed a strong transient downregulation over time, where ankle cartilage showed a transient increase in biosynthesis rates (Figures 5.2, 5.3, 5.4, Appendix 5.7.1). Mechanical injury alone and mechanical injury plus co-cultured joint capsule

only affected GAG loss in the 19-year-old cartilage significantly in the 1st mm at day 16 (Figure 5.5A). Ankle tissue showed to be more resilient to cartilage degradation measured through GAG loss (Figure 5.5C). This point, coupled with the trend that biosynthesis rates increased over time, provides a substantial difference between knee cartilage and ankle cartilage. The ankle cartilage appears to have the ability to turn the insult into a stimulatory event, while minimizing the amount of degradation compared to the control (FS). Knee cartilage, from both 1st and 2nd mm does not exhibit this trend, but responds in an opposite fashion to an injury insult, where the biosynthesis rates show substantial downregulation at early time points, and the GAG loss to the medium shows significant changes at later time points compared to the control (FS). Interestingly the 2nd mm of knee cartilage tended to exhibit large amounts of GAG loss, while maintaining comparable biosynthesis rates to the 1st mm. The surface area of the second mm plugs were all cut, assumably causing major damage to the intricate collagen and general ECM matrix. The 1st mm plugs still contained an intact superficial zone. This difference is likely a factor accounting for the difference in GAG loss between the 1st mm and 2nd mm of knee cartilage.

Taken together, it appears that our *in vitro* model of injury model mimic certain aspects of changes in bone-cartilage plugs harvested from patients as part of the surgical procedure involved in ACL repair. This work further verifies the viable model of mechanical injury co-cultured with joint capsule in human articular cartilage, and therefore vindicates the mechanical injury co-cultured with joint capsule model in bovine as has been reported in chapter 4 and which has been previously investigated [2].

5.5 Conclusion

An *in vitro* model of joint injury that includes the combination of mechanical injury to cartilage and subsequent co-culture with excised joint capsule mimics specific changes observed in human articular cartilage obtained from notchplasty post anterior cruciate ligament reconstructive surgery, as seen through IHC analysis. After *in vitro* injury, knee cartilage exhibited increased GAG loss and lower biosynthesis over time, while ankle cartilage exhibited less GAG loss over time and increased biosynthesis rates. The consequence of mechanical injury took 16 days to fully develop into a significant difference in GAG loss compared to FS. Biosynthesis rates in knee cartilage were significantly downregulated with the addition of mechanical injury at the first time point measured, two days after injury.

As previously reported, injurious conditions showed no significant difference in aggrecan species profile as examined by immunoblotting, up to six days after injury. Ongoing studies are aimed at further elucidating the molecular responses and cellular signaling pathways underlying the response of human tissue to combined mechanical injury and joint capsule co-culture.

5.6 References

1. Patwari, P., J. Fay, M.N. Cook, A.M. Badger, A.J. Kerin, M.W. Lark, and A.J. Grodzinsky, *In vitro models for investigation of the effects of acute mechanical injury on cartilage.* Clin Orthop Relat Res, 2001(391 Suppl): p. S61-71.
2. Lee, J.H., *Chondrocyte response to in vitro mechanical injury and co-culture with joint capsule tissue*, in *Biological Engineering Division.* 2005, Massachusetts Institute of Technology: Cambridge, MA. p. 162.
3. Thibault, M., A.R. Poole, and M.D. Buschmann, *Cyclic compression of cartilage/bone explants in vitro leads to physical weakening, mechanical breakdown of collagen and release of matrix fragments.* J. Orthop. Res., 2002. **20**(6): p. 1265-1273.
4. Torzilli, P.A., R. Grigiene, J. Borrelli, Jr., and D.L. Helfet, *Effect of impact load on articular cartilage: cell metabolism and viability, and matrix water content.* J Biomech Eng, 1999. **121**(5): p. 433-41.
5. Kurz, B., M. Jin, P. Patwari, D.M. Cheng, M.W. Lark, and A.J. Grodzinsky, *Biosynthetic response and mechanical properties of articular cartilage after injurious compression.* J Orthop Res, 2001. **19**(6): p. 1140-6.
6. Chen, C.T., N. Burton-Wurster, G. Lust, R.A. Bank, and J.M. Tekoppele, *Compositional and metabolic changes in damaged cartilage are peak-stress, stress-rate, and loading-duration dependent.* J Orthop Res, 1999. **17**(6): p. 870-9.
7. Loening, A.M., I.E. James, M.E. Levenston, A.M. Badger, E.H. Frank, B. Kurz, M.E. Nuttall, H.H. Hung, S.M. Blake, A.J. Grodzinsky, and M.W. Lark, *Injurious mechanical compression of bovine articular cartilage induces chondrocyte apoptosis.* Arch Biochem Biophys, 2000. **381**(2): p. 205-12.
8. Patwari, P., M.N. Cook, M.A. DiMicco, S.M. Blake, I.E. James, S. Kumar, A.A. Cole, M.W. Lark, and A.J. Grodzinsky, *Proteoglycan degradation after injurious compression of bovine and human articular cartilage in vitro: Interaction with exogenous cytokines.* Arthritis Rheum., 2003. **48**(5): p. 1292-301.
9. DiMicco, M.A., P. Patwari, P.N. Siparsky, S. Kumar, M.A. Pratta, M.W. Lark, Y.J. Kim, and A.J. Grodzinsky, *Mechanisms and kinetics of glycosaminoglycan release following in vitro cartilage injury.* Arthritis and Rheumatism, 2004. **50**(3): p. 840-848.
10. D'Lima, D.D., S. Hashimoto, P.C. Chen, C.W. Colwell, Jr., and M.K. Lotz, *Human chondrocyte apoptosis in response to mechanical injury.* Osteoarthritis Cartilage, 2001. **9**(8): p. 712-9.
11. Kurz, B., A. Lemke, M. Kehn, C. Domm, P. Patwari, E.H. Frank, A.J. Grodzinsky, and M. Schunke, *Influence of tissue maturation and antioxidants on the apoptotic response of articular cartilage after injurious compression.* Arthritis Rheum, 2004. **50**(1): p. 123-30.
12. Chen, C.T., N. Burton-Wurster, C. Borden, K. Hueffer, S.E. Bloom, and G. Lust, *Chondrocyte necrosis and apoptosis in impact damaged articular cartilage.* J Orthop Res, 2001. **19**(4): p. 703-11.
13. Lee, J.H., J.B. Fitzgerald, M.A. Dimicco, and A.J. Grodzinsky, *Mechanical injury of cartilage explants causes specific time-dependent changes in chondrocyte gene expression.* Arthritis Rheum, 2005. **52**(8): p. 2386-95.
14. Jubb, R.W. and H.B. Fell, *The effect of synovial tissue on the synthesis of proteoglycan by the articular cartilage of young pigs.* Arthritis Rheum, 1980. **23**(5): p. 545-55.

15. Fell, H.B. and R.W. Jubb, *The effect of synovial tissue on the breakdown of articular cartilage in organ culture.* Arthritis Rheum, 1977. **20**(7): p. 1359-71.
16. Vankemmelbeke, M.N., M.Z. Ilic, C.J. Handley, C.G. Knight, and D.J. Buttle, *Coincubation of bovine synovial or capsular tissue with cartilage generates a soluble "Aggrecanase" activity.* Biochem Biophys Res Commun, 1999. **255**(3): p. 686-91.
17. Kurz, B., J. Steinhagen, and M. Schunke, *Articular chondrocytes and synoviocytes in a co-culture system: influence on reactive oxygen species-induced cytotoxicity and lipid peroxidation.* Cell Tissue Res, 1999. **296**(3): p. 555-63.
18. Muehleman, C., D. Bareither, K. Huch, A.A. Cole, and K.E. Kuettner, *Prevalence of degenerative morphological changes in the joints of the lower extremity.* Osteoarthritis Cartilage, 1997. **5**(1): p. 23-37.
19. Patwari, P., S.A. Norris, S. Kumar, M.W. Lark, and A.J. Grodzinsky. *Inhibition of Bovine Cartilage Biosynthesis by Coincubation of Joint Capsule Tissue is Mediated by an Interleukin-1-Independent Signalling Pathway.* in *ORS*. 2003. New Orleans, Louisiana.
20. Frank, E.H., M. Jin, A.M. Loening, M.E. Levenston, and A.J. Grodzinsky, *A versatile shear and compression apparatus for mechanical stimulation of tissue culture explants.* Journal of Biomechanics, 2000. **33**(11): p. 1523-1527.
21. Sandy, J.D., J. Westling, R.D. Kenagy, M.L. Iruela-Arispe, C. Verscharen, J.C. Rodriguez-Mazaneque, D.R. Zimmermann, J.M. Lemire, J.W. Fischer, T.N. Wight, and A.W. Clowes, *Versican V1 proteolysis in human aorta in vivo occurs at the Glu441-Ala442 bond, a site that is cleaved by recombinant ADAMTS-1 and ADAMTS-4.* J Biol Chem, 2001. **276**(16): p. 13372-8.
22. Kenagy, R.D., J.W. Fischer, S. Lara, J.D. Sandy, A.W. Clowes, and T.N. Wight, *Accumulation and loss of extracellular matrix during shear stress-mediated intimal growth and regression in baboon vascular grafts.* J Histochem Cytochem, 2005. **53**(1): p. 131-40.
23. Richards, J.S., I. Hernandez-Gonzalez, I. Gonzalez-Robayna, E. Teuling, Y. Lo, D. Boerboom, A.E. Falender, K.H. Doyle, R.G. LeBaron, V. Thompson, and J.D. Sandy, *Regulated expression of ADAMTS family members in follicles and cumulus oocyte complexes: evidence for specific and redundant patterns during ovulation.* Biol Reprod, 2005. **72**(5): p. 1241-55.
24. Sandy, J.D. and C. Verscharen, *Analysis of aggrecan in human knee cartilage and synovial fluid indicates that aggrecanase (ADAMTS) activity is responsible for the catabolic turnover and loss of whole aggrecan whereas other protease activity is required for C-terminal processing in vivo.* Biochem J, 2001. **358**(Pt 3): p. 615-26.
25. Plaas, A., B. Osborn, Y. Yoshihara, Y. Bai, T. Bloom, F. Nelson, K. Mikecz, and J.D. Sandy, *Aggrecanolysis in human osteoarthritis: confocal localization and biochemical characterization of ADAMTS5-hyaluronan complexes in articular cartilages.* Osteoarthritis Cartilage, 2007. **15**(7): p. 719-34.
26. Stewart, M.C., A.J. Fosang, Y. Bai, B. Osborn, A. Plaas, and J.D. Sandy, *ADAMTS5-mediated aggrecanolysis in murine epiphyseal chondrocyte cultures.* Osteoarthritis Cartilage, 2006. **14**(4): p. 392-402.
27. Lark, M.W., J.T. Gordy, J.R. Weidner, J. Ayala, J.H. Kimura, H.R. Williams, R.A. Mumford, C.R. Flannery, S.S. Carlson, M. Iwata, and et al., *Cell-mediated catabolism of aggrecan. Evidence that cleavage at the "aggrecanase" site (Glu373-Ala374) is a*

primary event in proteolysis of the interglobular domain. J Biol Chem, 1995. **270**(6): p. 2550-6.

28. Westling, J., P.E. Gottschall, V.P. Thompson, A. Cockburn, G. Perides, D.R. Zimmermann, and J.D. Sandy, *ADAMTS4 (aggrecanase-1) cleaves human brain versican V2 at Glu405-Gln406 to generate glial hyaluronate binding protein.* Biochem J, 2004. **377**(Pt 3): p. 787-95.
29. Farndale, R.W., D.J. Buttle, and A.J. Barrett, *Improved quantitation and discrimination of sulphated glycosaminoglycans by use of dimethylmethylene blue.* Biochim Biophys Acta, 1986. **883**(2): p. 173-7.
30. Sandy, J., D. Cullan, T. Bloom, A. Plaas, and F. Nelson. *Immunolocalization of Aggrecanases and Aggrecan Fragments in Human Knee Joint Tissues in Early and End-Stage Osteoarthritis.* in *ORS*. 2006. Chicago IL.

5.7 Appendix

5.7.1 Biosynthesis Data- Radiolabel incorporation

■Day 2 ■Day 6 □Day 16

Bar indicates p-value < 0.05 between conditions

*** indicates p-value < 0.05 compared to FS**

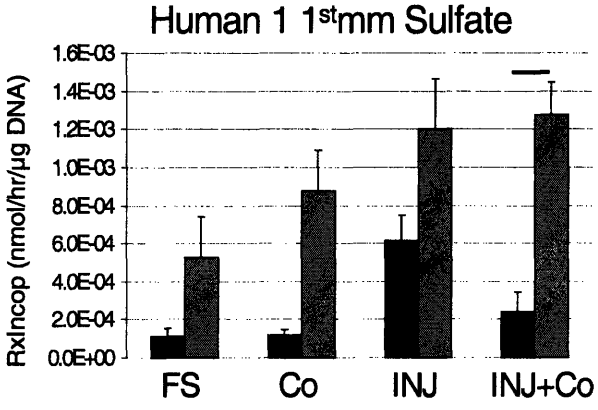

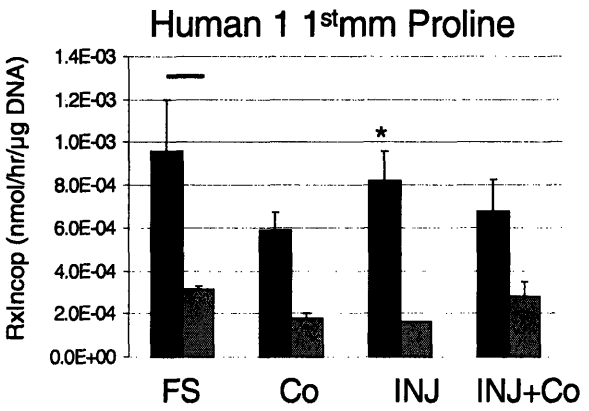

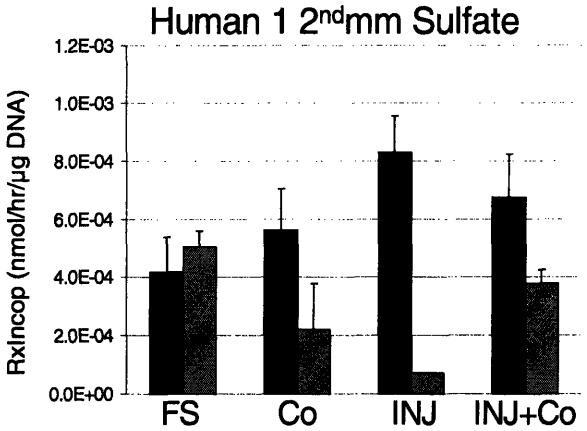

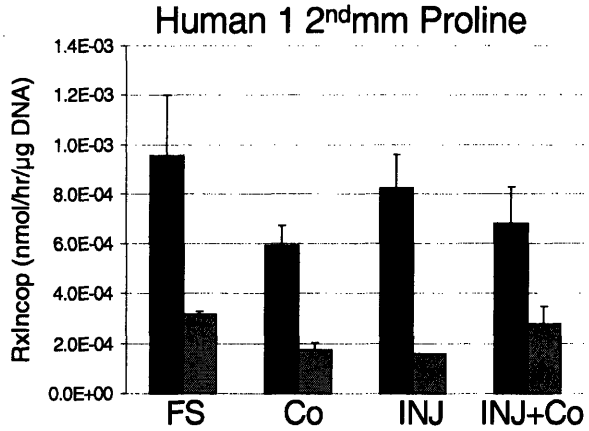

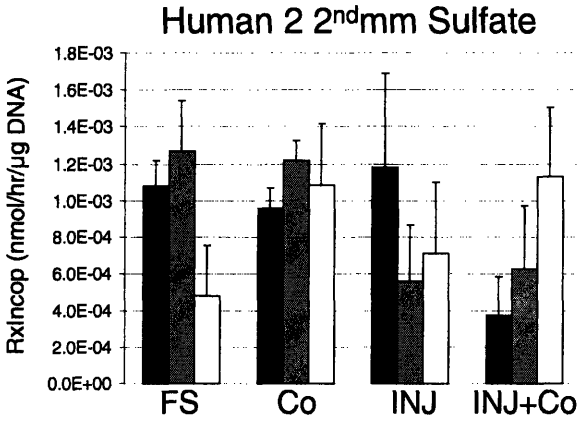

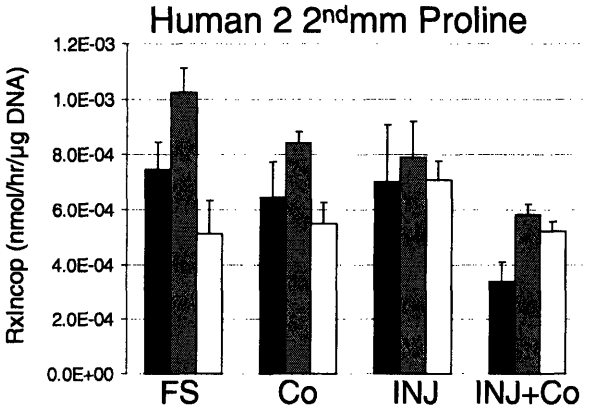

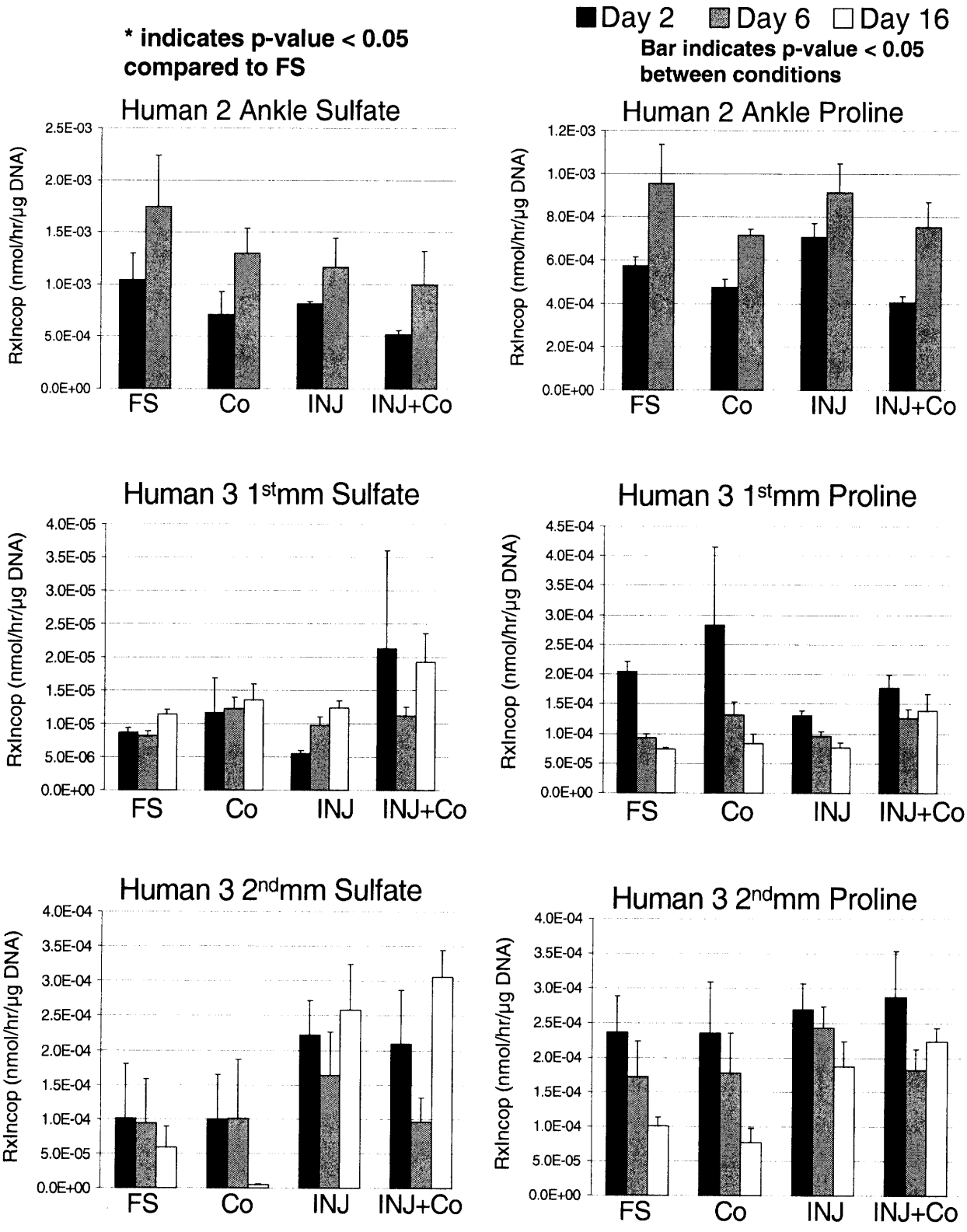
* indicates p-value < 0.05 compared to FS
Day 2
Day 6
Day 16
Bar indicates p-value < 0.05 between conditions
Human 2 Ankle Sulfate
Human 2 Ankle Proline
Human 3 1stmm Sulfate
Human 3 1stmm Proline
Human 3 2ndmm Sulfate
Human 3 2ndmm Proline
RxIncop (nmol/hr/µg DNA)
FS
Co
INJ
INJ+Co

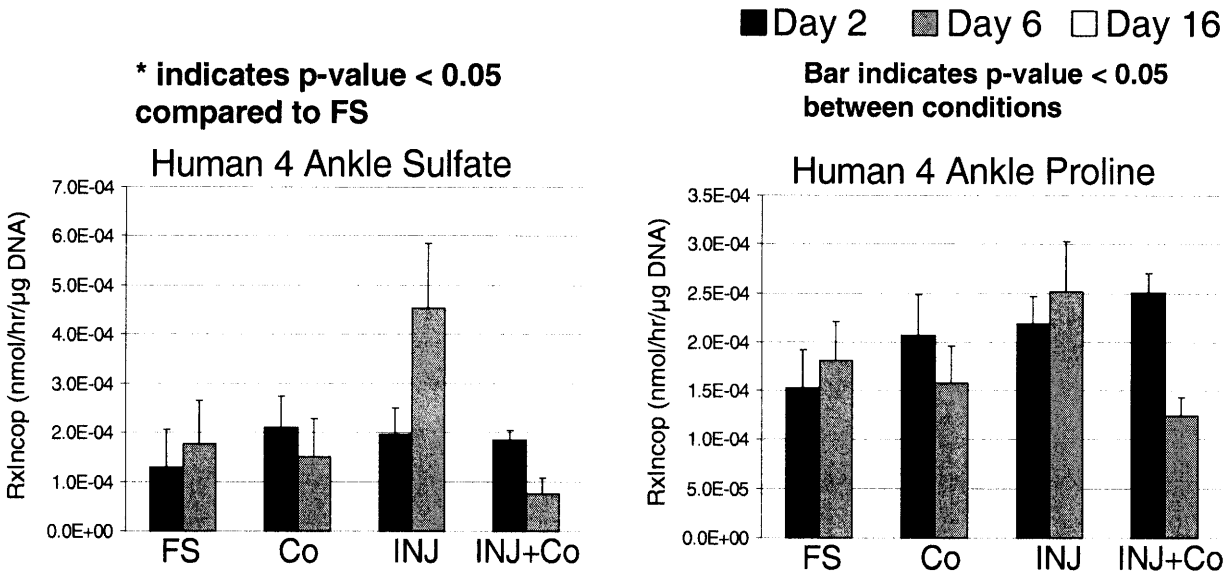
Day 2
Day 6
Day 16
* indicates p-value < 0.05 compared to FS
Human 4 Ankle Sulfate
RxIncop (nmol/hr/µg DNA)
7.0E-04
6.0E-04
5.0E-04
4.0E-04
3.0E-04
2.0E-04
1.0E-04
0.0E+00
FS
Co
INJ
INJ+Co
Bar indicates p-value < 0.05 between conditions
Human 4 Ankle Proline
RxIncop (nmol/hr/µg DNA)
3.5E-04
3.0E-04
2.5E-04
2.0E-04
1.5E-04
1.0E-04
5.0E-05
0.0E+00
FS
Co
INJ
INJ+Co

5.7.2 GAG Loss to the medium

*** indicates p-value < 0.05 compared to FS**

Day 2 Day 6 Day 16

Bar indicates p-value < 0.05 between conditions

Human 1 1stmm GAG Loss

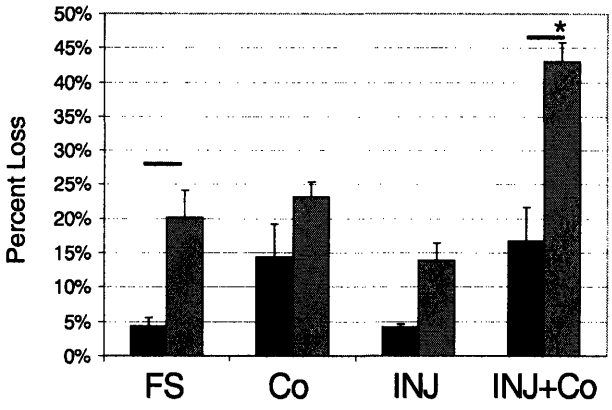

Human 1 2ndmm GAG Loss

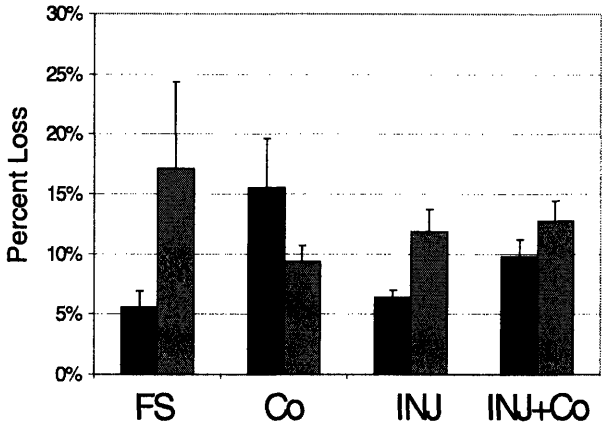

Human 3 1stmm GAG Loss

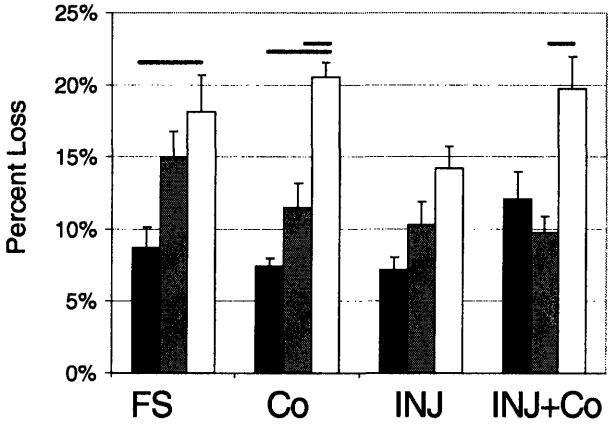

Human 3 2ndmm GAG Loss

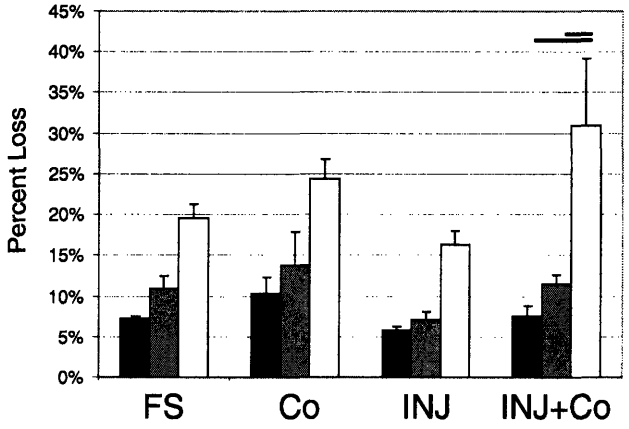

Human 3 Ankle GAG Loss

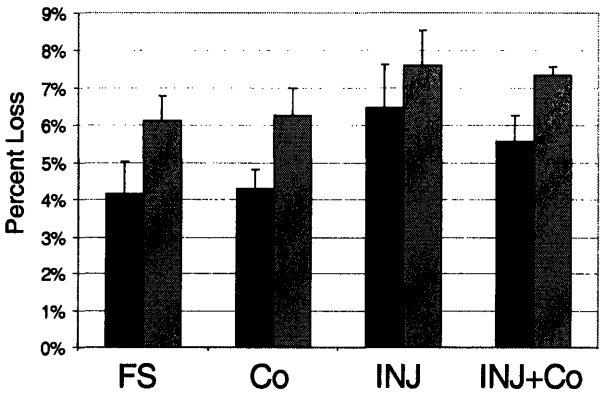

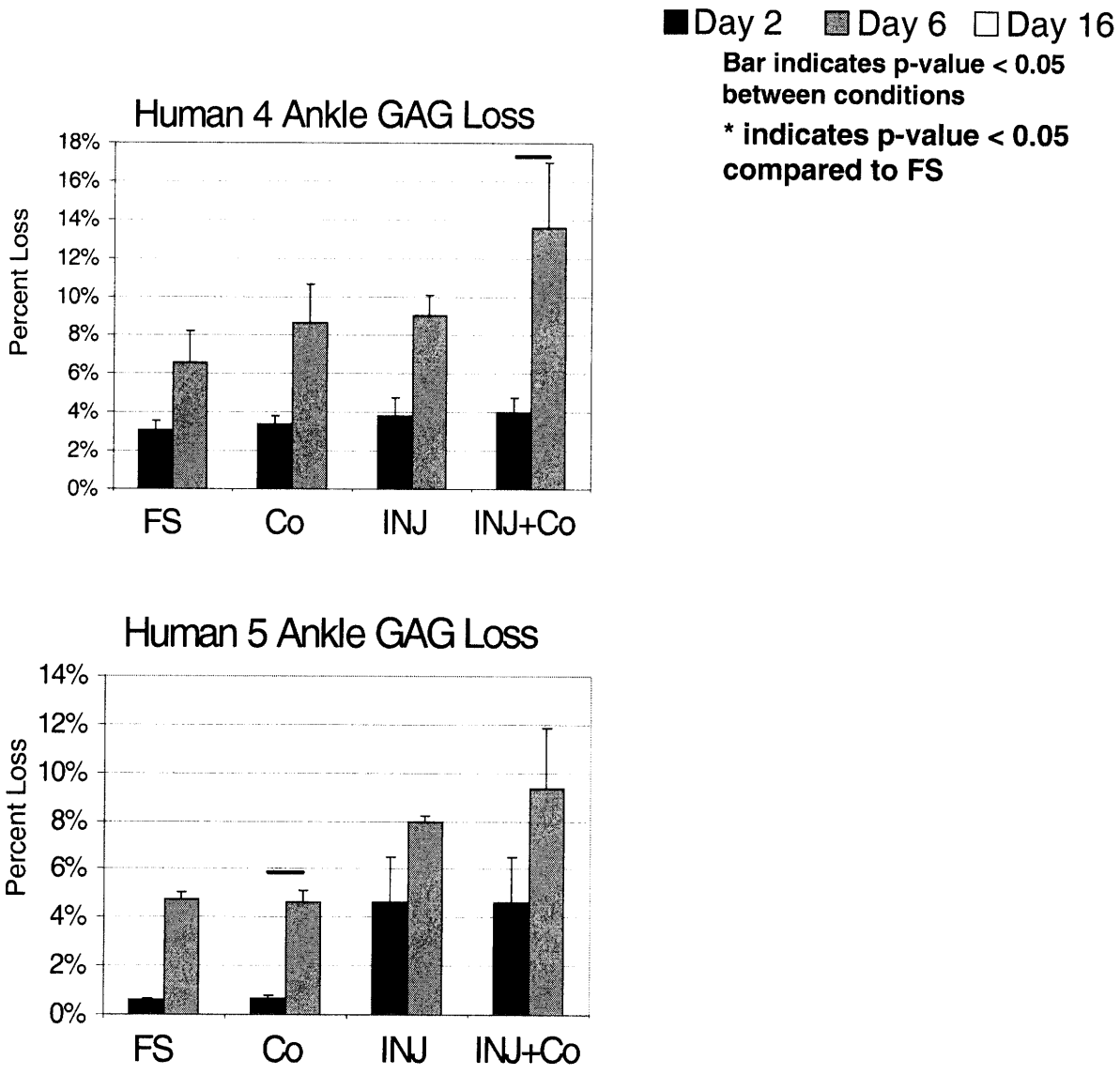
Day 2
Day 6
Day 16
Bar indicates p-value < 0.05 between conditions
* indicates p-value < 0.05 compared to FS
Human 4 Ankle GAG Loss
Percent Loss
18%
16%
14%
12%
10%
8%
6%
4%
2%
0%
FS
Co
INJ
INJ+Co
Human 5 Ankle GAG Loss
Percent Loss
14%
12%
10%
8%
6%
4%
2%
0%
FS
Co
INJ
INJ+Co

Chapter 6

The Effects of SODm on Cartilage Subjected to Cytokine Treatment Combined with Mechanical Injury

* This chapter is a manuscript in preparation for submission
(Wheeler, Cameron A., Perez, Anthony R., Wilkinson, Samuel, Kurz, Bodo, and Grodzinsky, Alan J.)

6.1 Introduction

Osteoarthritis (OA) is the most common disabling condition of man in the western world. OA is a disease of the joint, and includes cartilage, synovial capsule, connective and muscular tissue, as well as subchondral bone [1]. Adult cartilage is an avascular and hypoxic tissue, which chondrocytes, the cells within cartilage, are well adapted to. Recently, many researchers have sought to understand the role of oxygen levels and oxidative stress during the process of cartilage degradation [2, 3]. In particular, researchers have investigated the role of reactive oxygen species (ROS), which are byproducts of O_2 processing. These ROS include hydrogen peroxide, radicals (hydroxyl radical), ions (i.e. hypochlorite ion), and anions (superoxide anion). These ROS have been shown to oxidize nucleic acids, transcription factors, lipids, and different cellular components which hinder biologic activity, facilitate cell death, and promote extracellular matrix breakdown [4-9]. Studies have also shown that ROS scavengers or ROS production inhibitors decrease cartilage loss [10, 11]. ROS species have also been shown to be involved with chondrocyte apoptosis induced by mechanical injury [12-14].

Superoxide dismutase catalyzes the dismutation of superoxide into oxygen and hydrogen peroxide [15] As a protein SOD is not able to enter living cells. For that reason SOD mimetics (SODm), like Manganese(III)tetrakis (1-methyl-4-pyridyl) porphyrin pentachloride (Figure 6.1) have been used in many studies in order to influence ROS–dependent cell mechanisms. SODm has for example the potential to reduce chondrocyte apoptosis induced by injurious compression [12].

Figure 6.1 Superoxide Dismutase Mimetic

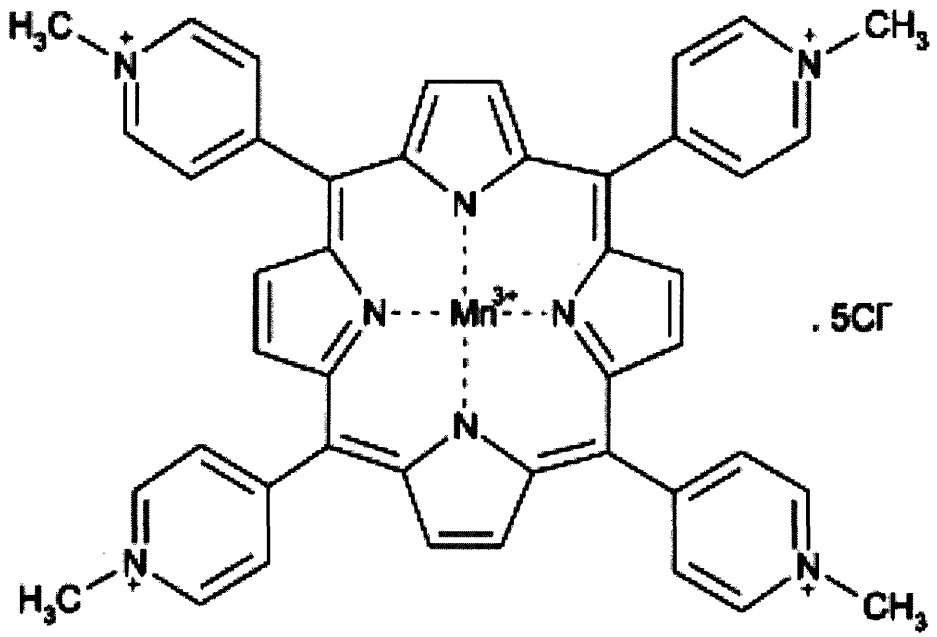

Figure 6.1 Superoxide dismutase mimetic structure, Manganese(III)tetrakis (1-methyl-4-pyridyl) porphyrin pentachloride.

Extra-cellular SOD, the major scavenger of ROS in extracellular spaces, is decreased in humans with OA, suggesting that inadequate controls of ROS plays a role in the pathophysiology of OA [16]. While it has been suggested that superoxide dismutase mimetic, SODm (cell permeable form of SOD), reduces cartilage degradation in mechanically-injured tissue, the mechanisms by which SODm affect chondrocyte transcription, translation, or post-translational machinery are not well known.

In vitro mechanical injury has been shown to increase hydraulic permeability [17] and water content [18-20], decrease stiffness [19, 21], and increase glycosaminoglycan (GAG) lost to the medium [19, 22-24]. Cells subject to this injury have been shown to decrease biosynthesis rates [19], undergo apoptosis and necrosis [12, 18, 19, 25], and have elevated levels of protease

transcript activity within the first 24 hours. Recent studies showed treatment with cytokines (e.g., IL-1, TNF-α, IL-6 [22, 26]) following injurious compression *in vitro* increased GAG loss and decreased biosynthesis greater than either mechanical injury or cytokine treatment alone.

The objectives of this study was to (1) more fully explore the degradative effects of mechanical injury and subsequent treatment of inflammatory cytokines on chondrocyte transcript levels in cartilage explants as well as on levels of tissue degradation (GAG loss), and (2) to test whether an antioxidant, specifically superoxide dismutase mimetic (SODm), could ameliorate the degradative effects on cartilage caused by mechanical injury followed by treatment with selected cytokines.

6.2 Materials and Methods

Tissue Harvest

Cartilage-bone plugs (9 mm in diameter) were harvested from the patello-femoral groove of 1-2 week old calves. Cartilage disks (1 mm thick x 3 mm diameter) were sliced and punched from the middle zone as described previously [27], and equilibrated for two days under free-swell conditions (37°C, 5% CO_2) in the presence of serum-free, 1% ITS supplemented feeding medium consisting of no phenol red, high glucose Dulbecco's modified essential medium supplemented with 10 nM Hepes Buffer, 0.1 mM nonessential amino acids, 20 μg/ml ascorbate, 100 units/ml penicillin, 100 μg/ml streptomycin, and 0.25 μg/ml amphoericin B.

Combined Injury Cytokine Model

After two days of equilibration, disks were allocated into one of 4 conditions: (1) free swell (FS), (2) FS with the addition of 2.5μM SODm (FS+SOD), (3) cartilage mechanically injured with the addition of 25 ng/mL TNF-α, 50 ng/mL IL-6, and 250 ng/mL sIL-6R and (4) injured cartilage with the addition of 25 ng/mL TNF-α, 50 ng/mL IL-6, 250 ng/mL sIL-6R, and 2.5μM SODm. SODm concentration was determined through a dose-dependent experiment (25, 2.5, 0.25, and 0.025 μM SODm) measuring key cartilage related gene transcripts (Appendix 6.1), as previously presented [28]. A custom designed incubator-housed loading apparatus [29] was used to compress cartilage disks. Each cartilage disk designated for mechanical injury was loaded individually in a polysulfone chamber allowing for radially-unconfined compression [19, 22, 23]. Cartilage disks were measured for height, compressed to a final strain of 50% at a velocity of 1mm/sec, and promptly removed and placed in fresh culture media as described previously [30]. Application of this strain and strain rate produced a peak stress on the order of 20MPa.

Gene Expression Time Courses

One hour prior to injury, plugs designated for SODm treatment were incubated under free swell conditions with medium supplemented with 2.5 μM SODm. At time = 0, plugs designated for injury were injured as prescribed and placed in medium that was supplemented with 25 ng/mL TNF-α, 50 ng/mL IL-6, and 250 ng/mL sIL-6R, and incubated at 37°C, 5% CO_2. At hours, 2, 8, 24, 48, and 72, plugs were flash frozen in liquid N_2 and placed in -80°C. Medium was changed every 48 hours. Each of the time point-conditions in the experiment contained 6 cartilage disks which were pooled and purposely matched across depth, location, and time to prevent any bias in the results. The gene expression experiment was repeated five times, using

five different animals for each experiment for an n=5. *Positive Control*: A positive control experiment was performed to illicit cellular responses to known reactive oxygen species. Cartilage disks were harvested as described above, and allowed to equilibrate for 2 days. At time t = 0, hydrogen peroxide at concentrations of 0, 10, 100, or 1000 μM was added to free swell plugs. Twenty-four hours post treatment, cartilage plugs were flash frozen and stored in -80°C. The gene expression experiment was repeated three times, using three different animals for each experiment for an n=3.

RNA Extraction and Quantization, Primer Design, and Real-Time PCR

Six disks for each time point and condition were taken from the -80° C freezer and pulverized. In order to prevent RNA degradation, the pulverizing apparatus was constantly cooled using liquid nitrogen. Trizol (Sigma, MO) was added, and the tissue was thoroughly homogenized. After chloroform was added, the mixture was transferred to pre-spun phase gel tubes and spun at 13,000 rpm for 10 minutes at 4° C. The supernatant was removed, and RNA was extracted using Qiagen RNAeasy mini kit protocol with recommended DNase digest (Qiagen). RNA was stored in 50 μl of RNase free water under -80° C conditions. RNA abundance and purity was measured using NanoDrop ND-1000 (NanoDrop Technologies, DE) with abundance ~80μg/ml and purity ~2 (260nm/280nm). 1μg of RNA was reverse transcribed using Applied Biosystems reagents as previously described [30]. Forward and reverse primers for 36 relevant genes (Table 6.1) were designed using Primer3 Software (http://fokker.wi.mit.edu/primer3/input.htm) and Primer Express (Applied Biosystems, CA) based on bovine genomic sequences, and standard curves were calculated as previously described [31].

Table 6.1. List of Cartilage relevant genes measured by qPCR

Housekeeping	Matrix Molecules	Proteinases	Proteinase Inhibitors	Apoptotic Gene
18s	Aggrecan	MMP-1	TIMP-1	Caspase-3
	Collagen2	MMP-3	TIMP-2	
	Link	MMP-9	TIMP-3	
	Fibromodulin	MMP-13		
	Fibronectin	ADAMTS-4		
		ADAMTS-5		
Transcrition Factors	**Growth Factors**	**Cytokines**	**Stress Activated Genes**	**Oxidative Factors**
Sox-9	IGF-1	IL-1b	CD-44	SOD1
Cox-2	IGF-2	IL-4	HAS2	SOD2
c-Fos	TGF-B	IL-6	iNOS	GPX-3
c-Jun	OP-1	TNF-a	HSP90	
	bFGF			

Table 6.1 List of 36 cartilage relevant genes measured by qPCR. Primer3 and Primer Express were used to design primers. Standard dilutions were used to calculate relative mRNA copy number.

Once cDNA was obtained, Real-Time PCR was performed using Applied Biosystems ABI 7900ht instrument and SYBR Green Master Mix (SGMM, Applied Biosystems, CA). SGMM was combined with cDNA, and RNase free water was combined with forward and reverse primers. Using a multi-pipette, 8 different samples of cDNA and SGMM were aliquoted into a 384 well plate, followed by 48 different primer and water mixes. Plates were run and inspected for proper amplification and melting curves using SDS 2.3 (Applied Biosystems, CA). Measured threshold values (Ct) were obtained through SDS 2.3 and converted to RNA copy number according to previously calculated primer efficiencies using standard curves.

Gene Expression Data Analysis

All data are shown as mean ± SEM. Under each condition and time point, each gene RNA copy number was normalized to the 18s housekeeping gene from that same condition and time point [30, 31]. 18s was chosen in light of recent studies showing the variation in expression of alternative housekeeping genes (i.e., GAPDH, β-actin) in response to certain conditions of loading of cartilage explants [32]. To examine the time course of gene expression, all conditions

were normalized to their corresponding free swell condition. Thus, gene expression values below or above 1 represent a decrease or increase in expression, respectively, compared to FS. Expression levels due to experimental error, as defined by 6σ from mean, were removed. The Wilcoxon sign-ranked test (a non-parametric test which incorporates the amount of data in the significance statistic and avoids the assumption of a parameter-based distribution) was used to judge significance at a p-value less than 0.05. *Clustering and Principle Component Analyses*: In addition to measuring changes in the expression magnitude of each gene, we further explored patterns of co-expression using principle component analysis (PCA) and clustering analysis performed on all normalized conditions (fold change compared to FS) and time points (2, 8, 24, 48, 72 hours) over 47 genes. This resulted in a 20 x 35 matrix which was standardized by expression amplitude as described previously [31]. After normalization of the data using PCA, the maximal dimensional space was reordered according to greatest dimensional variance where the first three detentions or principle components represent ~79% of the variance in the data [33, 34]. Once the principle components had been calculated, a k-means clustering algorithm was applied to cluster the components into k groups. The average and variance of each projected coordinate group was calculated to give the group centroid. Centroid vectors were formed by combining the three main principal components weighted by their projected centroid coordinate. The uniqueness of each group's expression patterns was evaluated by the Wilcoxon sign-ranked test and special separation between the centroids were measured and deemed significant through euclidean distance and student's t-test.

+/- Injury +/- Cytokine Models

To elucidate the effects of mechanical injury, cytokine treatment, and SODm treatment, plugs were allocated into one of eight different conditions: (1) free swell (FS), (2) FS with the

addition of 100 ng/mL TNF-α (FS+TNF), (3) mechanically-injured cartilage (INJ), and (4) mechanically-injured cartilage with the addition of 100 ng/mL TNF-α (INJ+TNF). Conditions (5)-(8) consisted of the first four conditions treated with 2.5μM SODm.

GAG Loss Time Course

One hour prior to injury, plugs designated for SODm treatment were incubated under free swell conditions with medium supplemented with 2.5 μM SODm. At time = 0, plugs designated for injury were injured and placed in their allocated medium conditions. Three days post injury, medium and plugs were collected and stored in -20°C until processing.

GAG Loss

The amount of sulfated glycosaminoglycan (GAG) content within the condition medium and within each cartilage plug was quantified using dimethylmethylene blue (DMMB) dye-binding assay [35]. Standard curves were generated using known amounts of GAG (Sigma, St. Louis, MO). Cartilage plugs were proteolytically digested by incubating overnight in protease K at 60°C. GAG from plugs was measured though DMMB dye. For ease of comparison, GAG loss data was expressed in percentage of GAG loss to the medium, normalized by the total GAG (GAG in medium + GAG in plug). Values were normalizes to FS to determine GAG loss-fold change compared to FS values. Each condition had a total of 5 distinct plugs which were matched across depth, location, and condition to ensure unbiased. This experiment was repeated with 6 different animals.

GAG Loss Analysis

All data are represented as mean ± SEM. A three-way analysis of variance with post-hoc Tukey was used to test significant differences in GAG loss data. P-values less than 0.05 were considered significant.

6.3 Results

Gene Expression

Similar to previous studies using injurious loading alone (no cytokines) [30], MMP-3, ADAMTS-5, TIMP-1, c-Fos, c-Jun, and TGF-β were upregulated in response to INJ, while aggrecan, SOX-9, IGF-2, IL-1β, and TNF-α remained largely unaffected (Figure 6.2A, Appendix 6.7.2).

Figure 6.2 Aggrecan and Collagen 2 Gene Expression

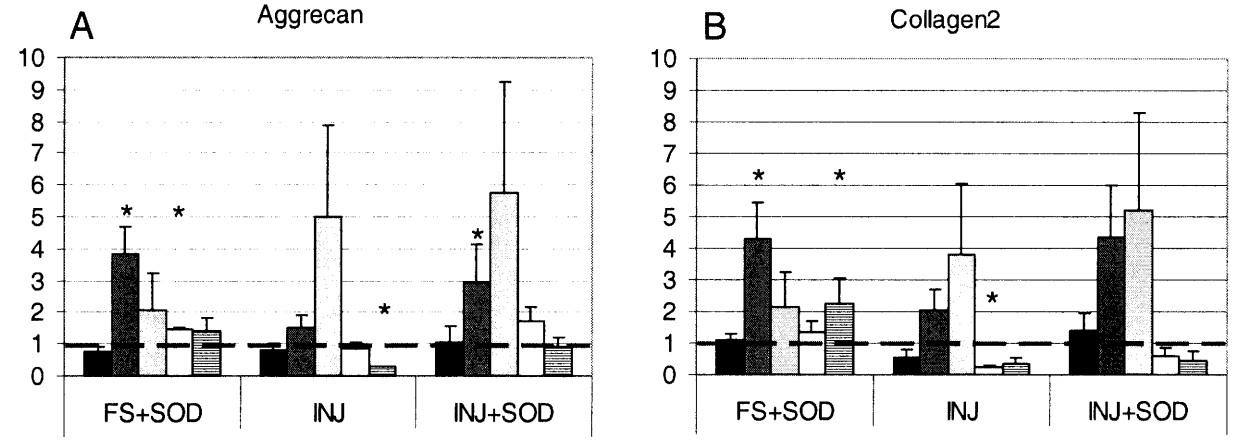

Figure 6.2 Aggrecan and collagen type II gene expression at 2, 8, 24, 48, and 72 hours after treatment. Data was plotted relative to FS conditions, and stars indicate significance (p-values < 0.05) between condition and corresponding FS value. Mean ± SEM.

When comparing the effects of SODm under FS or INJ, most genes, including: aggrecan, collagen II, link, fibromodulin, MMP-1, MMP-3, ADAMTS-4, ADAMTS-5, TIMP-1, TIMP-3, SOX-9, COX-2, c-Fos, c-Jun, IGF-1, IGF-2, TGF-β, bFGF, IL-1β, IL-4, IL-6, TNF-α, CD-44, HAS2, iNOS, and HSP90 were upregulated by SODm independent of INJ (Appendix 6.7.2), as exemplified by aggrecan and collagen type II (Figure 6.2A, 6.2B). MMP-3, MMP-9, MMP-13, ADAMTS-4, and ADAMTS-5 were severely upregulated by injury, and appeared to be further

stimulated by SODm treatment (Figure 6.3B, Appendix 6.7.2).

Figure 6.3 Caspase-3 and MMP-9 Gene Expression

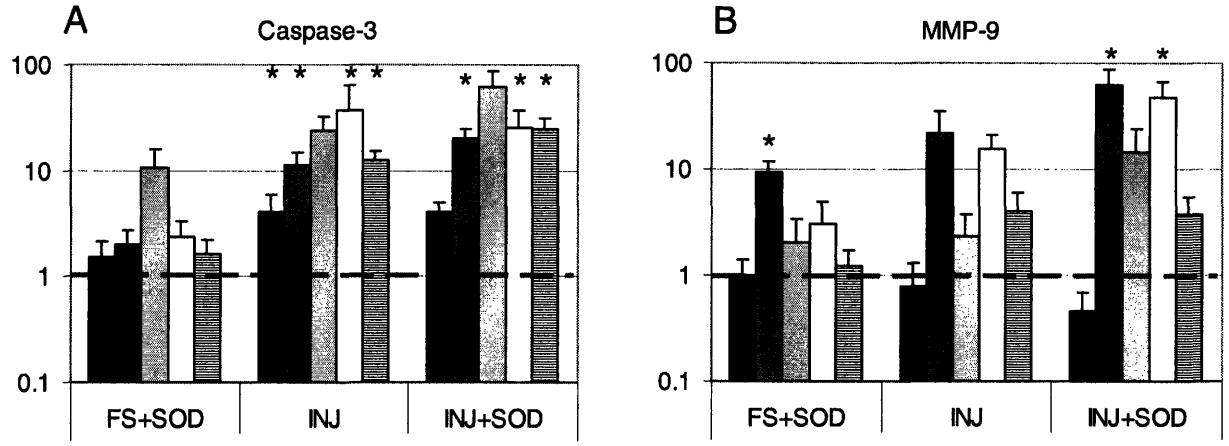

Figure 6.3 Caspase-3 and MMP-9 gene expression at 2, 8, 24, 48, and 72 hours after treatment. Data was plotted relative to FS conditions, and stars indicate significance (p-values < 0.05) between condition and corresponding FS value. Mean ± SEM.

TIMP-1 and TIMP-2 were expressed on the same order of magnitude as the key degradative enzymes, MMP-9, MMP-13, and ADAMTS-5 (Appendix 6.7.2). Cyclooxygenase 2 (COX-2) was highly upregulated with SODm treatment and was synergistically upregulated when injury and SODm were combined (Appendix 6.7.2). Osteogenic protein 1 (OP-1) was highly upregulated in response to injury, underlying the finding that OP-1 acts as an initial anabolic response to cartilage insult [36]. Also of note, basic fibroblast growth factor (bFGF) was highly upregulated with the addition of SODm and injury, individually and in combination (Appendix 6.7.2). This growth factor has been shown to negate the effect of key anabolic stimuli and can be interpreted as a negative or catabolic response to SODm treatment and injury [37]. Inducible nitric oxide synthase (iNOS) was highly upregulated in response to injury (as seen in chapter 3) and the treatment of SODm did not inhibit iNOS transcriptional activity (Appendix 6.7.2). Caspase-3 was significantly upregulated when exposed to INJ (Figure 6.3A). SODm did not appear to have a significant effect on caspase-3 transcripts under FS or INJ conditions. SOD2

showed little to no transcriptional effect of SODm treatment or injury (Appendix 6.7.2). SOD1 and GPX-3 were upregulated slightly with the addition of SODm and were significantly upregulated with INJ. SODm significantly downregulated SOD2 under FS conditions but had the opposite effect post INJ (Appendix 6.7.2).

Effects of SODm: Isolating the effects of SODm, under INJ, only aggrecan and collagen II showed a distinct monotonic transient up-regulation in the presence of SODm (Figure 6.4A, B).

Figure 6.4 Effects of SODm treatment- Aggrecan and Collagen 2

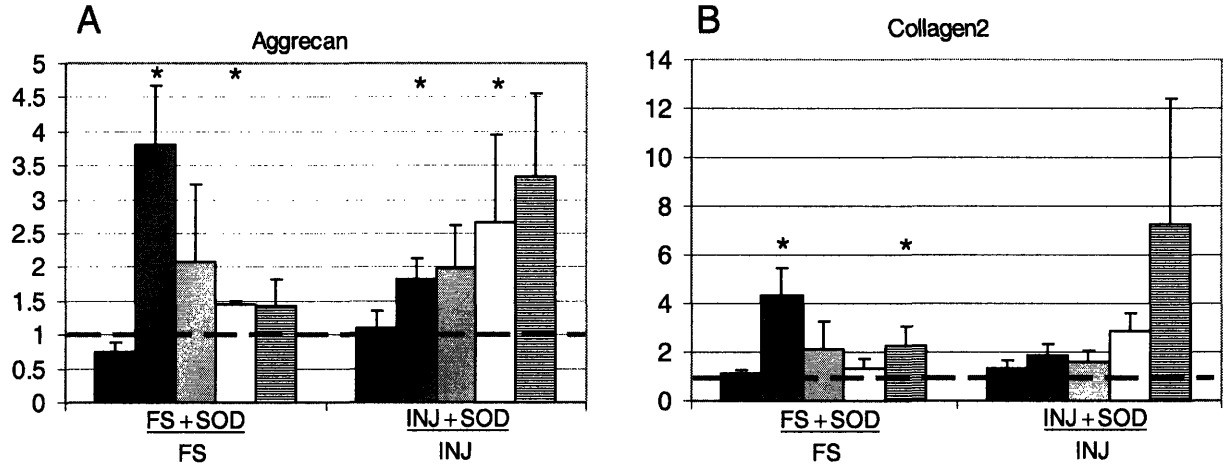

Figure 6.4 Effects of SODm treatment on aggrecan and collagen type II gene expression at 2, 8, 24, 48, and 72 hours after treatment. Data was plotted relative to corresponding loading conditions (FS or INJ), and stars indicate significance (p-values < 0.05) between SODm treatment and corresponding loading value. Mean ± SEM.

No genes measured were consistently downregulated by SODm under FS or INJ conditions, while most genes measured were upregulated by SODm (Appendix 6.7.4). Caspase-3, HAS2, TNF-α, bFGF, TGF-β, COX-2, TIMP-1, TIMP-3, and fibromodulin showed at least a ten-fold increase of expression with SODm treatment under FS and/or INJ conditions (Appendix 6.7.4).

Positive Control: H_2O_2 treatment differed from the profile obtained through the mechanical injury + cytokines model. Cartilage explants subject to 1000μm H_2O_2 did not

survive the treatment and no significant amount of mRNA could be extracted. Hydrogen peroxide dramatically decreased expression of aggrecan, ADAMTS-4, ADAMTS-5, SOX-9, c-Fos, and c-Jun at concentrations of 10μM and 100μM (Appendix 6.7.2). MMP-3 and collagen type II were upregulated with the treatment of H_2O_2 (Appendix 6.7.2). Yet aggrecan, c-Fos, c-Jun, ADAMTS-4, and ADAMTS-5 were upregulated in response to SODm treatment under H_2O_2 conditions, and MMP-3 was downregulated (Appendix 6.7.2).

Clustering: Clustering analysis of all conditions and all time points revealed 5 distinct groups of genes as seen plotted in principle component space (Figure 6.5).

Figure 6.5 Genes Clustered in PC Space

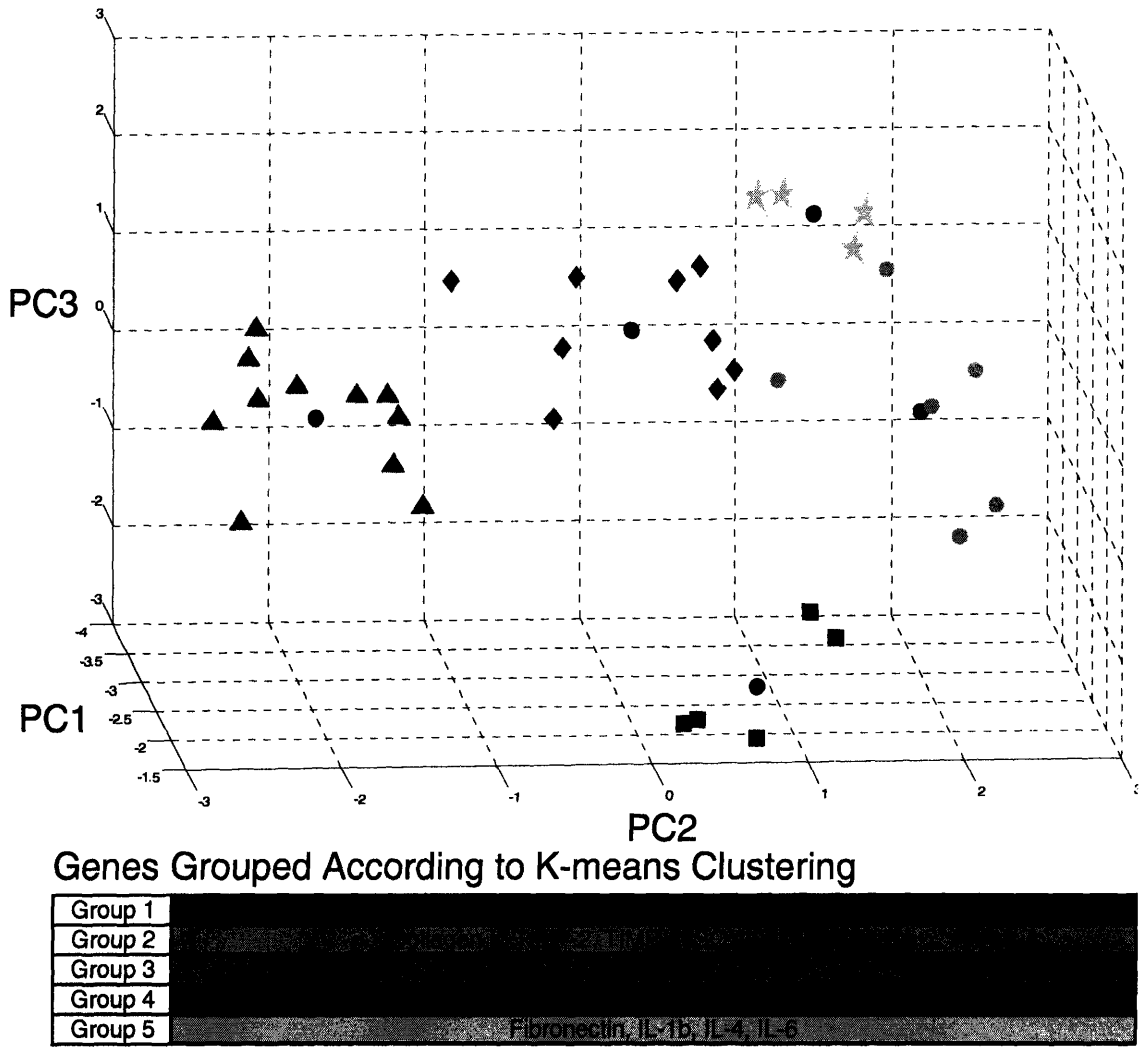

Figure 6.5 Standardized gene expression visualized in principle component space. Principle components 1, 2, and 3 represent 79% of the variance in the data. Genes were allocated to one of five distinct groups by way of k-means clustering. Large solid black circles denote the centroid of the corresponding group.

Group 1 was composed of potent proteinases MMP-13, ADAMTS-5; growth factors OP-1 and bFGF; all oxidative factors measures SOD1, SOD2, and GPX-3; as well as, CD-44, HAS2, iNOS, and Caspase-3. Group 2 was composed of the key ECM gene, Collagen II, protease inhibitors, TIMP-2, TIMP-3, as well as, SOX-9, IGF-1, and TNF-α. Group 3 was composed of most of the matrix metalloproteinases measured, MMP-1, MMP-3, MMP-9, as well as

ADAMTS-4, TIMP-1, Cox-2, c-Fos, c-Jun, and TGF-β. Group 4 was composed of key ECM genes, Aggrecan, Link, Fibromodulin, the growth factor, IGF-2, and HSP90. Group 5 was composed of the measured interleukins, IL-1β, IL-4, and IL-6, and Fibronectin. Following combined INJ + SODm treatment, Groups 1 and 2 (Figure 6.6A, B) were dominated by the effects of INJ, although SODm upregulated earlier (Group 1) and later (Group 2) time points. Group 3 (Figure 6.6C), containing mainly ECM molecules and proteinases, showed additive effects under the combination of INJ and SODm. Group 4 (Figure 6.6D) was upregulated and showed peaks under all conditions at 24 hours. Composed primarily of cytokines, Group 5 (Figure 6.6E) exhibited a strong effect at 8 hours for INJ, which was negated by addition of SODm.

Figure 6.6 Centroid Profile of Gene Expression

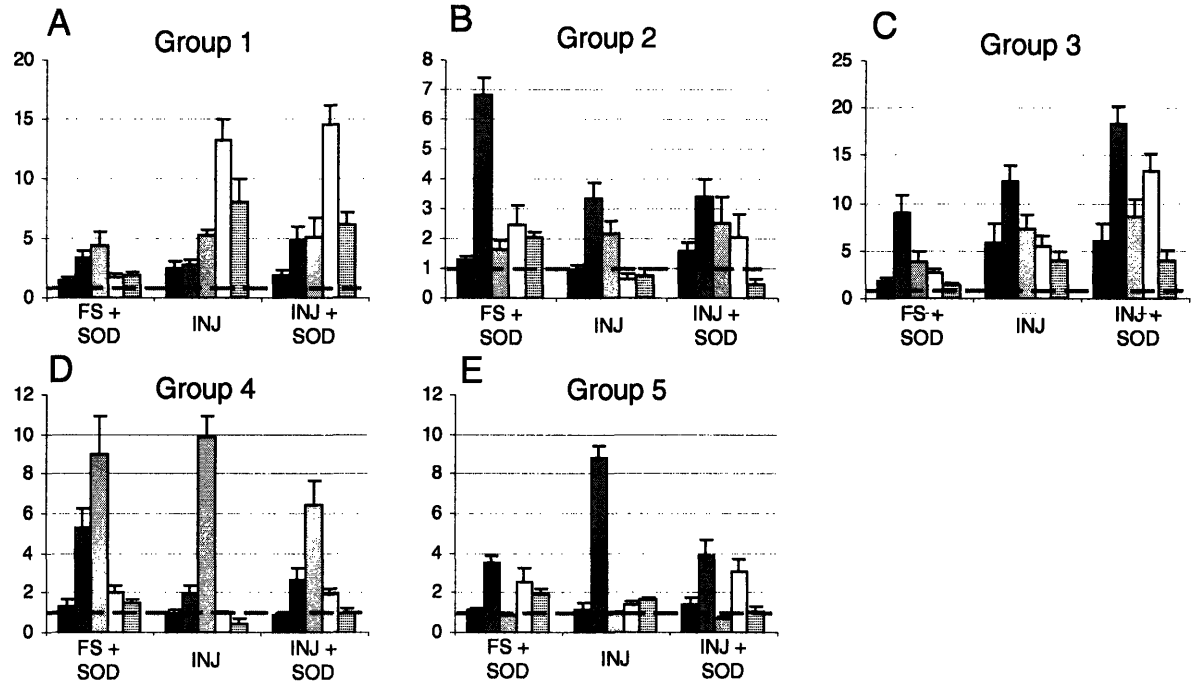

Group 1	MMP-13, ADAMTS-5, OP-1, bFGF,CD-44, HAS2, iNOS, Caspase-3, SOD1, SOD2, GPX-3
Group 2	Collagen II, TIMP-2, TIMP-3, SOX-9, IGF-1, TNF-a
Group 3	MMP-1, MMP-3, MMP-9, ADAMTS-4, TIMP-1, Cox-2, c-Fos, c-Jun, TGF-B
Group 4	Aggrecan, Link, Fibromodulin, IGF-2, HSP90
Group 5	Fibronectin, IL-1b, IL-4, IL-6

Figure 6.6 Five expression profiles represent the combination of FS + 2.5 μM SODm, INJ, and INJ + 2.5 μM SODm. Centroid profiles were calculated through the average projection coordinates of genes in each group, and transformed from principle component space through use of the calculated principle components. Mean ± SE (n varies based on group component number)

GAG Loss

To more fully understand and isolate the effects of cytokine treatment, mechanical injury, and the treatment of superoxide dismutase, GAG loss to the medium was measured under 8 different conditions; FS, mechanical injury, TNF-α treatment, and mechanical injury combined with cytokine treatment, all with or without SODm treatment. A 3-way ANOVA showed significant difference with TNF-α treatment ($p<0.001$), SODm treatment ($p<0.001$), and INJ ($p<0.001$) over all the data (Figure 6.7). As seen previously, bovine disks treated with TNF-α

had significantly higher GAG loss, even more pronounced by the combination of TNF-α + mechanical injury. SODm significantly increased GAG loss in TNF-α treatment alone (>2.75x FS conditions). Although not significant in all conditions measured, all conditions showed the trend of increasing GAG loss with SODm treatment (Figure 6.7).

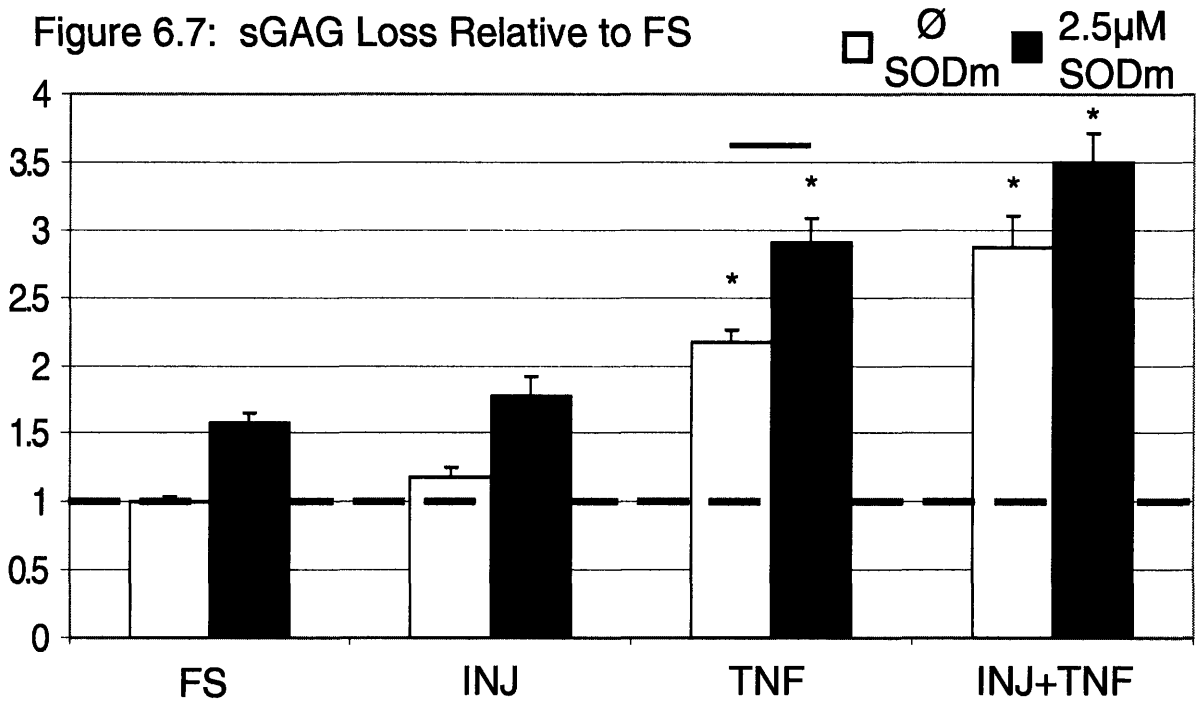

Figure 6.7 sGAG loss to the medium in free swell (FS), mechanical injury (INJ), TNF-α treatment (TNF), and mechanical injury with TNF-α treatment (INJ+TNF) and all conditions ± 2.5 μM SODm plotted relative to FS conditions. Stars indicate significance (p-values < 0.05) between condition and FS, and bar indicates significance between two conditions. Mean ± SEM.

6.4 Discussion

Gene Expression

All genes examined were strongly stimulated by SODm treatment under FS conditions suggesting SODm acts as a purely stimulatory factor. Consistent with the hydrogen peroxide

positive control experiment, genes were upregulated when treated with the combination of the strong oxidant hydrogen peroxide and SODm. Following INJ+C (mechanical injury + cytokine) treatment plus SODm, most gene transcription levels were upregulated; this pattern was most dramatic for aggrecan and IGF-2 (Figure 6.2A, Appendix 6.7.3). These findings suggest pro-anabolic activity when INJ+C disks were treated with antioxidant.

The INJ+C+SODm condition elevated expression of COX-2, OP-1, bFGF, iNOS, and HSP90 to levels greater than 100x FS. These highly responsive genes could be divided into two groups: anabolic response to injury insult or catabolic response to injury insult. As has been reported, OP-1 and HSP90 act as an initial anabolic response to injury, while COX-2, bFGF, and iNOS are clearly catabolic factors [38-40]. The mechanical injury and cytokine model of injury increased the magnitude of COX-2, OP-1, bFGF, iNOS, and HSP90 to a greater extent compared to mechanical injury alone or cytokine treatment alone [30]. SODm had little effect on Caspase-3 gene expression, although as expected, Caspase-3 was upregulated with INJ+C. Since SODm has been shown to inhibit nuclear blebbing after mechanical injury significantly [12] it might be suggested that the SODm effect on apoptosis is not based on an altered gene expression level of caspase-3, but on an inhibition of the activation of pre-existing caspases. As part of the apoptotic signaling pathway ROS seem to be generated at the mitochondrial membrane, resulting in mitochondrial dysfunction and subsequent activation of caspases by release of cytochrome C and other caspase activators [41-44]. SOD1 and GPX-3 responded positively through SODm treatment but were dominated by the INJ+C response. SODm downregulated the injury-dependent increase of SOD2 (primarily located in the mitochondria). Table 6.2 shows the distinct separation of the 5 clustered groups.

Table 6.2 Centroid Uniqueness

P-value of Centroid Separation	Centroid 1	Centroid 2	Centroid 3	Centroid 4
Centroid 2	0.016			
Centroid 3	0.021	0.031		
Centroid 4	0.032	0.051	0.037	
Centroid 5	0.064	0.107	0.116	0.036

Table 6.2. P-value of Centroid Profile Separation. P-values were obtained through student T-test, comparing centroid to centroid Euclidean distance. Degrees of freedom were taken as the number of genes in each group.

From clustering analyses, key cytokines (IL-1β, IL-4, and IL-6) were grouped together in group 5 (Figure 6.6E) where the 8-hour peak under INJ+C conditions was significantly downregulated by SODm treatment. These findings suggest a transcriptional mechanism by which the antioxidant may abrogate the negative effects of the INJ+C model by upregulating anabolic genes and downregulating cytokines. Examining the transcriptional effects of SODm on ADAMTS-4, SOX-9, c-Fos, c-Jun, IGF-2, TGF-B, IL-1b, CD-44, and HAS2, SODm appears to act via an INJ+C-dependent manner, whereas the transcriptional effects of SODm on fibronectin, IL-4, and IL-6 were independent of INJ+C (Appendix 6.7.4).

GAG Loss

Surprisingly, GAG loss was increased with the addition of SODm. After three days in culture, GAG loss is significantly increased compared to FS conditions, ranging from >2X FS with TNF-α alone, to nearly 3X FS with TNF-α and mechanical injury. These values increase to 3x with TNF-α alone and 3.5x with TNF-α and mechanical injury when 2.5 μM SODm is added. These data further support the increases in transcription activity under INJ+C conditions of MMP-1 (peak 10x FS), MMP-3 (peak 67x FS), MMP-9 (peak 62x FS), MMP-13(peak 26x FS),

ADAMTS-4 (peak 25x FS) and ADAMTS-5 (peak 69x FS) with the addition of SODm over the same time period measured. Previous studies have shown an upregulation of iNOS expression with the addition of N-acetyl-l-cysteine (NAC), an antioxidant like SODm which may suggest a role for antioxidants in GAG loss [45]. As a side note, NAC increased cell viability in isolated chondrocytes, as seen with SODm [46]. In this study, iNOS was upregulated to peak values of 125x FS under the treatment of SODm alone (FS + SODm). When mechanical injury, cytokine treatment, and SODm were combined, iNOS levels increased to peak values of 600x FS (Appendix 6.7.3). This correlation with increased iNOS and GAG loss with the presence of an antioxidant supports the idea that SODm mediates GAG loss through the increase of NO, a product of the upregulated iNOS.

This work supports the notion that SODm does not have the general ability to protect against cartilage matrix degradation. While SODm has been shown to decrease levels of apoptosis post injury, it appears that SODm does not have the ability to protect the cartilage matrix against the harmful effects of treatment with cytokines and/or mechanical injury and, in some cases, exacerbates matrix degradation.

6.5 Conclusion

In a complex model of injury, namely one composed of mechanical injury and treatment of destructive cytokines, SODm, an antioxidant, does not demonstrate the ability to abrogate the negative effects of this complex injurious assault on matrix degradation. On the contrary, the treatment of SODm tended to stimulate all genes measured. In particular, it increased protease transcript levels, as well as increased in GAG loss, a measure of cartilage degradation. The injury model elicited dramatic responses of COX-2, OP-1, bFGF, iNOS, and HSP90 to levels greater than 100 fold the control, suggesting these genes play a crucial role in the initial response to traumatic injury within the first three days. The magnitude of these gene transcripts has not been observed previously in the application of mechanical injury or cytokine treatment to our knowledge. As has previously been suggested, the combination of cytokine treatment and mechanical injury produced the most cartilage degradation, opening a possibly insightful *in vitro* model of osteoarthritis. Since ROS influence on signaling pathways in chondrocytes depends on the kind of ROS (superoxide versus hydrogen peroxide [1]), and SODm eliminates both superoxides and hydrogen peroxide, further studies are needed with antioxidants with greater specificity to determine the effect of ROS on chondrocytes. Whether antioxidants may serve as therapeutics for osteoarthritis for their ability to decrease cell death, or as targets for therapeutics because of their increased degradative effects on cartilage, as seen here, remains to be seen.

6.6 References

1. Henrotin, Y., B. Kurz, and T. Aigner, *Oxygen and reactive oxygen species in cartilage degradation: friends or foes?* Osteoarthritis Cartilage, 2005. **13**(8): p. 643-54.
2. Archer, C.W., S. Redman, I. Khan, J. Bishop, and K. Richardson, *Enhancing tissue integration in cartilage repair procedures.* J Anat, 2006. **209**(4): p. 481-93.
3. Wang, Y., L.F. Prentice, L. Vitetta, A.E. Wluka, and F.M. Cicuttini, *The effect of nutritional supplements on osteoarthritis.* Altern Med Rev, 2004. **9**(3): p. 275-96.
4. Lo, Y.Y., J.A. Conquer, S. Grinstein, and T.F. Cruz, *Interleukin-1 beta induction of c-fos and collagenase expression in articular chondrocytes: involvement of reactive oxygen species.* J Cell Biochem, 1998. **69**(1): p. 19-29.
5. Martin, G., R. Andriamanalijaona, S. Grassel, R. Dreier, M. Mathy-Hartert, P. Bogdanowicz, K. Boumediene, Y. Henrotin, P. Bruckner, and J.P. Pujol, *Effect of hypoxia and reoxygenation on gene expression and response to interleukin-1 in cultured articular chondrocytes.* Arthritis Rheum, 2004. **50**(11): p. 3549-60.
6. Henrotin, Y.E., P. Bruckner, and J.P. Pujol, *The role of reactive oxygen species in homeostasis and degradation of cartilage.* Osteoarthritis Cartilage, 2003. **11**(10): p. 747-55.
7. Tiku, M.L., S. Gupta, and D.R. Deshmukh, *Aggrecan degradation in chondrocytes is mediated by reactive oxygen species and protected by antioxidants.* Free Radic Res, 1999. **30**(5): p. 395-405.
8. Tiku, M.L., R. Shah, and G.T. Allison, *Evidence linking chondrocyte lipid peroxidation to cartilage matrix protein degradation. Possible role in cartilage aging and the pathogenesis of osteoarthritis.* J Biol Chem, 2000. **275**(26): p. 20069-76.
9. Mendes, A.F., M.M. Caramona, A.P. Carvalho, and M.C. Lopes, *Hydrogen peroxide mediates interleukin-1beta-induced AP-1 activation in articular chondrocytes: implications for the regulation of iNOS expression.* Cell Biol Toxicol, 2003. **19**(4): p. 203-14.
10. Kurz, B., B. Jost, and M. Schunke, *Dietary vitamins and selenium diminish the development of mechanically induced osteoarthritis and increase the expression of antioxidative enzymes in the knee joint of STR/1N mice.* Osteoarthritis Cartilage, 2002. **10**(2): p. 119-26.
11. Pelletier, J.P., V. Lascau-Coman, D. Jovanovic, J.C. Fernandes, P. Manning, J.R. Connor, M.G. Currie, and J. Martel-Pelletier, *Selective inhibition of inducible nitric oxide synthase in experimental osteoarthritis is associated with reduction in tissue levels of catabolic factors.* J Rheumatol, 1999. **26**(9): p. 2002-14.
12. Kurz, B., A. Lemke, M. Kehn, C. Domm, P. Patwari, E.H. Frank, A.J. Grodzinsky, and M. Schunke, *Influence of tissue maturation and antioxidants on the apoptotic response of articular cartilage after injurious compression.* Arthritis Rheum, 2004. **50**(1): p. 123-30.
13. Sandstrom, P.A., M.D. Mannie, and T.M. Buttke, *Inhibition of activation-induced death in T cell hybridomas by thiol antioxidants: oxidative stress as a mediator of apoptosis.* J Leukoc Biol, 1994. **55**(2): p. 221-6.
14. Cai, J. and D.P. Jones, *Superoxide in apoptosis. Mitochondrial generation triggered by cytochrome c loss.* J Biol Chem, 1998. **273**(19): p. 11401-4.

15. Henrotin, Y. and B. Kurz, *Antioxidant to treat osteoarthritis: dream or reality?* Curr Drug Targets, 2007. **8**(2): p. 347-57.
16. Regan, E., J. Flannelly, R. Bowler, K. Tran, M. Nicks, B.D. Carbone, D. Glueck, H. Heijnen, R. Mason, and J. Crapo, *Extracellular superoxide dismutase and oxidant damage in osteoarthritis.* Arthritis Rheum, 2005. **52**(11): p. 3479-91.
17. Thibault, M., A.R. Poole, and M.D. Buschmann, *Cyclic compression of cartilage/bone explants in vitro leads to physical weakening, mechanical breakdown of collagen and release of matrix fragments.* J. Orthop. Res., 2002. **20**(6): p. 1265-1273.
18. Torzilli, P.A., R. Grigiene, J. Borrelli, Jr., and D.L. Helfet, *Effect of impact load on articular cartilage: cell metabolism and viability, and matrix water content.* J Biomech Eng, 1999. **121**(5): p. 433-41.
19. Kurz, B., M. Jin, P. Patwari, D.M. Cheng, M.W. Lark, and A.J. Grodzinsky, *Biosynthetic response and mechanical properties of articular cartilage after injurious compression.* J Orthop Res, 2001. **19**(6): p. 1140-6.
20. Chen, C.T., N. Burton-Wurster, G. Lust, R.A. Bank, and J.M. Tekoppele, *Compositional and metabolic changes in damaged cartilage are peak-stress, stress-rate, and loading-duration dependent.* J Orthop Res, 1999. **17**(6): p. 870-9.
21. Loening, A.M., I.E. James, M.E. Levenston, A.M. Badger, E.H. Frank, B. Kurz, M.E. Nuttall, H.H. Hung, S.M. Blake, A.J. Grodzinsky, and M.W. Lark, *Injurious mechanical compression of bovine articular cartilage induces chondrocyte apoptosis.* Arch Biochem Biophys, 2000. **381**(2): p. 205-12.
22. Patwari, P., M.N. Cook, M.A. DiMicco, S.M. Blake, I.E. James, S. Kumar, A.A. Cole, M.W. Lark, and A.J. Grodzinsky, *Proteoglycan degradation after injurious compression of bovine and human articular cartilage in vitro: Interaction with exogenous cytokines.* Arthritis Rheum., 2003. **48**(5): p. 1292-301.
23. DiMicco, M.A., P. Patwari, P.N. Siparsky, S. Kumar, M.A. Pratta, M.W. Lark, Y.J. Kim, and A.J. Grodzinsky, *Mechanisms and kinetics of glycosaminoglycan release following in vitro cartilage injury.* Arthritis and Rheumatism, 2004. **50**(3): p. 840-848.
24. D'Lima, D.D., S. Hashimoto, P.C. Chen, C.W. Colwell, Jr., and M.K. Lotz, *Human chondrocyte apoptosis in response to mechanical injury.* Osteoarthritis Cartilage, 2001. **9**(8): p. 712-9.
25. Chen, C.T., N. Burton-Wurster, C. Borden, K. Hueffer, S.E. Bloom, and G. Lust, *Chondrocyte necrosis and apoptosis in impact damaged articular cartilage.* J Orthop Res, 2001. **19**(4): p. 703-11.
26. Sui, Y., X.-Y. Song, J. Lee, M. DiMicco, S. Blake, H.-H. Hung, I. James, M. Lark, and A. Grodzinsky. *Mechanical Injury Potentiates the Combined Effects of TNF-α and IL-6/SIL-6R on Proteoglycan Catabolism in Bovine Cartilage.* in *ORS*. 2007. San Diego, CA.
27. Sah, R.L.Y., Y.J. Kim, J.Y.H. Doong, A.J. Grodzinsky, A.H.K. Plaas, and J.D. Sandy, *Biosynthesis Response to Cartilage Explants to Dynamic Compression.* J. Orthop. Res., 1989. **7**: p. 619-636.
28. Wheeler CA, W.S., Grodzinsky AJ, Kurz B. *Antioxidant Superoxide Dismutase Stimulates Anabolic Factors and Decreases Catabolic Factors in Cartilage Subjected to Mechanical Injury and Inflammatory Cytokines* in *ORS*. 2007. San Diego.

29. Frank, E.H., M. Jin, A.M. Loening, M.E. Levenston, and A.J. Grodzinsky, *A versatile shear and compression apparatus for mechanical stimulation of tissue culture explants.* Journal of Biomechanics, 2000. **33**(11): p. 1523-1527.
30. Lee, J.H., J.B. Fitzgerald, M.A. Dimicco, and A.J. Grodzinsky, *Mechanical injury of cartilage explants causes specific time-dependent changes in chondrocyte gene expression.* Arthritis Rheum, 2005. **52**(8): p. 2386-95.
31. Fitzgerald, J.B., M. Jin, D. Dean, D.J. Wood, M.H. Zheng, and A.J. Grodzinsky, *Mechanical compression of cartilage explants induces multiple time-dependent gene expression patterns and involves intracellular calcium and cyclic AMP.* Journal of Biological Chemistry, 2004. **279**(19): p. 19502-19511.
32. Lee, C.R., S. Grad, J.J. Maclean, J.C. Iatridis, and M. Alini, *Effect of mechanical loading on mRNA levels of common endogenous controls in articular chondrocytes and intervertebral disk.* Anal Biochem, 2005. **341**(2): p. 372-5.
33. Alter, O., P.O. Brown, and D. Botstein, *Singular value decomposition for genome-wide expression data processing and modeling.* Proc Natl Acad Sci U S A, 2000. **97**(18): p. 10101-6.
34. Holter, N.S., M. Mitra, A. Maritan, M. Cieplak, J.R. Banavar, and N.V. Fedoroff, *Fundamental patterns underlying gene expression profiles: simplicity from complexity.* Proc Natl Acad Sci U S A, 2000. **97**(15): p. 8409-14.
35. Farndale, R.W., D.J. Buttle, and A.J. Barrett, *Improved quantitation and discrimination of sulphated glycosaminoglycans by use of dimethylmethylene blue.* Biochim Biophys Acta, 1986. **883**(2): p. 173-7.
36. Chubinskaya, S., M. Hurtig, and D.C. Rueger, *OP-1/BMP-7 in cartilage repair.* Int Orthop, 2007.
37. Im, H.J., C. Pacione, S. Chubinskaya, A.J. Van Wijnen, Y. Sun, and R.F. Loeser, *Inhibitory effects of insulin-like growth factor-1 and osteogenic protein-1 on fibronectin fragment- and interleukin-1beta-stimulated matrix metalloproteinase-13 expression in human chondrocytes.* J Biol Chem, 2003. **278**(28): p. 25386-94.
38. Im, H.J., P. Muddasani, V. Natarajan, T.M. Schmid, J.A. Block, F. Davis, A.J. van Wijnen, and R.F. Loeser, *Basic fibroblast growth factor stimulates matrix metalloproteinase-13 via the molecular cross-talk between the mitogen-activated protein kinases and protein kinase Cdelta pathways in human adult articular chondrocytes.* J Biol Chem, 2007. **282**(15): p. 11110-21.
39. Loeser, R.F., S. Chubinskaya, C. Pacione, and H.J. Im, *Basic fibroblast growth factor inhibits the anabolic activity of insulin-like growth factor 1 and osteogenic protein 1 in adult human articular chondrocytes.* Arthritis Rheum, 2005. **52**(12): p. 3910-7.
40. Loeser, R.F., C.A. Pacione, and S. Chubinskaya, *The combination of insulin-like growth factor 1 and osteogenic protein 1 promotes increased survival of and matrix synthesis by normal and osteoarthritic human articular chondrocytes.* Arthritis Rheum, 2003. **48**(8): p. 2188-96.
41. Kim, B.M. and H.W. Chung, *Hypoxia/reoxygenation induces apoptosis through a ROS-mediated caspase-8/Bid/Bax pathway in human lymphocytes.* Biochem Biophys Res Commun, 2007. **363**(3): p. 745-50.
42. Yang, J., L.J. Wu, S. Tashino, S. Onodera, and T. Ikejima, *Critical roles of reactive oxygen species in mitochondrial permeability transition in mediating evodiamine-induced human melanoma A375-S2 cell apoptosis.* Free Radic Res, 2007. **41**(10): p. 1099-108.

43. Orrenius, S., *Reactive oxygen species in mitochondria-mediated cell death.* Drug Metab Rev, 2007. **39**(2-3): p. 443-55.
44. Malik, F., A. Kumar, S. Bhushan, S. Khan, A. Bhatia, K.A. Suri, G.N. Qazi, and J. Singh, *Reactive oxygen species generation and mitochondrial dysfunction in the apoptotic cell death of human myeloid leukemia HL-60 cells by a dietary compound withaferin A with concomitant protection by N-acetyl cysteine.* Apoptosis, 2007. **12**(11): p. 2115-33.
45. Mathy-Hartert, M., G.P. Deby-Dupont, J.Y. Reginster, N. Ayache, J.P. Pujol, and Y.E. Henrotin, *Regulation by reactive oxygen species of interleukin-1beta, nitric oxide and prostaglandin E(2) production by human chondrocytes.* Osteoarthritis Cartilage, 2002. **10**(7): p. 547-55.
46. Tschan, T., I. Hoerler, Y. Houze, K.H. Winterhalter, C. Richter, and P. Bruckner, *Resting chondrocytes in culture survive without growth factors, but are sensitive to toxic oxygen metabolites.* J Cell Biol, 1990. **111**(1): p. 257-60.

6.7 Appendix

Appendix 6.7.1 SODm Dose Response

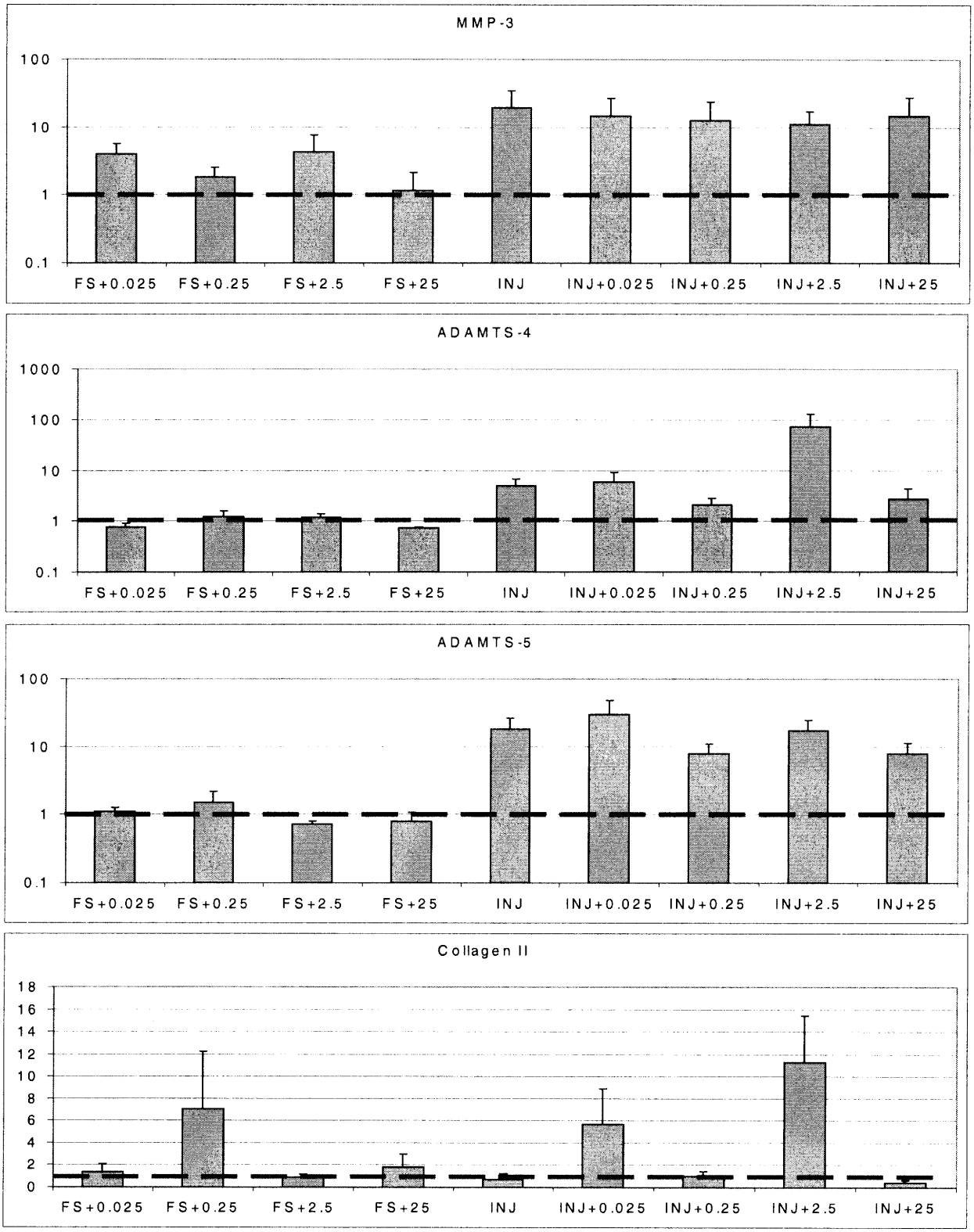

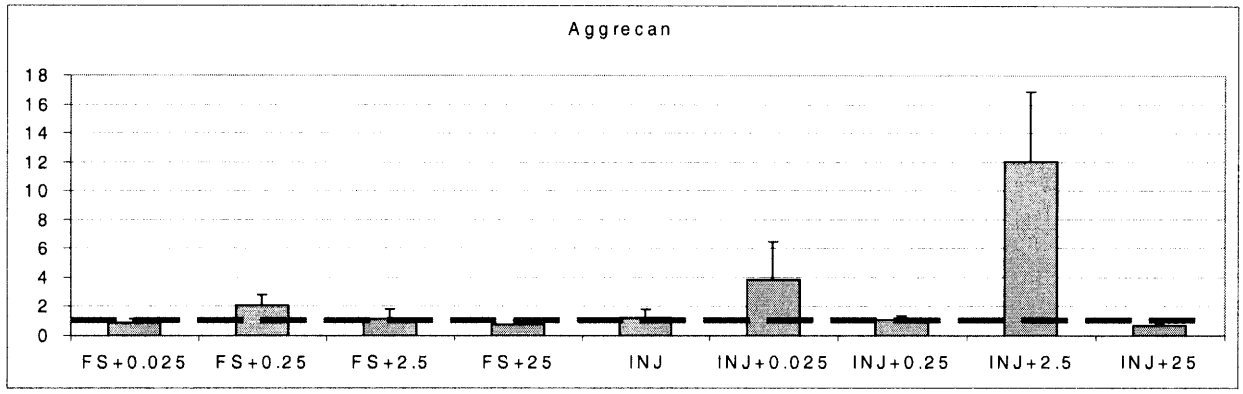
Aggrecan
18
16
14
12
10
8
6
4
2
0
FS+0.025
FS+0.25
FS+2.5
FS+25
INJ
INJ+0.025
INJ+0.25
INJ+2.5
INJ+25

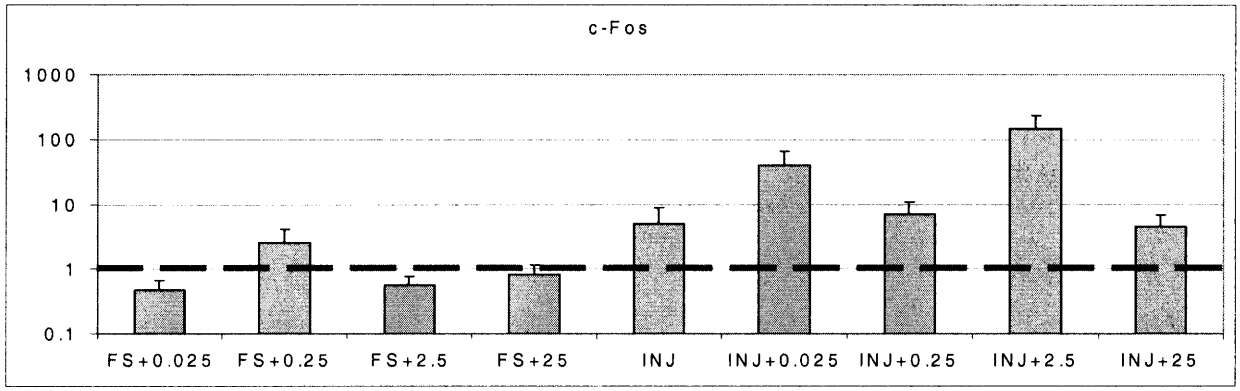
c-Fos
1000
100
10
1
0.1
FS+0.025
FS+0.25
FS+2.5
FS+25
INJ
INJ+0.025
INJ+0.25
INJ+2.5
INJ+25

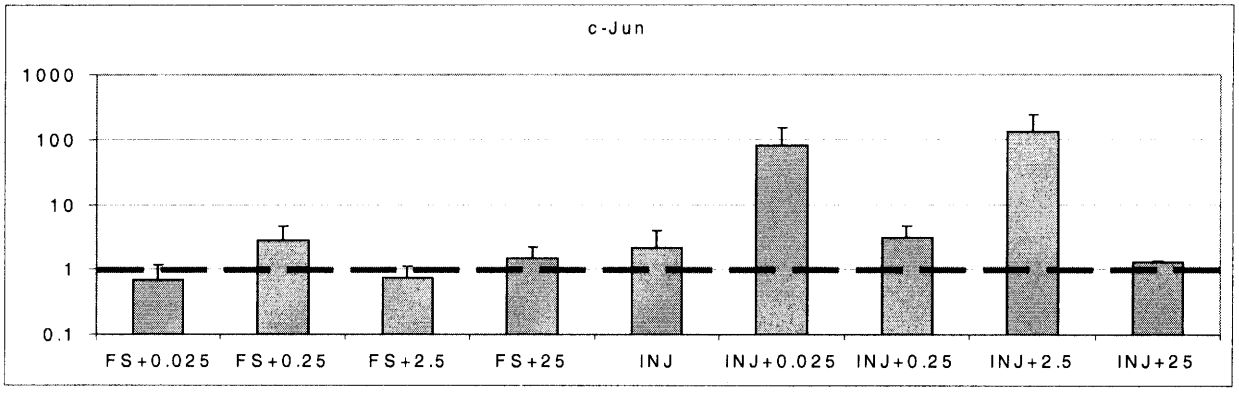
c-Jun
1000
100
10
1
0.1
FS+0.025
FS+0.25
FS+2.5
FS+25
INJ
INJ+0.025
INJ+0.25
INJ+2.5
INJ+25

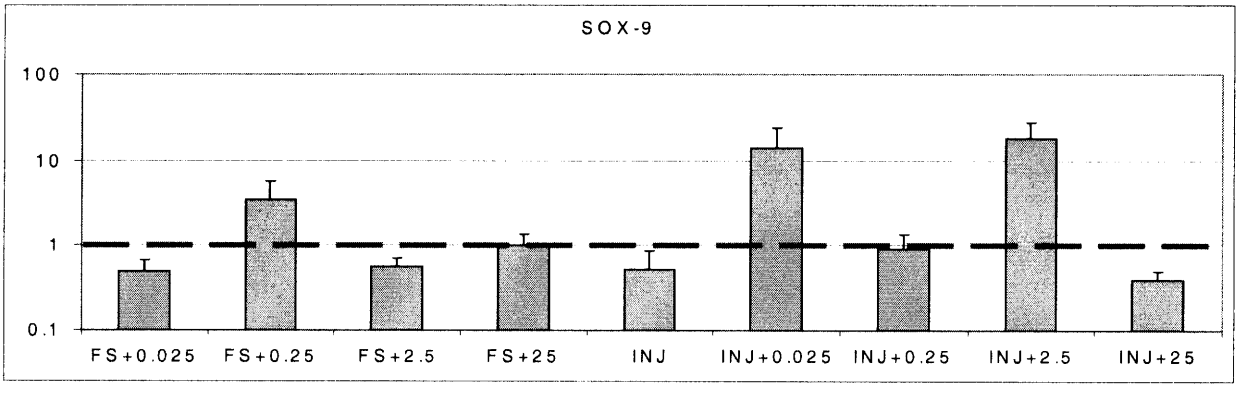
SOX-9
100
10
1
0.1
FS+0.025
FS+0.25
FS+2.5
FS+25
INJ
INJ+0.025
INJ+0.25
INJ+2.5
INJ+25

Appendix 6.7.2 H_2O_2 Positive Control

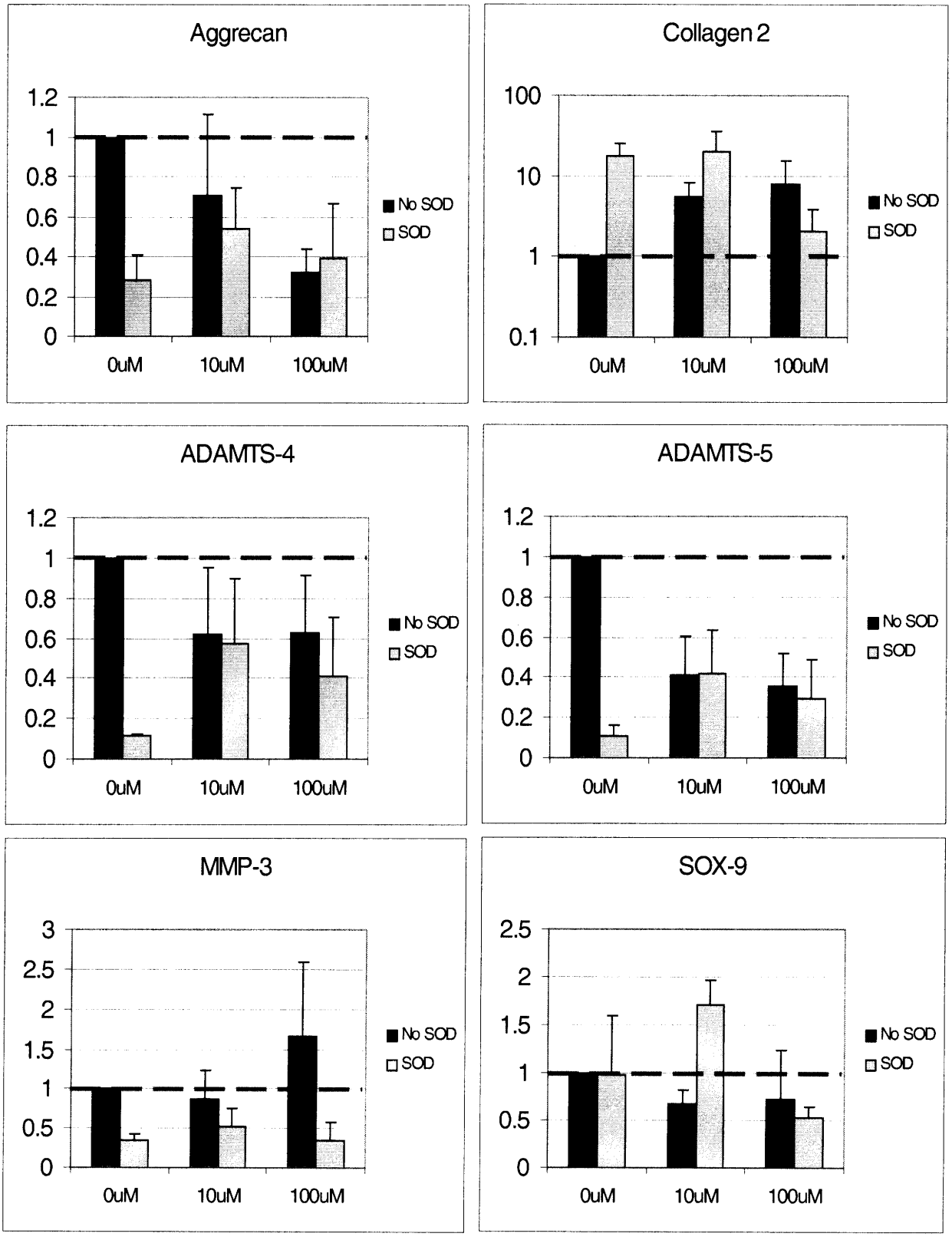

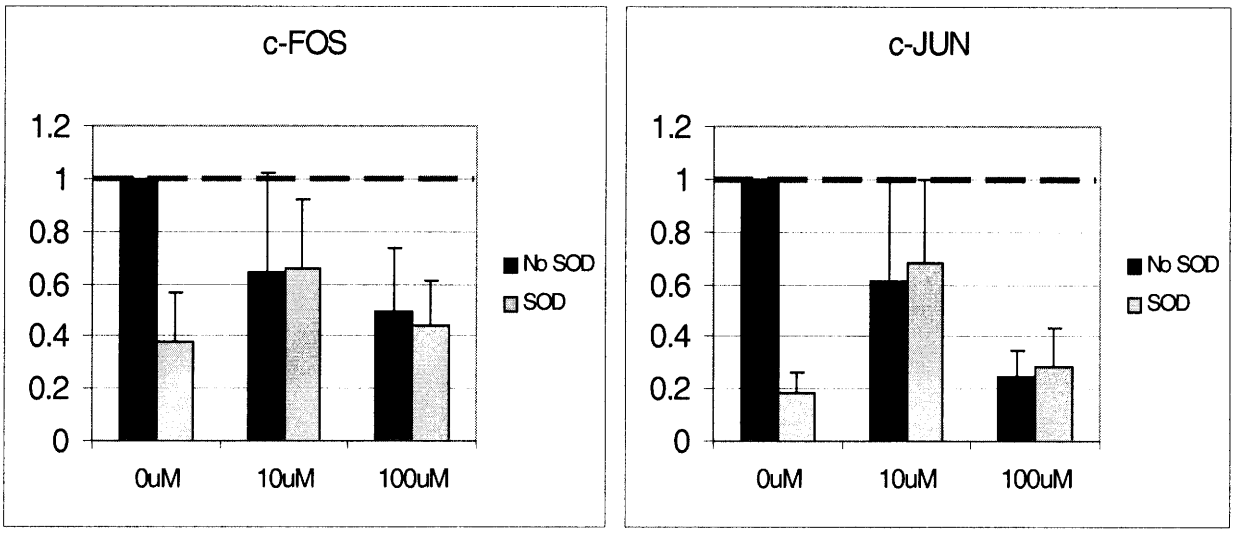
c-FOS
1.2
1
0.8
0.6
0.4
0.2
0
0uM
10uM
100uM
No SOD
SOD
c-JUN
1.2
1
0.8
0.6
0.4
0.2
0
0uM
10uM
100uM
No SOD
SOD

Appendix 6.7.3 Gene Expression 35 Cartilage Relevant Genes

■2hr■8hr□24hr□48hr▤72hr Mean ± SEM * = p-value<0.05 (n=5)

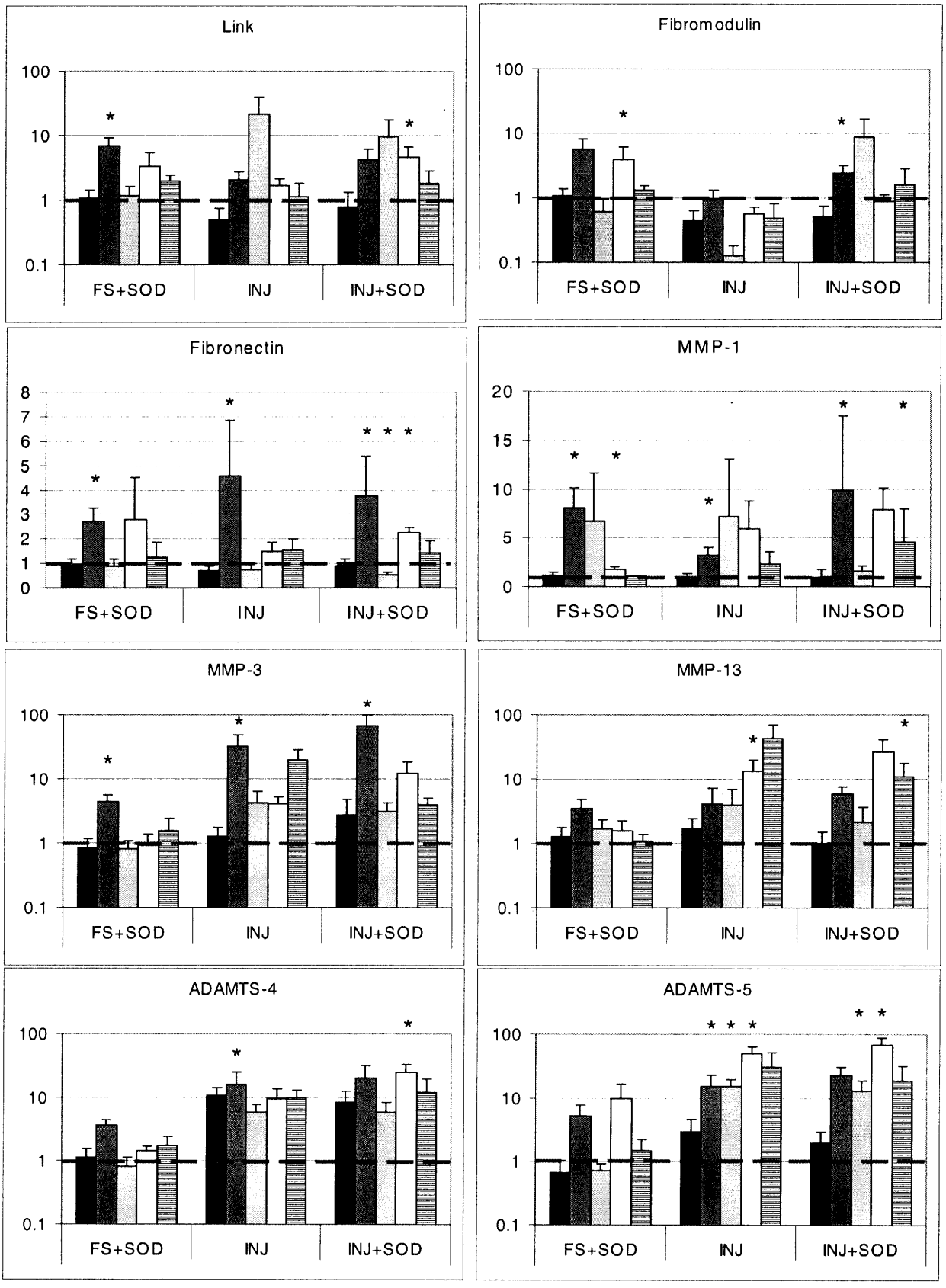

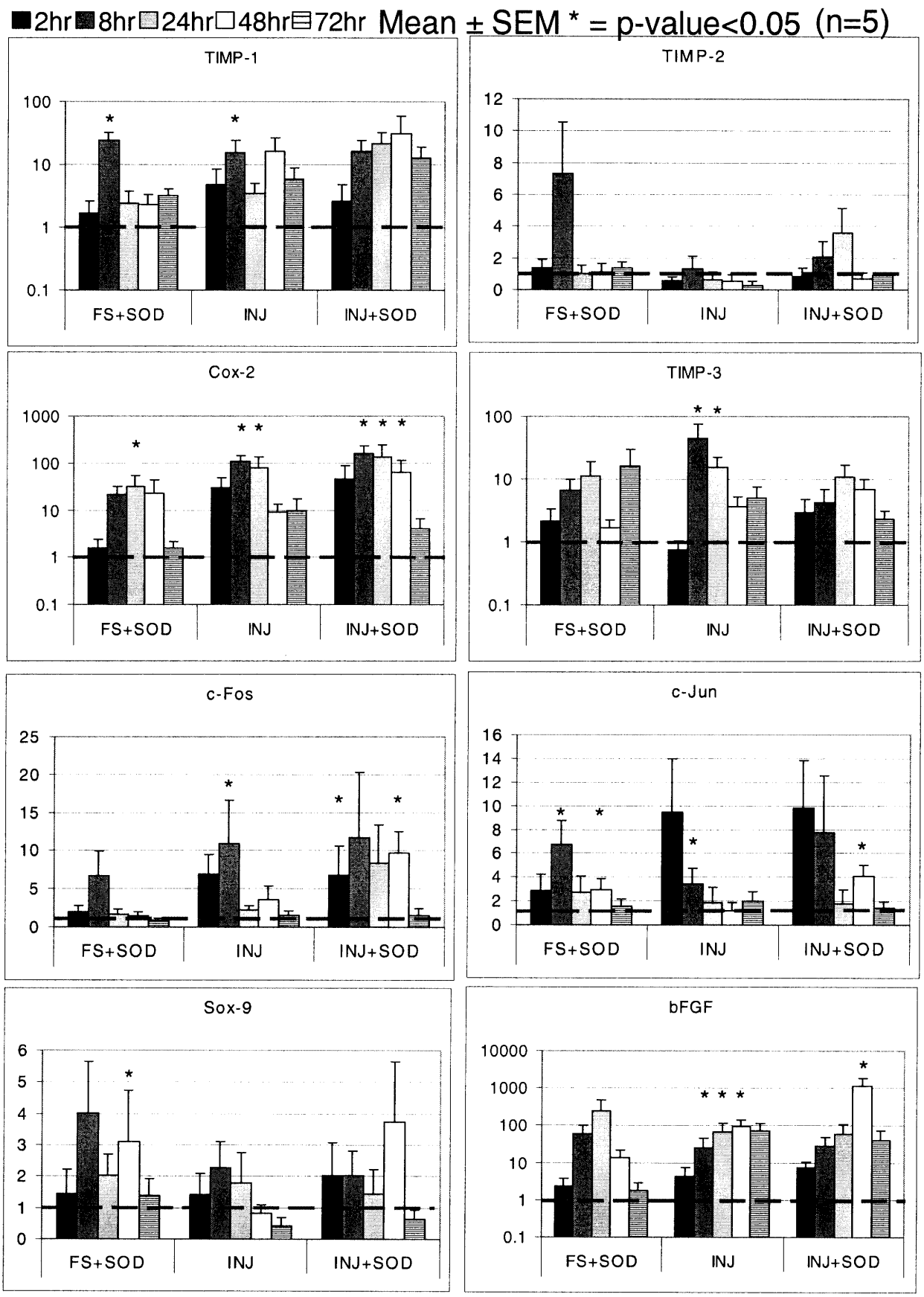
2hr 8hr 24hr 48hr 72hr Mean ± SEM * = p-value<0.05 (n=5)
TIMP-1
TIMP-2
Cox-2
TIMP-3
c-Fos
c-Jun
Sox-9
bFGF
FS+SOD
INJ
INJ+SOD

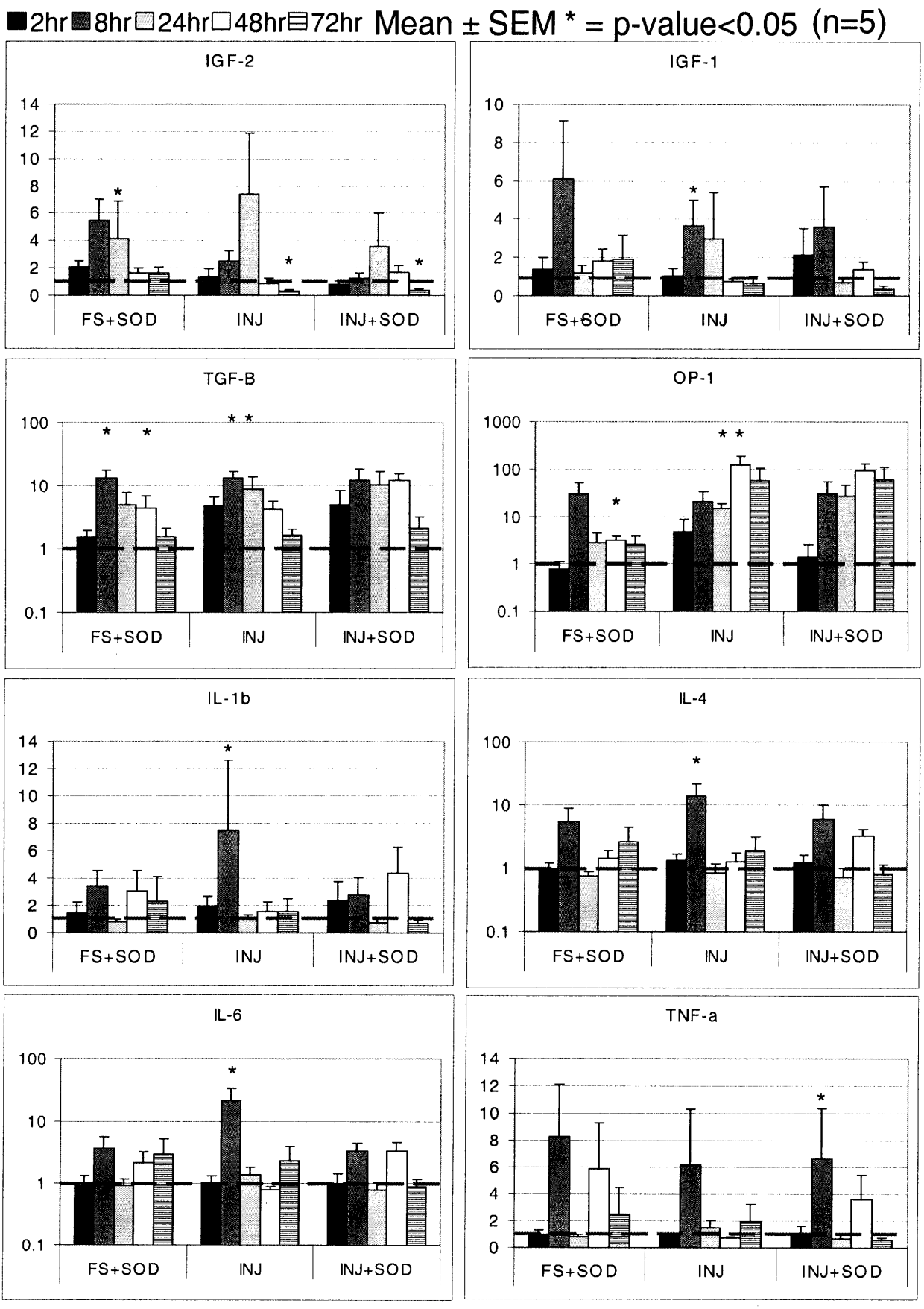
2hr 8hr 24hr 48hr 72hr Mean ± SEM * = p-value<0.05 (n=5)
IGF-2
IGF-1
TGF-B
OP-1
IL-1b
IL-4
IL-6
TNF-a
FS+SOD
INJ
INJ+SOD

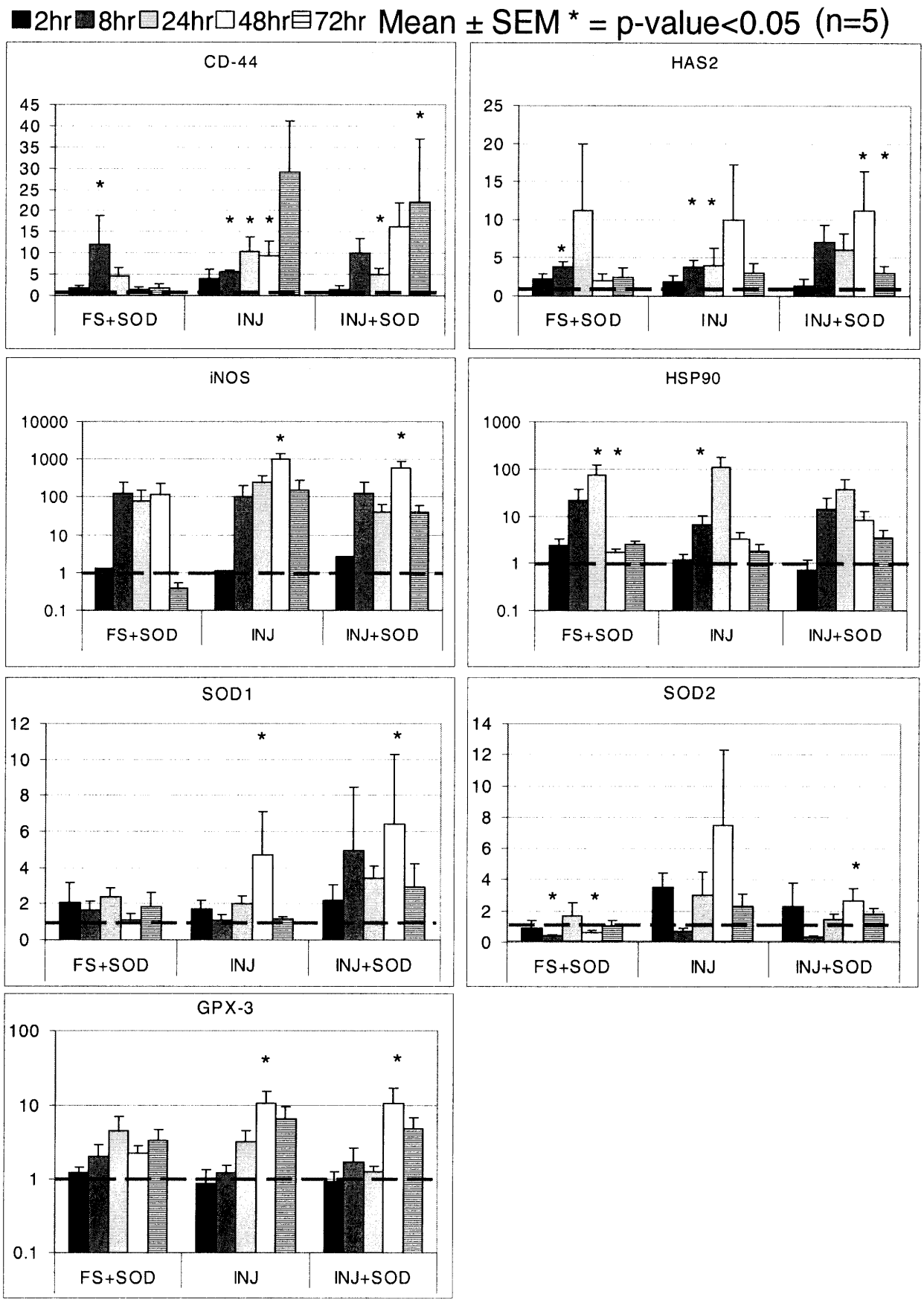
2hr 8hr 24hr 48hr 72hr Mean ± SEM * = p-value<0.05 (n=5)
CD-44
HAS2
iNOS
HSP90
SOD1
SOD2
GPX-3
FS+SOD
INJ
INJ+SOD

■2hr■8hr□24hr□48hr⊟72hr Mean ± SEM * = p-value<0.05 (n=5)

Appendix 6.7.4 The Effects of SODm on Gene Expression

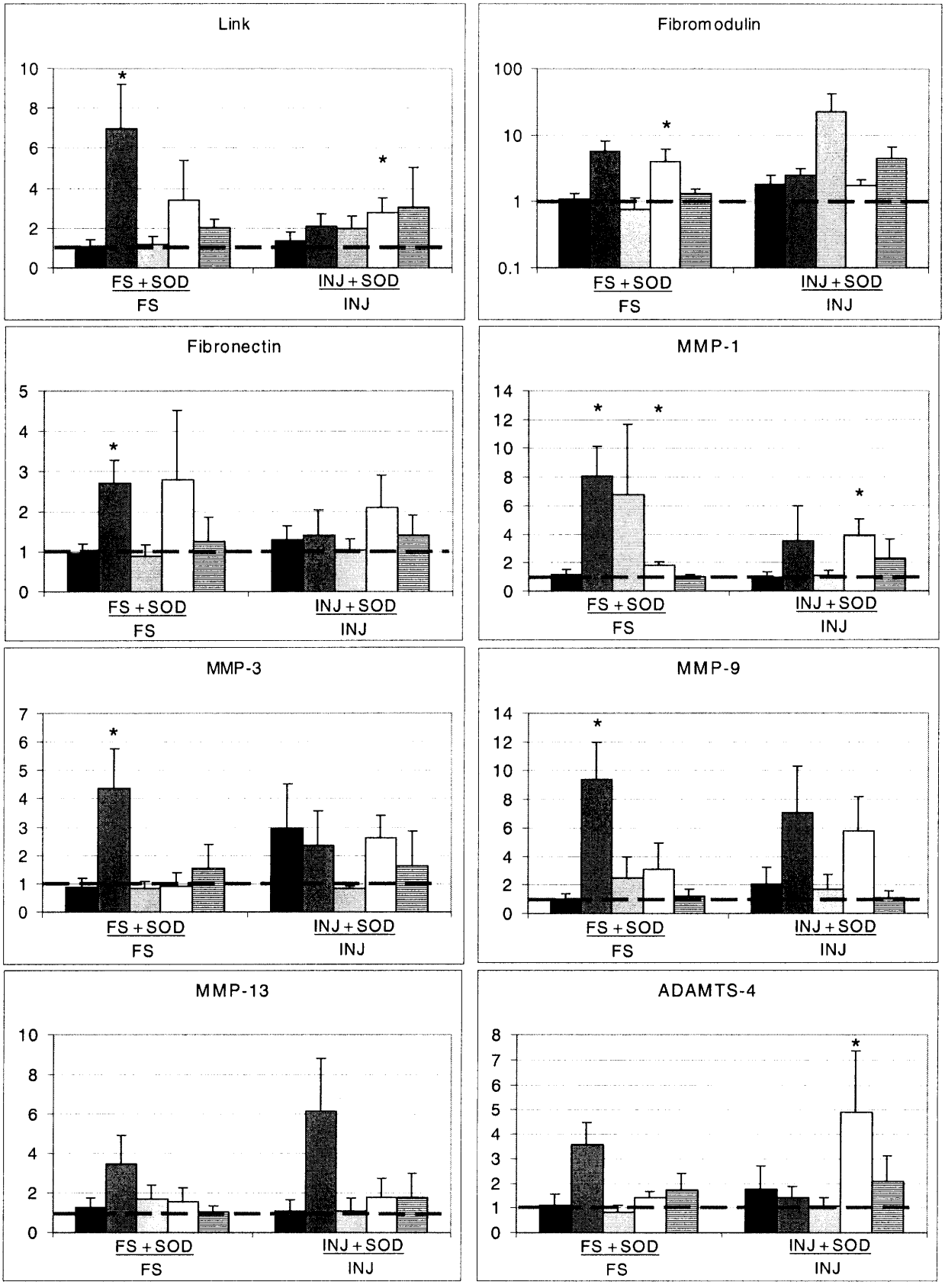

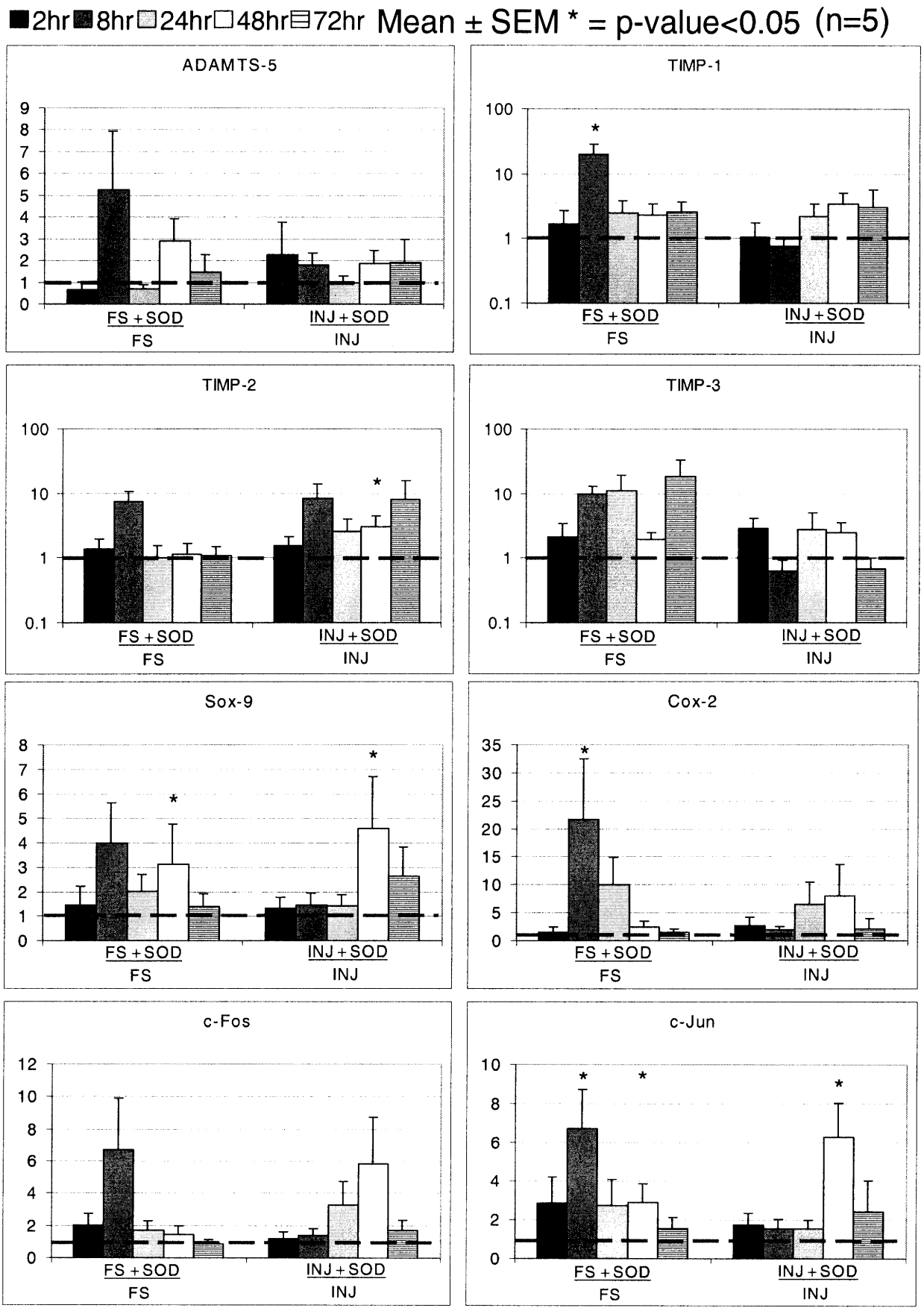
2hr 8hr 24hr 48hr 72hr Mean ± SEM * = p-value<0.05 (n=5)
ADAMTS-5
TIMP-1
TIMP-2
TIMP-3
Sox-9
Cox-2
c-Fos
c-Jun
FS + SOD
FS
INJ + SOD
INJ

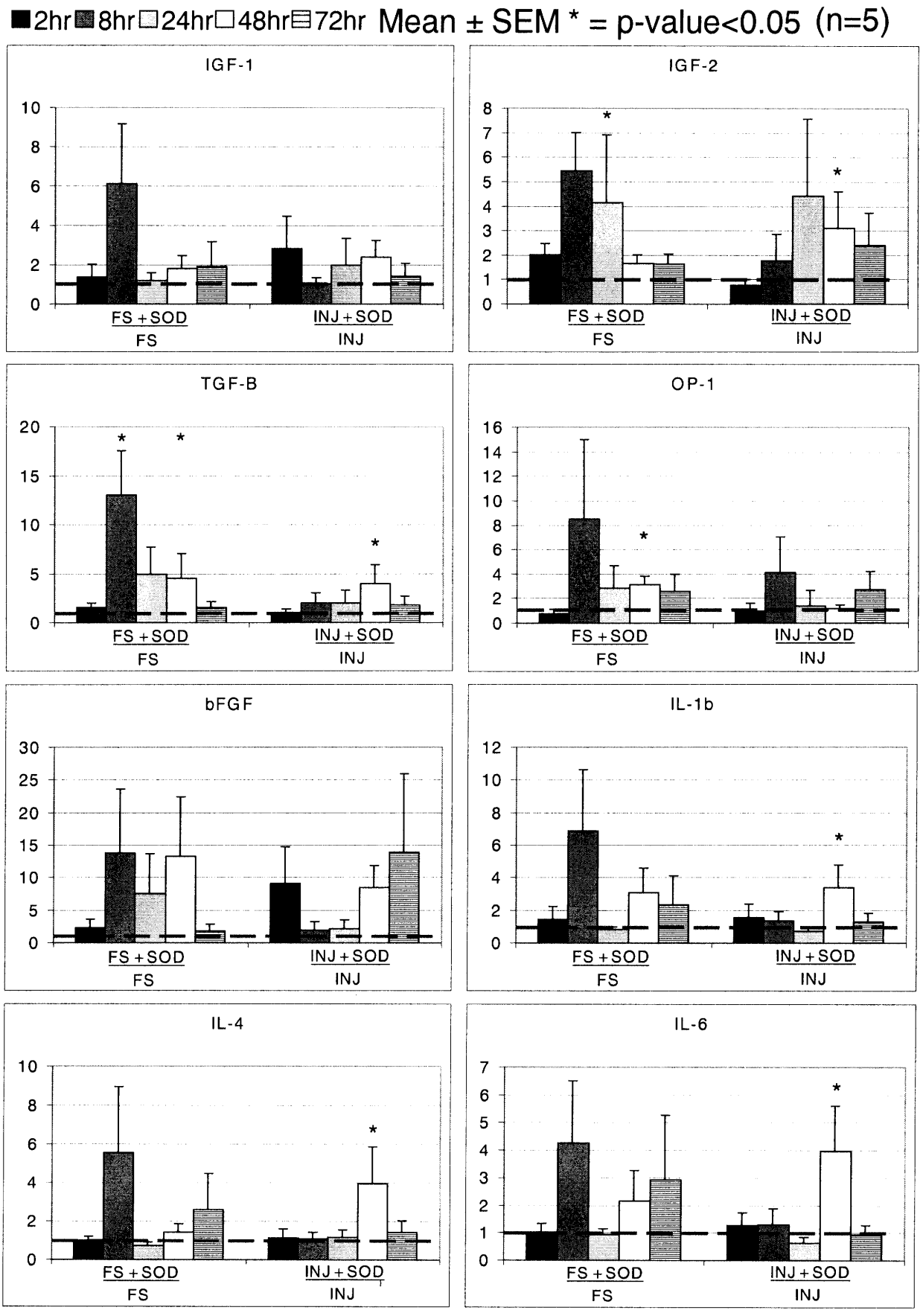
2hr 8hr 24hr 48hr 72hr Mean ± SEM * = p-value<0.05 (n=5)
IGF-1
IGF-2
TGF-B
OP-1
bFGF
IL-1b
IL-4
IL-6
FS + SOD
FS
INJ + SOD
INJ

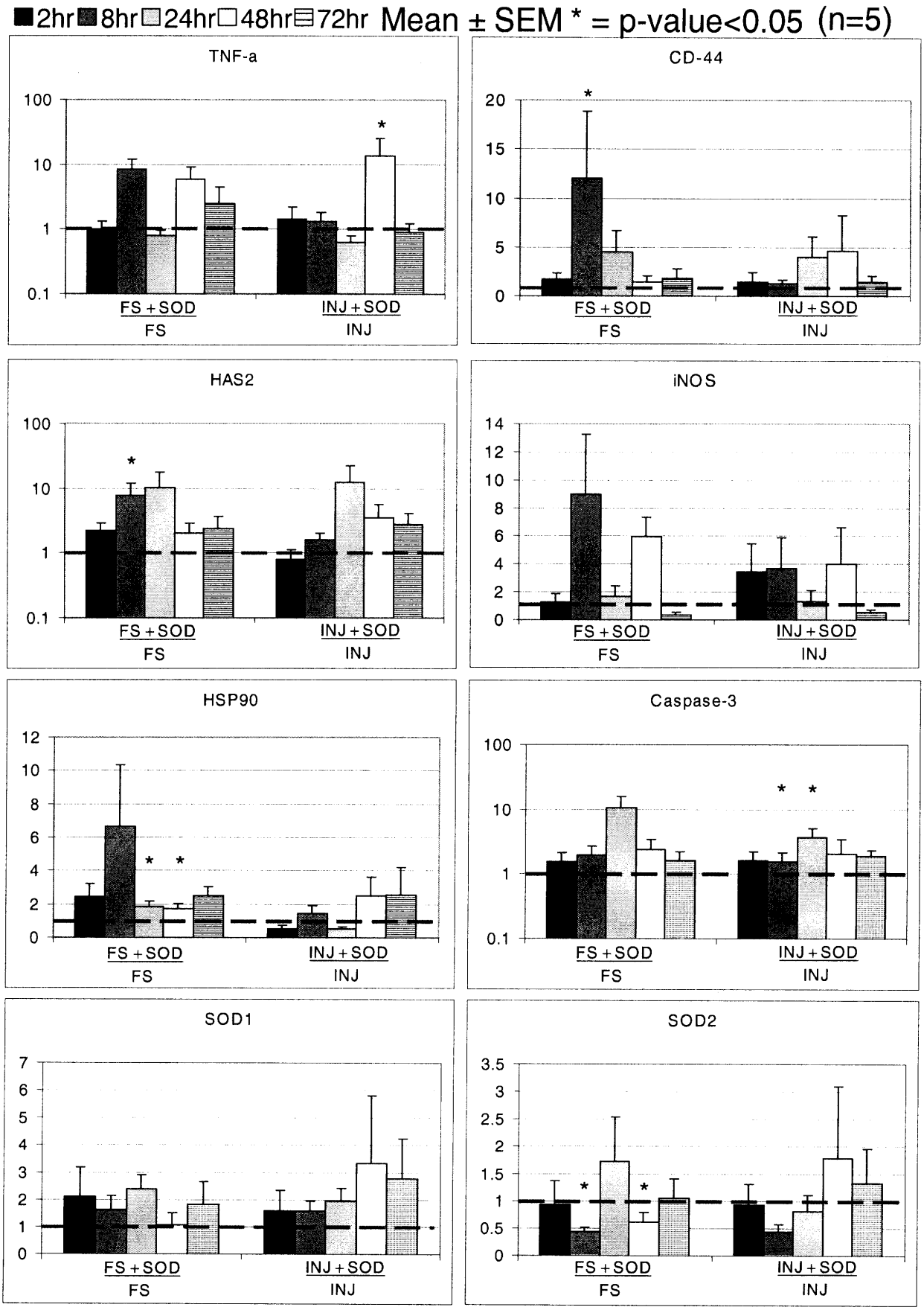
2hr 8hr 24hr 48hr 72hr Mean ± SEM * = p-value<0.05 (n=5)
TNF-a
100
10
1
0.1
FS + SOD
FS
INJ + SOD
INJ
CD-44
20
15
10
5
0
HAS2
iNOS
14
12
10
8
6
4
2
HSP90
12
Caspase-3
SOD1
7
6
5
4
3
2
1
0
SOD2
3.5
3
2.5
1.5
0.5

■2hr ▩8hr □24hr □48hr ▤72hr Mean ± SEM * = p-value<0.05 (n=5)

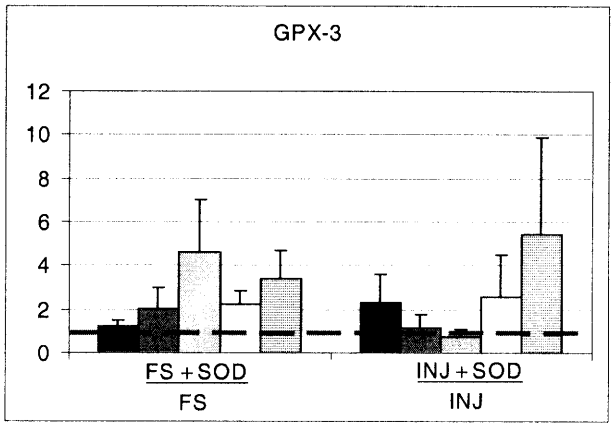

Chapter 7

Summary and Conclusion

The onset of osteoarthritis (OA) is a fascinating subject to study because of the multifactorial influences that contribute to the disease. While genetic and environmental factors play a role in the development of OA (obesity, exercise health, traumatic injury), the time scales at which these factors act and contribute to degradation of cartilage are on the order of years to decades. Given this complex etiopathogenesis, *in vitro* models of the onset of cartilage degradation have been developed to isolate specific aspects of mechanical compression, molecular communication (growth factor and cytokine), and tissue communication (joint capsule and synovium). This study investigated models of joint injury in combination with potential therapeutic agents having the ability to abrogate the negative effects of these *in vitro* injury models.

In Chapter 3, cartilage explants subjected to a ramp and hold compression with a final strain of 50% were treated with IGF-1. Experiments were performed to assess expression levels of a range of ECM related genes in response to static loading in the presence and absence of IGF-1. Through k-means clustering analysis, major co-expression trends were elucidated, grouping genes into highly responsive, non-responsive, and differentially active gene profile groups. The gene pairs MMP-1 and IGF-2, TIMP-3 and ADAMTS-5, and type II collagen and IGF-1 were consistently co-expressed in multiple clustering conditions, suggesting the possibility of strong regulation and control relationships between members of each pair.

Aggrecan and link protein responded to IGF-1 in a compression-dependent manner, whereas type II collagen and fibronectin appeared to respond to IGF-1 in a manner independent of compression. While aggrecan transcripts were significantly upregulated with the addition of IGF-1 under 0% compression, IGF-1 was unable to upregulate aggrecan when the cartilage explants were statically compressed to 50% strain. In comparing aggrecan gene expression to aggrecan synthesis, these data suggest that aggrecan synthesis is transcriptionally regulated by IGF-1 while the inhibition of aggrecan synthesis by compression is post-transcriptionally regulated. However, more studies are needed to elucidate the specific stimulatory mechanism(s) induced by IGF-1 and the post-translational inhibitory effects of compression.

Chapter 4 focused on an extensive study of the transcriptional, translational, and apoptotic effects of various models of injury in combination with growth factor stimulus. ECM genes were generally downregulated and proteases upregulated in response to Co, INJ, and/or INJ+Co, where genes responded most dramatically to INJ+Co for both short-term expression and longer-term expression. GF treatment failed to rescue the downregulation of ECM transcripts and the upregulation of protease transcripts. Clustering analysis of both short-term gene expression and longer-term gene expression showed distinct groupings of co-regulated genes. Joint capsule gene expression was also measured and revealed that protease expression is much higher in joint capsule than normal (free swelling) cartilage tissue. Growth factor treatment stimulated all genes measured in the JC, with the exception of ADAMTS-5. Examining the rates of biosynthesis, Co and INJ+Co dramatically affected uptake of ^{35}S and ^{3}H over the 16 day time period measured. After treatment with OP-1 and IGF-1, biosynthesis rates measured by ^{3}H-proline incorporation improved dramatically, while biosynthesis measured by ^{35}S-sulfate

incorporation only slightly increased. Dramatic amounts of apoptosis were measured after mechanical injury. JC appeared to have little effect on apoptosis. Growth factor treatment significantly decreased levels of apoptosis under mechanical injury alone. The *in vitro* models of injury, Co, INJ, and INJ+Co, mimic a physiologic system of *in vivo* injury. Growth factor treatment had a slightly stimulatory effect on biosynthesis rates, decreased apoptosis, and had little effect on recovering gene transcripts after injury. While OP-1 and IGF-1 have a positive effect on apoptosis, the data presented support the role of OP-1 and IGF-1 as remodeling factors, as opposed to anti-catabolic and pro-anabolic factors as has been previously reported. Further studies are needed to understand the mechanistic action of OP-1 and IGF-1 to clarify their reparative and possible therapeutic capabilities.

In Chapter 5 the model of mechanically injured cartilage co-cultured with excised joint capsule was examined using adult human tissue. The data showed that the combination of cartilage mechanical injury and subsequent co-culture with excised joint capsule strongly mimics certain changes in human articular cartilage obtained from notchplasty during reconstructive surgery following anterior cruciate ligament rupture, as seen through IHC analysis. After injury, knee cartilage exhibited increased GAG loss levels and lower biosynthesis rates, while ankle cartilage showed less GAG loss and increased biosynthesis rates over time. The conditions including mechanical injury took 16 days to fully develop a significant difference in GAG loss compared to FS controls. Biosynthesis rates in knee cartilage were significantly downregulated with the addition of mechanical injury at the first time point measured, two days after injury. As previously reported, injurious conditions showed no significant difference in aggrecan species profile as examined by immunoblotting, up to six days after injury. Ongoing studies are aimed at

further elucidating the molecular responses and cellular signaling pathways underlying the response of human tissue to combined mechanical injury and joint capsule co-culture.

In Chapter 6 a complex model of joint injury, consisting of mechanical injury to cartilage and subsequent treatment with inflammatory cytokines (TNF-α, IL-6, and IL-6R) in combination with an antioxidant, superoxide dismutase mimetic (SODm) was investigated at the level of transcription. SODm did not demonstrate the ability to abrogate the negative effects of this complex injurious assault. On the contrary, the treatment of SODm tended to stimulate all genes measured. In particular, it increased protease transcript levels, as well as increased in GAG loss, a measure of cartilage degradation. The injury model elicited dramatic responses of COX-2, OP-1, bFGF, iNOS, and HSP90 to levels greater than 100 fold the control, suggesting these genes play a crucial role in the initial response to traumatic injury within the first three days. The magnitude of these changes in gene transcript levels had not been observed previously in the application of mechanical injury or cytokine treatment to our knowledge. As has previously been suggested, the combination of cytokine treatment and mechanical injury produced the most cartilage degradation, opening a possibly insightful *in vitro* model of osteoarthritis. Since ROS influence on signaling pathways in chondrocytes depends on the kind of ROS (superoxide versus hydrogen peroxide), and SODm eliminates both superoxides and hydrogen peroxide, further studies are needed with antioxidants with greater specificity to determine the effect of ROS on chondrocytes. Whether antioxidants may serve as therapeutics for osteoarthritis for their ability to decrease cell death, or as targets for therapeutics because of their increased degradative effects on cartilage, as seen here, remains to be seen.

In conclusion, this work has extensively investigated the effects of multiple injury models including the combination of static compression, injurious loading, cytokine treatment, co-culture with injured or excised joint capsule, and selected combinations of these models. Through studies in both bovine cartilage and human cartilage, we have found these models mimic the onset of osteoarthritis. The growth factors and antioxidants, IGF-1, OP-1, and SODm, were tested to examine if they had the capability to abrogate the negative effects of these injury models. Taking a systems approach, through extensive measures of gene expression, cell viability, biosynthesis data, protein expression, and GAG loss, OP-1 and IGF-1 were unable to rescue transcriptional expressions due to injury, but were able to rescue cells from apoptosis, and slightly increase biosynthesis rates. The antioxidant, SODm, showed no ability to selectively diminish protease transcriptional activity, and cartilage treated with this antioxidant significantly increased GAG loss to the medium, while diminishing levels of apoptotic cells. Taken together, this work supports further investigation of 1) the mechanisms of action of OP-1, IGF-1, and SODm in order to elucidate their possible therapeutic value, and 2) the validation of *in vitro* injury models in mimicking the onset of OA.

Appendix A: Experimental Protocols

A.1 RNA Extraction Protocol- Bovine

Base & Top of Pulverizer

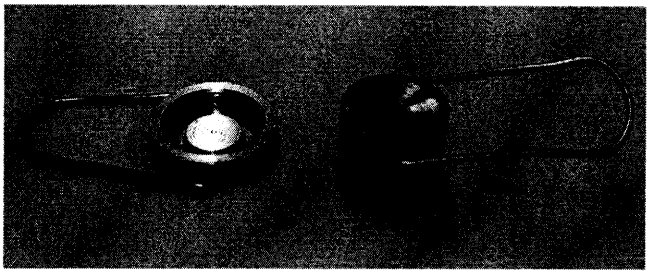

Stopper & pole

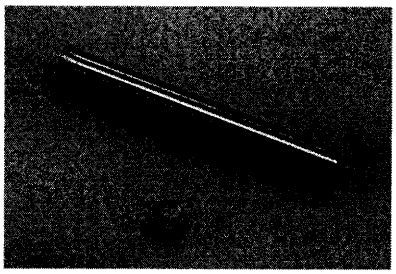

Pulverizer ready to pound

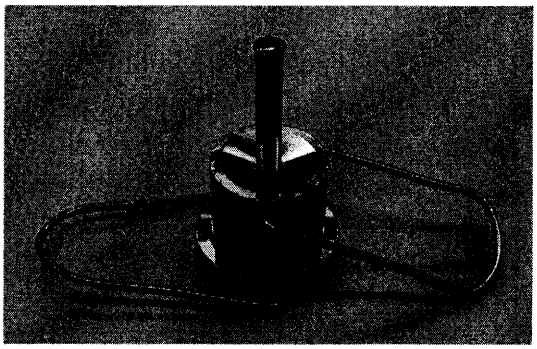

Pulverizer ready to freeze

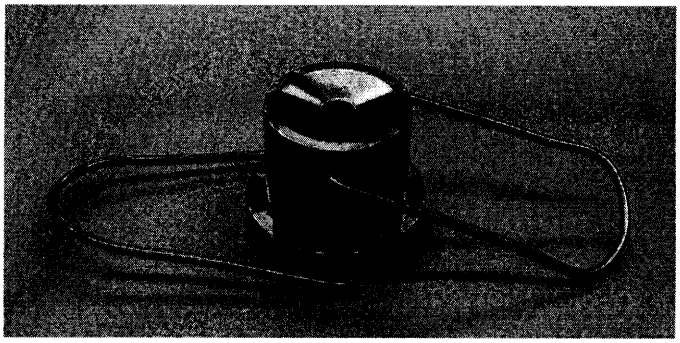

Tissue Tearor (Homogenizer)

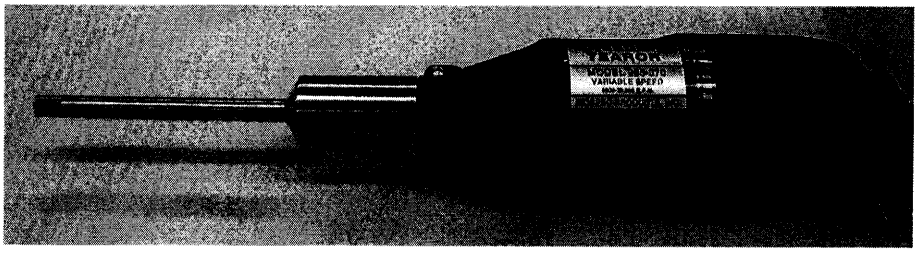

Sheath and Blade

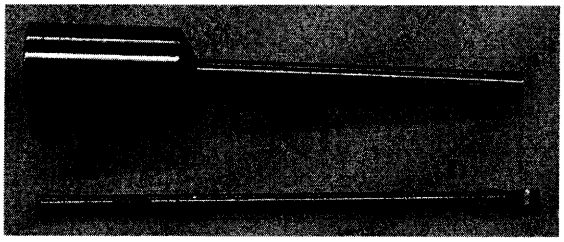

Blade is flush within sheath

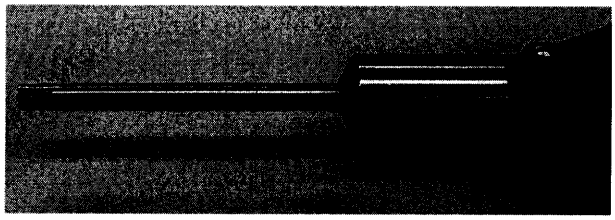

Tissue preparation

0) You should prepare/label all required tubes before starting. Also make up the **DNase** used in step 6 of the RNA extraction protocol ahead of time and store in ice bath. All steps for the RNA extraction are taken from the QIAGEN RNeasy MiniKit for animal tissue. Pages 54-55. Obtain volumes of **chloroform, 100% ethanol** and **RLT buffer** (with β-Me added). Add **20mls of DI water to two 50ml tubes** for cleaning the homogenizer. Pre-spin Eppendorf **phasegel** tubes for 15 seconds.
1) Samples should be stored by either flash-freezing in liquid nitrogen and placing in a –80C freezer, or placing in RNA*later* solution and placing in –80C freezer. It is best if cartilage has been dissected into multiple 3x3x1mm pieces.
2) Place pulverizer and pole in container and bathe in liquid nitrogen repeatedly to cool. Remove two samples from the -80°C freezer and place in ice bath. Cool pulverizer again with liquid nitrogen.
3) Remove pulverizer and bend its arms downwards. Add cartilage samples to top of pulverizer (make sure metal stopper is in place). Place pole into top base. Hit pole firmly 8-10 times with a hammer, while holding pole and top of pulverizer.
4) Lift top of pulverizer and gently tap pole to release metal stopper. Place a 5ml polypropylene tube beneath pulverizer, turn pulverizer sideways and tap pole on side of bench to release the smashed cartilage into tube. Place polypropylene tube with pulverized cartilage in -80 deg Freezer.**
5) Clean pulverizer with sterile gauss and if necessary re-cool with liquid nitrogen. Repeat steps 2 to 5 with next sample.
6) Remove all polypropylene tubes from -80 deg freezer, take off caps, and add **540µl of Trizol** to each. Ensure that cartilage is submerged in trizol; change tips.
7) All samples should now be pulverized and have Trizol added. Set up the homogenizer so that the blade is flush with the sheath.
8) Place homogenizer in first water tube, turn on and rinse, turn off, remove and shake dry. Repeat in second water tube. The second water tube should still look clean at the end of the Tissue preparation protocol.
9) Place homogenizer into first sample, turn onto low speed, and slowly increase speed. Sample should be homogenized in less than 20 seconds. Never turn tissue tearor past level 2. Place sample back in ice bath. Repeat steps 7 & 8 until finished.
10) Remove samples from ice bucket, wait 30 min for samples to soak in trizol.
11) Add **60µl of chloroform** (final 10%) to each tube.
12) Mix Trizol, chloroform, cartilage (should turn cloudy pink) and transfer sample to pre-spun phasegel tubes. Cut off end of pipette tips if cartilage repeatedly clogs pipette.
13) Spin phasegel tubes at maximum speed for 10 minutes at 4°C (room temperature if cold room centrifuge is not available).

RNA extraction

1) Make sure all QIAGEN reagents are ready. Buffer RPE should have ethanol added to the bulk volume when the kit is first used. Each month a 10ml aliquot of Buffer RLT mixed with 100X β-Mercaptoethanol must be made. β-Me is highly toxic and must remain in the chemical fume-hood.
2) The following steps are taken from the QIAGEN RNeasy Mini Protocol.
3) While the phasegel tubes are spinning add **250µl of 100% ethanol** to a set of RNase-DNase free 1.5ml centrifuge tubes. Then add **350µl of RLT buffer** (which contains β-Me).
4) Transfer the supernatant in a phasegel tube to the new centrifuge tube and immediately mix the supernatant, ethanol and RLT buffer. Transfer half the solution to the pink RNeasy spin column (less than 700µl). Repeat for each phasegel tube. Centrifuge spin columns for 15sec at 10,000 rpm, allowing 5sec for ramping up, then discard flow through. The RNA is now attached to the silica membrane in the pink tubes. Add the remaining sample from the centrifuge tube to the spin columns and spin again at 10,000rpm. Discard flow through.

   Steps 5 to 8 are the for **DNase digestion** to remove genomic DNA, and can be found in the QIAGEN RNeasy Mini Protocol (p98-99).
5) Pipette **350µl of Buffer RW1** into spin column and centrifuge for 15sec at 10,000rpm, allowing 5sec for ramping up. Discard flow-through into separate bin and reuse collection tube.
6) **Prepare ahead:** Make a mastermix of 10µl of DNase stock solution to 70µl of RDD Buffer per sample. Once dissolved DNase should be stored in the –20C freezer in aliquots. Thawed DNase aliquots should not be re-frozen, instead store in the 4°C fridge (generally choose aliquot size carefully).
7) Pipette **80µl aliquots of DNase mix** directly onto the spin column membrane, tap gently to ensure the entire membrane is covered. Incubate on bench top for 15 minutes at room temperature.
8) Pipette **350µl of Buffer RW1** into spin column and centrifuge for 15sec at 10,000rpm, allowing 5sec for ramping up. Discard flow-through and collection tubes into appropriate bins.

9) Place spin column into a **new 2ml collection tube**, add **500µl of Buffer RPE** (with ethanol previously added), centrifuge for 15sec at 10,000rpm, allowing 5sec for ramping up. Discard flow-through into separate bin and reuse collection tube.
10) Pipette **500µl of Buffer RPE** (with ethanol added) into spin column, centrifuge for 2 minutes at maximum speed. After spin remove spin column from collection tube and wipe the outside gently with sterile gauze to remove any residual ethanol, which may interfere with subsequent reactions.
11) Place spin column into 1.5ml collection tube (supplied, rounded bottom). Add 50µl of Rnase-Dnase free dH_2O from QIAGEN kit. Spin at 10,000rpm for 1 minute, and then place immediately in -80°C freezer, discard column.
12) Keep RNA in -80°C to minimize degradation.

A.2 RNA Extraction Protocol- Human Tissue

Small Scale Human Cartilage RNA Protocol – 11/21/04

This protocol is designed for harvesting intact RNA from ~ 0.05 – 0.2 g of snap frozen cartilage. Expected yields should be about 10-15 μg RNA/g tissue.

Suggested reagents and materials:

All materials should be molecular biology grade or higher, and RNase-free. Gloves should be worn at all times to prevent potential RNA degradation. Use of a fume hood is also recommended.

Ambion

Acid Phenol:$CHCl_3$ – cat # 9720
Phenol:$CHCl_3$:IAA – cat # 9730
1.5 ml Non-stick RNase free microfuge tubes – cat # 12450
Nuclease free water - cat # 9937

Pierce Chemicals

Aquasil Silanizing Fluid – cat # 42799

Sigma Aldrich

$CHCl_3$

Invitrogen

TriZol – cat # 15596-026

Zymo Research

RNA clean up kit #R1015

Other materials

SPEX Certiprep 6750 Freezer mill
SPEX Certiprep Microvials # 6753
Microfuge
2 ml screw cap sample tubes
Barrier-tip pipet tips
Liquid nitrogen
Dry Ice
Wet ice
Methanol
Vortexer
Eppendorf Phase Lock Gel (Heavy, 2.0 ml) – Brinkman Instruments cat # 955154045

1. Silanize grinding microvials as per manufacturer's instructions, including impactors and end caps. Air dry for 1 day in hood. Discard waste as appropriate. Store grinding microvials at -80 °C the day prior to RNA extraction, if possible..

2. Powder snap frozen cartilage (in liquid N2) using a SPEX 6750 Freezer mill. Pre-chill chamber and grinding vials in liquid nitrogen prior to use (minimum of 10-15 minutes is recommended).

Keep grinding vials cold at all times. Allowing the vials to warm even slightly will decrease RNA yield and quality dramatically.

Powdered tissue using the suggested settings: Cycles: 3

Pre Cool: 5 minutes

Cool between cycles: 2 minutes

Rate: 10

Powder time: 1 minute

3. Remove one end cap from grinding microvial, and gently transfer powdered cartilage into 2 ml screw cap tube on dry ice. Use 1-2 ml of TriZol per 100 mg tissue. Do not let powdered tissue warm up! Vortex for 1 minute. Ensure powder is totally resuspended in TriZol. Rotate for 1 hour at RT.

4. Pellet samples, 12,000 x g, 5' at 4 °C. Transfer supernatant to 1.5 ml eppendorf tubes. (At this point may need to split each sample equally into two tubes). Note initial starting volume. Add 0.2 volumes of $CHCl_3$ per tube. Vortex ~ 15 – 30 seconds. Incubate at RT for 3 minutes. Centrifuge for 15 minutes @ 12,000 x g, 4 °C. *Optional: Remove about 10% of lowest phase. Add another 0.2 volumes $CHCl_3$. Vortex for 15 seconds. Incubate at RT for 3 minutes. Centrifuge for 15 minutes @ 12,000 x g, 4 °C.*

   Transfer aqueous phase to fresh tubes.

5. Add one volume Ambion Acid Phenol:$CHCl_3$ and vortex. Incubate on ice, 10 minutes. Centrifuge at 15,000 x g, 15 minutes. Added back 100-200 µl dH_2O/tube and back extract. Transferred aqueous phase to fresh tubes. Repeat extractions with one volume Phenol:CHCl3:Isoamyl (25:24:1). Chill on ice 10 minutes. Centrifuge at 15,000 x g, 15 minutes, remove aqueous phase. Finally, extract aqueous phase with one volume $CHCl_3$, vortex briefly, and transfer to pre-spun Phase Lock Gel (Heavy, 2.0 ml) tubes. Centrifuge at 15,000 x g, 5 minutes. Remove upper aqueous phase. Determine final volume of the aqueous phase. Use this value for determining how much RNA binding buffer to add. Per sample, add 4 volumes Zymo Research RNA Binding Buffer.

6. Per sample, use one Zymo Research spin column/sample. Note: Binding capacity of columns are ~ 5 µg of total RNA (this is a minimum). Load each column with up to 700 µl of each sample in RNA Binding buffer (700 µl is max volume per load). Centrifuge 11,000 x g, 15 seconds. Discard flow through. Reload the column with more sample. Centrifuge 11,000 x g, 15 seconds. Discard flow through. Repeat if necessary. Remove flowthrough. Add 200 µl wash buffer. Spin at top speed, 15-30 seconds. Add another 200 µl wash buffer. Spin at top speed, 30-60 seconds. Discard collection tube. Switch to supplied 1.5 ml eppendorf tube for collection. Add 8 µl dH_2O. Spin at 11,000 x g, 15 seconds. Add another 8 µl dH_2O. Spin at 11,000 x g, 15 seconds. Volume is now 16 µl. Run out 1 µl/sample on the Agilent Bioanalyzer using the Nano kit. May want to also take OD's. Store remainder of samples at –80 °C.

Notes: For RNA amplification, DNase treatment is usually not required. If DNasing is deemed necessary, can do so prior to Zymo RNA spin column step.

A.3 Extracted RNA Measurements

Materials:

- Ice bucket
- Samples (with extracted RNA)
- DNase/RNase-free deionized water
- P2, with pipette tips

Procedure:

1. Place a maximum of 12 samples in the ice bucket and go to the Nanodrop instrument (located in the lab next door).
2. Lift the lever of the Nanodrop and spray eye with ethanol. Clean gently with a kimwipe.
3. Open the Nanodrop software and choose Nucleic Acids.
4. The software will ask you for a calibration measurement. Place 1ul of the DNase free water on the eye. Lower lever and click OK.
5. Change the DNA tab to RNA and change the wavelength from 230 to 260.
6. Place another drop of water on the eye and re-calibrate. Measure the sample (water) to check if the measurement is actually zeroed. Repeat re-calibrating until the measurement is zeroed with the water sample.
7. Clean the eye with a kimwipe and place 1ul of the sample on the eye and lower lever.
8. Enter the sample name and click Measure.
9. Repeat steps 6 and 7 until samples are done. The Nanodrop should be re-calibrated about every six samples.
10. After the samples are all measured, close the program. Save the excel file to a flash drive. (Desktop -> Shortcut to Yusuke, go up one directory -> Nucleic Acids -> Default -> Excel file, ordered by date)

A.4 Reverse Transcription of RNA to cDNA

0) Before commencing ethanol all surfaces, use alcohol wipes on pipettes, pens & trays. This is done to avoid contamination with proteins, RNAs, RNase and DNase, crucial! Also calculate the appropriate volume needed for 1µg of RNA. This should not be larger than 25µl.

1) If proceeding straight from a RNA extraction ensure that RNA is kept cold (but not frozen) by placing vials in an ice bucket and then placing in the 4°C fridge as calculation of RNA volumes can take some time. If RNA has been frozen and stored in the -80°C freezer then thaw it immediately before use, and then mix by pipetting.

2) Make a RT master mix using the following guide. Total reaction volume will be 40µl once RNA and H_2O have been added.

RT Reagents	x1 40µl
10x PCR buffer	4
$MgCl_2$	4
dNTP(5mM)	4
Random Hexamers	1
Rnase Inhibitor	1
Multiscribe Reverse Transcriptase	1

Mix thoroughly

Keep cold, remove from freezer only when needed, mix thoroughly by pipetting, (do not vortex as enzymes are fragile).

3) Generally multiply all the above equations by the number of cartilage samples you have to create a master mix. A total volume of 40µl was chosen here, but this can be scaled up or down depending on the total needed volume.

4) Aliquot 15µl of the mastermix into X different tubes. Then add the appropriate amount of H2O (25µl- volume of 1µg RNA). Last step, add the RNA, immediately put on thermocycler block, and run 4° program. This will ensure the mix does not degrade.

5) Load tubes into the thermocycler and follow these steps: **GoldRT2**

25°C 20 minutes	(hybridization)
42°C 30 minutes	(reverse transcription)
Hold 4°C	(wait for removal)

6) Although cDNA is significantly more stable than RNA and thus doesn't degrade as fast as RNA, quantitative RT-PCR aims to avoid degradation as much as possible. Hence, move cDNA into the -20°C as soon as possible after the thermocycler reaches 4°C.

A.5 Standard Curve Measurements for qPCR Primers

1. Make primer stock by adding H2O to lyophilized primers. Make up 100 μmolar of Primer. Add (10*(nmole)) μL of H2O to stock.
2. Make up Aloquats by diluting primer stock by 20:1
    a. Use 200 μL eppindorf tubes, add 180 μL of H2O
    b. Add 10 μL of for and 10 μL of rev.
3. Amplify stock cDNA by adding new primer, SGMM, H20, and cDNA
    a. For 20μL, 10μL SGMM, 1.5 μL cDNA, 2 μL Primer, and 6.5 μL H20
4. Use RealPCR protocol on PCR machine
5. Purify the product- Centri-Spin Column
    a. Tap column to insure powder is at the bottom
    b. Add 650 μl of H20
    c. Pipette vigorously till mixed.
    d. Vortex, both top and bottom
    e. Let sit at room temp for at least 2 hrs.
    f. Take off Top and Bottom cap
    g. Spin columns in throw away tubes provided for 2 min at 3000rpms
    h. Empty flow through, dab bottom membrane with gauze.
    i. Carefully pipette 20-50μL of cDNA into center of column, avoid the edges!
    j. Place in labeled 1.5 mL eppindorf tube, and position the column in previous orientation in centrifuge.
    k. Spin Columns for 2 min a 3000rpms
6. Dilute purified cDNA amplification.
    a. Make a series of 5 10:1 dilutions, this will dilute the cDNA ~10^6 times.
    b. Then make a series of 5, 2:1 dilutions.
7. Plate these 5 2:1 dilution along with No Template Controls (NTC)

A.6 Finding/Designing Primers for qPCR

Finding
http://www.ncbi.nlm.nih.gov/Genomes/index.html
search under locuslink

search under nucleotide
http://www.ncbi.nlm.nih.gov/entrez/query.fcgi?db=Nucleotide&itool=toolbar
Bovine [orgn] IL-1
Click on gene ID = #####

Look at CDS coding region

Making
Primer3: http://frodo.wi.mit.edu/cgi-bin/primer3/primer3_www.cgi
Paste sequence in window
Change Product size ranges to 80-120
Primer GC% 40 to 60;
Click Pick Primers
Check primer3 results, look at any, and 3'. Want low any and low 3'
Want low pair any comp, and low pair 3' comp.

Blast
http://www.ncbi.nlm.nih.gov/blast/Blast.cgi?CMD=Web&LAYOUT=TwoWindows&AUTO_FORMAT=Semiauto&PAGE=Nucleotides&NCBI_GI=yes&FILTER=L&HITLIST_SIZE=100&SHOW_OVERVIEW=yes&AUTO_FORMAT=yes&SHOW_LINKOUT=yes
Check forward Sequence given by Primer3
Check reverse transcribed reverse seq. given by Primer3
Check to see if other genes are coded by primer given

Alternatively, use Primer Express (Applied Biosystems) to design primers. With sequences obtained, ensure proper design through Blast.

Ordering
Use Integrated DNA Technologies, http://www.idtdna.com/Home/Home.aspx
Create User/Password

A.7 Primer Inventory

	Gene	Forward Sequence	Reverse Sequence	Slope	Offset
1	AGGRECAN	CCTGAACGACAAGACCATCGA	TGGCAAAGAAGTTGTCAGGCT	-0.912	27.560
2	COLLAGEN 1 *	AATTCCAAGGCCAAGAAGCATG	GGTAGCCATTTCCTTGGTGGTT	-1.151	27.880
3	COLLAGEN 2	AAGAAGGCTCTGCTCATCCAGG	TAGTCTTGCCCCACTTACCGGT	-0.912	23.960
4	COLLAGEN 9	AATTTGCCCTCCTTGTTCGA	CCTTTCCACGCCAATCAT	-1.018	20.284
5	COLLAGEN 11	CTGATGTGGCCTACCGAGTGT	AGCAGAGAGAAATCTTTGGGAAAA	-1.253	27.969
6	FIBROMODULIN	ACAACCAGCTGCAGAAGATCC	TTCATGACATCCACCACGGT	-1.222	30.260
7	FIBRONECTIN	ACTGCCCACTCCTACAACCA	CAAAGGCATGAAGCACTCAA	-1.051	32.001
8	DECORIN	GCTCCTTTGGTGAAATTGGA	ACACGCAGCTCCTGAAGAGT	-1.025	19.340
9	LINK PROTEIN	AAGCTGACCTACGACGAAGCG	CGCAACGGTCATATCCCAGA	-1.005	27.840
10	CD44	GTCCTATGCGGAAACCTCAA	CTGCCCACACCTTCTCCTAC	-0.998	21.830
11	HAS2	GCACATCTGGAAGGAAAACC	AAAATCACACCACCCAGGAG	-0.930	20.446
12	OSTEOCALCIN**	AGGGGTGAGTCTCATGCCAGTG	CCAAGGCAGATGTGAGAGCAGG	-0.910	21.594
13	COMP	GTGCCAGGGCGACTTTGAT	TCTCCGGACACACATCGATCT	-0.852	14.635
14	MMP-1	GGACTGTCCGGAAATGAGGATCT	TTGGAATGCTCAAGGCCCA	-1.057	35.590
15	MMP-3	CACTCAACCGAACGTGAAGCT	CGTACAGGAACTGAATGCCGT	-1.130	30.540
16	MMP-9	TCCCTTCCTTGTCAAGAGCAA	TACTTGGCGCCCAGAGAAGAA	-1.439	33.279
17	MMP-13	TCTTGTTGCTGCCCATGAGT	GGCTTTTGCCAGTGTAGGTGTA	-1.068	33.369
18	ADAMTS-1	CGACACAAGAGAGGAAAGATGG	CATCACTTTACCCGCTGCTAT	-0.961	17.019
19	ADAMTS-4	CTGGGCCATGTCTTCAGCAT	GGCGGGAGGTGCTCTCA	-1.041	25.001
20	ADAMTS-5	CTCCCATGACGATTCCAA	AATGCTGGTGAGGATGGAAG	-1.110	31.777
21	TIMP-1	TCCCTGGAACAGCATGAGTTC	TGTCGCTCTGCAGTTTGCA	-1.237	30.966
22	TIMP-2	CCAGAAGAAGAGCCTGAACCA	TGATGTTCTTCTCCGTGACCC	-1.210	32.170
23	TIMP-3	TTTGGCACGATGGTCTACACC	CCTCAAGCTTAAGGCCACAGA	-1.028	35.753
24	SOX-9	TGAAGAAGGAGAGCGAGGAG	GTCCAGTCGTAGCCCTTGAG	-1.127	25.149
25	C-FOS	CTCCACTTCATCCTAGCGGC	GCCCCCACTCAGATCAAGAG	-0.755	35.500
26	C-JUN	AGCTGGAGCGCCTAATCATACA	CCTCCTGCTCATCTGTCACGTT	-1.063	33.810
27	INOS	AGGAGATAGAAACAACAGGAACC	TGCCATCTGGCATCTGGTAGC	-1.354	23.676
28	18S	TCGAGGCCCTGTAATTGGAA	GCTATTGGAGCTGGAATTACCG	-1.104	22.970
29	6S*	TCGTGACTCCACGAGTTCTG	TGGCCTCCTTCATTCTCTTG	-1.111	31.614
30	G3PDH	ATCAAGAAGGTGGTGAAGCAGG	TGAGTGTCGCTGTTGAAGTCG	-1.073	27.173
31	B-ACTIN	GATGAGATTGGCATGGCTTT	GTCACCTTCACCGTTCCAGT	-0.800	25.000
32	IGF-1**	CAGCAGTCTTCCAACCCAAT	GAAGAGATGCGAGGAGGATG	-0.986	31.063
33	IGF-2	TTCTACTTCAGCCGACCATCC	TGGCACAGTAAGTCTCCAGCA	-1.089	23.144
34	OP-1	GGGCTTTTCCTACCCCTA	CACGAGATTGACGAAGCTCA	-0.909	21.984
35	BFGF	GCCATAATCGGAACAGCACT	AGGAATGCACTGTGGAGCTT	-0.730	15.857
36	TGFB	CACGTGGAGCTGTACCAGAA	ACGTCAAAGGACAGCCACTC	-0.859	31.834
37	VEGF	TCCCTGTGGGCCTTGCT	CGTCTGCGGATCTTGTACAAAC	-0.889	20.857
38	LIF	CAACATCACGAGAGACCAGAAG	TCTAGTTGGCACCACGTATAGG	-1.135	28.752
39	IL-1B	GAAGAGCTGCATCCAACACC	ATGCAGAACACCACTTCTCG	-1.037	24.609
40	IL-4	GCGGACTTGACAGGAATCTC	TTCAGCGTACTTGTGCTCGT	-0.862	21.817
41	IL-6**	TGAGTGTGAAAGCAGCAAGG	AGCAAATCGCCTGATTGAAC	-1.257	31.807
42	TNFA	ACGGTGTGAAGCTGGAAGAC	CCCTGAAGAGGACCTGTGAG	-1.237	30.316
43	IL-6R**	GCACACCCGTCGTATTCTTT	TGTCAGATTCAAGGCTGCTG	-0.887	15.482
44	COX-2	AAAAGCTGGGAAGCCTTTTC	GCTCTTTCCTCCCTTTCACA	-1.127	25.149
45	TXNIP	CAAGTTCGGCTTTGAGCTTC	GCTGGGACGATCAAGAAAAG	-0.930	22.290
46	LUBRICIN*	AGGAATGCACTGTGGAGCTT	GCCATAATCGGAACAGCACT		
47	HSP90	AAACTGTATGTCCGCCGTGT	AGATGTTCAGGGGGAGGTCT	-1.090	26.400
48	CASPASE-3	GAAGTCTGACTGGAAAACCC	GAAGTCTGCCTCAACTGGTA	-0.999	18.891
49	ALPL	CCATGGTGAGTGACACAGACAA	GGCCCGTTGCCGTACA	-1.010	15.511
50	SOD1	TGGAGACCTGGGCAATGTG	ACAATATCCACGATGGCAACAC	-0.794	19.215
51	SOD2	AGGTCGGTTCACTCGGAAAGA	GGCGGTCCCTCTCCAACTA	-0.871	18.620
52	GPX-3**	AGGGGTGAGTCTCATGCCAGTG	CCAAGGCAGATGTGAGAGCAGG	-1.130	14.267

* These primers were not used in this work

** These primers could be redesigned to improve efficiency

A.8 Bovine DNA Standard and Assay using Hoechst 33258 Dye

Material:

10x TEN Buffer located in 4° stock
1mg/mL Hoechst 33258 Dye (10,000x) located in 4° stock
Stock DNA solution at 10μg/ml located in -20° stock
Tris buffer at 50mM located in 4° stock

DNA Dye Solution Mixing Procedure:

- Add 45mL of DI H_2O and 5mL of 10x TEN buffer into a 50mL test tube
- Mix well and add 5μl of 1mg/mL of Hoechst 33258 dye into the 1x TEN buffer
- Mix well and wrap the test tube with aluminum foil to protect the dye from light. The dye will have a final concentration of 0.1μg/mL Hoechst 33258.

Procedure:

- Digest cartilage plugs in proteinase K solution
- Make up standard solutions using following chart:

Tube	DNA conc. μg/mL	Tris Buffer	DNA stock 10μg/mL
1	10	0 μl	200 μl
2	5	100 μl	100 μl
3	4	120 μl	80 μl
4	3	140 μl	60 μl
5	2	160 μl	40 μl
6	1	180 μl	20 μl
7	0	200 μl	0 μl

- Plate 20μl of each standard and 20μl of each sample into a microflour 2 black 96 well plate making sure to duplicate all samples including the standards using the template below. Plate standards in descending order of concentration.

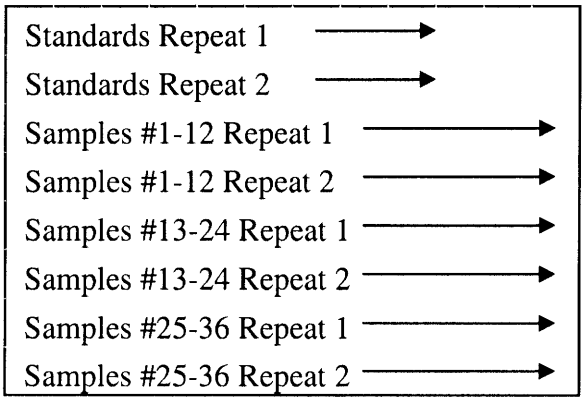

- Use 12-channel pipette to add 180µl of 0.1µg/mL Hoechst dye to each well
- Put plate in the Victor machine and select the DNA quantification protocol in the Victor software. Follow the on screen instructions to read plate.

Post Processing:

In order to process the raw data produced by this assay, a DNA standard curve must be made. DNA concentrations can then be calculated.

- Open the Microsoft Excel Template called 'MIT_Bovine_DNA_assay_template'
- Paste the raw data obtained from the Victor plate reader into the highlighted area in the 'Data Columns' tab
- Click on the 'DNA standard template' tab to view the standard curve
- Click on the 'DNA analysis' tab to view the concentration of DNA in each well as well as the average DNA concentration of the two repeats for each sample

A.9 GAG Standard and the GAG Assay with Maxy Machine

This is the general assay for sulfated GAGs (CS6, CS4, HS, KS). Chondroitin-6-sulfate is used as the standard because of its prevalence in articular cartilage.

Objective: DMMB Assay for GAG content

Material:

Tris buffer at 50mM located in 4° stock
GAG dye solution (DMMB Dye) located under bench 5
Stock GAG solution at 2mg/ml located in -20° stock

Procedure:

- Digest cartilage plugs in proteinase K solution
- Dilute samples so that GAG concentrations fall in the range of the standards
  - For digested bovine cartilage samples, dilute 1:40 in Tris buffer
  - For bovine media samples, dilute to 1:20 in Tris buffer
- Make up standard solutions using following chart:

Tube	Tris Buffer	Transfer	GAG conc. µg/ml
1	900µl	100 µl of 2mg/ml stock solution	200 µg/ml
2	100µl	100 µl from tube 1	100 µg/ml
3	100µl	100 µl from tube 2	50 µg/ml
4	100µl	100 µl from tube 3	25 µg/ml
5	100µl	100 µl from tube 4	12.5 µg/ml
6	100µl	100 µl from tube 5	6.25 µg/ml
7	100µl	100 µl from tube 6	3.125 µg/ml
8	100µl	100 µl from tube 7	1.5625 µg/ml
9	100µl	0	0 µg/ml

- Plate 20µl of each standard and 20µl of each sample into each well making sure to duplicate all samples including the standards using the template below. Plate standards in descending order:

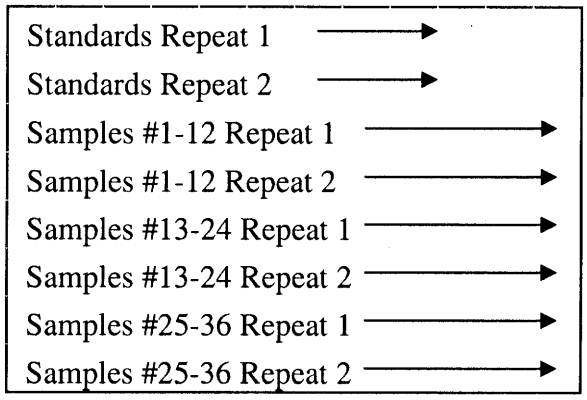

- Use 12-channel pipette to add 180µl of DMMB dye to each well
- Turn on the Molecular Devices Kinetic Microplate Reader machine
- Select 520nm wavelength for reading
- Load plate and click "Read Plate"

Post Processing:

In order to process the raw data produced by this assay, a GAG standard curve must be made. GAG concentrations can then be calculated.

- Open the Microsoft Excel Template called 'MIT_GAG_assay_template'
- Paste the raw data obtained from the Kinetic Microplate Reader into the highlighted area in the 'Data Columns' tab
- Click on the 'GAG standard template' tab to view the standard curve
- Click on the 'GAG analysis' tab to view the concentration of GAG in each well as well as the average GAG concentration of the two repeats for each sample

A.10 Human DNA Standard and Assay using CyQUANT Dye

Material:

Molecular Probes CyQUANT Cell Proliferation Assay Kit located in -20° stock which contains:

- CyQUANT GR Dye (Component A) at 400x
- Cell-lysis buffer (Component B) at 20x
- λ DNA standard (Component C) at 100μg/mL

DNAse free H_2O located in 4°

DNAse located in -20° stock

DNAse Pretreatment

In order to correct for the presence of RNA in the cell, samples that have been treated with DNAse will also be analyzed.

- Remove 50μl of each sample into 2ml 12-tube strips
- Add 3μl of DNAse to each sample
- Incubate at room temperature for one hour

DNA Dye Solution Mixing and λ DNA Preparation Procedure:

- Calculate the volume of CyQUANT GR/Lysis Buffer that will be needed by multiplying the number of samples to be tested by 800μl, then adding 3mL for standards. 800μl of the buffer/dye solution is allotted for each sample because each sample must be tested 4 times: 2 repeats of the sample treated with DNAse, and two repeats of untreated sample.
- Using this volume, dilute the cell-lysis buffer (Component B) 20-fold in DNAse free H_2O
- Make a 400 to 1 dilution of the CyQUANT GR Dye (Component A) in the 1x cell-lysis Buffer
- 1.5mL of 1μg/mL λ DNA will be needed for the standard curve. Place 1.485mL of 1x CyQUANT GR/Lysis Buffer solution into a 2mL tube.
- Add 15μl of λ DNA standard (Component C) at 100μg/mL. The final concentration of DNA will be 1μg/mL

DNA Standard Curve and Assay Procedure:

- Make up standard solutions in the first two rows of a microflour 2 black 96 well plate using following chart:

Well Num	CyQUANT GR/Lysis Buffer (µl)	1µg/mL DNA in CyQUANT GR/Lysis Buffer (µl)	Final DNA Concentration (ng/mL)
1	0	200	1000
2	40	160	800
3	80	120	600
4	120	80	400
5	160	40	200
6	180	20	100
7	190	10	50
8	198	2	10
9	200	0	0

- Duplicate all standards using the template below.
- Once the DNAse treated samples have been incubation for one hour, plate 20µl of each sample into the microflour 2 black 96 well plate making sure to duplicate all samples, using the template below. More samples can be added to additional plates using the same pattern.

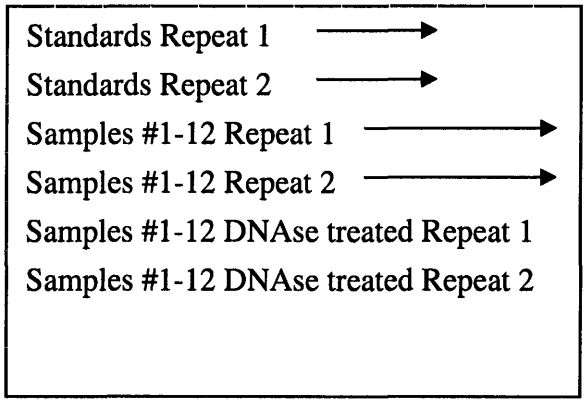

- Use 12-channel pipette to add 180µl of 1x CyQUANT GR/Lysis Buffer solution to each well
- Put plate in the Victor machine and select the CyQUANT protocol in the Victor software. Follow the on screen instructions to read plate.

A.11 Radiolabel Scintillation Counting Using Microbeta Plate Reader

Material:

Perkin Elmer Optiphase Supermix Scintillation fluid located under bench 5
Optically clear plastic film located under Microbeta machine
Disposable 24 well flexible plates located above Microbeta Machine

Procedure:

Preparing Samples

- Use clear 24 well disposable flexible plates. Plates are in boxes on the shelf above the Microbeta machine
- Pipette 50-100µl of each sample and standard into wells. The amount of sample plated is dependant on the volume of proteinases K solution used to digest the samples. If 1mL was used, plate 100ul of each sample. If 500uL of proteinases K was used, plate 50ul. A volume of 50uL should always be used for standards. Duplicate each sample and standard in alternating rows, e.g., plate one set of samples in rows A and C and the next set in rows B and D like in the following figure:

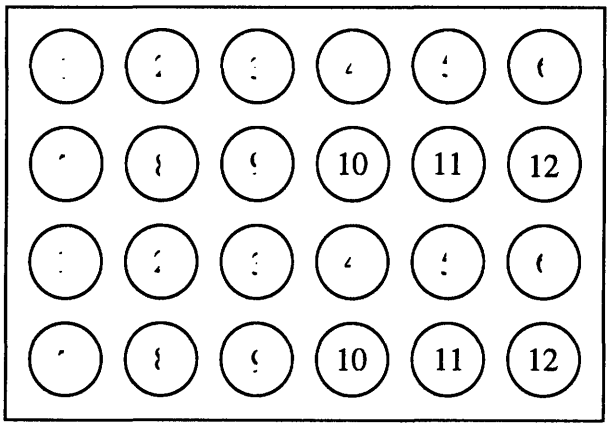

Samples #1-6 Repeat 1

Samples #7-12 Repeat 1

Samples #1-6 Repeat 2

Samples #7-12 Repeat 2

- Pipette 1mL scintillation fluid into each well using a repeating pipette. Be sure not to spill fluid on the black part of the plate.
- Cover plate with optically clear plastic film and seal with the roller. Run over the boarders of each well with a spatula to ensure the wells are sealed.
- Shake all plates on the orbital shaker for 5-10 minutes, or until scintillation fluid is homogenous
- Load flexible plates into white plate cassettes. These can be found in the drawer under the Microbeta machine
- Place cassettes into the machine. The Microbeta machine can hold a maximum of 15 plates. Place a "STOP" cassette above the last plate if reading fewer than 15 plates.

Reading Plates

- Start Microbeta Windows Workstation
- Choose protocol group "General" and click "Open"
- Choose the protocol you wish to use, e.g., "n Adjusted Dual Label"
- Click "Protocol" under the "Edit" heading to edit the count time
- Click "Plate map…" to view and edit the order the wells will be reported
- Click "Output" to change what will be included in the output file and to create a new output file
- Click "Start…" A window will appear that will let you select which shelf to start counting on. The machine will start at this shelf and continue until it hits the "STOP" plate.
- Click on "Live Display" to view the counting progress

Appendix B: Nitric Oxide Project

Nitric oxide enhances aggrecan degradation by aggrecanase in response to TNF-α but not IL-1β treatment at a post-transcriptional level in bovine cartilage explants. *

* This chapter has appeared as a paper in Osteoarthritis and Cartilage (Stevens AL, Wheeler CA, Tannenbaum SR, Grodzinsky AJ. Nitric oxide enhances aggrecan degradation by aggrecanase in response to TNF-alpha but not IL-1beta treatment at a post-transcriptional level in bovine cartilage explants. Osteoarthritis Cartilage. 2007 Oct 9)

Abstract

Objective: The objective of this study was to determine the role of NO in TNF-α–induced matrix damage, compared to IL-1β, in bovine cartilage explant cultures.

Methods: Cartilage explants were subjected to treatment with TNF-α (100 ng/ml), IL-1β (10 ng/ml) and to the nitric oxide synthase inhibitor, N-methylarginine (L-NMA; 1.25 mM) for 26, 50 or 120 hours (5 days). The collected medium was analyzed for sGAG, nitrate and nitrite, MMP activity by zymography, and aggrecan degradation by immunoblotting of aggrecan G1 and aggrecan-G1-NITEGE fragments. RNA was extracted from the 26 and 50 hour treated explants for real-time PCR analyses.

Results: TNF-α and IL-1β treatment caused a 3-5 fold increase in sGAG release with an increase in aggrecanase specific aggrecan breakdown and an increase in nitrate and nitrite production. L-NMA treatment inhibited almost 50% of the sGAG release caused by TNF-α treatment, with concomitant decrease in the aggrecanase-specific-NITEGE neo-epitope of aggrecan released into the medium. No L-NMA effect was identified with IL-1β. TNF-α and IL-1β both increased ADAMTS4 and ADAMTS5 transcription with no effect by L-NMA, suggesting that nitric oxide regulates aggrecanase activity at a post-transcriptional level in response to TNF-α. TNF-α and IL-1β both caused an increase in protease transcription (MMP3, MMP13, ADAMTS4 and ADAMTS5) and in pro-inflammatory enzymes iNOS and COX2, as well as a decrease in matrix protein transcription, including collagen II, aggrecan, fibromodulin and link, protein (IL-1β only), and an increase MMP-3 and MMP-9 secretion. L-NMA had no effect on gene transcription or MMP secretion.

Conclusion: Nitric oxide regulates aggrecanase activity at a post-transcriptional level in response to TNF-α treatment while having no effect on IL-1β treated cartilage explants.

Introduction

Nitric oxide (NO) is a neutral free radical product of nitric oxide synthase (NOS) with potent biological effects through its actions on cGMP production as well as through various oxidative and nitrosative chemistries that have been shown to modulate gene expression and to alter protein structure and function [1]. NO production by chondrocytes was first discovered by Stadler et al. who showed that, in vitro, chondrocytes produce substantial amounts of NO in response to interleukin 1 beta (IL-1β) and to lipopolysaccharide (LPS) [2]. Since these first reports, numerous studies have shown that chondrocytes or cartilage explant cultures from most species produce NO via inducible nitric oxide synthase (iNOS) in response to IL-1β, IL-1α, LPS, and tumor necrosis factor alpha (TNF-α) [3, 4], as well as IL-17, IL-18, interleukin 1 converting enzyme (ICE), and fibronectin fragments [5-7].

The inflammatory cytokines TNF-α and IL-1 contribute to disease processes in rheumatoid arthritis (RA) and likely in osteoarthritis (OA). TNF-α was identified in synovial exudates of RA and OA joints [8, 9]. In RA patients, TNF-α may contribute to IL-1 production as determined by anti-TNF-α therapy [10], and TNF-α alone or in combination with IL-1 may cause cartilage breakdown and a decrease in new matrix synthesis by chondrocytes *in vitro* [11]. TNF-α production by OA synovial cells and in synovial fluid and serum may be elevated in OA [10, 12, 13], and OA cartilage explants may be more sensitive to IL-1 and TNF-α treatment [14-16]. TNF-α receptor, TNF-R p55, is elevated in chondrocytes near OA lesions, and this expression correlates with sGAG depletion [17]. These data together suggest that TNF-α as well as IL-1 may play a role in cartilage breakdown in OA.

To determine whether NO production plays a role in mediating the pro-catabolic and anti-anabolic effects of inflammatory mediators, *in vitro* studies have used the NOS inhibitors, L-NMA (L-N-methyl-arginine), N_{ω}-nitro-L-arginine methyl ester (L-NAME), aminoguanidine, and L-NIO (N-iminoethyl-L-ornithine), to evaluate the role of NO in IL-1-induced changes in chondrocyte metabolism and matrix degradation in explant, hydrogel, and monolayer culture. With the exception of bovine explant studies [18], inhibiting NOS partially reversed IL-1-induced inhibition of proteoglycan synthesis in cartilage explants or chondrocyte cultures [4, 19, 20]. TNF-α can decrease proteoglycan synthesis in a NO dependent manner [21], and the exogenous NO donor, SNAP, may also decrease proteoglycan synthesis. Cao et al. found that NO decreased collagen synthesis[22]. Studies on matrix degradation have shown that inhibiting NO production may enhance [18, 23, 24] or have no effect [25] on IL-1β-induced aggrecan degradation as measured by sGAG release. IL-1-induced NO was also found to enhance gelatinase [2, 26, 27] and alter stromelysin (MMP-3) [18, 26] expression or activity. While most studies on inhibition of NOS are associated with IL-1 treatment, other inflammatory cytokines, such as TNF-α, are capable of mediating cartilage damage and enhancing NO production. Thus, understanding the contributions of NO with other cytokines may be important in determining their role in cartilage degradation.

The purpose of this study was to characterize the role of NO in matrix degradation in response to TNF-α and compare it to the effects of NO following IL-1β treatment using a non-specific NOS inhibitor, N-methylarginine (L-NMA). We found that inhibition of NOS by L-NMA decreased sGAG release in response to TNF-α by almost 50%, with a concomitant decrease in release of aggrecan-G1-NITEGE fragments specific for aggrecanase-mediated aggrecan degradation. No L-NMA effect was seen with IL-1β treatment. L-NMA did not alter

ADAMTS4 or ADAMTS5 transcription in response to cytokine treatment. Gene transcription profiling of a panel of inflammatory molecules, proteases, and matrix proteins showed that TNF-α and IL-1β both inhibited transcription of matrix proteins including collagen II, aggrecan, link protein, and fibromodulin, while enhancing matrix proteases and inflammatory factors such as MMP-3, MMP-13, iNOS, and COX2, all with no effect of L-NMA. Overall these data suggest that NO plays a role in TNF-α–induced aggrecan release at a post-transcriptional level by altering ADAMTS4 or ADAMTS5 protein expression or post-translational modification, and that TNF-α and IL-1β appear to promote aggrecan degradation through different mechanisms of aggrecanase regulation.

Methods

Reagents: ITS medium supplement and NOS inhibitor, N-methyl-arginine, were from Sigma (St Louis, MI). Recombinant human IL-1β and TNF–α were from R&D systems (Minneapolis, MN), PAGE gels were from BioRad (Hercules, CA). Protease-free chondroitinase and keratanase II were from Seikagaku (Japan). Common chemicals were purchased from ICN, Mallenkrodt, or Sigma.

Cartilage explant harvest and culture: Articular cartilage disks were obtained from the patello-femoral groove of 1-2 week old bovine calves as described previously [28]. Cartilage-bone cylinders (9-mm-diameter) were cored from the patello-femoral groove, perpendicular to the joint surface. Two 1-mm-thick slices were then microtomed from the middle zone and a 6-mm diameter dermal punch was then used to core a 6-mm diameter by 1-mm thick disk from the center of each of the 9-mm slice. The explants were cultured in high glucose DMEM with 1% ITS as described previously with medium change every other day prior to treatment [29]. Explants were weighed two days prior to the start of cytokine treatment.

TNF–α, IL-1β, and L-NMA treatments: Cartilage explants were allowed to rest 7 days in culture, and were then treated with 10 ng/ml IL-1β or 100 ng/ml TNF–α or left untreated in 2 ml of medium without 1% ITS. After 2 hours, half the explants were further treated with 1.25 mM L-NMA. Experiments utilized 5-8 different joints (5-8 different animals) with at least two explants per joint per condition. Every 24 hours over 5 days, cultures underwent a 10% (200 µl) medium removal and supplementation. After day 5 of treatment, medium and explants were collected, pooled to each treatment group, and stored at -80 °C. For real time PCR analyses explants were cultured for 24 or 48 hours after the addition of L-NMA and snap frozen in liquid nitrogen.

Sulfated Glycosaminoglycan (sGAG) Assay: sGAG released to the medium was measured as an indicator of aggrecan degradation and assessed via the dimethylmethylene blue (DMMB) assay using shark chondroitin C as a standard, as described previously [30].

Nitrate/Nitrite Analysis: Medium samples were diluted 1:2 in water prior to nitrate and nitrite analysis by Griess assay [31]. Total nitrogen oxides were determined by cadmium column reduction of nitrate to nitrite followed by direct nitrite detection by Griess reaction. Nitrite was assayed directly, and nitrate was calculated as the difference between the total nitrogen oxides and nitrite.

Gelatin and Casein Zymography for MMPs: Zymograms were performed as described [32]. Briefly, conditioned medium from day 5 was mixed with 4X non-reducing SDS-sample buffer and electrophoresed in 10%/12% gelatin or casein zymogram gels. Proteases were renatured in 2.5% triton X-100 solution, and placed in solution of 50 mM Tris and 5 mM $CaCl_2$ for 18 hours at 37°C. Gels were then fixed and stained with Coomassie brilliant blue and

destained until bands became visible and distinct. EDTA was added to the incubation buffer to verify MMP activity. MMP-3 and MMP-9 were verified by immunoblot.

Desalting and deglycosylation: Samples were desalted by ethanol precipitation or by dialysis with deglycosylation. The medium equivalent of 10-20 μg sGAG was precipitated by the addition of 3 volumes of ice-cold ethanol. The samples were resuspended (50 mM Tris-Acetate, 10mM EDTA) and sequentially deglycosylated beginning with 5 mU of protease-free chondroitinase ABC for three hours followed by 0.1 mU of keratanase II and 0.1 mU of endo-β-galactosidase for an additional four hours. Equal amounts of sGAG were loaded for aggrecan western blots.

Western blot analysis. Concentrated samples (10-15 μl) were subjected to denaturing SDS-PAGE on a 4-15% gradient gel run at 15 mA for 2 hours. Proteins were then transferred to Immobilon (PVDF) membrane, and proteins were detected using a monoclonal antibody to the aggrecan-NITEGE neoepitope in the interglobular domain of aggrecan associated with aggrecanase degradation (from C. Flannery, Wyeth Pharmaceuticals).

RNA extraction and real time PCR: For each condition (untreated, L-NMA, TNF-α ±, L-NMA, IL-1β ± L-NMA), 2-3 cartilage explants per condition per joint, from a total of 8 joints (8 animals) were taken at 26 and 50 hours of culture, pulverized under liquid nitrogen and homogenized in Trizol (Invitrogen, San Diego,CA). As described previously [33], homogenates were transferred to Phase Gel tubes according to the manufacturer's instructions (Eppendorf, Hamburg, Germany) and spun at 10,000 rpm for 10 minutes at 4°C. The clear RNA containing supernatant was removed from Phase Gel tubes and subjected to RNAeasy mini-kit clean-up (Qiagen, Chatsworth, CA) according to manufacturer's instructions. RNA quantification was determined by nano-drop method measuring absorbance at 260 nm and 280 nm, which gave the

concentration of RNA extracted from the tissue and the purity of the extract; the average 260/280 absorbance ratio for all samples was 2.12 ± 0.1. Equal amounts of RNA were subjected to reverse transcription using AmpliTaq-Gold reverse transcription kit (ABI, Foster City, CA) to generate cDNA for real time PCR analysis. Real time PCR analysis was performed with Applied Biosystems SYBR-Green master mix in combination with cDNA and primers, using the ABI prism 7900HT real time 384-well plate PCR instrument. Both forward and reverse primers were designed using Primer3 software based on the bovine genomic sequence [33]. Primers from 32 genes relevant to cartilage homeostasis were used: 18S-RNA, aggrecan, collagen II, fibromodulin, fibronectin, proteoglycan link protein, MMP1, MMP3, MMP9, MMP13, ADAMTS4, ADAMTS5, TIMP1, TIMP2, TIMP3, COX2, iNOS, G3PDH, β-actin, IGF-1, IGF2, TGF-β, TNF-α, IL-1β, IL-4, IL-6, TXNIP, HSP90, CD44, HAS2, bFGF, and OP-1. Standard curve analysis was performed on each primer to determine the efficiency of amplification and proper primer concentration. The measured cycle threshold (CT) was determined and converted to relative copy number using information from standard curves for comparisons.

Data analysis and statistics: Real time PCR data for each gene were first normalized to 18S-RNA; data from each sample were then normalized to the untreated control sample within each sample set (animal), and these normalized data were pooled across all animals and are reported as the mean +/- SEM (n=8) for each condition. Principal component analysis and k-means clustering were performed on the PCR data using components of the Matlab Statistics toolbox [33]. Cluster analysis was performed[33] on a (31 x 5 x 2) matrix of data derived from the set of 31 genes (i.e., all genes but 18S), 5 treatment conditions (each normalized to untreated control), and 2 time points (26 or 50 hrs). Each time point was also clustered individually to test the robustness of the co-expressed gene groupings. The Kruskal-Wallis test and Wilcoxon sign-

rank test with Bonferroni correction for multiple comparisons were used to determine statistical significance of the L-NMA effect and of pair-wise comparisons between treatments, respectively. For the sGAG and nitrate/nitrite assays, multi-way ANOVA followed by a post-hoc Student's t-test with Bonferroni correction for multiple comparisons were used to determine statistical significance defined as $p < 0.05$. All statistical analyses were performed using Matlab (Natick, MA) or Systat 11 (Richmond, CA).

Results

Nitrate/Nitrite: Nitrite and total nitrate plus nitrite were determined by the Griess assay as described by Green et al. [31]. IL-1β and TNF–α both increased accumulated nitrate and nitrite compared to the untreated control ($p < 0.001$) (Figure 1). The relative amounts of nitrite and nitrate were similar between the two cytokine treatments by day 5 (data not shown). Treatment of samples with L-NMA inhibited NO production to levels at or near untreated controls.

Sulfated glycosaminoglycan release: sGAG loss, which is known to be predominantly the result of aggrecan degradation in cartilage explants, was measured by DMMB assay. TNF–α and IL-1β caused 3-4 fold increase in sGAG release to the medium compared to control samples (Figure 2; $p<0.001$ for TNF-α and IL-1β compared to controls at all time points). Treatment with L-NMA partially inhibited TNF–α induced sGAG release ($p<0.003$, all time points). However with the exception of the 24-hour time point, L-NMA had no effect on IL-1β-induced sGAG release ($p = 0.015$ first 24 hours; $p > 0.745$ for all other points). No L-NMA effect was seen in the absence of cytokine treatment. These results suggest that NO was partially responsible for sGAG release in response to TNF–α treatment, but had little or no effect on IL-1β treatment.

Western analysis for aggrecanase generated aggrecan-G1 neo-epitope: To investigate whether L-NMA was able to decrease sGAG release by decreasing aggrecanase mediated

proteolysis of aggrecan, immunoblots were performed to probe for the aggrecan-NITEGE-COOH neoepitope generated by aggrecanase activity (Figure 3). A 60-80 kDa band was visible in the TNF-α and IL-1β treated lanes but not in the untreated (control) lanes of the immunoblot. While the addition of L-NMA to IL-1β treatment had no effect on the anti-NITEGE-stained band, samples treated with TNF–α and L-NMA showed a marked decrease compared to the sample treated with TNF-α alone. This result suggests that the decrease in sGAG release seen with the addition of L-NMA to TNF–α treatment was related to decreased aggrecanase-specific proteolysis of aggrecan.

Zymography for Metalloproteinase Measurements: To examine MMP expression and activity, zymography was performed on medium samples at the end of the experiment. Samples subjected to IL-1β treatment and, to a lesser extent, TNF-α treatment showed a diffuse clearing containing a doublet between 50 kDa and 75 kDa (with the lower band most prominent) by casein zymography (Figure 4A), representing secreted pro-MMP-3. No activated MMP-3 band (at 45 kDa) was visible in any of the samples. Gelatin zymography (Figure 4B) demonstrated two bands running in between 75 kDa and 50 kDa in all samples, which represent the pro- and the active forms of MMP-2. In addition, a ~90 kDa band indicative of pro-MMP-9 was present only in the cytokine treated samples. No differences in MMP-2, MMP-3, or MMP-9 were seen with L-NMA treatment, as assessed by zymography.

Real time PCR analyses: To determined whether cytokine ± L-NMA treatments altered transcription of aggrecanases, other proteases, matrix molecules, cytokines, and growth factors, real time PCR analysis of a 32-gene set was performed on explants from 8 different animals subjected to 26 and 50 hours of IL-1β or TNF-α treatment ± L-NMA, or L-NMA alone. Relative copy numbers were normalized to 18S-RNA and expressed in terms of the fold increase or

decrease compared to untreated control samples within each set. Expression of both ADAMTS4 and ADAMTS5 was elevated in response to TNF-α and IL-1β treatment (though little increase at 50 hours for ADAMTS5), with no statistically significant effect of added L-NMA at either the 26 hour or the 50 hour time point (Figure 5A). To elucidate the main expression patterns and identify groups of genes co-expressed under different treatment conditions, gene clustering was performed. The results are shown in principal component space (Figure 6); the first three principal components accounted for ~95% of the variance in the data. K-means clustering (31 genes, 5 normalized conditions, 2 time points) showed that the genes segregated well into two spatially distinct groups with group centroids as indicated (Figure 6). The centroid profiles (showing each condition for each group) are represented in Figure 5B,C as the mean ± SEM of each centroid. Group 1 genes (Figure 5B) had little response or were slightly down regulated by IL-1β and TNF-α treatment, while Group 2 genes were up regulated by IL-1β and TNF-α (Figure 5C). For each individual gene in Groups 1 and 2, the average-fold-change ± SEM is listed in Table 1 (with TNF-α and IL-1β each compared to control, TNF-α compared to TNF-α + L-NMA, and IL-1β compared to IL-1β + L-NMA); asterisks represent statistical significance for the comparison ($p<0.05$). While addition of L-NMA often slightly decreased gene transcription compared to IL-1β or TNF-α alone, this decrease was not statistically significant for any individual gene.

Discussion

IL-1β and, to a lesser extent, TNF–α, can induce chondrocyte-mediated matrix degradation, with loss of aggrecan typically preceding collagen degradation [34]. Previous studies explored the role of NO in IL-1β–induced aggrecan degradation; however, to our knowledge, this is the first study to test the effect of NO on TNF-α–induced sGAG release and to explore its

underlying mechanism. Cartilage explants treated with the NOS inhibitor, L-NMA, showed marked inhibition of TNF–α–induced sGAG release and concomitant production of aggrecan G1-NITEGE fragments, indicating a decrease in aggrecan proteolysis by aggrecanase. In contrast, L-NMA did not alter IL-1β–induced sGAG release or the generation of aggrecan-G1-NITEGE fragments. Real time PCR analyses showed no significant effect of L-NMA alone on expression of ADAMTS4 or ADAMTS5 or a panel of 30 other matrix genes, proteases and cytokines. Together, these results suggest that NO plays a role in the post-transcriptional regulation of aggrecanases in response to TNF-α, while NO has no effect on IL-1β induced aggrecan degradation. Thus, TNF-α and IL-1β utilize different pathways of expression or activation of aggrecanases to mediate aggrecanolysis, with that of TNF-α being regulated in part by an NO mediated post-transcriptional processing of ADAMTS4 and ADAMTS5.

NO can mediate its effects through enhancing cGMP, increasing protein nitrosation or protein nitration which may serve as an important regulatory mechanism at the level of the cell or individual proteins. NO concentration and chemistry, which depends in part of oxygen free radicals, may determine its role as a second signal mediator. Treatment of cartilage with cytokines caused an increase in NO production (Figure 1, $p<0.001$ for IL-1β and TNF-α vs. control for both nitrate and nitrite). In addition, TNF–α or IL-1β resulted in similar amounts of nitrate and nitrite, each corresponding to approximately half of the NO production, suggesting that NO chemistry was similar for both cytokine treatments. L-NMA decreased NO to control levels for both cytokines (cytokine + L-NMA vs. control not significant). Equal nitrate and nitrite production with both TNF-α and IL-1β treatment suggests that the effects of NO likely depend on cellular processes induced with each cytokine treatment and not NO chemistry.

The role of NO in matrix degradation associated with TNF-α may be quite different than that with IL-1β. In this study, L-NMA treatment inhibited TNF-α–induced sGAG loss by ~50% (Figure 2). While we know of no previous reports of the effects of NO treatment with TNF-α alone, van Bezooijen et al. [35] showed no measurable effect of L-NMA on cartilage damage induced by the combination of TNF-α and IL-17, compared to the cytokine combination alone as assessed by Alcian blue staining for sGAG. We found that L-NMA had no effect on sGAG loss following IL-1β treatment (Figure 2), similar to the findings of Bird et al.[25] using equine cartilage explants. In contrast, Stefanovic-Racic found that L-NMA in the presence of IL-1β significantly increased sGAG release compared to IL-1β alone, using bovine, human, and rabbit explants[18, 23]. Regarding other matrix degrading signals, Pichika et al. [36] showed that inhibiting NO resulted in a matrix protective effect when cartilage was treated with fibronectin fragments, similar to the effect seen with TNF-α (Figure 2). The effects of NO appear to depend on the cytokines or other signals with which it is produced and with which it signals. NO appears to play a distinctly degradative role in TNF-α (but not in IL-1β) treated cartilage.

Because aggrecanases are known to mediate aggrecan degradation in response IL-1β and TNF-α [37, 38], we hypothesized that the mechanism of L-NMA inhibition of TNF–α-induced sGAG release was through a decrease in aggrecanase cleavage of aggrecan at the Glu^{373}-Ala^{374} site in the interglobular domain [37, 39]. Immunoblot analysis of the medium using an antibody to the aggrecan-$NITEGE^{373}$ fragment showed that L-NMA + TNF-α resulted in less fragment release than TNF-α alone (Figure 3), consistent with decreased sGAG release (Figure 2). And while L-NMA did not alter sGAG release induced by IL-1β, there was no decrease in aggrecan-$NITEGE^{373}$ fragment release either. These results suggest that NO is partially responsible for TNF-α–induced aggrecanase activity in cartilage explants.

While aggrecanases are the main mediator of aggrecanolysis early in response to IL-1β and TNF-α treatment, NO has also been implicated in activation of MMPs through the disruption of the cysteine switch present in the zymogens[40]. Therefore, zymography was used to evaluate the effects of L-NMA on expression and activation of selected MMPs in response to cytokine treatment. IL-1β (and to a lesser extent, TNF-α) increased pro-MMP-3 secretion to the medium with no effect of L-NMA on activation or secretion (Figure 4A). Pro-MMP-9 was expressed in response to cytokine treatment, while MMP-2 was present under all conditions. L-NMA had no effect on MMP-2 or MMP-9 secretion or activation. MMP-3 and MMP-9 protein in the medium correlated well with the gene expression data (Figure 5,6; Table 1). These zymography results were also similar to those of Dozin et al.[41], who saw no effect of NOS inhibition on MMPs with chondrocyte monolayers treated with IL-1α and TNF-α in combination. Zymography failed to show evidence of an active MMP-3 band and no effect of L-NMA was observed, suggesting NO mediates aggrecan degradation in response to TNF-α by enhancing aggrecanase and not MMP-3 activity.

While ADAMTS1, 8, 9, 15, 16, and 18 have aggrecanase activity[42, 43], only ADAMTS4 and 5 are known to potently cleave the Glu^{373}-Ala^{374} site forming the aggrecan-NITEGE fragment[44]. We thus focused on ADAMTS4 and ADAMTS5 to explore the possible mechanism by which NO may be mediating an increase in aggrecanase activity. Because ADAMTS4 and ADAMTS5 proteins could not be reliably identified in tissue or medium samples (data not shown), we examined the effects of NO inhibition on gene expression of ADAMTS4 and 5 as well as a panel of genes associated with cartilage homeostasis (Table 1). We hypothesized that changes in expression of aggrecanases in response to cytokine and L-NMA treatments would likely occur approximately 24 hours before sGAG release to the medium, allowing time for

protein expression and diffusion of aggrecan fragments out of the tissue. Since the rate of sGAG release was maximal between days 2 and 4 of treatment (Figure 2), real time PCR analysis was performed on explants at 26 and 50 hours after treatment with IL-1β or TNF-α ± L-NMA. While IL-1β and TNF-α treatment caused significant changes in gene expression of many of the genes tested including ADAMTS4 and ADAMTS5 (Figure 5, Table 1), L-NMA treatment did not alter transcription of any genes evaluated in this study at either 26 or 50 hours.

Previous studies using young bovine explants showed significant increases in transcription of ADAMTS4 after 24 hours of treatment with IL-1α [45] and IL-1β [46], while ADAMTS5 was up-regulated by TNF-α [46]. Here, we observed a strong increase in ADAMTS5 expression with TNF-α and IL-1β at 26 hours but little increase at 50 hours (Figure 5A). In contrast, ADAMTS4 showed a sustained increase in expression at 26 and 50 hours with both IL-1β and TNF-α (Figure 5A). Interestingly, while TNF-α caused a greater average increase in ADAMTS4 and 5 transcription than IL-1β (Table 1), IL-1β treatment resulted in greater sGAG release. In addition, L-NMA did not significantly alter transcription of either ADAMTS4 or 5 in response to either cytokine treatment. Thus, the NO mediated regulation of ADAMTS4 and/or 5 activity in response to TNF-α is likely post-transcriptional and may be at the level of either translation or post-translational modification such as proteolysis[45]. ADAMTS4 and 5 do undergo proteolysis, which is known to change its binding affinity and proteolytic specificity of aggrecan cleavage sites [44, 45, 47]. Although less is known about ADAMTS5, some work on ADAMTS4 suggests that its activity may be regulated in part through a combination of proteolysis and/or protein-protein interactions rather than by protein expression[45, 48, 49]. Further work to explore the role of NO in modulating possible ADAMTS4 activators or inhibitors may be warranted. While it is possible that NO could play a more direct role in ADAMTS4 and/or 5

activity through direct chemical modification, this would still require a difference in ADAMTS4 and 5 protein expression between TNF-α and IL-1β in order to explain a TNF-α specific NO effect. But based on our findings, changes in aggrecanase transcription cannot account for the effects of L-NMA on TNF-α induced aggrecan degradation or the differential effects of L-NMA between IL-1β and TNF-α.

While previous studies have not reported changes in expression via qPCR for the broad panel of genes examined here (Table 1), we note several useful comparisons. Sasaki et al. reported a NO dependent increase in bFGF and MMP-9 gene expression by rabbit chondrocytes in monolayer in response to IL-1β[50]. While we did find an increase in the mean transcription level of bFGF and MMP-9 at 26 and 50 hours with TNF-α and IL-1β (not statistically significant), no L-NMA effect was observed. In the present study, inducible nitric oxide synthase (iNOS), responsible for chondrocyte production of NO, was elevated in response to both IL-1β and TNF-α ($p<0.05$), as was COX-2, MMP-3, and MMP-13 but not IL-6 or MMP-1. With the exception of IL-6 and MMP-1, these findings were consistent with the reported effects of IL-1β on human chondrocytes[51] and effects on MMPs in human OA cartilage using TNF-α and IL-1β receptor inhibitors[52] as well as equine cartilage in response to TNF-α[53]. Decreases in matrix geme expression (e.g., collagen II, aggrecan, fibromodulin, and link protein) were more pronounced at 50 hours than 26 hours suggesting that effects of IL-1β and TNF-α on matrix gene expression may occur later compared to the up regulation of matrix degrading enzymes[54] ($p<0.05$ TNF-α and IL-1β compared to control for collagen alpha 1(II), aggrecan, fibromodulin, and link protein (IL-1 only) at 50 hrs). The inhibitory effect of IL-1β and TNF-α on aggrecan and collagen synthesis is well characterized.

In summary, NO plays an enhancing role in TNF-α (but not IL-1β) induced aggrecanase-mediated aggrecan degradation. Inhibiting NO production with L-NMA caused no changes in ADAMTS4 or ADAMTS5 gene transcription; however, L-NMA partially inhibited aggrecanase-mediated aggrecan degradation in response to TNF-α suggesting that NO must play a role in regulating aggrecanases at a post-transcriptional level. At the same time, inhibiting NOS had no detectable effects on IL-1β or TNF-α induced MMP expression, activation, or the gene expression of various other matrix proteins, cytokines or growth factors after 26 or 50 hours of cytokine treatment. IL-1β and TNF-α–enhanced transcription of inflammatory genes such as iNOS and COX2 as well as matrix degrading enzymes MMP-3 and MMP-13 at 26 hours, and both cytokines decreased collagen II, aggrecan, link protein and fibromodulin at 50 hours, consistent with known effects of these cytokines and with no effect of L-NMA. These findings support the hypothesis of a post-transcriptional role for NO in regulating aggrecanase activity in response to TNF-α treatment, and the hypothesis that TNF-α and IL-1β regulate aggrecanase activity though different mechanisms.

Acknowledgements:

We thank J. Glogowski for technical assistance with the nitrate/nitrite analysis, and Dr. Carl Flannery for the aggrecan-G1-NITEGE neo-epitope antibody and ADAMTS4 and ADAMTS5 antibody used in this study. This research was funded in part by NIH grants AR45779 and CA26731, and a fellowship from NDSEG fellowship (ALS).

References

1. Miersch S, Mutus B. Protein S-nitrosation: biochemistry and characterization of protein thiol-NO interactions as cellular signals. Clin Biochem 2005;38(9):777-91.
2. Stadler J, Stefanovic-Racic M, Billiar TR, Curran RD, McIntyre LA, Georgescu HI, et al. Articular chondrocytes synthesize nitric oxide in response to cytokines and lipopolysaccharide. J Immunol 1991;147(11):3915-20.
3. Palmer RM, Hickery MS, Charles IG, Moncada S, Bayliss MT. Induction of nitric oxide synthase in human chondrocytes. Biochem Biophys Res Commun 1993;193(1):398-405.
4. Hauselmann HJ, Oppliger L, Michel BA, Stefanovic-Racic M, Evans CH. Nitric oxide and proteoglycan biosynthesis by human articular chondrocytes in alginate culture. FEBS Lett 1994;352(3):361-4.
5. Olee T, Hashimoto S, Quach J, Lotz M. IL-18 is produced by articular chondrocytes and induces proinflammatory and catabolic responses. J Immunol 1999;162(2):1096-100.
6. Cai L, Suboc P, Hogue DA, Fei DT, Filvaroff EH. Interleukin 17 induced nitric oxide suppresses matrix synthesis and protects cartilage from matrix breakdown. J Rheumatol 2002;29(8):1725-36.
7. Boileau C, Martel-Pelletier J, Moldovan F, Jouzeau JY, Netter P, Manning PT, et al. The in situ up-regulation of chondrocyte interleukin-1-converting enzyme and interleukin-18 levels in experimental osteoarthritis is mediated by nitric oxide. Arthritis Rheum 2002;46(10):2637-47.
8. Yocum DE, Esparza L, Dubry S, Benjamin JB, Volz R, Scuderi P. Characteristics of tumor necrosis factor production in rheumatoid arthritis. Cell Immunol 1989;122(1):131-45.
9. Di Giovine FS, Nuki, G., Duff, G. W. Tumor necrosis factor in synovial exudates. Annals of the Rheum 1988;47:768-772.
10. Brennan FM, Chantry D, Jackson A, Maini R, Feldmann M. Inhibitory effect of TNF alpha antibodies on synovial cell interleukin-1 production in rheumatoid arthritis. Lancet 1989;2(8657):244-7.
11. Saklatvala J. Tumour necrosis factor alpha stimulates resorption and inhibits synthesis of proteoglycan in cartilage. Nature 1986;322(6079):547-9.
12. Hrycaj P, Stratz T, Kovac C, Mennet P, Muller W. Microheterogeneity of acute phase proteins in patients with clinically active and clinically nonactive osteoarthritis. Clin Rheumatol 1995;14(4):434-40.
13. Schlaak JF, Pfers I, Meyer Zum Buschenfelde KH, Marker-Hermann E. Different cytokine profiles in the synovial fluid of patients with osteoarthritis, rheumatoid arthritis and seronegative spondylarthropathies. Clin Exp Rheumatol 1996;14(2):155-62.
14. Pelletier JP, DiBattista JA, Roughley P, McCollum R, Martel-Pelletier J. Cytokines and inflammation in cartilage degradation. Rheum Dis Clin North Am 1993;19(3):545-68.
15. Ismaiel S, Atkins RM, Pearse MF, Dieppe PA, Elson CJ. Susceptibility of normal and arthritic human articular cartilage to degradative stimuli. Br J Rheumatol 1992;31(6):369-73.
16. Westacott CI, Ismaiel, S., Langkamer, V. G., Atkins, R. M., Elson, C. J. . Human Articular Cartilage Degradation and Chondrocyte Expression of TNF-alpha Receptors. In: Transactions of the Orthopaedic REsearch Society; 1993; San Francisco, CA; 1993. p. 739.
17. Westacott CI, Barakat AF, Wood L, Perry MJ, Neison P, Bisbinas I, et al. Tumor necrosis factor alpha can contribute to focal loss of cartilage in osteoarthritis. Osteoarthritis Cartilage 2000;8(3):213-21.

18. Stefanovic-Racic M, Morales TI, Taskiran D, McIntyre LA, Evans CH. The role of nitric oxide in proteoglycan turnover by bovine articular cartilage organ cultures. J Immunol 1996;156(3):1213-20.
19. Taskiran D, Stefanovic-Racic M, Georgescu H, Evans C. Nitric oxide mediates suppression of cartilage proteoglycan synthesis by interleukin-1. Biochem Biophys Res Commun 1994;200(1):142-8.
20. Hickery MS, Palmer, R. M. J., Charles, I. G., Moncada, S., Bayliss, M. T. The role of Nitric Oxide in the IL-1- and TNF-alpha induced inhibition of proteoglycan synthesisi in human articular cartilage. In: Transactions of the Orthopaedic Research Society; 1994 February 21-24, 1994; 1994. p. 77.
21. Goodstone NJ, Hardingham TE. Tumour necrosis factor alpha stimulates nitric oxide production more potently than interleukin-1beta in porcine articular chondrocytes. Rheumatology (Oxford) 2002;41(8):883-91.
22. Cao M, Westerhausen-Larson A, Niyibizi C, Kavalkovich K, Georgescu HI, Rizzo CF, et al. Nitric oxide inhibits the synthesis of type-II collagen without altering Col2A1 mRNA abundance: prolyl hydroxylase as a possible target. Biochem J 1997;324 (Pt 1):305-10.
23. Stefanovic-Racic M, Mollers MO, Miller LA, Evans CH. Nitric oxide and proteoglycan turnover in rabbit articular cartilage. J Orthop Res 1997;15(3):442-9.
24. Bird JL, May S, Bayliss MT. Nitric oxide inhibits aggrecan degradation in explant cultures of equine articular cartilage. Equine Vet J 2000;32(2):133-9.
25. Bird JL, Wells T, Platt D, Bayliss MT. IL-1 beta induces the degradation of equine articular cartilage by a mechanism that is not mediated by nitric oxide. Biochem Biophys Res Commun 1997;238(1):81-5.
26. Murrell GA, Jang D, Williams RJ. Nitric oxide activates metalloprotease enzymes in articular cartilage. Biochem Biophys Res Commun 1995;206(1):15-21.
27. Tamura T, Nakanishi T, Kimura Y, Hattori T, Sasaki K, Norimatsu H, et al. Nitric oxide mediates interleukin-1-induced matrix degradation and basic fibroblast growth factor release in cultured rabbit articular chondrocytes: a possible mechanism of pathological neovascularization in arthritis. Endocrinology 1996;137(9):3729-37.
28. Sah RL, Kim YJ, Doong JY, Grodzinsky AJ, Plaas AH, Sandy JD. Biosynthetic response of cartilage explants to dynamic compression. J Orthop Res 1989;7(5):619-36.
29. Kisiday JD, Kurz B, DiMicco MA, Grodzinsky AJ. Evaluation of medium supplemented with insulin-transferrin-selenium for culture of primary bovine calf chondrocytes in three-dimensional hydrogel scaffolds. Tissue Eng 2005;11(1-2):141-51.
30. Farndale RW, Buttle DJ, Barrett AJ. Improved quantitation and discrimination of sulphated glycosaminoglycans by use of dimethylmethylene blue. Biochim Biophys Acta 1986;883(2):173-7.
31. Green LC, Wagner DA, Glogowski J, Skipper PL, Wishnok JS, Tannenbaum SR. Analysis of nitrate, nitrite, and [15N]nitrate in biological fluids. Anal Biochem 1982;126(1):131-8.
32. Clark IM. Matrix Metalloproteinase Protocols. Clifton, NJ: Humana Press; 2001.
33. Fitzgerald JB, Jin M, Dean D, Wood DJ, Zheng MH, Grodzinsky AJ. Mechanical compression of cartilage explants induces multiple time-dependent gene expression patterns and involves intracellular calcium and cyclic AMP. J Biol Chem 2004;279(19):19502-11.
34. Pratta MA, Yao W, Decicco C, Tortorella MD, Liu RQ, Copeland RA, et al. Aggrecan protects cartilage collagen from proteolytic cleavage. J Biol Chem 2003;278(46):45539-45.

35. Van Bezooijen RL, Van Der Wee-Pals L, Papapoulos SE, Lowik CW. Interleukin 17 synergises with tumour necrosis factor alpha to induce cartilage destruction in vitro. Ann Rheum Dis 2002;61(10):870-6.
36. Pichika R, Homandberg GA. Fibronectin fragments elevate nitric oxide (NO) and inducible NO synthetase (iNOS) levels in bovine cartilage and iNOS inhibitors block fibronectin fragment mediated damage and promote repair. Inflamm Res 2004;53(8):405-12.
37. Sandy JD, Flannery CR, Neame PJ, Lohmander LS. The structure of aggrecan fragments in human synovial fluid. Evidence for the involvement in osteoarthritis of a novel proteinase which cleaves the Glu 373-Ala 374 bond of the interglobular domain. J Clin Invest 1992;89(5):1512-6.
38. Arner EC, Hughes CE, Decicco CP, Caterson B, Tortorella MD. Cytokine-induced cartilage proteoglycan degradation is mediated by aggrecanase. Osteoarthritis Cartilage 1998;6(3):214-28.
39. Flannery CR, Lark MW, Sandy JD. Identification of a stromelysin cleavage site within the interglobular domain of human aggrecan. Evidence for proteolysis at this site in vivo in human articular cartilage. J Biol Chem 1992;267(2):1008-14.
40. Gu Z, Kaul M, Yan B, Kridel SJ, Cui J, Strongin A, et al. S-nitrosylation of matrix metalloproteinases: signaling pathway to neuronal cell death. Science 2002;297(5584):1186-90.
41. Dozin B, Malpeli M, Camardella L, Cancedda R, Pietrangelo A. Response of young, aged and osteoarthritic human articular chondrocytes to inflammatory cytokines: molecular and cellular aspects. Matrix Biol 2002;21(5):449-59.
42. Zeng W, Corcoran C, Collins-Racie LA, Lavallie ER, Morris EA, Flannery CR. Glycosaminoglycan-binding properties and aggrecanase activities of truncated ADAMTSs: comparative analyses with ADAMTS-5, -9, -16 and -18. Biochim Biophys Acta 2006;1760(3):517-24.
43. Porter S, Clark IM, Kevorkian L, Edwards DR. The ADAMTS metalloproteinases. Biochem J 2005;386(Pt 1):15-27.
44. Tortorella MD, Liu RQ, Burn T, Newton RC, Arner E. Characterization of human aggrecanase 2 (ADAM-TS5): substrate specificity studies and comparison with aggrecanase 1 (ADAM-TS4). Matrix Biol 2002;21(6):499-511.
45. Patwari P, Gao G, Lee JH, Grodzinsky AJ, Sandy JD. Analysis of ADAMTS4 and MT4-MMP indicates that both are involved in aggrecanolysis in interleukin-1-treated bovine cartilage. Osteoarthritis Cartilage 2005;13(4):269-77.
46. Caterson B, Flannery CR, Hughes CE, Little CB. Mechanisms involved in cartilage proteoglycan catabolism. Matrix Biol 2000;19(4):333-44.
47. Flannery CR, Zeng W, Corcoran C, Collins-Racie LA, Chockalingam PS, Hebert T, et al. Autocatalytic cleavage of ADAMTS-4 (Aggrecanase-1) reveals multiple glycosaminoglycan-binding sites. J Biol Chem 2002;277(45):42775-80.
48. Pratta MA, Scherle PA, Yang G, Liu RQ, Newton RC. Induction of aggrecanase 1 (ADAM-TS4) by interleukin-1 occurs through activation of constitutively produced protein. Arthritis Rheum 2003;48(1):119-33.
49. Gao G, Plaas A, Thompson VP, Jin S, Zuo F, Sandy JD. ADAMTS4 (aggrecanase-1) activation on the cell surface involves C-terminal cleavage by glycosylphosphatidyl inositol-anchored membrane type 4-matrix metalloproteinase and binding of the activated proteinase to chondroitin sulfate and heparan sulfate on syndecan-1. J Biol Chem 2004;279(11):10042-51.

50. Sasaki K, Hattori T, Fujisawa T, Takahashi K, Inoue H, Takigawa M. Nitric oxide mediates interleukin-1-induced gene expression of matrix metalloproteinases and basic fibroblast growth factor in cultured rabbit articular chondrocytes. J Biochem (Tokyo) 1998;123(3):431-9.
51. Saas J, Haag J, Rueger D, Chubinskaya S, Sohler F, Zimmer R, et al. IL-1beta, but not BMP-7 leads to a dramatic change in the gene expression pattern of human adult articular chondrocytes--portraying the gene expression pattern in two donors. Cytokine 2006;36(1-2):90-9.
52. Kobayashi M, Squires GR, Mousa A, Tanzer M, Zukor DJ, Antoniou J, et al. Role of interleukin-1 and tumor necrosis factor alpha in matrix degradation of human osteoarthritic cartilage. Arthritis Rheum 2005;52(1):128-35.
53. Richardson DW, Dodge GR. Dose-dependent effects of corticosteroids on the expression of matrix-related genes in normal and cytokine-treated articular chondrocytes. Inflamm Res 2003;52(1):39-49.
54. Aigner T, McKenna L, Zien A, Fan Z, Gebhard PM, Zimmer R. Gene expression profiling of serum- and interleukin-1 beta-stimulated primary human adult articular chondrocytes--a molecular analysis based on chondrocytes isolated from one donor. Cytokine 2005;31(3):227-40.

Figure Legends

Figure 1: Five-day accumulated total nitrate and nitrite release to the medium (nmol/mg wet weight) as a measure of NO production plotted as mean +/- SEM from greater than 3 explants per joint pooled from from 5 different joints (animals) (* $p<0.001$ cytokine compared to control and ** $p<0.01$ cytokine compared to cytokine + NMA)

Figure 2: Accumulated sGAG release to medium over five day cytokine treatment in the presence or absence of L-NMA plotted as mean +/- SEM. IL-1β and TNF-α alone cause a 3-5 fold increase in sGAG release compared to untreated controls ($p<0.001$ for all points). L-NMA inhibited roughly half the sGAG release caused by treatment with TNF-α ($p<0.01$ for all time points).

Figure 3: Anti-Aggrecan-G1-NITEGE-COOH Western blot to probe mechanism of sGAG loss in response to IL-1β and TNF-α treatment with and without NOS inhibitor, L-NMA. A band is visualized in all cytokine-treated conditions; however, the TNF-α + L-NMA band is significantly lighter than that with TNF-α alone or with IL-1β ± L-NMA. This immunoblot is representative of five different experiments and corresponding blots.

Figure 4. Casein (4A) and Gelatin (4B) zymograms of 5 day culture medium. (A) The casein zymogram for both IL-1β and IL-1β - L-NMA contains a 54 kDa band, corresponding to pro-MMP-3 that appears as a doublet, with a lighter upper band and a brighter lower band. A faint doublet is seen for TNF-α treatment and, in addition, a 90 kDa band is seen with all cytokine treatments. (B) The gelatin zymogram contained a 72 kDa band (arrow) and a lower 65 kDa band in all samples, corresponding to the pro- and active forms of MMP-2, respectively.

Only cytokine treated samples had a 92 kDa band corresponding to MMP-9. L-NMA had no effect on MMP-3, MMP-9 or MMP-2 expression or activation as seen in medium samples.

Figure 5: Relative gene expression by real-time PCR and clustering analyses. (5A) Expression of ADAMTS4 and ADAMTS5 at 26 and 50 hour time points, relative to controls, in response to treatment with L-NMA alone, IL-1β ± L-NMA and TNF-α ± L-NMA. (5B) Centroid profile for gene cluster 1 (group-1 genes) which showed decreased expression or were unchanged in response to cytokine treatment. Centroids represent 26 and 50 hour time points clustered together. (5C) Centroid profile for gene cluster 2, showing genes that were upregulated in response to cytokine treatment. (Groups produced from clustering 26 hours alone (see Table 1) vs. 26 and 50 hours together were identical, except IGF-2 and TIMP-3 in Table 1 swapped groups. The * indicates statistical significance compared to the untreated control sample by pair-wise comparison (Wilcoxan Sign Rank test with Bonferroni correction for multiple comparison; $p<0.05$)

Figure 6: Projection plot of gene behavior represented by the first three principal components. The genes readily separated into 2 clusters which correspond to genes that respond positively to IL-1β and TNF-α treatment (triangles = Group 2 of Table 1) and those genes that either did not respond or responded negatively to the cytokine treatment (squares; Group 1). The black circles indicate the group centroids which are significantly different from each other ($p<0.001$; Student's t-Test).

Table Caption

Table 1: Genes probed by real time PCR, represented as the mean fold change over control +/-SEM at 26 hours. Groups were determined using clustering analysis of data from the 26 hour time point. The expression data for the individual genes show similar trends at the 50 hour time point. The * indicates statistical significance compared to the untreated control sample by pair-wise comparison (Wilcoxan Sign Rank test with Bonferroni correction for multiple comparison; $p<0.05$). Data represent experiments from eight animals with 2 or 3 explants pooled per animal for RNA extraction.

Table 1

GENE *Group 1*	*NMA*	*TNF-α*	*TNF-α/ TNF+NMA*	*IL-1β*	*IL-1β/ IL-1b+NMA*
Aggrecan	0.98+/-0.06	**0.74+/-0.07***	1.17+/-0.14	0.91+/-0.05	1.12+/-0.24
Collagen II	0.98+/-0.13	0.73+/-0.11	1.14+/-0.27	0.81+/-0.10	1.31+/-0.19
Fibromodulin	1.18+/-0.12	**0.59+/-0.06***	0.98+/-0.08	0.86+/-0.06	0.91+/-0.05
Link protein	1.0+/-0.10	**0.46+/-0.06***	0.95+/-0.07	0.81+/-0.08	1.09+/-0.15
TIMP-2	0.99+/-0.12	**0.53+/-0.03***	1.12+/-0.16	**0.50+/-0.08***	0.76+/-0.12
TIMP-3	0.61+/-0.11	1.1+/-0.37	4.07+/-3.18	0.97+/-0.27	1.52+/-0.53
MMP-1	0.88+/-0.09	0.92+/-0.08	1.02+/-0.10	0.98+/-0.09	1.15+/-0.08
G3DPH	0.90+/-0.12	0.72+/-0.15	0.93+/-0.21	0.89+/-0.19	0.82+/-0.16
b-actin	0.95+/-0.08	0.81+/-0.06	0.92+/-0.05	0.86+/-0.07	1.03+/-0.07
IGF-1	1.0+/-0.13	**0.50+/-0.12***	1.05+/-0.21	0.64+/-0.10	1.33+/-0.27
IL-4	0.82+/-0.11	0.78+/-0.11	1.10+/-0.26	0.91+/-0.13	1.27+/-0.23
IL-6	0.77+/-0.13	0.82+/-0.15	1.56+/-0.38	1.1+/-0.16	1.33+/-0.30
TXNIP	0.92+/-0.09	**0.55+/-0.05***	0.87+/-0.09	**0.66+/-0.05***	0.91+/-0.06
HAS2	1.0+/-0.12	**0.49+/-0.03***	0.95+/-0.11	**0.47+/-0.04***	1.01+/-0.12
Group 2					
Fibronectin	0.96+/-0.08	**1.60+/-0.15***	1.16+/-0.10	**1.41+/-0.15***	1.20+/-0.16
MMP-3	1.0+/-0.18	**11+/-2.7***	1.75+/-0.43	**34+/-9.1***	1.80+/-0.53
MMP-9	1.1+/-0.24	115+/-60	1.11+/-0.24	74+/-54	0.79+/-0.17
MMP-13	0.83+/-0.17	**12+/-4.4***	1.87+/-0.66	**76+/-23***	1.31+/-0.17
ADAMTS4	0.98+/-0.09	**8.0+/-1.1***	1.24+/-0.16	**5.9+/-1.4***	1.26+/-0.14
ADAMTS5	1.26+/-0.23	**68+/-9.1***	1.28+/-0.24	**17.4+/-6.9***	1.15+/-0.17
TIMP-1	10.1+/-0.16	**4.6+/-1.3***	1.40+/-0.38	**3.4+/-0.64***	1.24+/-0.19
COX2	1.2+/-0.11	**11.4+/-2.7***	1.13+/-0.20	**17.6+/-5.0***	1.28+/-0.27
NOS2	1.5+/-0.57	**4513+/-1495***	1.04+/-0.31	**894/-183***	1.94+/-0.70
IGF-2	0.99+/-0.10	0.92+/-0.08	0.94+/-0.17	1.1+/-0.11	0.96+/-0.11
TGF-beta	0.92+/-0.07	2.3+/-0.20	0.91+/-0.06	**1.7+/-0.18***	1.10+/-0.08
TNF-alpha	2.0+/-0.98	2.5+/-1.6	0.91+/-0.13	3.7+/-2.6	1.27+/-0.22
IL-1beta	0.95+/-0.12	4.4+/-2.8	1.35+/-0.25	4.3+/-2.4	1.33+/-0.34
HSP90	0.85+/-0.07	**2.2+/-0.27***	1.21+/-0.11	1.3+/-0.14	1.06+/-0.08
CD44	1.0+/-0.17	**20+/-3.0***	1.06+/-0.09	**11+/-2.1***	1.27+/-0.16
bFGF	9.0+/-7.0	1722+/-1109	10.56+/-5.86	61+/-48	8.66+/-4.91
OP-1	1.6+/-0.41	**80+/-16***	1.32+/-0.28	**26+/-10***	1.42+/-0.31

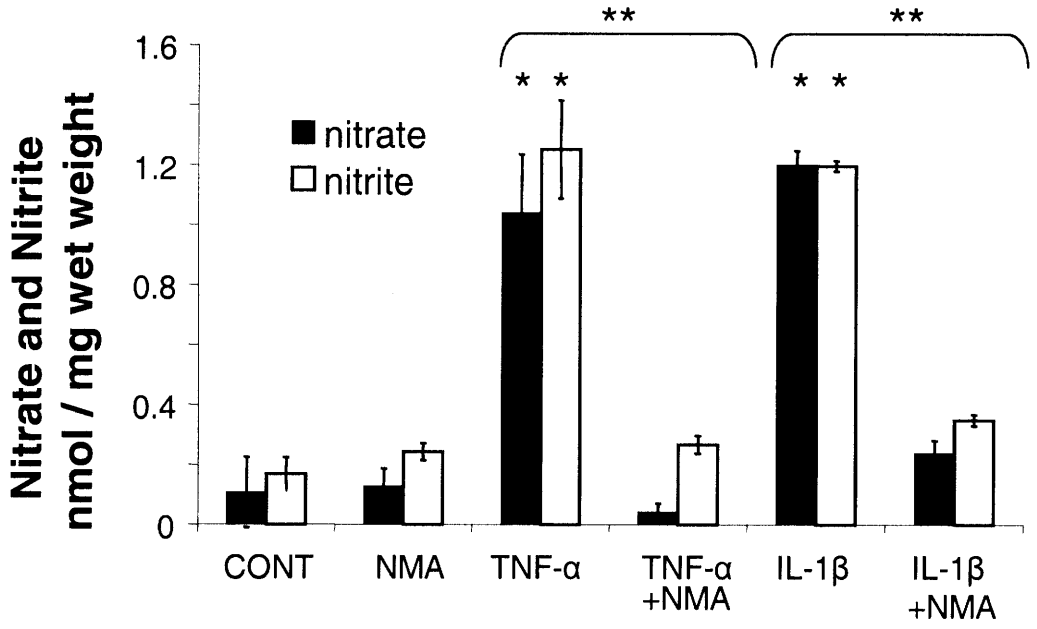
Nitrate and Nitrite
nmol / mg wet weight
1.6
1.2
0.8
0.4
0
nitrate
nitrite
**
**
* *
* *
CONT
NMA
TNF-α
TNF-α
+NMA
IL-1β
IL-1β
+NMA

Figure 1

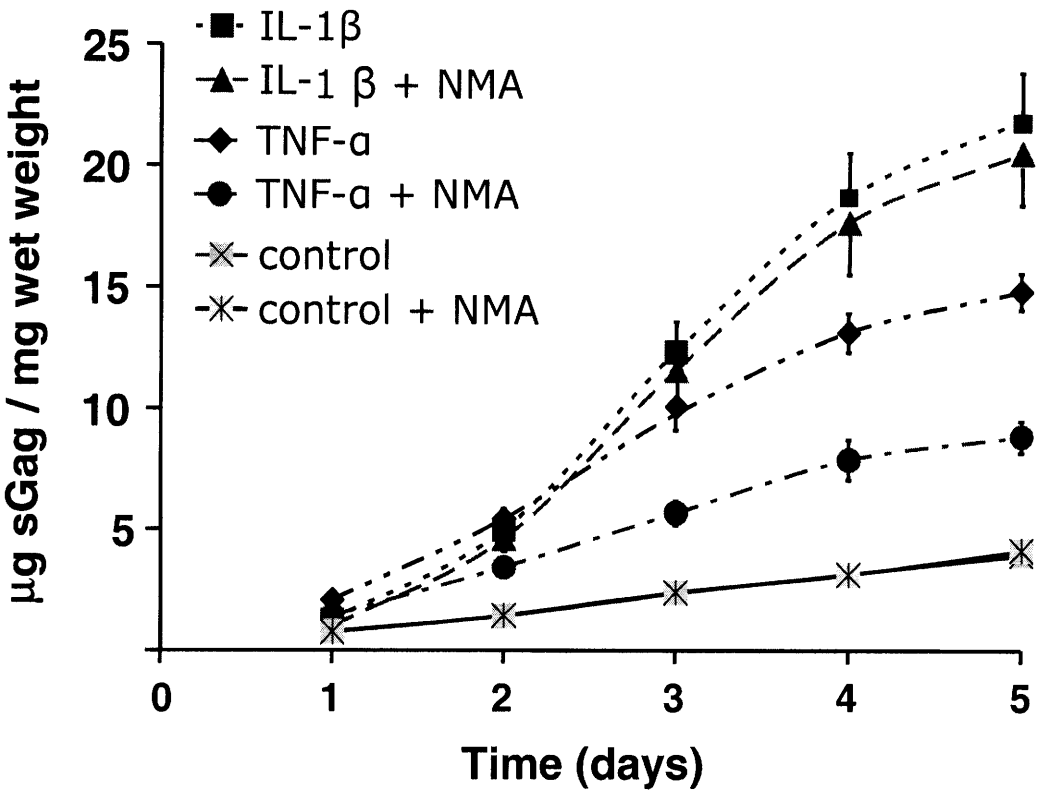
IL-1β
IL-1 β + NMA
TNF-α
TNF-α + NMA
control
control + NMA
µg sGag / mg wet weight
25
20
15
10
5
0
1
2
3
4
5
Time (days)

Figure 2

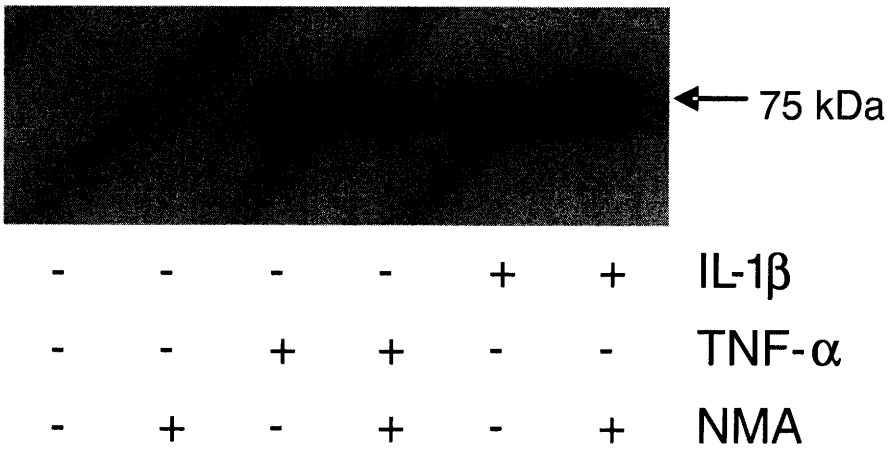

Figure 3

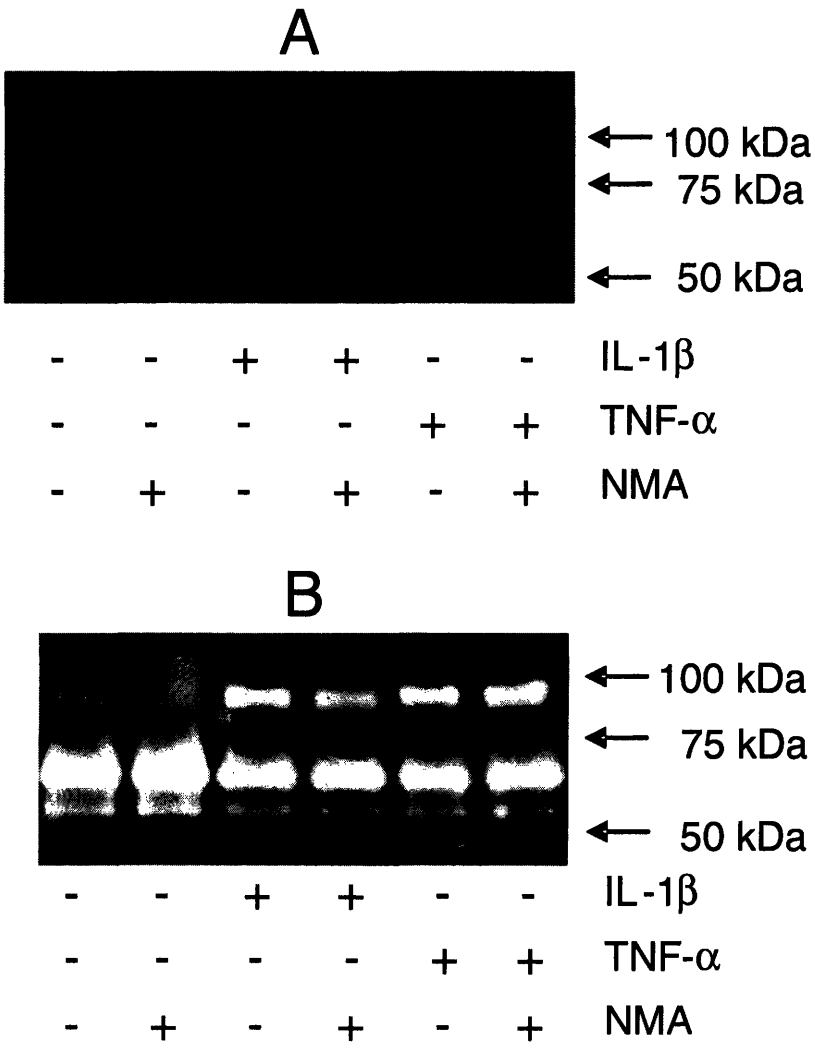
A
100 kDa
75 kDa
50 kDa
- - + + - - IL-1β
- - - - + + TNF-α
- + - + - + NMA
B
100 kDa
75 kDa
50 kDa
- - + + - - IL-1β
- - - - + + TNF-α
- + - + - + NMA

Figure 4

Figure 5

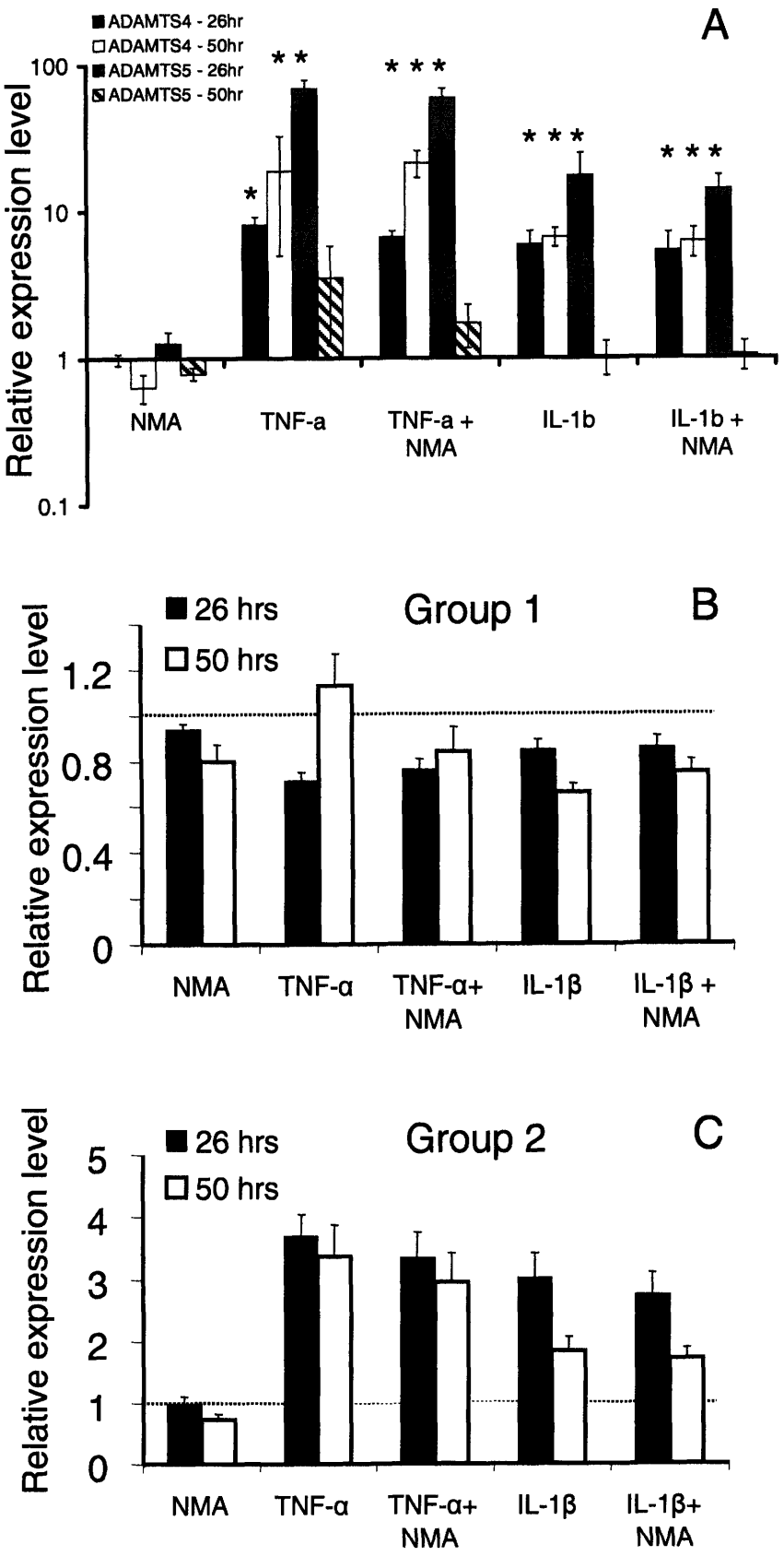
A
ADAMTS4 - 26hr
ADAMTS4 - 50hr
ADAMTS5 - 26hr
ADAMTS5 - 50hr
Relative expression level
100
10
1
0.1
NMA
TNF-a
TNF-a + NMA
IL-1b
IL-1b + NMA
B
Group 1
26 hrs
50 hrs
Relative expression level
1.2
0.8
0.4
0
NMA
TNF-α
TNF-α+ NMA
IL-1β
IL-1β + NMA
C
Group 2
26 hrs
50 hrs
Relative expression level
5
4
3
2
1
0
NMA
TNF-α
TNF-α+ NMA
IL-1β
IL-1β+ NMA

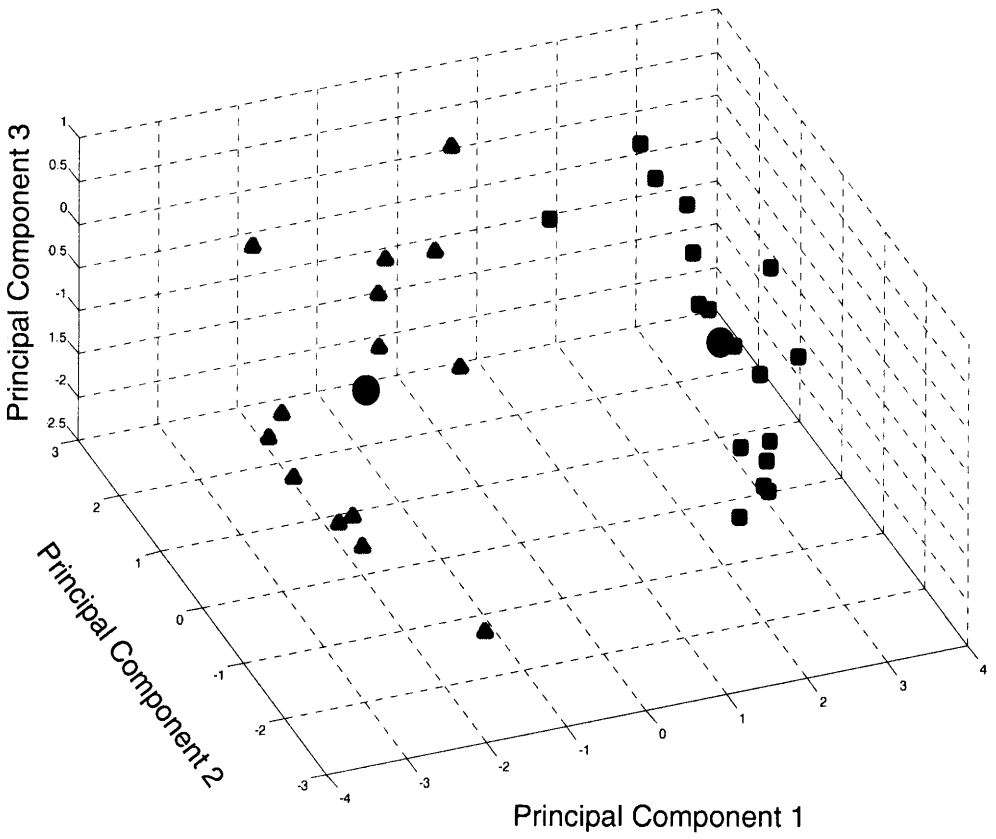
Principal Component 3
1
0.5
0
0.5
-1
1.5
-2
2.5
3
Principal Component 2
2
1
0
-1
-2
-3
-4
Principal Component 1
-4
-3
-2
-1
0
1
2
3
4

Figure 6